

**ANALYTICAL STUDY OF BASE ISOLATION SYSTEM
ON MEDIUM-RISE REINFORCED CONCRETE
BUILDING FOR INDIAN SUBCONTINENT**

भारतीय उपमहाद्वीप के लिए मध्यम-राइज़ प्रबलित कंक्रीट बिल्डिंग
पर बेस आइसोलेशन सिस्टम का विश्लेषणात्मक अध्ययन

A

Thesis

Submitted for the Award of the Ph.D. degree of

**PACIFIC ACADEMY OF HIGHER
EDUCATION AND RESEARCH UNIVERSITY**

By

M. TAMIM TANWER

मो. तमीम तंवर

Under the supervision of

Dr. TANVEER AHMED KAZI

Professor

Pacific Academy of Higher Education
& Research University, Udaipur



FACULTY OF ENGINEERING

DEPARTMENT OF CIVIL ENGINEERING

**PACIFIC ACADEMY OF HIGHER EDUCATION
AND RESEARCH UNIVERSITY, UDAIPUR**

2023

DECLARATION

I, **Mr. M. TAMIM TANWER, S/o Mr. M. ASLAM TANWER** resident of Surat, Gujarat, hereby declare that the research work incorporated in the present thesis entitled “**ANALYTICAL STUDY OF BASE ISOLATION SYSTEM ON MEDIUM-RISE REINFORCED CONCRETE BUILDING FOR INDIAN SUBCONTINENT**” (भारतीय उपमहाद्वीप के लिए मध्यम-राइज़ प्रबलित कंक्रीट बिल्डिंग पर बेस आइसोलेशन सिस्टम का विश्लेषणात्मक अध्ययन) is my original work. This work (in part or in full) has not been submitted to any University for the award or a Degree or a Diploma. I have properly acknowledged the material collected from secondary sources wherever required.

I solely own the responsibility for the originality of the entire content.

Signature of the Candidate

Date:

FACULTY OF ENGINEERING
PACIFIC ACADEMY OF HIGHER EDUCATION AND
RESEARCH UNIVERSITY, UDAIPUR

Dr. TANVEER AHMED KAZI
Professor

CERTIFICATE

It gives me an immense pleasure in certifying that the thesis entitled “ANALYTICAL STUDY OF BASE ISOLATION SYSTEM ON MEDIUM-RISE REINFORCED CONCRETE BUILDING FOR INDIAN SUBCONTINENT” (भारतीय उपमहाद्वीप के लिए मध्यम-राइज़ प्रबलित कंक्रीट बिल्डिंग पर बेस आइसोलेशन सिस्टम का विश्लेषणात्मक अध्ययन) and submitted by **Mr. M. TAMIM TANWER** is based on the research work carried out under my guidance. He have completed the following requirements as per Ph.D. regulations of the University;

- (i) Course work as per the university rules.
- (ii) Residential requirements of the university.
- (iii) Regularly presented Half Yearly Progress Report as prescribed by the university.
- (iv) Published / accepted minimum of two research paper in a refereed research journal.

I recommend the submission of thesis as prescribed/notified by the University.

Date:

Name and Designation of Supervisor

Dr. TANVEER AHMED KAZI
Professor
Pacific Academy of Higher Education
& Research University, Udaipur

COPYRIGHT

I, **Mr. M. TAMIM TANWER**, hereby declare that the Pacific academy of higher education and research university, Udaipur, Rajasthan, shall have the rights to preserve, use and disseminate this dissertation entitled **“ANALYTICAL STUDY OF BASE ISOLATION SYSTEM ON MEDIUM-RISE REINFORCED CONCRETE BUILDING FOR INDIAN SUBCONTINENT”** (भारतीय उपमहाद्वीप के लिए मध्यम-राइज़ प्रबलित कंक्रीट बिल्डिंग पर बेस आइसोलेशन सिस्टम का विश्लेषणात्मक अध्ययन) in print or in electronic format for the academic research.

Date:

Signature of Candidate

Place:

ACKNOWLEDGEMENT

First and foremost, praises and thanks to the God, the Almighty, for his showers of blessings throughout my research work to complete the research successfully.

I would like to express my deep and sincere gratitude to my research supervisor, **Dr. Tanveer Ahmed Kazi**, Professor, Pacific Academy of Higher Education & Research University-Udaipur, for giving me the opportunity to do research and providing invaluable guidance throughout this research. His dynamism, vision, sincerity and motivation have deeply inspired me. He has taught me the methodology to carry out the research and to present the research works as clearly as possible. It was a great privilege and honor to work and study under his guidance. I am extremely grateful for what he has offered me. I would also like to thank him for his friendship, empathy, and great sense of humor. I am extending my heartfelt thanks to his wife, family for their acceptance and patience during the discussion I had with him on research work and thesis preparation.

I am extremely grateful to **my family** for their love, prayers, caring and sacrifices for educating and preparing me for my future.

I thank the management of Pacific Academy of Higher Education & Research University-Udaipur, for their support to do this work.

Finally, my thanks go to all the people who have supported me to complete the research work directly or indirectly.

M. Tamim Tanwer

PREFACE

An earthquake is a very dangerous natural disaster i.e. brought on by the tectonic plates moving within the earth's core. Many constructions fall as a result of earthquakes, causing fatalities among people. The Base Isolation System is a technique for minimizing an earthquake's effects on the building by absorbing its shaking forces. In order to minimize base shear, increase time & storey-displacement, and decrease storey-drift, the design of base isolation bearing is optimized from the cumulative load of column of fixed base structure.

Here, we are considering the design of G+12 & G+22 storey RC building with fixed base and isolated base. For design of a based isolated structure, LRB and TFPB are used. Analyzing and designed of these two type of structure with different model case are carried out by response spectrum method in ETABS 2016 software. LRB & TFPB are design according to axial load, biaxial load and uniaxial load (Cumulative load from fixed base modal). Time period, base shear, story displacement, story-drift, percentage reduction in steel, and overall cost economy will be determined for all model situations after evaluating the framework. With the use of LRB and TFPB as base isolators, it is found from this study that time period and story displacement increased while base shear, story drift, percentage of steel reduction, and overall cost were reasonably enhanced.

LIST OF CONTENTS

CHAPTER- I INTRODUCTION		1-7
1.1	Preamble	1
1.2	General Overview	1
1.3	Motion Caused by Earthquakes	3
	1.3.1 Features of Earthquakes	3
	1.3.2 Concept of Resonance	4
	1.3.3 RS - Response Spectrum	5
1.4	Structure Reaction	5
	1.4.1 Consequence of Surface Acceleration	5
	1.4.2 Effects of Stiffness and Ductility	6
	1.4.3 Damping's Impacts	6
1.5	Thesis Organization	6
CHAPTER- II COMPONENTS OF BASE ISOLATION SYSTEM		8-15
2.1	Preamble	8
2.2	Parts of Base Isolation Systems	8
2.3	Elastometric Bearing	8
	2.3.1 Natural Rubber Bearing (NRB)	8
	2.3.2 Lead Rubber Bearing (LRB)	10
	2.3.3 High Damping Natural Rubber Bearing (HDRB)	11
2.4	Moving Mechanisms	11
	2.4.1 Natural Friction Bearing	11
	2.4.2 Cable Friction Bearing	12
	2.4.3 Resilient Friction Base Isolators	13
	2.4.4 Friction Pendulum Bearing	14
2.5	Limiting Devices	15

CHAPTER- III LITERATURE REVIEW OF BASE ISOLATION SYSTEM		16-29
3.1	Preamble	16
3.2	Literature Survey	16
3.3	Observations from Literature Survey	28
3.4	Summary	29
CHAPTER- IV METHODOLOGY OF RESEARCH		30-55
4.1	Preamble	30
4.2	Scope of Work	30
4.3	Objectives of the Study	31
4.4	Hypothesis	32
4.5	Sample Model	32
	4.5.1 G+12 Storey Model Details	32
	4.5.2 G+22 Storey Model Details	35
4.6	Sample Model Case	38
	4.6.1 Case (a) G+12 Storey Reinforced Concrete (RC) Structure	38
	4.6.2 Case (b) G+22 Storey Reinforced Concrete (RC) Structure	39
4.7	Important Design Factors	39
	4.7.1 Loads	39
	4.7.2 Analytical Procedures	39
	4.7.3 Design Philosophies	40
	4.7.4 Building Components Design	41
4.8	Design Calculation for R.C.C.	42
	4.8.1 Analysis Method	42
4.9	Research Methodology	54
4.10	Summary	55

CHAPTER- V DESIGN OF BASE ISOLATION BEARING		56-164
5.1	Preamble	56
5.2	Design of LRB for G+12 Storey RC Structure.	56
	5.2.1 LRB for Biaxial Load - 1638 KN	56
	5.2.2 LRB for Uniaxial Load - 2487 KN	64
	5.2.3 LRB for Axial Load - 3920 KN	72
5.3	Design of Triple Friction Pendulum Bearing (TFPB) for G+12 Storey RC Structure.	80
	5.3.1 TFPB for Biaxial Load - 1638 KN	80
	5.3.2 TFPB for Uniaxial Load - 2487 KN	90
	5.3.3 TFPB for Axial Load - 3920 KN	100
5.4	Design of Lead Rubber Bearing (LRB) for G+22 Storey RC Structure.	110
	5.4.1 LRB for Biaxial Load - 3342 KN	110
	5.4.2 LRB for Uniaxial Load - 4627 KN	118
	5.4.3 LRB for Axial Load - 6860 KN	126
5.5	Design of Triple Friction Pendulum Bearing (TFPB) for G+22 Storey RC Structure.	134
	5.5.1 TFPB for Biaxial Load - 3342 KN	134
	5.5.2 TFPB for Uniaxial Load - 4627 KN	144
	5.5.3 TFPB for Axial Load - 6860 KN	154
5.6	Summary	164
CHAPTER- VI ANALYSIS OF RESULTS		165-197
6.1	Preamble	165
6.2	Result Comparison for Case (a) G+12 Storey Reinforced Concrete (RC) Structure. (Case-I with Case-II).	165
	6.2.1 Time Period.	165
	6.2.2 Base Shear.	166

	6.2.3 Storey-Displacement.	167
	6.2.4 Storey-Drift.	169
	6.2.5 Steel Reduction.	171
	6.2.6 Overall Cost Economy.	172
6.3	Result Comparison for Case (a) G+12 Storey Reinforced Concrete (RC) Structure. (Case-I with Case-III).	173
	6.3.1 Time Period.	173
	6.3.2 Base Shear.	174
	6.3.3 Storey-Displacement.	175
	6.3.4 Storey-Drift.	177
	6.3.5 Steel Reduction.	179
	6.3.6 Overall Cost Economy.	180
6.4	Result Comparison for Case (b) G+22 Storey Reinforced Concrete (RC) Structure. (Case-IV with Case-V).	181
	6.4.1 Time Period.	181
	6.4.2 Base Shear.	182
	6.4.3 Storey-Displacement.	183
	6.4.4 Storey-Drift.	185
	6.4.5 Steel Reduction.	187
	6.4.6 Overall Cost Economy.	188
6.5	Result Comparison for Case (a) G+22 Storey Reinforced Concrete (RC) Structure. (Case-IV with Case-VI).	189
	6.5.1 Time Period.	189
	6.5.2 Base Shear.	190
	6.5.3 Storey-Displacement.	191
	6.5.4 Storey-Drift.	193
	6.5.5 Steel Reduction.	195

	6.5.6 Overall Cost Economy.	196
6.6	Summary	197
CHAPTER- VII CONCLUSIONS		198-199
7.1	Future Work	199
BIBLIOGRAPHY		200-206
APPENDIX		

LIST OF FIGURES

Figure No.	Particulars	Page No.
1	Tacoma Narrows Bridge: Excessive Deformation and Subsequent Collapse Due To Resonance.	5
2	NRB Schematic	9
3	LRB Schematic	10
4	Cable Friction Bearing Schematic	12
5	Resilient Friction Base Isolators Schematic	13
6	Friction Pendulum Bearing Schematic	14
7	Fixed & Isolated Base Structure Model	17
8	Elevation Views and Bare Frame Case Study	18
9	Plan & Elevation G+6 Storey Model	19
10	3D Model of 8-Storey Office Building	21
11	Buildings Elevation with and Without Base Isolators.	22
12	Analytical Model - Fixed & Isolated Base	23
13	2-Storey Sample Model	24
14	3D Model of G+ 5 Storeys	25
15	3D View of G+10 Storey in SAP2000 Model	26
16	Buildign A & Building B Model	28
17	G+12 Storey Sample Model - Plan	34
18	G+12 Storey Sample Model - Elevation	35
19	G+22 Storey Sample Model - Plan	37
20	G+22 Storey Sample Model - Elevation	38
21	Sample Material Property – Concrete M20	44
22	Sample Material Property – Steel Fe500	45
23	Sample Section Property – Slab	46

24	Sample Section Property – Beam	47
25	Sample Section Property – Column	48
26	Sample Diaphragm Data	49
27	Sample Mass Source Data	49
28	Sample Response Spectrum Function Property	50
29	Sample Modal Case	51
30	Sample Load Patterns	52
31	Sample Load Cases	52
32	Sample Load Combination	53
33	LRB Schematic	56
34	LRB Input Values in ETABS for Biaxial Load 1638 KN - Direction U_1	62
35	LRB Input Values in ETABS for Biaxial Load 1638 KN - Direction U_2 & U_3	63
36	LRB Schematic	64
37	LRB Input Values in ETABS for Uniaxial Load 2487 KN - Direction U_1	70
38	LRB Input Values in ETABS for Uniaxial Load 2487 KN - Direction U_2 & U_3	71
39	LRB Schematic	72
40	LRB Input Values in ETABS for Axial Load 3920 KN - Direction U_1	78
41	LRB Input Values in ETABS for Axial Load 3920 KN - Direction U_2 & U_3	79
42	TFPB Schematic	80
43	TFPB Input Values in ETABS for Biaxial Load 1638 KN - Direction U_1	88
44	TFPB Input Values in ETABS for Biaxial Load 1638 KN - Direction U_2 & U_3	89
45	TFPB Schematic	90

46	TFPB Input Values in ETABS for Uniaxial Load 2487 KN - Direction U_1	98
47	TFPB Input Values in ETABS for Uniaxial Load 2487 KN - Direction U_2 & U_3	99
48	TFPB Schematic	100
49	TFPB Input Values in ETABS for Axial Load 3920 KN - Direction U_1	108
50	TFPB Input Values in ETABS for Axial Load 3920 KN - Direction U_2 & U_3	109
51	LRB Schematic	110
52	LRB Input Values in ETABS for Biaxial Load 3342 KN - Direction U_1	116
53	LRB Input Values in ETABS for Biaxial Load 3342 KN - Direction U_2 & U_3	117
54	LRB Schematic	118
55	LRB Input Values in ETABS for Uniaxial Load 4627 KN - Direction U_1	124
56	LRB Input Values in ETABS for Uniaxial Load 4627 KN - Direction U_2 & U_3	125
57	LRB Schematic	126
58	LRB Input Values in ETABS for Axial Load 6860 KN - Direction U_1	132
59	LRB Input Values in ETABS for Axial Load 6860 KN - Direction U_2 & U_3	133
60	TFPB Schematic	134
61	TFPB Input Values in ETABS for Biaxial Load 3342 KN - Direction U_1	142
62	TFPB Input Values in ETABS for Biaxial Load 3342 KN - Direction U_2 & U_3	143
63	TFPB Schematic	144
64	TFPB Input Values in ETABS for Uniaxial Load 4627 KN - Direction U_1	152

65	TFPB Input Values in ETABS for Uniaxial Load 4627 KN - Direction U_2 & U_3	153
66	TFPB Schematic	154
67	TFPB Input Values in ETABS for Axial Load 6860 KN - Direction U_1	162
68	TFPB Input Values in ETABS for Axial Load 6860 KN - Direction U_2 & U_3	163

LIST OF TABLES

Table No.	Particulars	Page No.
1	Damping Coefficient, B_D or B_M	57
2	Seismic Coefficient C_V	57
3	Vulcanized Natural Rubber Compounds	57
4	Damping Coefficient, B_D or B_M	64
5	Seismic Coefficient C_V	65
6	Vulcanized Natural Rubber Compounds	65
7	Damping Coefficient, B_D or B_M	72
8	Seismic Coefficient C_V	73
9	Vulcanized Natural Rubber Compounds	73
10	Damping Coefficient, B_D or B_M	111
11	Seismic Coefficient C_V	111
12	Vulcanized Natural Rubber Compounds	111
13	Damping Coefficient, B_D or B_M	118
14	Seismic Coefficient C_V	119
15	Vulcanized Natural Rubber Compounds	119
16	Damping Coefficient, B_D or B_M	126
17	Seismic Coefficient C_V	127
18	Vulcanized Natural Rubber Compounds	127
19	Comparison of Time Period of Fixed Base Structure (Case-I) and	165

	LRB Base Structure (Case-II).	
20	Comparison of Base Shear of Fixed Base Structure (Case-I) and LRB Base Structure (Case-II).	166
21	Comparison of Storey-Displacement of Fixed Base Structure (Case-I) and LRB Base Structure (Case-II).	167
22	Comparison of Storey-Drift of Fixed Base Structure (Case-I) and LRB Base Structure (Case-II).	169
23	Comparison of Steel Reduction of Fixed Base Structure (Case-I) and LRB Base Structure (Case-II).	171
24	Comparison of Overall Cost Economy of Fixed Base Structure (Case-I) and LRB Base Structure (Case-II).	172
25	Comparison of Time Period of Fixed Base Structure (Case-I) and TFPB Base Structure (Case-III).	173
26	Comparison of Base Shear of Fixed Base Structure (Case-I) and TFPB Base Structure (Case-III).	174
27	Comparison of Storey-Displacement of Fixed Base Structure (Case-I) and TFPB Base Structure (Case-III).	175
28	Comparison of Storey-Drift of Fixed Base Structure (Case-I) and TFPB Base Structure (Case-III).	177
29	Comparison of Steel Reduction of Fixed Base Structure (Case-I) and TFPB Base Structure (Case-III).	179
30	Comparison of Overall Cost Economy of Fixed Base Structure (Case-I) and TFPB Base Structure (Case-III).	180
31	Comparison of Time Period of Fixed Base Structure (Case-IV) and LRB Base Structure (Case-V).	181

32	Comparison of Base Shear of Fixed Base Structure (Case-IV) and LRB Base Structure (Case-V).	182
33	Comparison of Storey-Displacement of Fixed Base Structure (Case-IV) and LRB Base Structure (Case-V).	183
34	Comparison of Storey-Drift of Fixed Base Structure (Case-IV) and LRB Base Structure (Case-V).	185
35	Comparison of Steel Reduction of Fixed Base Structure (Case-IV) and LRB Base Structure (Case-V).	187
36	Comparison of Overall Cost Economy of Fixed Base Structure (Case-IV) and LRB Base Structure (Case-V).	188
37	Comparison of Time Period of Fixed Base Structure (Case-IV) and TFPB Base Structure (Case-VI).	189
38	Comparison of Base Shear of Fixed Base Structure (Case-IV) and TFPB Base Structure (Case-VI).	190
39	Comparison of Storey-Displacement of Fixed Base Structure (Case-IV) and TFPB Base Structure (Case-VI).	191
40	Comparison of Storey-Drift of Fixed Base Structure (Case-IV) and TFPB Base Structure (Case-VI).	193
41	Comparison of Steel Reduction of Fixed Base Structure (Case-IV) and TFPB Base Structure (Case-VI).	195
42	Comparison of Overall Cost Economy of Fixed Base Structure (Case-IV) and TFPB Base Structure (Case-VI).	196
43	Summary of Result Analysis	197

LIST OF GRAPHS

Graph No.	Particulars	Page No.
1	Parametric Variation of Time Period of Fixed Base Structure (Case-I) and LRB Base Structure (Case-II).	165
2	Parametric Variation of Base Shear of Fixed Base Structure (Case-I) and LRB Base Structure (Case-II).	166
3	Parametric Variation of Storey-Displacement of Fixed Base Structure (Case-I) and LRB Base Structure (Case-II).	168
4	Parametric Variation of Storey-Drift of Fixed Base Structure (Case-I) and LRB Base Structure (Case-II).	170
5	Parametric Variation of Time Period of Fixed Base Structure (Case-I) and TFPB Base Structure (Case-III).	173
6	Parametric Variation of Base Shear of Fixed Base Structure (Case-I) and TFPB Base Structure (Case-III).	174
7	Parametric Variation of Storey-Displacement of Fixed Base Structure (Case-I) and TFPB Base Structure (Case-III).	176
8	Parametric Variation of Storey-Drift of Fixed Base Structure (Case-I) and TFPB Base Structure (Case-III).	178
9	Parametric Variation of Time Period of Fixed Base Structure (Case-IV) and LRB Base Structure (Case-V).	181
10	Parametric Variation of Base Shear of Fixed Base Structure (Case-IV) and LRB Base Structure (Case-V).	182
11	Parametric Variation of Storey-Displacement of Fixed Base Structure (Case-IV) and LRB Base Structure (Case-V).	184
12	Parametric Variation of Storey-Drift of Fixed Base Structure	186

	(Case-IV) and LRB Base Structure (Case-V).	
13	Parametric Variation of Time Period of Fixed Base Structure (Case-IV) and TFPB Base Structure (Case-VI).	189
14	Parametric Variation of Base Shear of Fixed Base Structure (Case-IV) and TFPB Base Structure (Case-VI).	190
15	Parametric Variation of Storey-Displacement of Fixed Base Structure (Case-IV) and TFPB Base Structure (Case-VI).	192
16	Parametric Variation of Storey-Drift of Fixed Base Structure (Case-IV) and TFPB Base Structure (Case-VI).	194

LIST OF SYMBOLS & ABBREVIATIONS

Symbols	Abbreviations
EQ	Earthquake
RS	Response Spectrum
RC	Reinforced Concrete
NRB	Natural Rubber Bearing
LRB	Lead Rubber Bearing
TFPB	Triple Friction Pendulum Bearing
HDRB	High Damping Rubber Bearing
LDRB	Low Damping Rubber Bearing
FPB	Friction Pendulum Bearing
FD	Friction Damper
FS	Friction Slider
FF	Floor Finish
LL	Live Load
E	Youngs Modulus
G	Shear Modulus
K	Modification Factor
ε_b	Elongation of Rubber at Break
f_{py}	Yield Strength of Core

σ_a	Allowable Normal Stress
F_s	Shear Yield Strength of Steel
f_y	Yield Strength of Steel Plate
IS	Indian Standards
GL	Ground Level

CHAPTER – I

INTRODUCTION



1.1 Preamble

In the present chapter, the study area's history is covered. This is followed by the justification for selecting the current research question and the thesis' organizational structure.

1.2 General Overview

Designing a stiff and robust structure that can withstand expected lateral stresses and can withstand earthquakes using conventional "brute force" methods. This approach might not be the most economical one. This method has the drawback that all lateral forces generated by the seismic ground motion must be absorbed by the building. The aforementioned issue can be prevented using the base isolation system.

The base isolation technique seemed to be created in an effort to lessen earthquakes' influence on structures when seismic strikes, also, it's been demonstrably among the most successful techniques in recent years. Installing the support devices that isolate the building from ground tremors brought caused by earthquakes constitutes base isolation. The input forcing feature is enabled by base isolation to be filtered and the structure to be protected against acceleration-induced seismic forces. Ground movement occurs during earthquakes while the structure barely moves if it is separated from the ground. Whereas this technique had first been developed in the 1900s, it wasn't until the 1970s that it became a useful method for seismic design.

The Base isolation's main goal is to significantly diminish the structure's ability to absorb the pressures and energy caused by an earthquake. To do this, a framework is placed on a lateral stiffness-low support mechanism, which causes only mild motion in the structure itself when an earthquake occurs and causes considerable motion in the ground. Movement of the framework as the support bearings' flexibility increases, challenges with how they relate to the ground when subjected to wind loads may arise.

According to research by Skinner and McVerry (1975), a base isolator with hysteric force-displacement qualities can withstand wind-induced horizontal stresses while still providing the essential high dumping, force limitation, and flexibility under

earthquake stresses (Skinner & McVerry, 1975).

A basis for using a two-degree-of-freedom linear dynamic system was introduced by Connor in 2002 to analyze the reaction of the base isolation Mechanism. By shifting the system's actual fundamental frequency out of the region at which a quake would produce the most powerful inertia forces, base isolation reduces seismic reactivity. Increased support bearing flexibility (or a decrease in their stiffness) lengthens the system's corresponding natural period. Period is raised over the range of the surface trembling brought by earthquakes, preventing resonance & lowering seismographic acceleration response (Connor, 2002).

The performance of a base isolation system in a framework is based on specifications of bearing mechanisms that isolate the framework from surface vibrations. The lateral inertia forces brought on by earthquakes on a structure are reduced by a building's prolonged effective period and the base isolated structure's isolation from the support mechanisms' low rigidity. Understanding how the parameters of the framework's support systems affect the seismic performance of isolated structures is therefore critical. A number of base isolation devices, such as friction devices (PTFE sliding bearings), yielding steel devices, laminated elastomeric rubber bearings, lead rubber bearings, and lead extrusion devices, have been developed to achieve this goal.

In contrast to unisolated structures, base isolation systems, according to Andriono [1990], greatly lower the superstructure's lateral stiffness and ductility requirements. Due to the reduction of materials used for lateral systems and the simplicity of structural detailing, cost savings are made possible. Additionally, base isolation gives the designer access to a larger selection of architectural forms and structural materials (Andriono, 1990).

In addition to the technical feasibility, the early stages of design should focus on the economic feasibility. Construction expenses, earthquake insurance premiums, earthquake damage costs, maintenance costs, market share loss, and potential responsibility are the primary considerations (Charng, 1998).

According to Skinner and McVerry [1975], the cost of creating buildings with the required level of seismic resistance may frequently be greatly diminished as a result of the current base isolation procedures (Skinner & McVerry, 1975).

Base isolation is a seismic safety technology that has gained popularity over the last few decades for both buildings and the stuff inside of them. Base isolation is a method for seismic retrofitting old buildings, designing buildings with moving parts, high-risk structure, and structure with special significance after quakes, among other things.

Base isolation has advantages over traditional methods in the aforementioned situations because it offers far higher protection from extreme seismic events. It is thought that base isolations systems can solve a variety of design problems.

1.3 Motion Caused by Earthquakes

It is vital to determine the applied forces in order to comprehend how buildings move. This section will go over the main, underlying problems with earthquakes.

1.3.1 Features of Earthquakes

The following are the primary aspects of earthquake ground motion that an engineer must comprehend:

- period
- amplitude of displacement
- amplitude of velocity
- increase in acceleration
- range of ground motion frequency

Additionally, structures possess a set of inherent frequencies respond to that which determine them. Its fundamental recurrence is the lowest. The basic recurrence resonance arises as the produced earthquake recurrence gets closer to it. A designer must make sure that the frequency response of the building is higher than the seismic frequency range. An approximation of the relationship between a building's n floors and the basic period T is provided by a general theory that is very helpful in the early design.

$$T = \frac{n}{10} \quad (1.1)$$

With six floors and a story elevation of 15 feet, a building that is 90 feet tall would have a period of roughly 0.6 sec.

1.3.2 Concept of Resonance

As previously indicated, Engineers are required to create structures that their response to ground motion occurs at frequencies that are distinct from those of earthquakes. Resonance happens when the response frequency of the building is similar to or nearly equal to the frequency of surface motion. The horizontal resonance pressures on a structure are amplified when resonance increases the building reaction, which can have catastrophic effects. A well-known illustration of this is the Tacoma Narrows Bridge, instance of a catastrophic failure brought on by resonance. Instead of ground motion, the Tacoma Narrows Bridge collapsed due to oscillating in response to wind vorticity, who's frequency matched one of the torsion modes of tremors within the structure about the orientation along the long axis of the deck. Although reverberations caused by wind is outside the study's parameters, a wonderful example of the disastrous collapse caused by resonance is the Tacoma Narrows Bridge.



Figure-1. Resonance-Induced Severe Deformation and Eventual Collapse of the Tacoma Narrows Bridge.

1.3.3 RS - Response Spectrum

The spectrum of response of the structure to ground movement for different frequencies are readily shown by a RS. A graph of RS structure, which displays the high response rates of velocity against the duration of excitation, is a standard way to see the spectrum (inverse of frequency). The fundamental mode frequency of a building is first determined by engineers, who then use the aforementioned graph to calculate the acceleration that an earthquake will have on a building. The inter-story drift of a structure determines the degree of structural damage it will sustain. Therefore, when examining the way a structure responds to tremors, it's crucial for analyzing the structure to determine its reaction frequencies.

1.4 Structure Reaction

The primary factors influencing building reaction and earthquake damage will be briefly covered in the section that follows. A building may sustain a variety of damages, ranging from modest surface finish cracking to significant cracks inside the primary structural elements, which could lead to total structural damage. Structure-related destruction (damage to structural members brought on by deformations) and non-structural damage are the two categories into which damage is commonly divided. Damage to the structure could result in considerable property damage and death. Although non-structural damage has the potential to result in fatalities, it is largely associated with the injuries and probable infrastructure damage.

1.4.1 Consequences of Surface Acceleration

Understanding how a structure is harmed by ground acceleration requires applying the Second Law of Motion, that states that the force exerted against an object equals the the body's mass times its acceleration. As a result, the forces acting on a building rise together with acceleration. Therefore, an engineer must lessen the building's acceleration in order to lower forces on the structure. The inertia force is defined as the sum of mass and acceleration. The structure deforms as a result of the inertia

force brought on by ground motion. Beams, columns, lateral braces, bearing mills, interconnections and additional internal structures are all affected.

1.4.2 Effects of Stiffness and Ductility

Height, materials, connections, lateral systems, and other factors all affect stiffness. The lateral forces that the structure experiences as a result of ground motion are significantly influenced by stiffness. Accelerations equal to those of the ground will be experienced by an endlessly stiff edifice. Therefore, the more rigid the framework, the greater the lateral inertia forces that result from ground motion on the framework. System for base isolation successfully lowers the system's similar rigidity, which lowers the inertia forces acting on the structure.

The most critical element determining a building's seismic performance in traditional seismic design is its ductility. A building's ductility must be sufficient to survive any earthquakes it may suffer over the course of its lifetime. The primary duty of an engineer building a quakes structure is to do this.

1.4.3 Damping's impacts

Damping is characterized as the gradual decrease in oscillation amplitude. Every structure has some natural damping. An oscillatory object wouldn't ever come to a halt without dampening. Internal friction in buildings causes damping, which loses input energy. The ability of a building to dissipate earthquake energy depends on its intrinsic damping, which increases with size.

1.5 Thesis Organization

Current Chapter (Introduction) provides a succinct summary of the topic of current research, the impetus for the current study, and an outline of the thesis's organizational structure.

Chapter 2 (Components of Base Isolation System) contains components of the numerous kinds of base isolation system.

Chapter 3 (Literature review of Base Isolation System) contains the review of literature in the field of numerous kinds of base isolation system.

Chapter 4 (Methodology of Research) the chapter contains the scope of present work, objectives defined based on the identification of the gap in existing research, the hypothesis of thesis and overall design methodology.

Chapter 5 (Base Isolation Bearing Design). In this chapter the Base Isolation System: LRB) & TFPB are design according to axial load, biaxial load and Tri-axial load (Cumulative load from fixed base modal).

Chapter 6 (Analysis & Results Summary). In this chapter the result obtained from all the model: Time period, Base Shear, Storey-Drift, Storey-Displacement, Steel reduction and overall cost economy is analyzed and a Results summary is made for comparison along with graph.

Chapter 7 (Conclusions & Recommendation). In this Chapter the entire work of this thesis is concluded & Recommendation based on the conclusion.

The resources consulted for this project have been cited at the respective places of use and listed in the Bibliography chapter.

.

CHAPTER – II

COMPONENTS OF BASE ISOLATION SYSTEM



2.1 Preamble

Chapter 2 provides components of the different types of base isolation systems.

2.2 Parts of Base Isolation Systems

Since seismic isolation system has become more popular over the past few decades, the technology is advanced and there are many different base isolation systems available. Elastometric devices and gliding devices are the two main groups into which the devices could be separated. Above isolation techniques, which both have some inherent dampening, are used to shift the fundamental building frequency outside of the earthquake excitation range, which lowers accelerations and lowers the associated lateral inertia forces. A particular collection of characteristics, such as lateral rigidity, yield strength, maximum deformations under severe seismic loading, residual deformation, and the ability to revert to the original location, etc., define the devices of both groups. The aforementioned specifications for several devices that are currently on the market are outlined in this chapter.

2.3 Elastometric Bearing

Since they are made of elastometric material, elastometric devices live up to their name and are effective. Their resilience is their main benefit. Deformations caused by service load and durability, however, can be a problem. NRB, LRB and HDRB are examples of popular elastometric devices. In this part, the specifics of the aforementioned technologies will be covered.

2.3.1 Natural Rubber Bearing (NRB)

Natural rubber or neoprene is used to make laminated rubber bearings, another name for natural rubber bearings, synthetic rubber used for its strength and durability and for its resemblance to natural rubber in behavior (Ehrlich, Flexner, Carruth, & Hawkins, 1980). Figure 2 depicts natural rubber bearing setup.

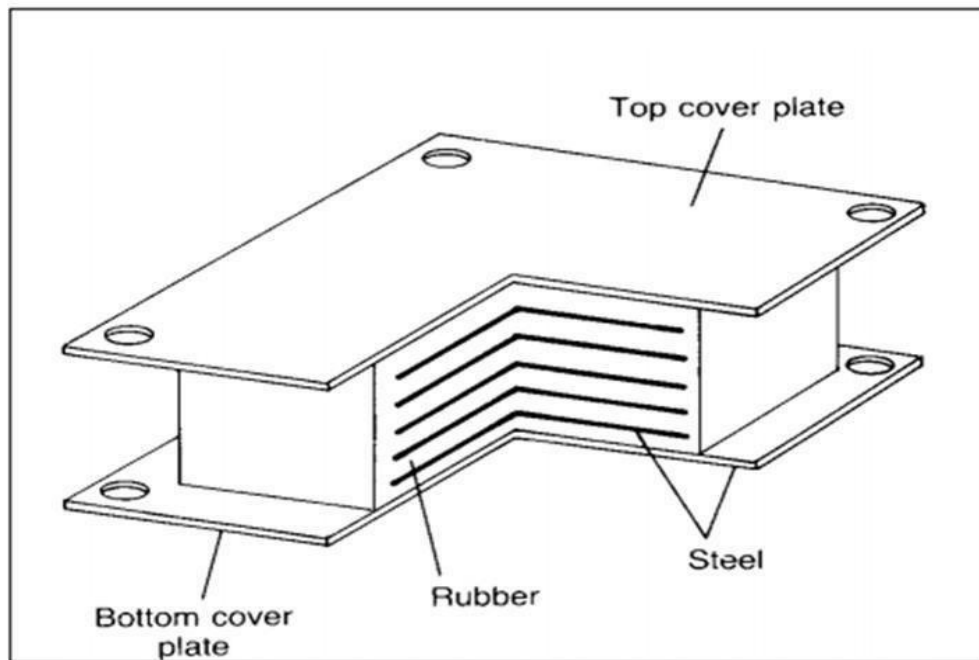


Figure-2. NRB Schematic

Shim layers made of rubber and steel alternate in natural rubber bearings. In order to create a composite bearing, these layers are fused together using the crosslinking process under temperatures and pressure. Shims made of steel stiffen the bearings vertically and stop an isolated structure from wobbling. Shims made of steel also prevent latex prevent blowing up when under severe axial compressive loads. Shims have no impact on the bearings' axial stiffness because this property is governed by the elastic material's shear modulus. The bearings are sandwiched between two sizable endplates to make it easier to attach the foundations and isolator mat.

The main drawbacks of natural rubber bearings are their poor absorption and low stiffness, which make them incapable of withstanding service wind loads. Natural rubber bearings typically have a 2-3% critical damping. In order to cope with service and strong seismic loads, natural rubber bearing support structures typically need further damping mechanisms, including such viscous or hysteretic dampers. However, damping qualities can be improved by altering the elastometric material's characteristics.

NRB, however, are easy to install and produce. Additionally, it is simple to understand, analyze, and consequently design their behavior. Neoprene and Natural rubber are recognized to keep a stable shear modulus during age, hence the impacts of creep and

stiffness degradation over time are minimal. (Naeim & Kelly, 1999).

2.3.2 Lead Rubber Bearing (LRB)

LRB are far better able to provide enough rigidity for wind loads and superior damping properties than NRB. Apart from the presence of any number of cylindrical metals inserts in centre, as seen in Figures 3, the LRB arrangement is same as of natural rubber bearings. Whenever the lead plug and rubber are being used together, the device behaves bilinearly. When there are lower delivery wind loads, high rigidity of the lead plug, which draws the majority of the load, and arrangement is very stiff. At very strong seismic stresses, lead deforms plastically, lowering the device's stiffness to just that of rubber. The lead plug's plastic deformation results in a hysteretic loss of energy as well. During intense events, the lead plug changes shape similarly to rubber, but rather produces heat or discharges by transforming kinematic energy into heat. Therefore, the plug's hysteretic nature aids in minimizing the amount of energy which the structure has collected. As a result, LRB possess desirable hysteretic damping qualities, which improves the system's structural response. Amount of energy lost depends on the maximum bearing displacement. LRB are indeed easily installed, produce, interpret, and create. (Naeim & Kelly, 1999).

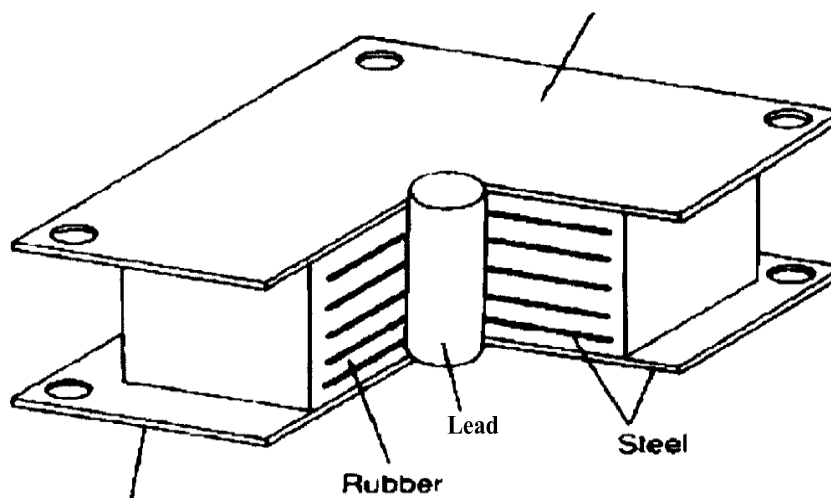


Figure-3. LRB Schematic

2.3.3 High Damping Rubber Bearing (HDRB)

HDRB replace existing damping mechanisms. Their composition is similar to that of NRB, with the exception of the elastometric material used. A greater amount of damping is possible with the use of additives such as carbon, lubricants, and resins. By using fillers, the damping was enhanced to 20–30 percent of the critical damping.

HDRB have strong hardness and high yielding at shear strains under 20%. For controlling deformations during service wind loads, this behavior is helpful. With stresses larger than 120%, stiffness and absorption both increase. As a result, when subjected to significant earthquake loads, this behaviour efficiently absorbs energy, limits deformations, and provides sufficient rigidity for service wind forces. HDRB have the same benefits as the aforementioned devices in terms of with ease production & use. (Naeim & Kelly, 1999).

2.4 Moving Mechanisms

The ability of moving mechanism to remove effect of torsion in irregular constructions is their main benefit. This is as a result of the fact that the axial force exerted on a sliding mechanism by mass is proportionate to the frictional force used in sliding devices. As a result, torsional effects in asymmetric buildings are eliminated since the centre of rigidity of the isolation system and the centre of gravity of the building coincide (Kunde & Jangid, 2003) and (Trombetti, Ceccoli, & Silvestri, 2001). Pure friction devices, robust friction-based devices, and friction pendulums are some of the frequently used sliding base isolation devices. The following section will go over the specifics of the aforementioned devices. They can also be employed for a variety of constructions because of their susceptibility to seismic excitation frequency content.

2.4.1 Natural Friction Bearing

The first kind of sliding mechanism are natural friction bearings. They effectively stand in for a sliding joint that separates the ground from superstructure. Because the load is insufficient to overcome the friction force at rest, the framework behaves like a fixed base building when subjected to service wind loads. High seismic stresses cause static friction to disappear, and the bearing moves. Effort is lost in the bearings through

Coulomb damping caused by friction. The axial force and the friction coefficient determine the lateral force necessary to remove static resistance. By choosing the right resources for the bearings' sliding surfaces, the friction factor can be managed. Two significant limitations are the need for routine servicing to maintain a steady friction factor as the bearings ages and the challenge of getting the building to center on its own following a quake (Kunde & Jangid, 2003).

2.4.2 Cable Friction Bearing

Figure 4 depicts the basic layout of cable friction bearings. A typical sliding bearing, strong tension cables, and, if required, a fracture fastened in the centre make up the apparatus. Restrainer cables prevent excessive superstructure displacement during severe earthquake events. It's not intended to break, the shear bolt during light and moderate earthquakes, preventing the need to replace the bearing. The shear bolt snaps under intense earthquake pressures, causing sliding to become active. As a result, there is a reduction in the transfer of seismic forces to the superstructure. Friction between the teflon and stainless steel plates dissipates energy while cables prevent excessive relative displacements (Wancheng, Binbin, Pakchiu, Xinjian, & Zhaojun, 2012).

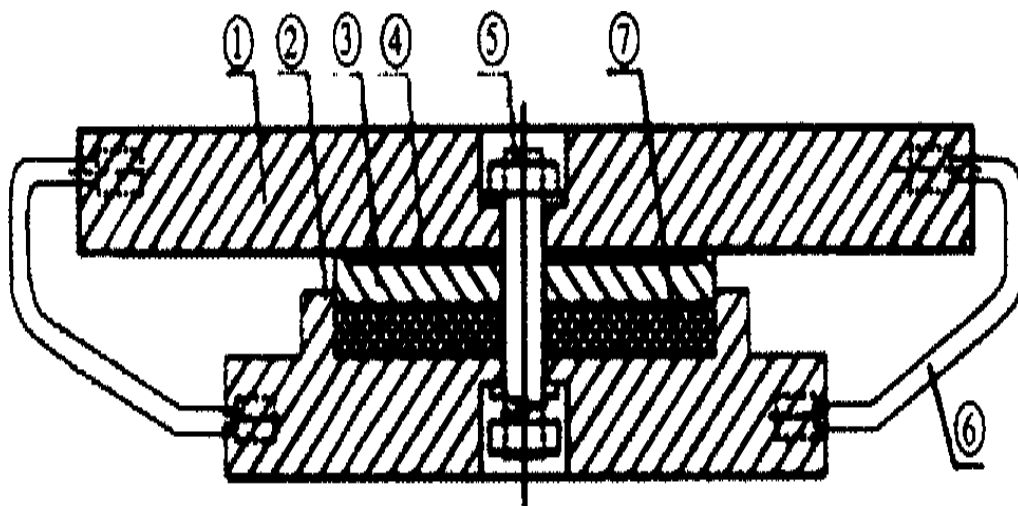


Figure-4. Cable Friction Bearing Schematic

2.4.3 Resilient Friction Base Isolators

Figure 5 shows numerous flat metal plates make up the durable friction-base isolators with a center or outer rubber cores that can glide past one another. The rings are covered in an extremely flexible rubber band that shields them from dust and rust. Teflon is applied to the sliding plates to lessen friction. The rubber cores aid in distributing the horizontal deformation and pace uniformly along the isolator's height. Identification of resilient friction-base isolators is based on the sliding components' friction coefficient and the rubber cores' overall lateral stiffness. It is possible to sustain service wind loads thanks to the friction that generates between the plates. The principal energy dissipater during seismic stresses is friction damping, as rubber has a limited ability to dampen. Rubber cores are simply inserted and not attached to the sliding rings, creating a sturdy friction-base isolator is a pretty simple process. (Mostaghel & Khodaverdia, 1987).

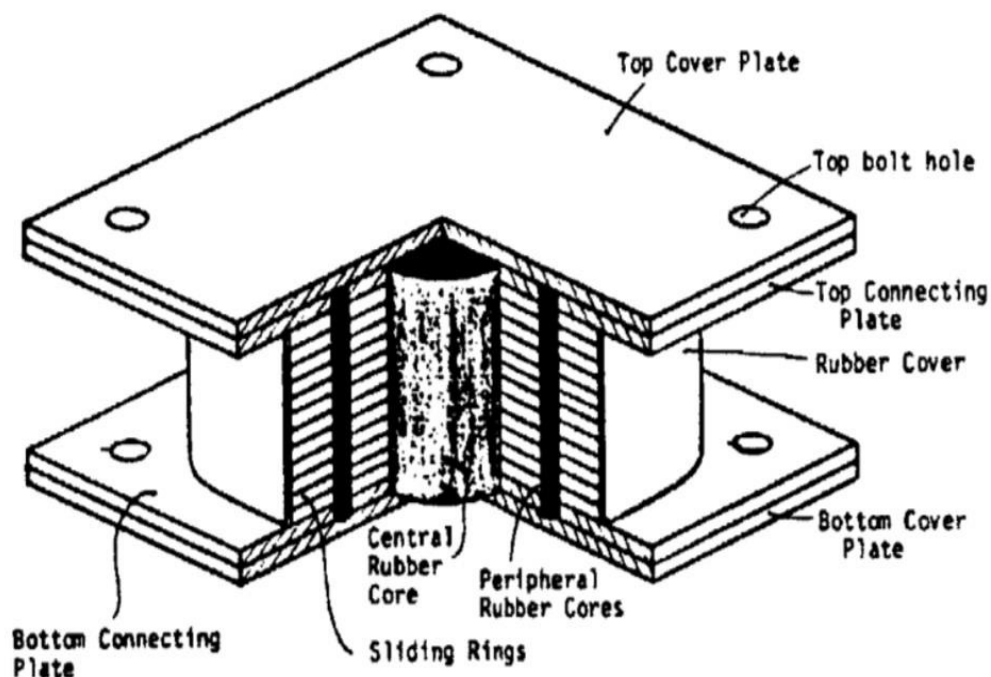


Figure-5. Resilient Friction Base Isolators Schematic

2.4.4 Friction Pendulum Bearing (FPB)

The motions of sliding and pendulum are combined in friction pendulum bearings. A FPB is shown schematically in Figure 6. They consist of a concave spherical mounted on the surface of a chrome surface, which is supported by an articulated slider. The slider is protected by a layer of Teflon or some other coated bearing material. Friction coefficient at high speeds around the two plates is 0.1, & 0.05 at low speeds. Devices using friction pendulums function as fuses and are triggered by quake stresses similarly to conventional sliding bearings that are more than that of the static friction value. These bearings deliver horizontal loads that consist of a mixture of static friction and restoring force by elevating the round surface.

The bearing's restoring force is inversely related to the concave surface's curvature radius and proportionate to the weight the bearing is able to support. As a result of static friction, these bearings do not deflect (display stiffness) when subjected to service wind loads, which is an exceptionally desirable quality. Moreover, Due to transverse force within a given bearing is inversely related to the amount of the structure's burden that it supports, the centre of stiffness of the support system and the structure's centers of mass are inextricably linked, preventing the likelihood of torsional effects. In shake-table experiments, this property has been verified by (Zayas, Low, & Mahin, 1987). FPS also exhibit strong stability and little susceptibility to the frequency content of seismic excitation (Mokha, Constantinou, Reinhorn, & Zayas, 1991).

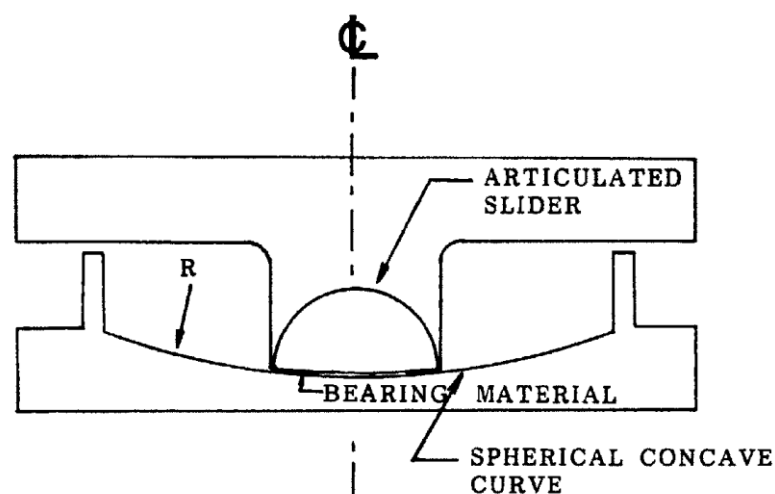


Figure-6. Friction Pendulum Bearing Schematic

2.5 Limiting Devices

Limiting devices may be needed in event of a severe quake to keep the structure from moving. This is crucial for elastometric bearing systems since they are susceptible to instability at large lateral strains. Excessive lateral deflections run the risk of colliding with nearby structures, which could result in serious injuries or even fatalities.

To prevent the bearing systems from deflecting excessively, stiff or flexible devices may be used. However, if a building collides with a limiting device during an earthquake, structural amplitudes could increase and cause localized damage to the structure or support system which happen as a result of impact. Therefore, creating a suitable restricting configuration is a crucial step inside the base isolation design stage.

CHAPTER – III

LITERATURE

REVIEW FOR BASE

ISOLATION SYSTEM



3.1 Preamble

Chapter 3 contains the review of literature in the field of numerous kinds of base isolation system. The literature survey leading to the identification of research gaps and the research objectives along with the thesis hypothesis in brief are described in this chapter.

3.2 Literature Survey

Numerous studies have been conducted on various base isolation system types in order to understand their effects and to determine the best configuration and performance-improving methods. The necessary literature searches were conducted through national and international journals, periodicals, books, conferences, and online sources of recent data.

Regarding a multi-story reinforced concrete structure, Donato Cancellara and Fabio De Angelis [2016] studied the seismic behavior with two different base isolators. The base isolation systems were created in accordance with the EC2 and EC8 seismic codes in Europe. A fundamentally isolated structure is chosen, one that exhibits pronounced plan irregularity. The building chosen has a considerable irregularity in the layout and is a basic standalone structure. The structure's performance exposed to seismic occurrences is evaluated by a comparative analysis. The HDRB and LRB, both of which are simultaneously activated with FS, have been taken into consideration in the analysis (FS). The three-dimensional base isolated structure is subjected to an analysis that is dynamically nonlinear. For the assessment of the structure's seismic response, recorded accelerograms for ground motions in both directions that are consistent with the reference elastic response spectrum were employed. The dissipative capacity of LRB isolators is better than that of HDRB isolators, spanning from 15% to 30% more. The analysis's findings demonstrate the need to limit LRB's higher dissipative capacities because they could result in larger inter-storey drift values because other vibration modes contributed more than the initial one. Despite being predominantly maintained in the elastic zone in the layout, the overstructure, this must be taken into account when analysing the framework. It is recommended to take these factors into account while designing a system so that, by effectively avoiding the downsides, only the advantages

of the LRB's enhanced dissipative qualities are utilized. LRB isolators have very little dependence on the strain history. The LRB isolators' hysteretic cycles are significantly more robust and stable, which is a considerable advantage. When FS are used in parallel with FS isolators, which have low friction coefficient values, it has been possible to assess how much more the isolation system will dissipate. In order to achieve the goal of base isolating the structure effectively when quake, Friction Sliders (FS) positioned in the right location in the design correspond with elastomeric isolators looks to be a workable alternative in multi-story RC buildings. In comparison to other alternative solutions, this one is also distinguished by lower economically price (Cancellara & Angelis, 2016).

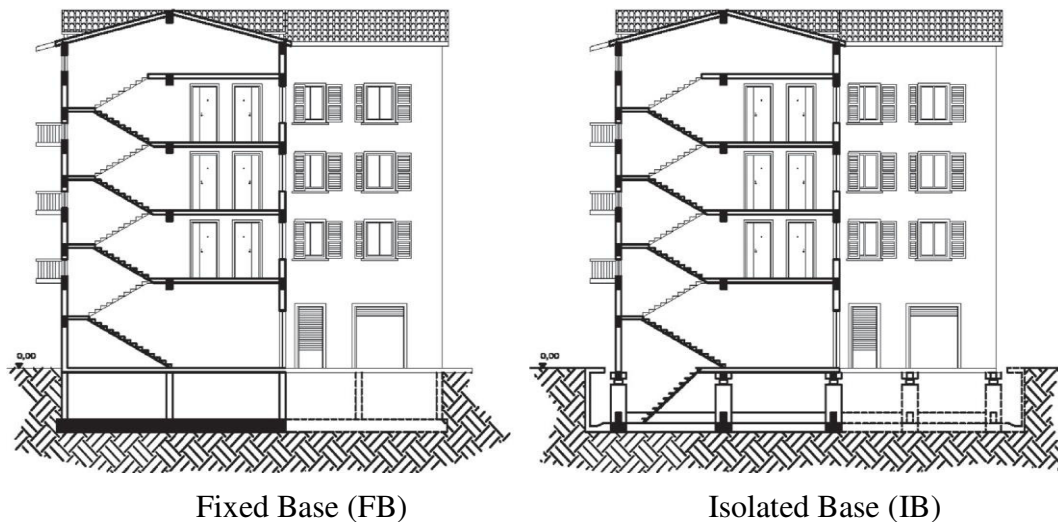


Figure-7. Fixed & Isolated Base Structure Model.

The irregular seismic reactions of typical moment frame buildings upgraded with a number of passive protection devices are discussed in Ahmet Hilmi Dering and Esra Mete Guneyisi's [2020] study. For this purpose, base isolators such as LRB, FPB, and HDRB were taken into consideration. Friction damper (FD) was used as a mechanism for dissipating energy. Comparative research was done on the efficiency of the dampers and isolation systems. One of the study's key conclusions that a single control strategy couldn't always reach a level of performance equivalent to that of a fully functional system, but the base isolation and friction damper systems worked together to successfully achieve this goal within the case study framework. Due to the enormous horizontal stiffness of the friction device, the use of FD successfully reduced the

displacement demand, while base isolation methods, particularly elastomeric bearings, significantly increased horizontal displacement. For instance, FD resulted in a 65.6% reduction in average displacement. The largest average displacement increments, however, were produced by LRB and HDRB, at 67 and 74.5%, respectively. The biggest average base shear reductions were achieved by LRB and FD + LRB, both of which achieved reductions of nearly 84%, significantly higher than the 43.9% achieved by FD when used alone. LRB and HDRB may offer a more effective means of reducing structural vibration than FD and FPB. Extra lead core dissipation capacity and FD braking effect allowed for a clear observation of the dominance of FD + LRB on the nonlinear response (Deringol & Gunyesi, 2020).

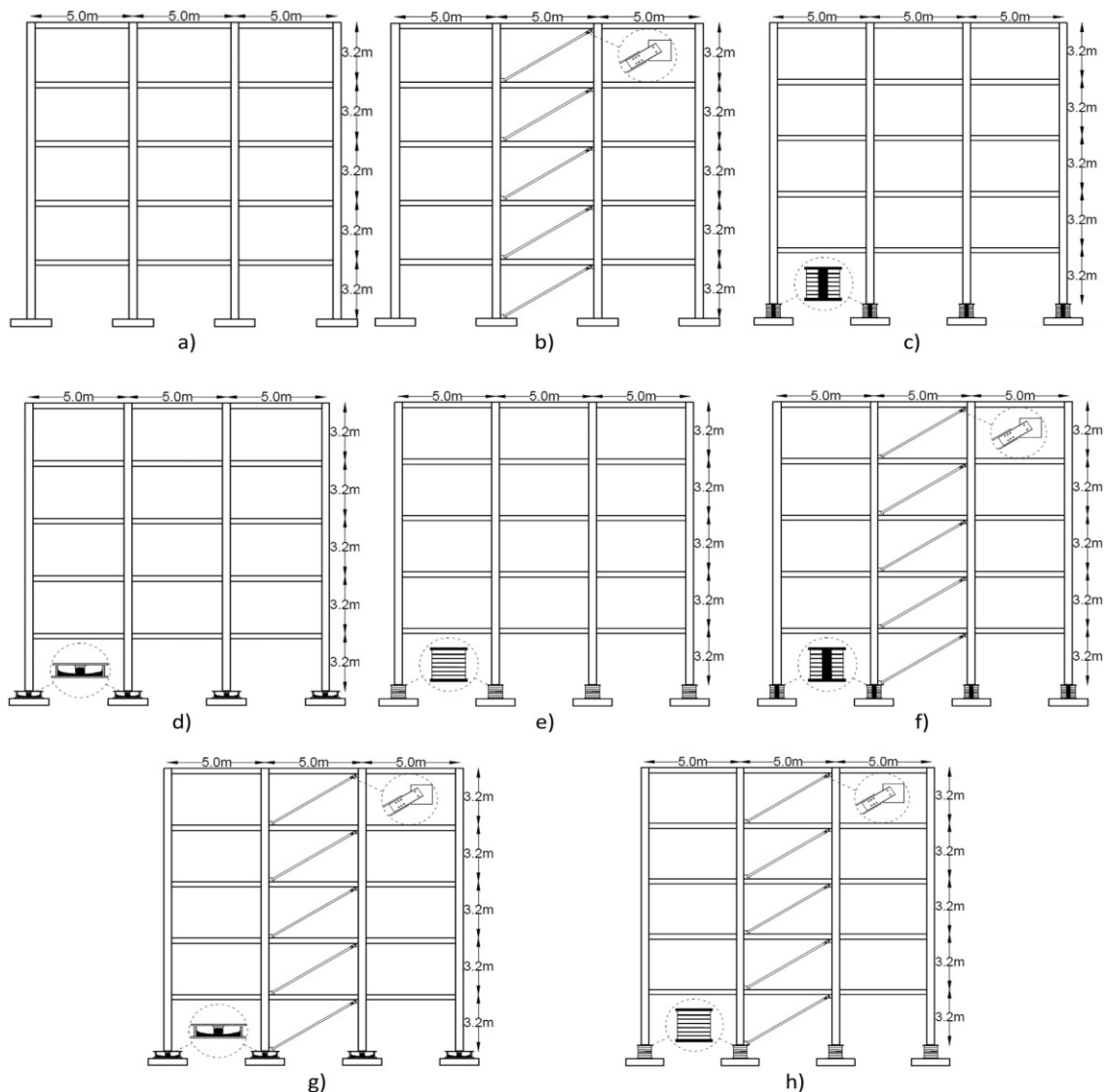


Figure-8. Elevation Views and Bare-Frame Case Study (Deringol & Gunyesi, 2020).

SAP 2000 software was used to analyse Nitya M and Arathi S's [2016] plus-shaped G+6 storey with friction isolation and rubber isolation. With and without base isolation conditions, nonlinear seismic Time History data are used for the analysis. On the earthquakes in EL Centro, 1940, It has been done to analyze time history. Therefore, the effectiveness of RC buildings in dynamic conditions is examined in this work with base isolation, and the results are compared with those of buildings without base isolation. Base isolation, it has been found, lengthens the building's lifespan and correspondingly reduces base shear. The base isolation significantly lengthens the building's lifespan and, as a result, minimizes the base shear. Up to 75% less base shear than a fixed one exists. The lengthening of the time for structures with isolated bases ensures that the structure is entirely excluded from the earthquake's resonance range. Analysis reveals that for the isolated structure, the basic period is about doubled. The maximum acceleration and, consequently, the earthquake-induced stresses on the structure are reduced as the fundamental cycle increases. It is evident from the graph & tables that the storey displacements are significantly longer for isolated buildings and that they are nearly identical for all storeys. In comparison to a friction isolator, the rubber isolator has a larger displacement (Nitya & Arathi , 2016).

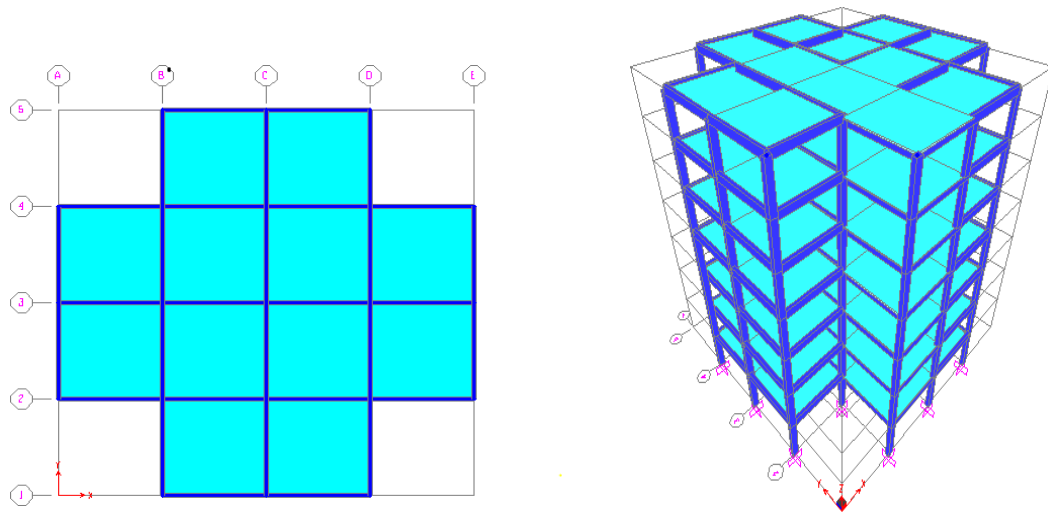


Figure-9. Plan & Elevation G+6 Storey Model

Tessy Thomas and Dr. Alice Mathai [2016] conducted research utilising the ANSYS 14.5 software's finite element base isolator model. Analysis was also done on the friction pendulum's behaviour as a base isolator. For various storey load levels, the base

isolator's nonlinear static analysis is conducted. Conclusion: Stress intensity value increases along with the load value of number of storey. The stress intensity value up to 30 stories is within acceptable bounds, hence a base isolator can be constructed for a building with 22 to 30 stories. This investigation clearly shows that the slider's movement generates an introduce uncertainty force that functions as the necessary damping to absorb the energy of the earthquake (Thomas & Mathai , 2016).

Using SAP 2000 software, M. Vijayakumar, Mr. S. Manivel, and Mr. A. Arokiaprakash [2016] assess a G+25 storey building square in plan. Buildings using the base isolation technique perform substantially better than those with fixed bases. Analysis has been done on the parameters, including displacement and drift. Therefore, it can be shown that base isolation has a bigger displacement than fixed base. The building's story drift is the key regulating factor. The study demonstrates that base isolation significantly reduces drift. Despite the fact that base isolation is more expensive to instal, its effectiveness shows that it is necessary in hospitals, public spaces, and important structures. It was discovered that the usage of base isolation in seismically active areas improved the performance of various bracing systems (Vijaykumar, Manivel, & Arokiaprakash, 2016).

Mital Desai and Prof. Roshni John [2015] Utilizing the Response Spectrum Method, an eight-story skyscraper has been examined. Software called STAAD Pro has been used for dynamic analysis. Variables that are compared between isolated and non-isolated buildings. Comparing the base isolated building to the fixed base building, frequency has decreased. In seismic analysis, fundamental mode is much more effective. In fundamental mode, frequency is lowest in the LRB structure compared to HDRB and LDRB. When isolators are present, acceleration is decreased. In comparison to the other two types of isolators, LRB construction provides the least acceleration. When a base is isolated, the base shear is significantly reduced. When a structure is LRB isolated as opposed to a fixed base framework, the base shear is reduced by 47%. When the structure is separated with HDRB and LDRB as opposed to the fixed base structure, the variation in base shear is 33% and 34%, respectively. Compared to the non-isolated structure, displacement has increased in each of the three isolators. In comparison to

HDRB and LDRB, Lead Rubber Bearing has the highest average displacement. Due to the isolator's presence, storey drift has significantly decreased. In comparison to a non-isolated building, HDRB, LDRB, and LRB constructions all experienced a reduction in storey drift at a height of 9 metres of 13%, 13%, and 15%, respectively. We can draw the conclusion that isolated buildings perform better than non-isolated ones. In comparison to high- and low-damping rubber bearings, lead rubber bearings perform better (Desai & John, 2015).

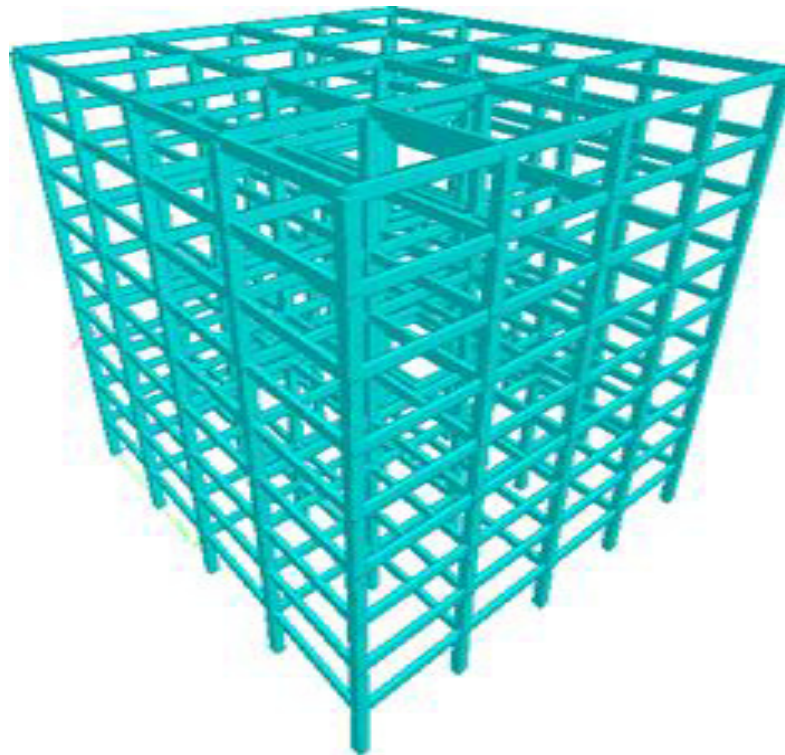


Figure-10. 3D Model of 8-Storey Office Building

A G+9 storey square building was examined using SAP 2000 software by Naveen K, Dr. H.R. Prabhakara, and Dr. H. Eramma [2015]. According to the results of the time history study for the El Centro earthquake, top storey lateral displacement is reduced by 35% for ten-storey regular buildings and by 36% for ten-storey mass irregular buildings. A building's mass irregularity creates torsion, as may be demonstrated by examining the outcomes in both horizontal displacements X and Y axes. It has been discovered that base separated buildings do not have inter-storey drifts. This indicates that when base isolators are used, the structure moves rigidly. Inter-storey drifts for mass irregular buildings are bigger than for regular buildings (Naveen, Prabhakara, &

Eramma, 2015).

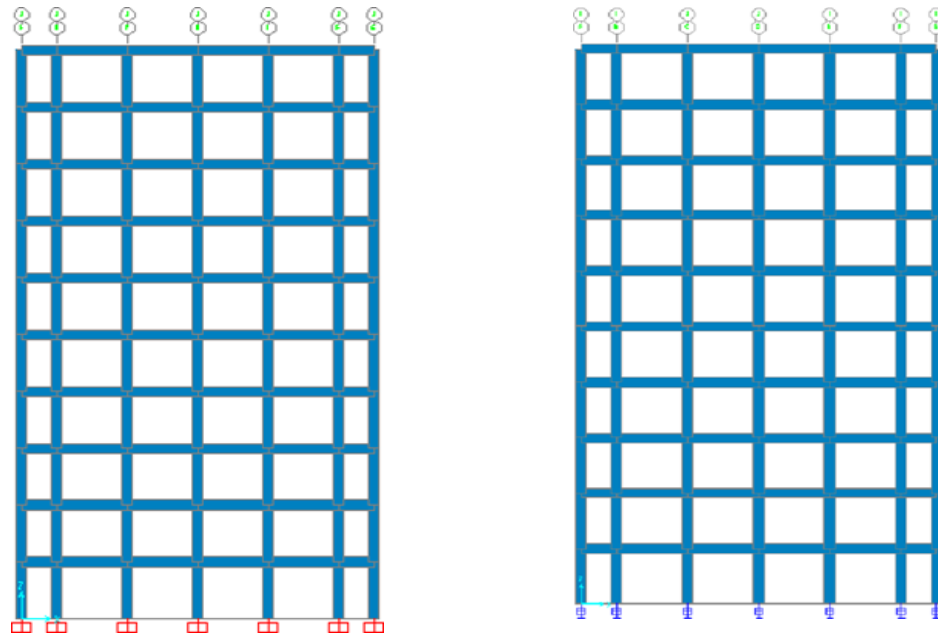


Figure-11. Buildings Elevation with and without Base Isolators.

Meena Noorzai, M.N. Bajad and Neha Dodal [2015] The seismic impact of a G+25 story frame building is compared with a fixed base building vs an isolated building. The G+25 story RCC frame structure is designed with base isolation using the ETAB programme. LRB is utilized as an isolator, and the report demonstrates that the values for lateral loads are significantly reduced when using lead rubber. Base-isolated structures have lower lateral deflection and lower moment values than fixed base structures because the lateral displacement at the base never equals zero. The base separation separates the structure from the load caused by earthquakes while maintaining a longer fundamental lateral period than a fixed basis. A method known as base isolation shields a structure from the potentially harmful effects of a seismic movement. The ground may be moving during an earthquake, but the structure will remain still if it separates from the ground. The ETABS programme was used to create the G+25 storeys frame structure with base isolation. LRB is used as the isolator since it produces better results for the frame structure over the fixed base structure than any other isolation method (Noorzai, Bajad, & Dodal, 2015).

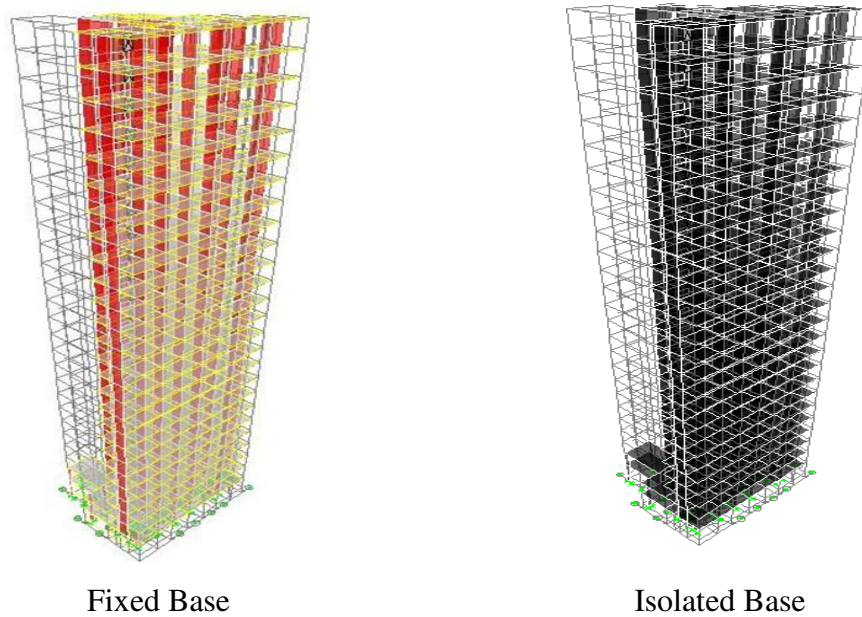


Figure-12. Analytical Model – Fixed & Isolated Base.

G+5 storey building is studied using SAP 2000 software by Prof. R.B. Ghodke and Dr. S.V. Admane [2015] increases with building height, but displacement in base-isolated buildings and displacement in permanent base isolation decreases. Additionally, base isolation results in less displacement as compared to fixed bases (Ghodke & Admane, 2015).

According to Dia Eddin Nassani and Mustafa Wassef Abdul majeed [2015], quake effect on fixed-base and Isolated base structures are evaluated in their study. The SAP 2000 software is used to examine two different G+4 story structures, the first of which is a regular structure and the second of which is an irregular structure. Based on their findings, base isolation can be used to lessen the structure's reactivity. The base isolation system increases displacement while decreasing base shear force and story drifts, according to a comparison of the findings of the base-isolated condition and the fixed-base condition (Dia & Mustafa, 2015).

Mazhar Khan and S.V. Bakre [2015] A G+5 steel frame building was used to evaluate how it responded to seismic loading under both standard fixed base conditions and base isolation conditions. The four kinds of isolators listed above were created based on the weight and natural cycle of the superstructure. In SAP2000, the building was modelled.

It was modelled in the same programme using the isolators' design values. The structure was then designated for the four various types of isolated and stationary bases. On the building underneath the permanent base and the several isolator bases, a time history analysis was done. The time history analysis in SAP2000 utilized two alternative time histories that were chosen for use. In comparison to fixed base structures, base isolated structures have a longer time duration. The framework is more adaptable as a result. Because of its flexibility, the structure is less affected by seismic forces as storey displacement rises. This lessens the strong impact of the seismic force's impulse, which would otherwise inflict more damage to fixed base framework. For a fundamentally isolated framework, the relative displacement of the joint has decreased. Thus, it will contribute to minimizing the negative impacts of the seismic force. Base Due to the more flexible material used in base isolators, deformation is larger. Base shear for an independent has significantly decreased (Khan & Bakre, 2015).

S. Keerthana, K. Balamonica, and K. Sathish Kumar [2015] One of the effective methods for designing earthquake-resistant constructions is base isolation. If base isolation is applied, the structure's acceleration time history is regulated, but the structure's displacement is increased. By designing the isolator in a nonlinear form that is simple to implement, the massive displacements seen in the isolated structure may be controlled. There was a 58% decrease in acceleration and an 85% rise in displacement. When the non-linear characteristics of the isolators were taken into account, a further 38% decrease in displacement could be seen (Keerthana, Sathish Kumar, & Balamonica, 2015).

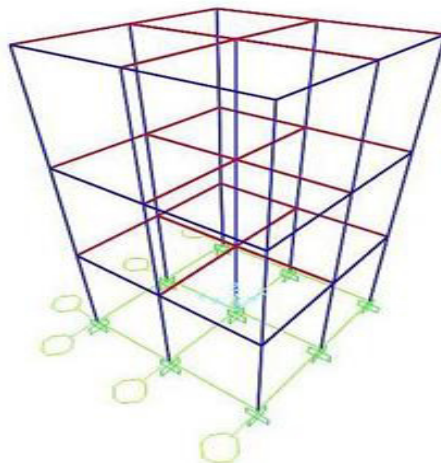


Figure-13. 2-Storey Sample Model

Ganga Warriar A, Balamonica K, Sathish Kumar K and Dhanalakshmi [2015] The installation of isolators modifies acceleration on buildings and displacement. The building's displacement grows as its acceleration decreases. If the isolator is made of a non-linear material, the displacement rise can be decreased. The non-linear isolator additionally adds more damping to the system (Warriar, Balamonica , & Sathish Kumar , 2015).

Anusha R Reddy and Dr. V Ramesh [2015] two structures are taken into consideration: a G+13-story building and a G+5-story building that were both planned and assessed using ETABS. Both structures are given lead rubber isolators, and under zone v and soil type II, assessments of the time history and linear response spectra in both case were conducted. After installing a rubber base isolator, G+13 and G+5 storey structures' mode periods rose by 19% and 47%, respectively. It has been determined that the rubber isolator's flexible nature, which was provided, extended the mode period (Reddy & Ramesh , 2015).

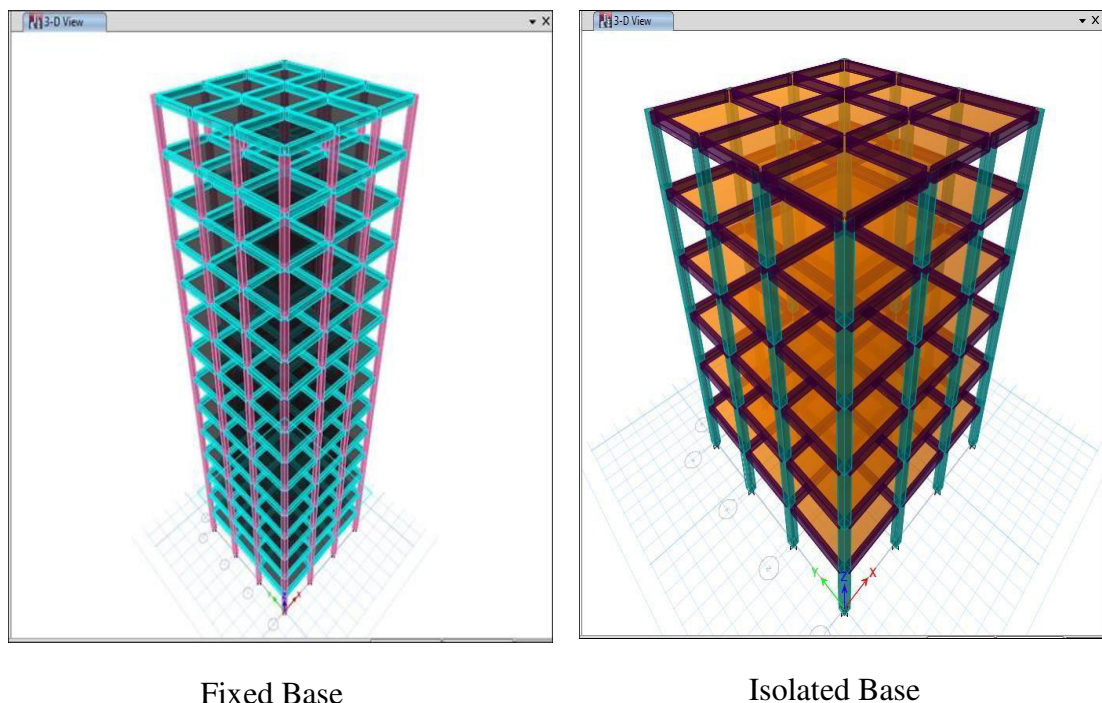


Figure-14. 3D Model of G+ 5 Storeys

Pallavi Wamanrao Taywade and Madhuri Narayan Savale [2015] Seismic base isolation has shown to be a dependable technique for designing earthquake-resistant structures. The efficiency of this approach is greatly influenced by the design of isolation mechanisms and meticulous planning. Extensive study has been done on a variety of isolation device types that have been proposed. They are capable of serving the objective in practically all circumstances. Systems for effective isolation must be flexible enough to respond to different seismic events. In addition, the current devices are pricey, so work is needed to design devices that are affordable in order to make isolation practical for common buildings (Taywade & Savale, 2015).

Khloud El-Bayoumi [2015] Using concrete slab pieces that were 0.2 meter wide and IPE300 column and beam sections, a prototype model of a (25*15) m, 10-story skyscraper was constructed. In earlier iterations of SAP2000, TFPB was typically modelled as a set of friction bearings, seeking to approximate the behaviour of the isolator as closely as possible. However, after utilising the new TFPB feature, it is now clear that new versions of SAP2000 v-16.0 and later are more moderate for the analysis of base-isolated framework since these versions have an actual model of TFP bearing, so we can get results with actual isolator behaviour (El-Bayoumi , 2015).

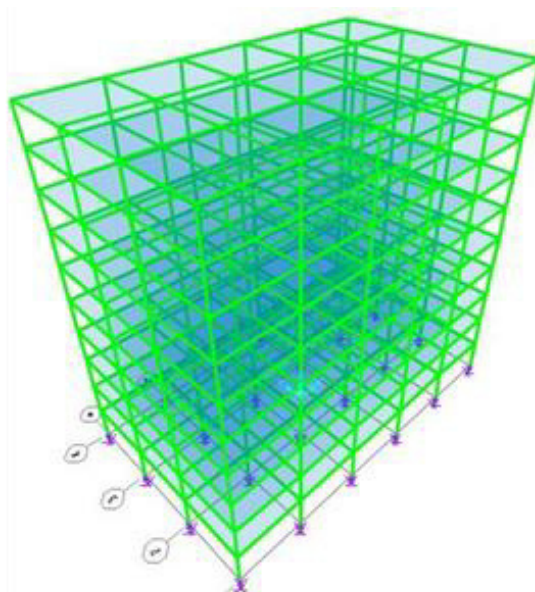


Figure-15. 3D View of G+10 Storey in SAP2000 Model

G. Arya, Alice T.V and Alice Mathai [2015] ANSYS was used to model the HDRB and conduct nonlinear finite element analysis. The largest displacement that the isolator can experience without losing stability is equal to 350% of the rubber layer's thickness. Although the isolator can withstand a 400% shear strain, the bearing may be damaged if the tensile tension is too high. The isolator can be employed for accelerations of about 0.3 g and can tolerate cyclic displacements. The induced stresses were discovered to be within the acceptable range (Arya, Alice, & Mathai, 2015).

Sarah Moretti, Alba Trozzo, Vesna Terzic, Gian Paolo Cimellaro and Stephen Mahin [2014] G+2, the base isolated system dramatically reduces average harm and recovery time in two Oakland, California, buildings: a healthcare institution and a school. The results are decrease significantly that occurs at the building's base when an isolated system is used. The range of the repair cost savings for the hospital occupancy with an average of 85%, and for the school with an average of 76%. This significant decrease in the price of base-isolated system impact restoration is primarily attributable to the prevention of damage to costly structural elements and accessories in addition to the avoidance of damage to non-structural components. Compared to fixed-base buildings, repair times for standalone buildings are 3–6 times shorter. A base-isolated building's resilience will be higher and its downtime will be greatly reduced as a result of the drastic reduction in maintenance time (Moretti, Trozzo, Terzic, Cimellaro, & Mahin , 2014).

Sima Rezaei, Gholamreza Ghodrati Amiri and Pejman Namiranian [2014] To assess the system's seismic response during near-field motions, three alternative TFPB geometry configurations and FS are evaluated. The findings reveal a notable decrease in isolated structure reaction when compared to fixed base structures, but a striking rise in displacement induced at the ground level of isolated structures during near-fault earthquakes. Additionally, the results demonstrate that base displacement will increase with corresponds to period, acceleration, inter-story drifts & base shear will decrease (REZAEI, AMIRI, & NAMIRANIAN, 2014).

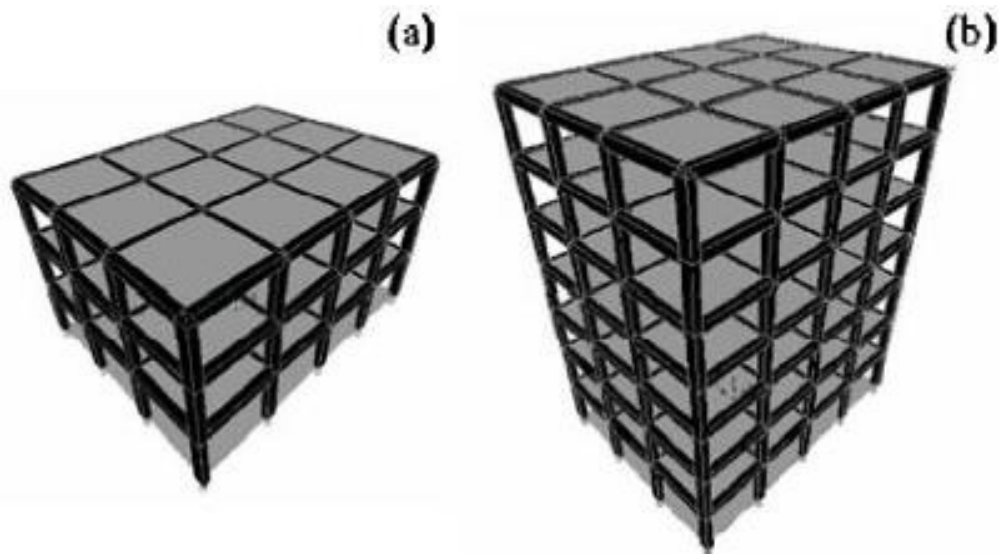


Figure-16. Building A & Building B Model

Prerna Nautiyal, Saurabh Singh and Geeta Batham [2014] The Indian standard offers various expressions for estimating the building structure's natural period while taking or ignoring the stiffness of the infill wall. When masonry infill stiffness is taken into account, the structure becomes more rigid, which decreases the natural period and increases response acceleration and, in turn, seismic forces (base shear and corresponding lateral forces at each storey) (Nautiyal, Singh, & Batham , 2013).

3.3 Observations from Literature Survey

- Base isolation greatly lengthens the building's lifespan and hence lowers base shear.
- Base isolation approach significantly improves a building's performance over fixed base one.
- LRB's performance is superior than that of HDRB and LDRB.
- When compared to other isolation systems, LRB is employed as an isolator because it produces effective results for frame structures over fixed base structures.
- Increases with height of building displacement decreases in base- isolated framework and displacement in fixed base isolation.
- The displacement is increased while the base shear and story drifts are decreased.
- The main factors that contribute to a significant decrease in the cost of base-isolated system damage repairs are the prevention of damage to costly technology and

structural parts as well as the reduction of non-structural component damage.

3.4 Summary

In current chapter, the research gaps are identified by means of the literature survey and the observation are identified from the literature survey.

CHAPTER – IV

METHODOLOGY OF RESEARCH



4.1 Preamble

This chapter contains the scope of present work, objectives defined based on the identification of the gap in existing research, the hypothesis of thesis and overall design methodology.

4.2 Scope of Work

With certain base isolators going back to the early 1900s, base isolation systems for major framework have been around for a very long time. Base isolation bearings are mounted between the framework and the foundation of an isolated construction. While permitting some relative transverse motion between the framework and the ground, the isolation bearings provide strong support in the upward direction. Structure reaction to seismic shaking is decreased by the adaptability of the framework and the ground.

A method called base isolation gives the new structure earthquake resistance. The base isolation system offers a particularly rigid vertical component to the base level of the superstructure in connection to the substructure, which decouples the framework from the horizontal ground motion caused by earthquakes. It modifies the basic lateral period (T_a), through damping dissipates energy, and lessens the amount of horizontal forces that are transmitted to the floor acceleration & inter-story drift. The building's structural framework will fluctuate violently in tune with the earthquake frequency. The framework is less likely to collapse if it is possible to change the framework's natural cycle so that it does not coincide with earthquake frequency. This is precisely the job of a base isolator. The base damper makes the structure less rigid, which brings down the fundamental frequency. In such situation, instead of resonating with the vibrations, the top of the framework will respond to them as a hard unit. In other words, the base isolator bends to lessen the effects of surface motion on the superstructure as the building's base shift with the earth.

The seismic isolation approach is an innovative seismic design technique meant to shield the framework from seismic danger, lessen the energy and pressures it is subjected to, and prevent it from directly resisting such forces. If the foundation is firmly connected to the deck, the entire force of a quake will be delivered promptly and

without any frequency change to the remaining framework. Shear force is applied to the foundation of buildings by earthquakes, which shake the base of structures laterally. The building will fall down if a force of this magnitude has the same frequency as the inherent frequency of the structure. The key idea underlying base isolation is enabling the base to move slightly to the side in order to extend the structure's fundamental time period. Because of the lengthening of the period, the structure will be less vulnerable to seismic pressures and sustain less structural damage. Among the most successful strategies for preventing structural damage from seismic strikes has been the deployment of base isolation techniques, which has grown popular in last two decades. This is due to the fact that the impacts of an earthquake attack are limited by base isolation, the structure is mainly decoupled from ground motion by a flexible base, and structural response accelerations are often lower than ground acceleration. Because of the base's enhanced flexibility, the structure's natural period has expanded enough to move its frequency outside the range of the dominant earthquake frequency. Additionally, the building's ability to dissipate seismic energy and withstand excessive horizontal displacement.

In summary, it is vital to analyze the best base isolation system capable to operate them efficiently and cost effectively in RCC construction industries.

In the current study the objective is to optimize the base isolation bearing by comparing results for Time period, Base shear, Storey-Drift, Storey-Displacement, Percentage steel reduction and cost economy obtained from G+12 & G+22 Storey RC structure with fixed & isolated system base.

4.3 Objectives of the Study

In this work, optimization of base isolation system is performed for objectives given below:

- Study computer-aided software's functionality “ETABS 2016”.
- Preparation of building drawing in AutoCAD.
- Model generation in computer aided software “ETABS 2016”.

- Evaluation and creation of G+12 & G+22 Storey RC structure with fixed & isolated base.
- Design of base isolation bearing.
- Evaluation of results obtained from G+12 & G+22 Storey RC structure with fixed & isolated base for Time period, Base shear, Storey-Drift, Storey-Displacement, Percentage steel reduction and cost economy.

4.4 Hypothesis

In the current study, we shall try to maintain the following:

- Comparison of the time periods between fixed and isolated base structure.
- Comparison of Base shear between structure with fixed & isolated base structure.
- Comparison of Storey-Displacement between structure with fixed & isolated base structure.
- Comparison of Storey-Drift between structure with fixed & isolated base structure.
- Comparison of Percentage steel reduction between structure with fixed & isolated base structure.
- Comparison of cost economy between structure with fixed & isolated base structure.

4.5 Sample Model

This study aims at comparison of structure with fixed base & isolated base for both short and long period of earthquake excitation for Indian subcontinent.

The structure of G+12 & G+22 Storey Reinforced Concrete structure with fixed base & isolated base is considered for study and results carried out is to be differentiate like Time period, Base shear, Storey-Drift, Storey-Displacement, Percentage steel reduction and cost economy.

4.5.1 G+12 Storey Model Details:

Properties

➤ X-direction	=	4000 mm (7-bay)
➤ Y-direction	=	4000 mm (7-bay)
➤ Beam	=	230 x 450 mm
➤ Column	=	450 x 450 mm (Base)
	=	375 x 375 mm (Plinth to Storey-7)
	=	300 x 300 mm (Storey-8 to Terrace)
➤ Ceiling height	=	3000 mm
➤ Plinth level	=	450 mm from G.L.
➤ Foundation depth	=	2100 mm from G.L.
➤ Wall	=	115 mm
➤ Slab depth	=	125 mm

Load

➤ FF	=	1.5 KN/m ²
➤ LL	=	3 KN/m ²

Earthquake Load

➤ EQ Method	=	Response Spectrum IS 1893:2016
➤ Zone	=	3
➤ Soil	=	Hard Soil (Type-I)

- Damping = 5%
- Model Combination Method = SRSS

Material

- Concrete Grade = M20 [20 N/mm^2]
 - Steel Grade = Fe500 [500 N/mm^2]
 - Concrete density = 25 KN/m^3
 - Bricks masonry density = 20 KN/m^3
 - Rebar density = 78.5 KN/m^3
 - Design basis : Limit State
- IS: 456-2000

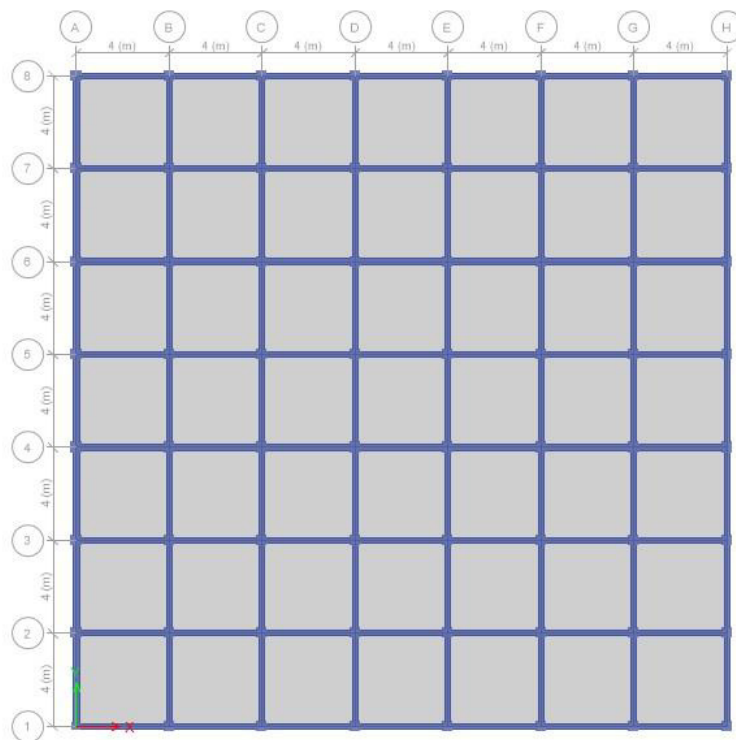


Figure-17. G+12 Storey Sample Model - Plan

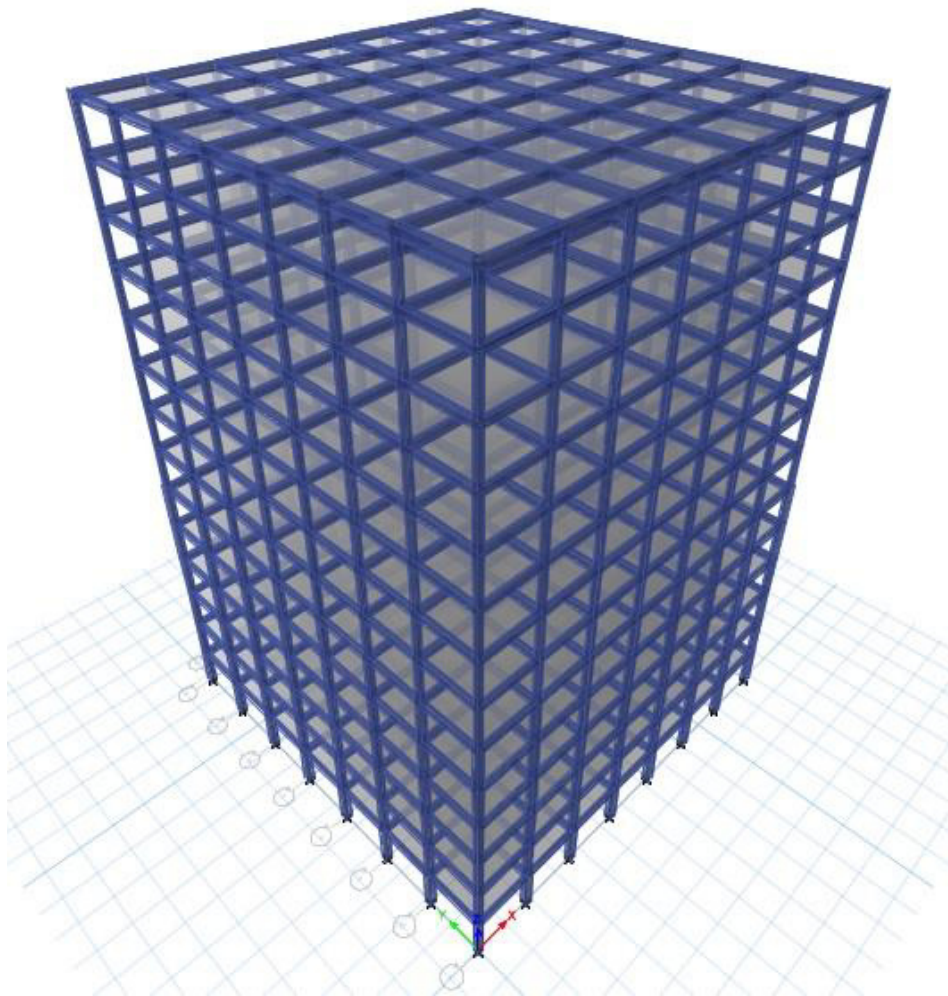


Figure-18. G+12 Storey Sample Model - Elevation

4.5.2 G+22 Storey Model Details:

Properties

➤ X-direction	=	4000 mm (12-bay)
➤ Y-direction	=	4000 mm (12-bay)
➤ Beam	=	230 x 450 mm
➤ Column	=	525 x 525 mm (Base)
	=	450 x 450 mm

		(Plinth to Storey-7)
	=	375 x 375 mm
		(Storey-8 to Storey-16)
	=	300 x 300 mm
		(Storey-16 to Terrace)
➤ Ceiling height	=	3000 mm
➤ Plinth level	=	450 mm from G.L.
➤ Foundation depth	=	2100 mm from G.L.
➤ Wall	=	115 mm
➤ Slab depth	=	125 mm

Load

➤ FF	=	1.5 KN/m ²
➤ LL	=	3 KN/m ²

Earthquake Load

➤ EQ Method	=	Response Spectrum IS 1893:2016
➤ Zone	=	3
➤ Soil	=	Hard Soil (Type-I)
➤ Damping	=	5%
➤ Model Combination Method	=	SRSS

Material

➤ Concrete Grade	=	M20 [20 N/mm ²]
➤ Steel Grade	=	Fe500 [500 N/mm ²]
➤ Concrete density	=	25 KN/m ²

- Bricks masonry density = 20 KN/m²
- Rebar density = 78.5 KN/m³
- Design basis : = Limit State
IS:456-2000

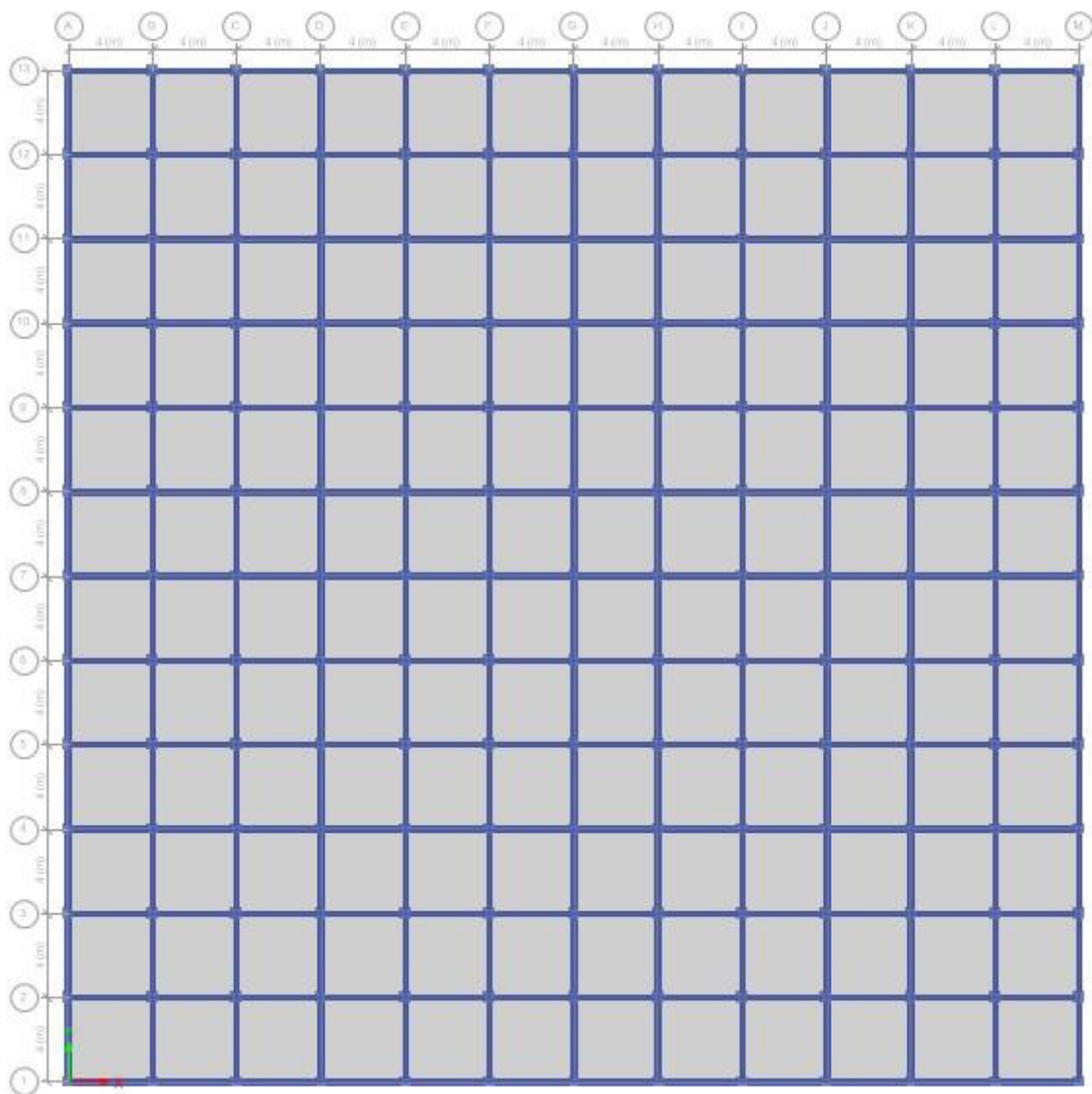


Figure-19. G+22 Storey Sample Model - Plan

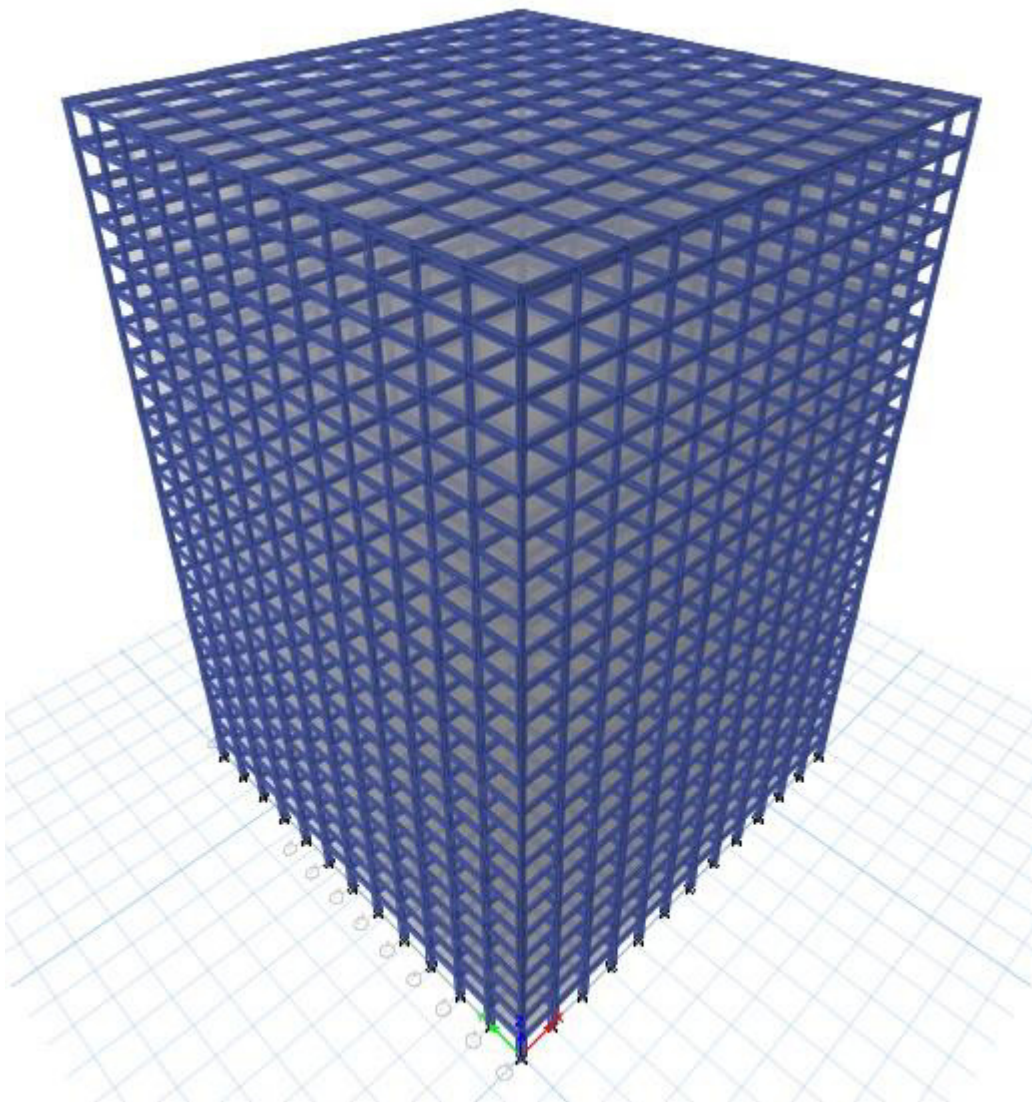


Figure-20. G+22 Storey Sample Model - Elevation

4.6 Sample Model Case

Following cases are considered for analysis and design of structure

4.6.1 Case (a) G+12 Storey Reinforced Concrete (RC) Structure

Case-I: Fixed Base Structure.

Case- II: LRB Base Structure.

Case-III: TFPB Base Structure.

4.6.2 Case (b) G+22 Storey Reinforced Concrete (RC) Structure

Case-IV: Fixed Base Structure.

Case- V: LRB Base Structure.

Case-VI: TFPB Base Structure.

4.7 Important Design Factors

4.7.1 Loads

Throughout its useful life, a building is susceptible to the following loads.

i. Dead Load

The weight of all the walls, wall panels, floors, and roofs, as well as the total weight of the building's different permanent structures, make up the dead loads in a building.

ii. Live Load

Live loads, also known as superimposed loads, are all moving or fluctuating loads brought on by humans or other occupants, including their furniture, temporary storage, machinery, and other items. Every load on floors must be a live load, excluding dead loads. In IS 875: 1987, several live loads acting on the various floors are listed.

iii. Earthquake Load

During a quake, the framework is subject to EQ load. It will affect the structure horizontally. It also goes by the name seismic force.

4.7.2 Analytical Procedures

Plane grid method, Plane frame method, and Space frame method are the three building methodologies that have been utilised to analyse reinforced concrete structures.

The most precise and ideal way of analysis is the space frame method. For human computations, this approach is challenging to use, but it works well for computer-assisted analysis.

The rigidity of pillars is included for analysis in the space frame approach. Beams are created as structural systems with end supports that are fixed. Columns will have axial loads and moments in the directions X and Y included into their design. Additionally, biaxial bending into the footing is required.

4.7.3 Design Philosophies

For the creation of reinforced concrete structures, three design philosophies have been employed namely, the working stress method, the ultimate load approach, and the limit state method. Currently, the IS 456-2000 advises against using the limit state method of design. However, the working stress technique of design has also been kept. Below is a short introduction to the limit state method.

i. Limit State Method (IS 456-2000)

The goal is to achieve an acceptable chance that the structure won't become unusable over its lifetime. Therefore, this approach is founded on the idea that the structure should be able to resist the working load safely throughout its lifetime and also meet the serviceability requirement. The following limit states in the design are looked at:

ii. Limit State of Collapse:

According to the ultimate capacity carrying capacities, it corresponds to failure but does not necessarily entail total collapse. The following limit states are associated with it: flexion, compression, shear, and torsion.

iii. Limit State of Serviceability:

It is consistent with the progression of severe deformation. This condition is equivalent to Deflection on Vibration and Cracking.

4.7.4 Building Component Design

The sections below give a quick overview of explanation of the major framework elements, as well as the analysis and design methodology.

i. Slabs

Depending on the aspect ratio, slabs can be either one-way or two-way. When $(l_y/l_x) > 2$, the aspect ratio. It is intended to be a one-way slab. However, when the aspect ratio is 2, it is created as a two-way slab.

- ❖ One-way slabs are constructed with a beam in mind because they are one metre wide.
- ❖ Based on the border criteria, two-way slabs are further divided into nine categories as stated in IS456:2000.
- ❖ The two-way slabs are constructed using edge strips and central strips, respectively.

ii. Beams

These are the primary flexural members that support the slab. The columns that the beam is supported by transfer the loads to. Beams can have cross-sections that are square, rectangular, or flanged. With regard to the support offered. Beams can be double- or single-reinforced.

iii. Column

They are the vertical skeleton structural elements, and their cross-sectional shapes can be rectangular, square, round, etc. The effective length of the columns and the loads acting on them, which then in turn have an impact on the kind of floor system, the spacing between the columns, the number of stories, etc., determine the dimensions of the section. The column is often designed to withstand axial compression as well as uni- or bi-axial bending moments caused by the frame's movement. Additionally, it is preferable to limit the columns' unsupported length by include the proper tie beams; otherwise, slender columns may have to be created.

iv. Footing

These are the components that are available at ground surface to transfer the column's load to the soil. Flexure, one-way shear, and two-way shear are taken into account when designing the footing. Depending on the soil carrying capacity, a foundation area is provided.

4.8 Design Calculation for R.C.C.**4.8.1 Analysis Method**

There are several ways to analyse a multistory building:

i. Approximate Methods

- ❖ Substitute frame method
- ❖ Portal frame method
- ❖ cantilever frame method

ii. Computer Methods

- ❖ Matrix methods
- ❖ Finite Element methods
- ❖ Finite difference methods

Computer-aided software is the most accurate way out of all those mentioned above. Software like STRUDS 2008, STADD PRO V8i, ETABS, and ANSYS, among others, is available on the market for computer-aided structural analysis and design. The computer aided software "ETABS 2016" analyses the entire project. This software operates in three modes to model, analyse, and design the structure. The ETABS 2016 analytical process is as follows:

a. Modelling

The steps in this technique are as follows:

- ❖ Story and grid system
- ❖ Define & assign material property

- ❖ Define & assign section property
- ❖ Define & assign spring property
- ❖ Define & assign Diaphragms
- ❖ Define Response spectrum functions
- ❖ Define Mass source
- ❖ Define Modal cases
- ❖ Define load pattern
- ❖ Define load cases
- ❖ Define load combination
- ❖ Check warnings

b. Run Analysis

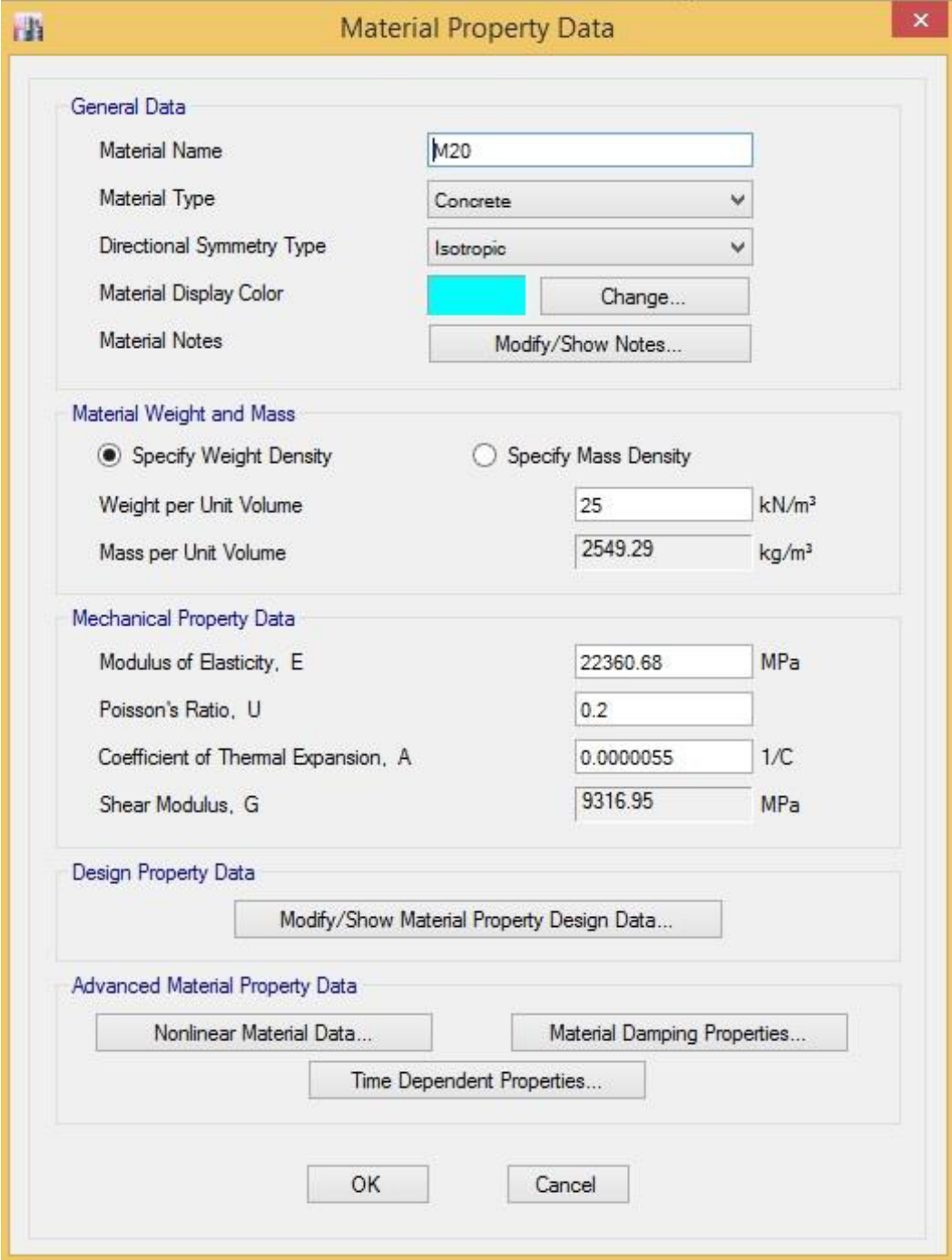
This process consists of the following procedure:

- ❖ Time period
- ❖ Base shear
- ❖ Storey-Displacement
- ❖ Storey-Drift
- ❖ Reactions (Cumulative load)

c. Concrete Frame Design

This process consists of the following procedure:

- ❖ Design parameters preferences
- ❖ Design of section
- ❖ Steel quantity

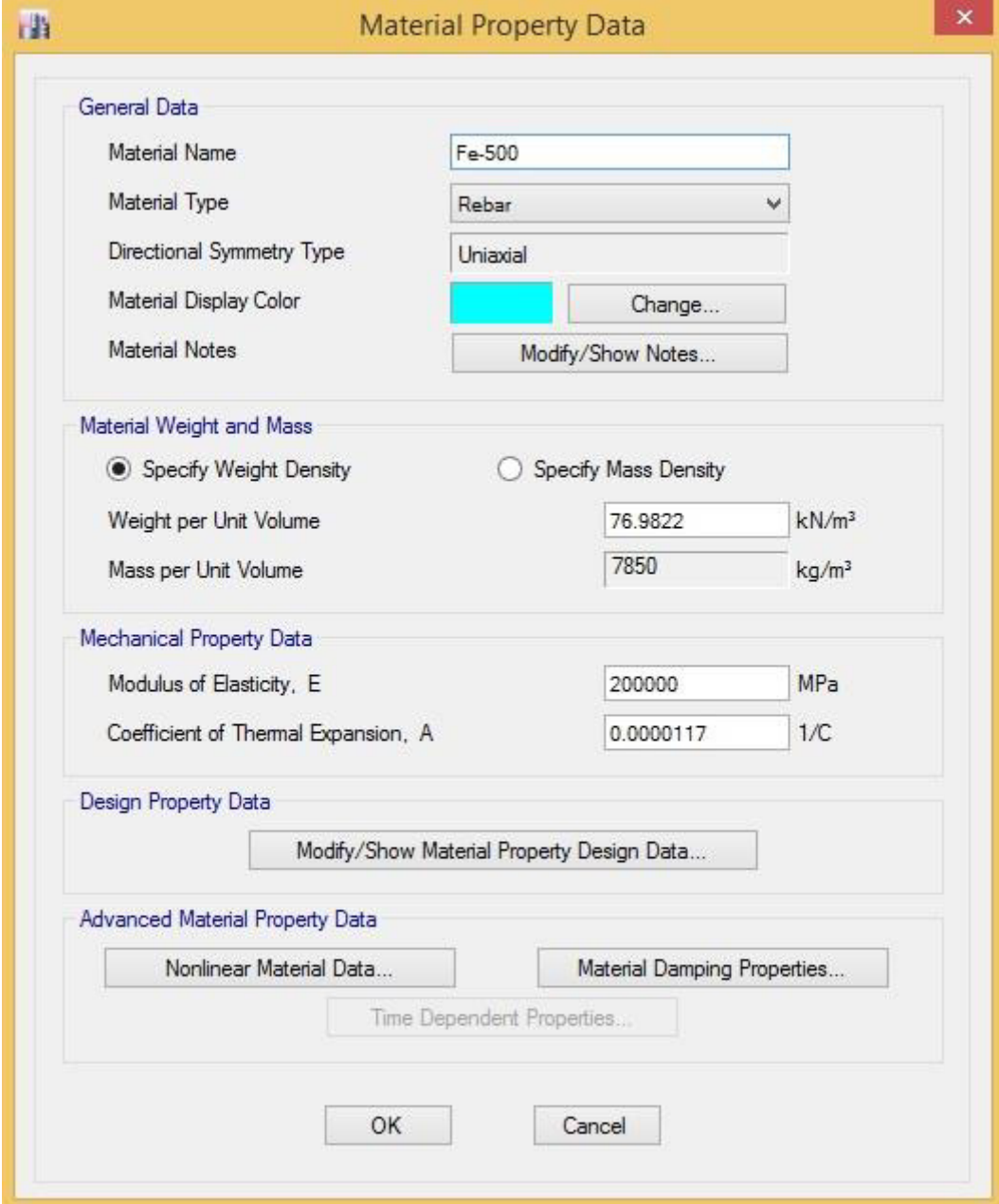


The image shows a software dialog box titled "Material Property Data" with a yellow border and a red close button in the top right corner. The dialog is organized into several sections:

- General Data:** Contains fields for "Material Name" (M20), "Material Type" (Concrete), "Directional Symmetry Type" (Isotropic), "Material Display Color" (a cyan color swatch with a "Change..." button), and "Material Notes" (with a "Modify/Show Notes..." button).
- Material Weight and Mass:** Features two radio buttons: "Specify Weight Density" (selected) and "Specify Mass Density". Below are input fields for "Weight per Unit Volume" (25 kN/m³) and "Mass per Unit Volume" (2549.29 kg/m³).
- Mechanical Property Data:** Includes input fields for "Modulus of Elasticity, E" (22360.68 MPa), "Poisson's Ratio, U" (0.2), "Coefficient of Thermal Expansion, A" (0.0000055 1/C), and "Shear Modulus, G" (9316.95 MPa).
- Design Property Data:** Contains a single button labeled "Modify/Show Material Property Design Data...".
- Advanced Material Property Data:** Contains three buttons: "Nonlinear Material Data...", "Material Damping Properties...", and "Time Dependent Properties...".

At the bottom of the dialog are "OK" and "Cancel" buttons.

Figure-21. Sample Material Property – Concrete M20



The image shows a software dialog box titled "Material Property Data" with a yellow header bar and a red close button. The dialog is organized into several sections with expandable/collapsible headers. The "General Data" section is expanded, showing fields for Material Name (Fe-500), Material Type (Rebar), Directional Symmetry Type (Uniaxial), Material Display Color (a cyan square), and Material Notes. The "Material Weight and Mass" section is also expanded, showing radio buttons for "Specify Weight Density" (selected) and "Specify Mass Density", with input fields for Weight per Unit Volume (76.9822 kN/m³) and Mass per Unit Volume (7850 kg/m³). The "Mechanical Property Data" section is expanded, showing Modulus of Elasticity, E (200000 MPa) and Coefficient of Thermal Expansion, A (0.0000117 1/C). The "Design Property Data" section is collapsed, showing a button to "Modify/Show Material Property Design Data...". The "Advanced Material Property Data" section is collapsed, showing buttons for "Nonlinear Material Data...", "Material Damping Properties...", and "Time Dependent Properties...". At the bottom are "OK" and "Cancel" buttons.

Section	Property	Value	Unit
General Data	Material Name	Fe-500	
	Material Type	Rebar	
	Directional Symmetry Type	Uniaxial	
	Material Display Color	Cyan	
	Material Notes		
Material Weight and Mass	Specify Weight Density	<input checked="" type="radio"/>	
	Specify Mass Density	<input type="radio"/>	
	Weight per Unit Volume	76.9822	kN/m³
	Mass per Unit Volume	7850	kg/m³
Mechanical Property Data	Modulus of Elasticity, E	200000	MPa
	Coefficient of Thermal Expansion, A	0.0000117	1/C
Design Property Data	Modify/Show Material Property Design Data...		
Advanced Material Property Data	Nonlinear Material Data...		
	Material Damping Properties...		
	Time Dependent Properties...		

Figure-22. Sample Material Property – Steel Fe500

Slab Property Data

General Data

Property Name: S - 125mm M20

Slab Material: M20

Notional Size Data: Modify/Show Notional Size...

Modeling Type: Shell-Thin

Modifiers (Currently User Specified): Modify/Show...

Display Color: Change...

Property Notes: Modify/Show...

Property Data

Type: Slab

Thickness: 125 mm

OK Cancel

Figure-23. Sample Section Property – Slab

Frame Section Property Data

General Data

Property Name: B - 9 x 18 M20

Material: M20

Notional Size Data: Modify/Show Notional Size...

Display Color: Change...

Notes: Modify/Show Notes...

Shape

Section Shape: Concrete Rectangular

Section Property Source

Source: User Defined

Section Dimensions

Depth: 450 mm

Width: 230 mm

Property Modifiers

Modify/Show Modifiers...
Currently User Specified

Reinforcement

Modify/Show Rebar...

OK
Cancel

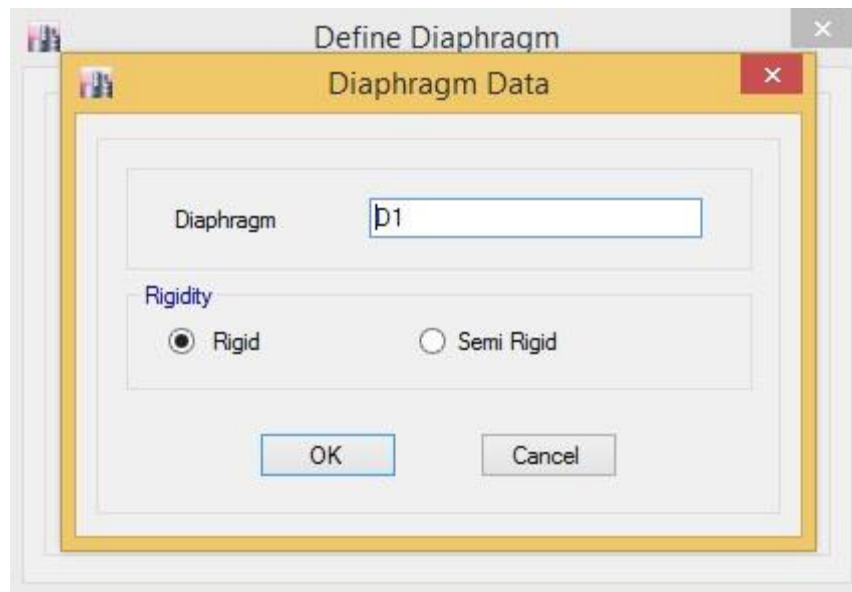
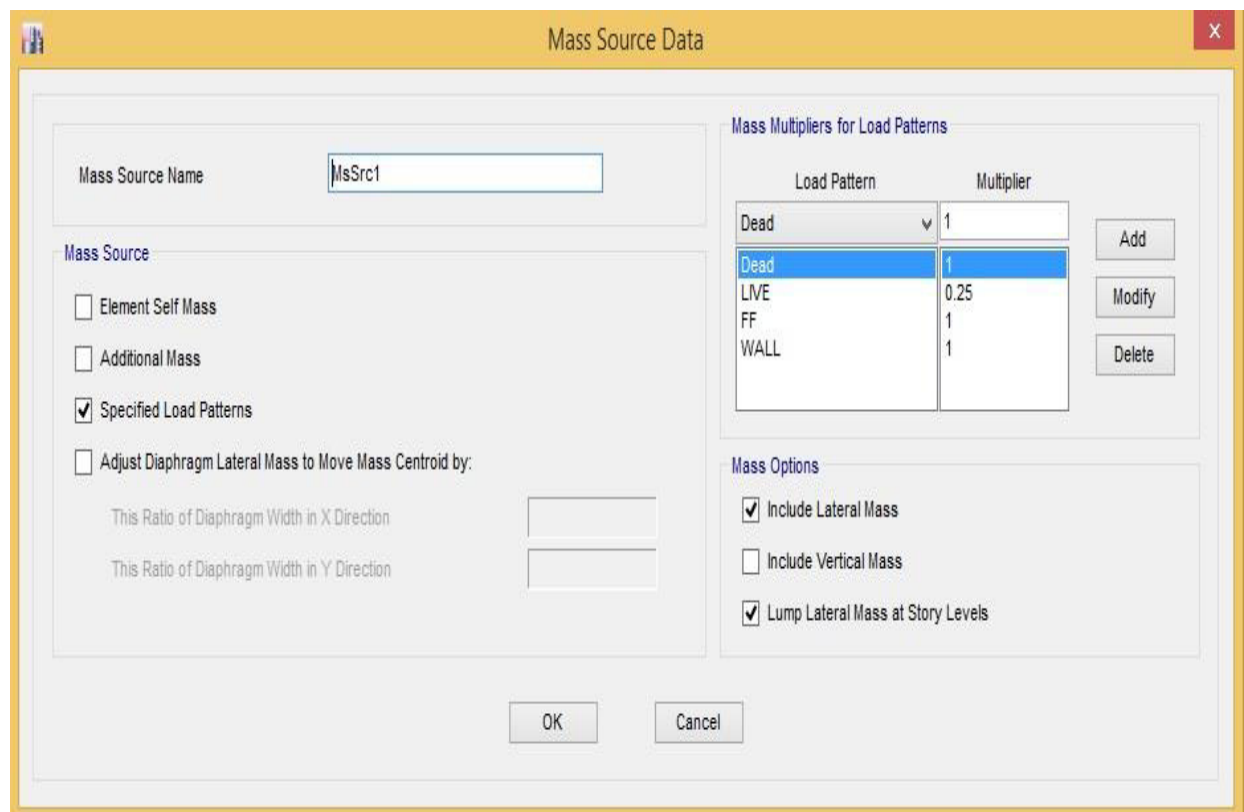
Show Section Properties...

Figure-24. Sample Section Property – Beam

The screenshot shows a software window titled "Frame Section Property Data" with a yellow title bar and a close button (X) in the top right corner. The window contains several sections for configuring a column section:

- General Data:** Includes fields for "Property Name" (C - 18 x 18 M20), "Material" (M20), "Notional Size Data" (Modify/Show Notional Size...), "Display Color" (a blue color swatch with a Change... button), and "Notes" (Modify/Show Notes...).
- Shape:** Includes a "Section Shape" dropdown menu set to "Concrete Rectangular".
- Section Property Source:** Includes a "Source" dropdown menu set to "User Defined".
- Section Dimensions:** Includes input fields for "Depth" (450 mm) and "Width" (450 mm).
- Reinforcement:** Includes a "Modify/Show Rebar..." button.
- Property Modifiers:** Includes a "Modify/Show Modifiers..." button and the text "Currently User Specified".
- Diagram:** A square diagram on the right shows the reinforcement layout with 18 bars (9 top, 9 bottom) and a blue crosshair indicating the section dimensions.
- Buttons:** At the bottom right are "OK" and "Cancel" buttons. At the bottom center is a "Show Section Properties..." button.

Figure-25. Sample Section Property – Column

**Figure-26. Sample Diaphragm Data****Figure-27. Sample Mass Source Data**

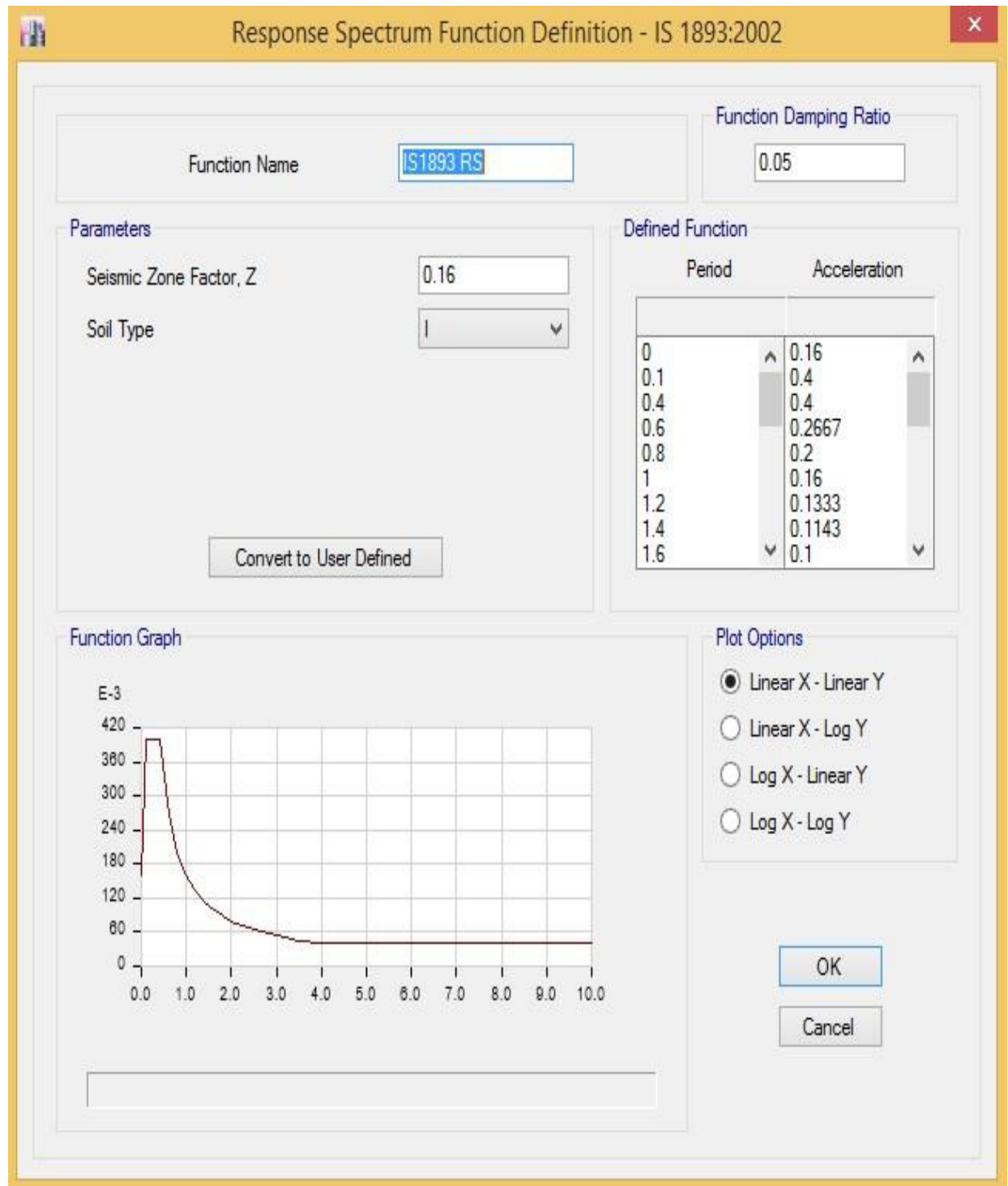
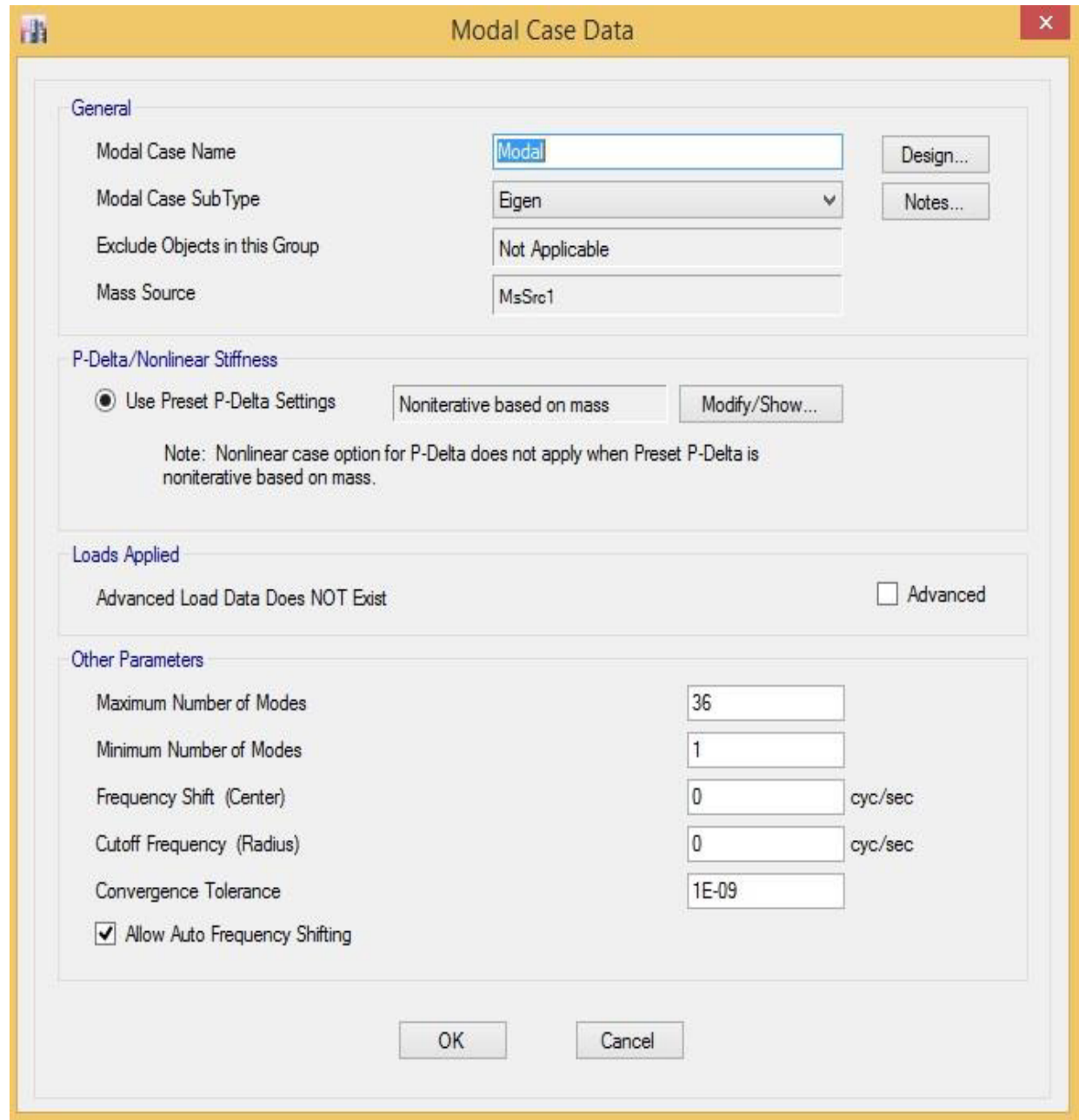


Figure-28. Sample Response Spectrum Function Property



The image shows a software dialog box titled "Modal Case Data". It is divided into several sections: "General", "P-Delta/Nonlinear Stiffness", "Loads Applied", and "Other Parameters".

- General:** Contains fields for "Modal Case Name" (set to "Modal"), "Modal Case SubType" (set to "Eigen"), "Exclude Objects in this Group" (set to "Not Applicable"), and "Mass Source" (set to "MsSrc1"). There are "Design..." and "Notes..." buttons.
- P-Delta/Nonlinear Stiffness:** Features a radio button for "Use Preset P-Delta Settings" (which is selected), a text field for "Noniterative based on mass", and a "Modify/Show..." button. A note states: "Note: Nonlinear case option for P-Delta does not apply when Preset P-Delta is noniterative based on mass."
- Loads Applied:** Includes a checkbox for "Advanced Load Data Does NOT Exist" (unchecked) and an "Advanced" checkbox (unchecked).
- Other Parameters:** Contains input fields for "Maximum Number of Modes" (36), "Minimum Number of Modes" (1), "Frequency Shift (Center)" (0 cyc/sec), "Cutoff Frequency (Radius)" (0 cyc/sec), and "Convergence Tolerance" (1E-09). There is also a checked checkbox for "Allow Auto Frequency Shifting".

At the bottom of the dialog are "OK" and "Cancel" buttons.

Figure-29. Sample Modal Case

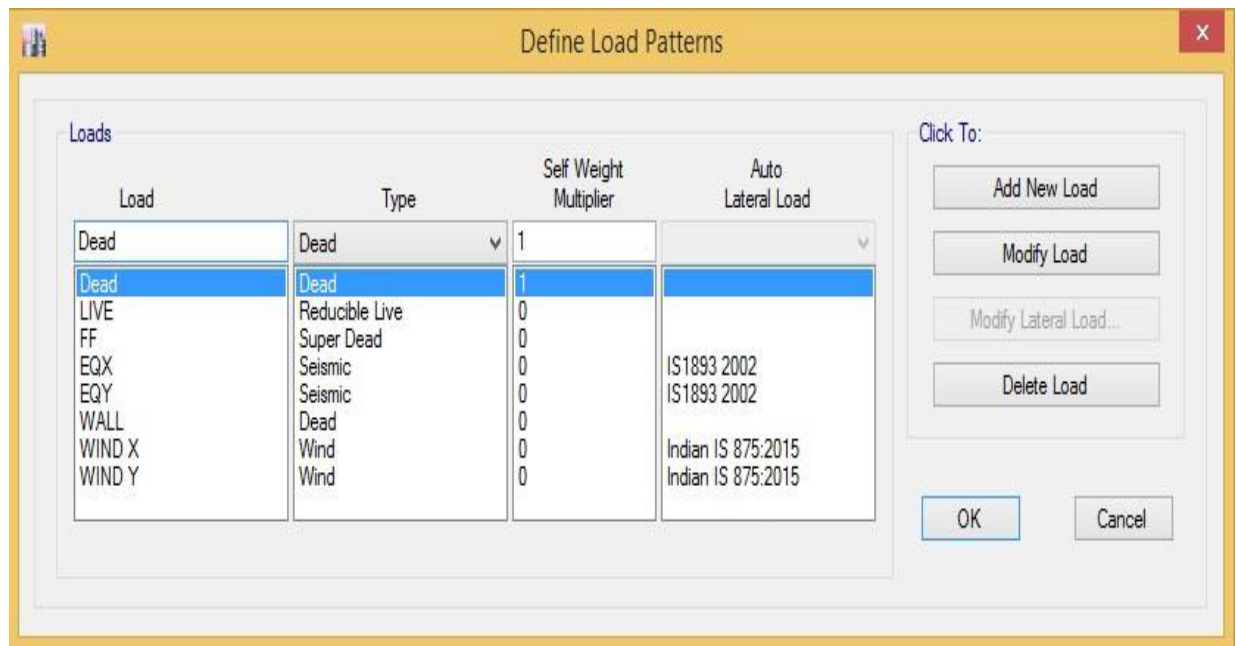


Figure-30. Sample Load Patterns

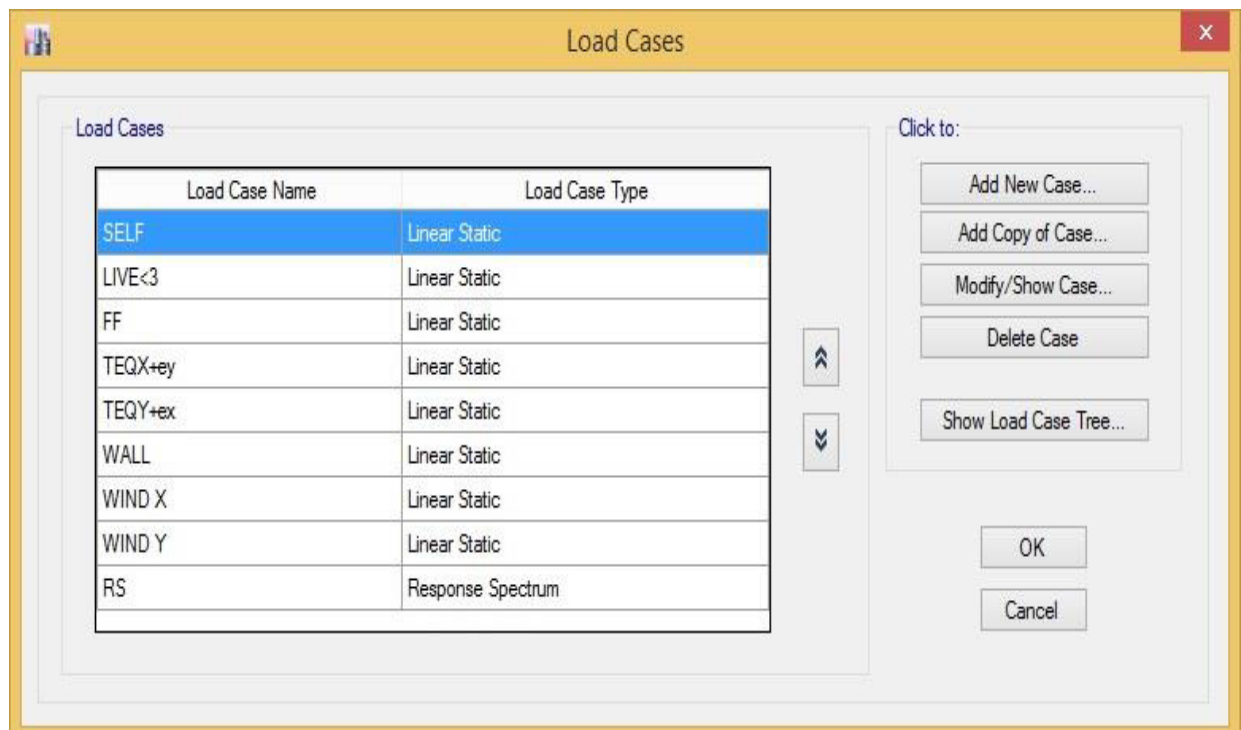


Figure-31. Sample Load Cases

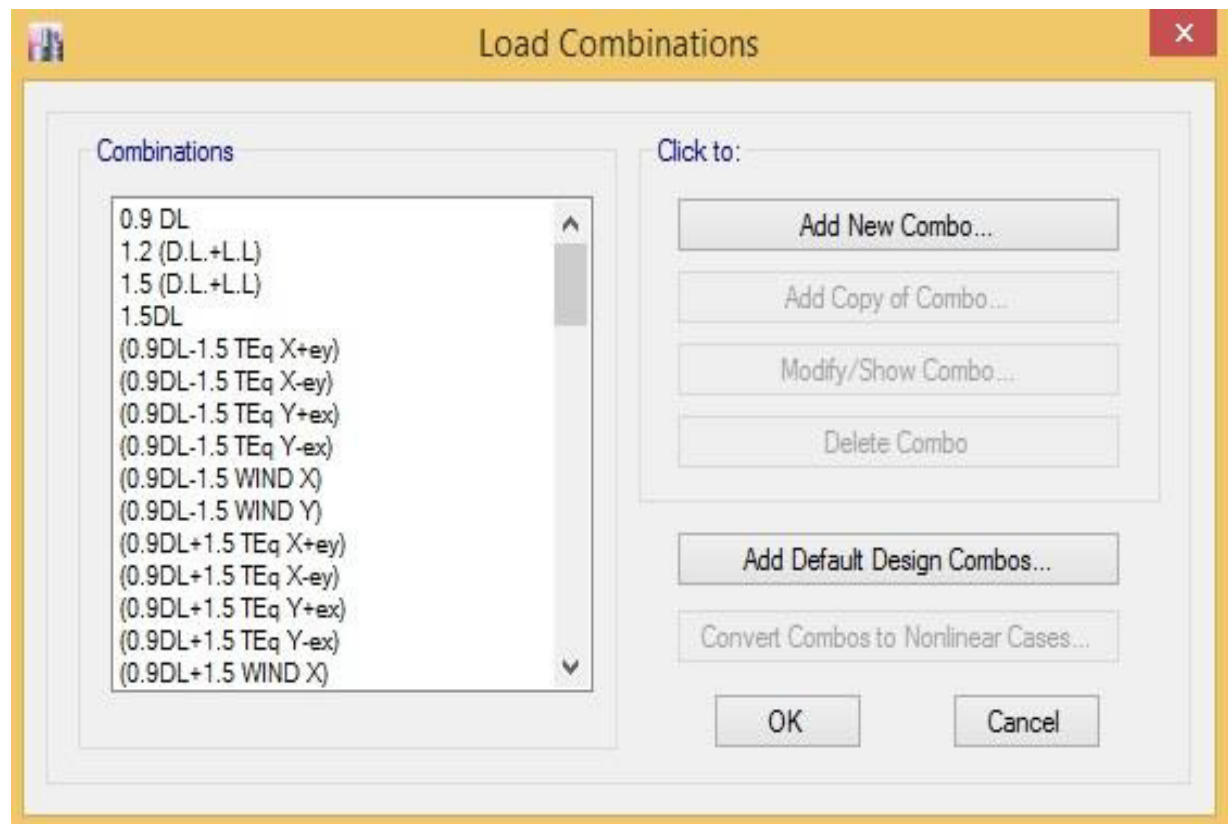
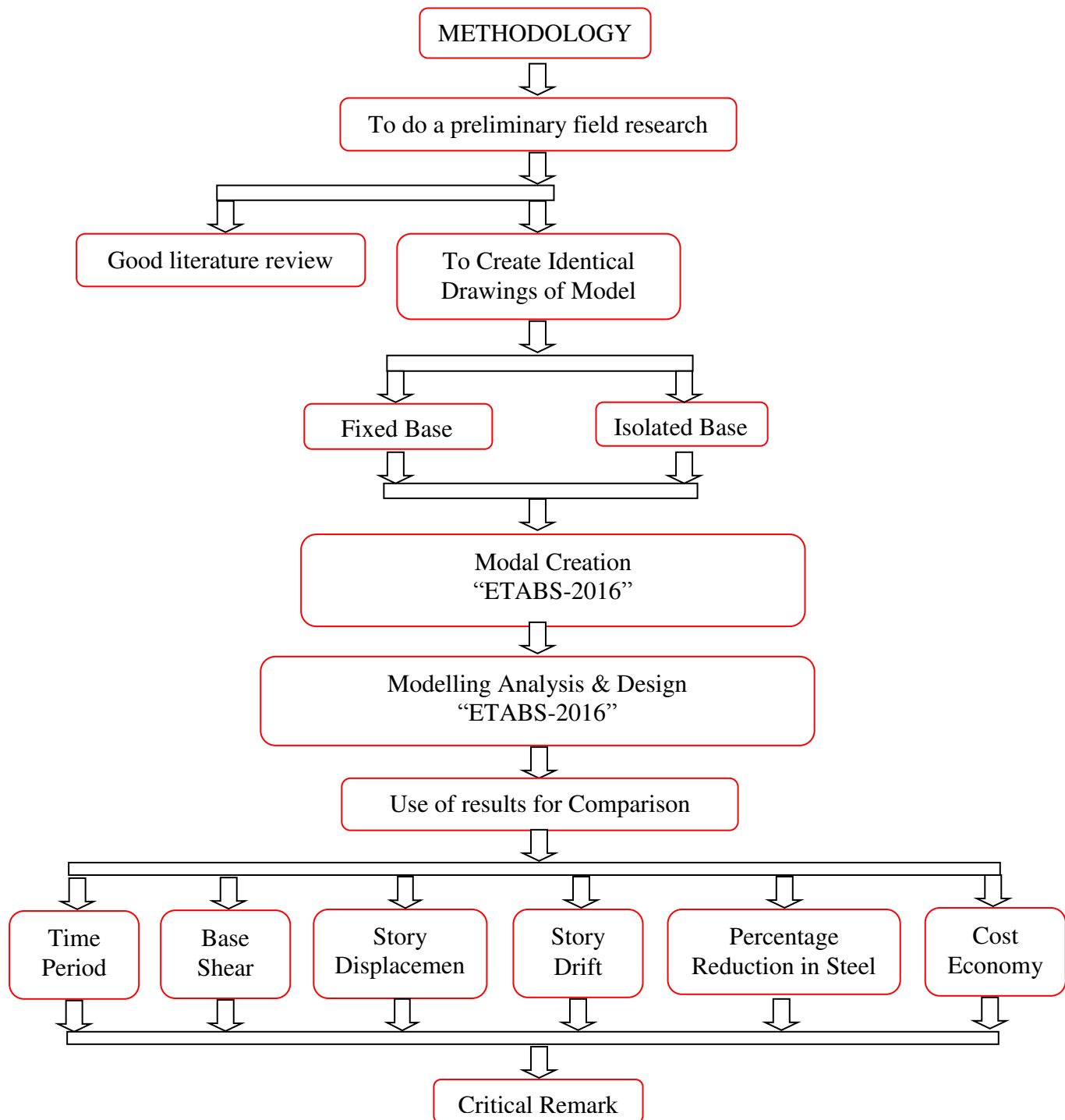


Figure-32. Sample Load Combination

4.9 Research Methodology



- From preliminary field study & healthy literature review, Sample Model is created using CAD tools.
- Validation of computer aided structure designing software “ETABS-2016”.
- Fixed base Model generation in “ETABS-2016”.
- Analysis & design of fixed base Model in “ETABS-2016”.
- Design of Base isolator using cumulative load of fixed base Model.
- Base isolator Model generation in “ETABS-2016”.
- Result obtained from all the above sample Model cases (4.6) are compared.

4.10 Summary

In the current chapter, the objectives of the study are defined from the identification of the gap in existing research by means of the literature survey. With the formulated objectives, Hypothesis are identified and to fulfill the same, sample models with different case are prepared and presented in this thesis.

CHAPTER – V

DESIGN OF BASE ISOLATION BEARING



5.1 Preamble

In this chapter the Base Isolation Bearing: LRB & TFPB are design according to axial load, biaxial load and Tri-axial load (Cumulative load from fixed base modal).

5.2 Design of LRB for G+12 Storey RC Structure.

For the analysis & design of LRB, the cumulative load at the base is obtained from the fixed based design modal in ETABS-2016. This load is categorized into three groups viz. Axial load, Biaxial load and Uniaxial load.

5.2.1 LRB for Biaxial Load - 1638 KN

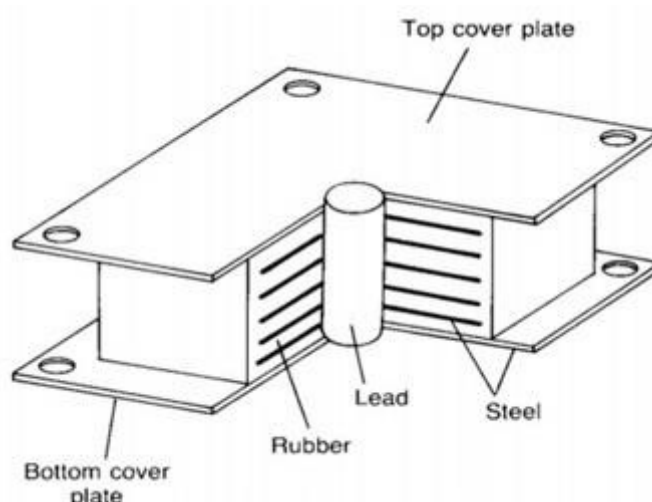


Figure-33. LRB Schematic

Biaxial Load (W)	= 1638 kN.
Time Period (T_D)	= 2.5 sec.
Design Shear Strain (γ_{max})	= 50%
	= 0.5 kN/m ² .
Effective Damping (ξ_{eff})	= 5%
	= 0.05 For U1,U2,U3.

Table-1. Damping Coefficient, B_D or B_M

EFFECTIVE DAMPING, β_D OR β_M (PERCENTAGE OF CRITICAL)	B_D OR B_M FACTOR
$\leq 2\%$	0.8
5%	1.0
10%	1.2
20%	1.5
30%	1.7
40%	1.9
$\geq 50\%$	2.0

Table-2. Seismic Coefficient C_v

SOIL PROFILE TYPE	SEISMIC ZONE FACTOR, Z				
	$Z=0.075$	$Z=0.15$	$Z=0.2$	$Z=0.3$	$Z=0.4$
S_A	0.06	0.12	0.16	0.24	$0.32N_v$
S_B	0.08	0.15	0.20	0.30	$0.40N_v$
S_C	0.13	0.25	0.32	0.45	$0.56N_v$
S_D	0.18	0.32	0.40	0.54	$0.64N_v$
S_E	0.26	0.50	0.64	0.84	$0.96N_v$
S_F	See Footnote 1				

Damping Coefficient (B_D) = 1.0 (UBC-97, Vol-2, Pg. No. 414)

Seismic Coefficient (S_D) = 0.54 (UBC-97, Vol-2, Pg. No. 35)

Table-3. Vulcanized Natural Rubber Compounds

Hardness IRHD ± 2	Young's Modulus E (MPa)	Shear Modulus G (MPa)	Material Constant k	Elongation at Break Min, %
37	1.35	0.40	0.87	650
40	1.50	0.45	0.85	600
45	1.80	0.54	0.80	600
50	2.20	0.64	0.73	500
55	3.25	0.81	0.64	500
60	4.45	1.06	0.57	400

Choosing 60 for analysis in critical circumstances

$$E = 4.45$$

$$= 4450 \text{ kN/m}^2$$

$$G = 1.06$$

$$= 1060 \text{ kN/m}^2$$

$$K = 0.57$$

$$\varepsilon_b = 4$$

$$= 400\%$$

$$f_{py} = 8500 \text{ kN/m}^2$$

$$\sigma_a = 7840 \text{ kN/m}^2$$

Typically 7 to 8.5 Mpa, Consult the manufacturer

$$F_s = 164640 \text{ kN/m}^2$$

$$f_y = 274400 \text{ kN/m}^2$$

(A) LRB - Analysis

- i. The effective horizontal stiffness K_{effH}

$$K_{\text{effH}} = \frac{W}{g} \left(\frac{2\pi}{T_D} \right)^2$$

$$K_{\text{effH}} = 1054.69 \text{ kN/m}$$

Direction U_2 & U_3

- ii. Design displacement (D_D)

$$D_D = \left(\frac{g}{4\pi^2} \right) \times \frac{S_D T_D}{B_D}$$

$$= 0.33546 \text{ m.}$$

- iii. Yield strength Q_d

$$Q_d = \frac{W_D}{4 \times D_D} = \frac{\pi}{4} \times K_{\text{effH}} \times \xi_{\text{effH}} \times D_D$$

$$= 27.788 \text{ kN}$$

iv. Yield Stiffness

$$K_U = 10 K_d$$

Where, K_d = Post yield stiffness

K_U = Pre yield stiffness

Note- Based on the findings of the trials, the initial elastic stiffness was calculated to be between 9 and 16 K_d .

$$K_d = K_{effH} - \frac{Q_d}{D_D}$$

$$= 971.854 \text{ kN/m.}$$

$$K_U = 10 K_d$$

$$= \mathbf{9718.54 \text{ kN/m.}}$$

v. Post yield stiffness ratio.

$$\frac{K_d}{K_U} = \frac{971.854}{9718.54}$$

$$= \mathbf{0.1}$$

Direction U2 & U3

(B) LRB - Developmenti. Area of lead core (A_p)

$$A_p = \frac{Q_d}{f_{py}}$$

$$= 0.00327 \text{ m}^2.$$

ii. Dia of lead core (d_p)

$$A_p = \frac{\pi d^2}{4}$$

$$d_p = \sqrt{\frac{4A_p}{\pi}}$$

$$= 0.06452 \text{ m.}$$

iii. Thickness of rubber layer (t_r)

$$t_r = \frac{D_D}{\gamma_{max}}$$

$$= 0.67092 \text{ m.}$$

- iv. The Shape factor (S)

$$\frac{E(1+2kS^2)}{G} \geq 400,$$

$$S = 9.09409$$

For $S < 10$, Take $S = 10$

- v. Compressive modulus of rubber & steel (E_c)

$$\begin{aligned} E_c &= E(1+2kS^2) \\ &= 511750 \text{ kN/m}^2. \end{aligned}$$

- vi. Effective area of bearing (A_o)

$$\begin{aligned} A_o &= W / \sigma_a \\ &= 0.20893 \text{ m}^2. \end{aligned}$$

- vii. Shear strain's effective area (A_1)

$$\begin{aligned} \frac{6SW}{E_c \times A_1} &\leq \frac{\epsilon_b}{3} \\ &= 0.14404 \text{ m}^2. \end{aligned}$$

- viii. Elastic Stiffness K_r

$$\begin{aligned} K_d &= K_r \times \frac{1+12 \times A_p}{A_o} \\ &= 818.219 \text{ kN/m}. \end{aligned}$$

- ix. Effective area of individual rubber layer (A_{sf})

$$\begin{aligned} A_{sf} &= \frac{\pi d^2}{4} \\ &= 0.51789 \text{ m}^2. \end{aligned}$$

- x. Diameter of rubber (d)

$$d = \sqrt{\frac{4A_{sf}}{\pi}}$$

$$= 0.81203 \text{ m.}$$

- xi. Effective vertical stiffness (k_v)

$$K_v = \frac{E_c \times A_{sf}}{t_r}$$

$$\mathbf{K_v = 395022 \text{ kN/m.} \quad \text{Direction } U_1}$$

- xii. Reduction factor - Damping (β)

$$\beta = 2 \times \cos^{-1} \left(\frac{D_D}{d} \right)$$

$$= 2.29.$$

- xiii. Reduced area (A_2)

$$A_2 = \frac{d^2 \times (\beta - \sin \beta)}{4}$$

$$= 0.25348 \text{ m}^2.$$

- xiv. LRB - Details

$$A = 0.25348 \text{ m}^2. \quad (\text{Max Area of } A_0, A_1, \& A_2)$$

$$d = 0.56811 \text{ m}$$

$$\text{No. of rubber layer (N)} = t_r/t \quad (\text{where } t = 0.0203)$$

$$= 33.0491$$

$$\text{Say (N)} = 34.00$$

- xv. Steel Plate thickness (t_s)

$$t_s = \frac{2 \times W \times 2t}{A \times F_s}$$

$$t_s = 0.00319 \geq 0.002 \text{ m.}$$

xvi. Total height of bearing (h_b)

$$h_b = N \times (t_s + 2 \times 0.0025) + t_r$$

$$h_b = 0.94929 \text{ m.}$$

(C) Input Values in ETABS:

The screenshot shows the 'Link/Support Directional Properties' dialog box. The 'Identification' section includes fields for Property Name (B), Direction (U1), Type (Rubber Isolator), and NonLinear (No). The 'Linear Properties' section includes Effective Stiffness (395022 kN/m) and Effective Damping (0.05 kN-s/m). The dialog has OK and Cancel buttons at the bottom.

**Figure-34. LRB Input Values in ETABS for Biaxial Load 1638 KN
Direction U_1**

Link/Support Directional Properties

Identification

Property Name	B
Direction	U2
Type	Rubber Isolator
NonLinear	Yes

Linear Properties

Effective Stiffness	1054.69	kN/m
Effective Damping	0.05	kN-s/m

Shear Deformation Location

Distance from End-J	0	m
---------------------	---	---

Nonlinear Properties

Stiffness	9718.54	kN/m
Yield Strength	27.79	kN
Post Yield Stiffness Ratio	0.1	

OK Cancel

**Figure-35. LRB Input Values in ETABS for Biaxial Load 1638 KN
Direction U_2 & U_3**

5.2.2 LRB for Uniaxial Load - 2487 KN

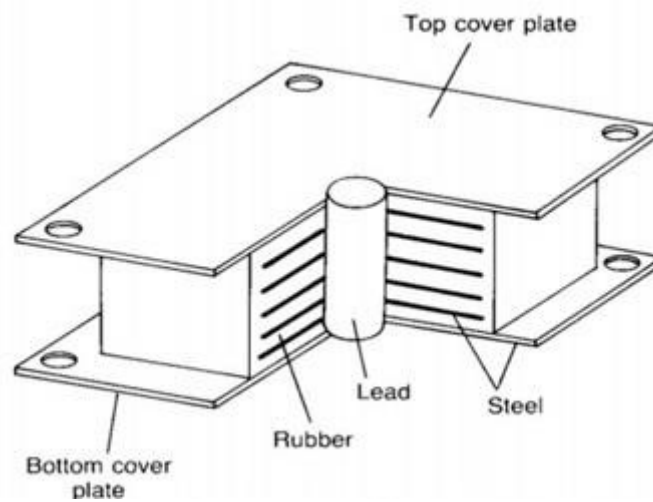


Figure-36. LRB Schematic

Uniaxial Load (W)	= 2487 kN.
Time Period (T_D)	= 2.5 sec.
Design Shear Strain (γ_{\max})	= 50%
	= 0.5 kN/m ² .
Effective Damping (ξ_{eff})	= 5%
	= 0.05 For U1,U2,U3.

Table-4. Damping Coefficient, B_D or B_M

EFFECTIVE DAMPING, β_D OR β_M (PERCENTAGE OF CRITICAL)	B_D OR B_M FACTOR
$\leq 2\%$	0.8
5%	1.0
10%	1.2
20%	1.5
30%	1.7
40%	1.9
$\geq 50\%$	2.0

Table-5. Seismic Coefficient C_v

SOIL PROFILE TYPE	SEISMIC ZONE FACTOR, Z				
	$Z=0.075$	$Z=0.15$	$Z=0.2$	$Z=0.3$	$Z=0.4$
S_A	0.06	0.12	0.16	0.24	$0.32N_y$
S_B	0.08	0.15	0.20	0.30	$0.40N_y$
S_C	0.13	0.25	0.32	0.45	$0.56N_y$
S_D	0.18	0.32	0.40	0.54	$0.64N_y$
S_E	0.26	0.50	0.64	0.84	$0.96N_y$
S_F	See Footnote 1				

Damping Coefficient (B_D) = 1.0 (UBC-97, Vol-2, Pg. No. 414)

Seismic Coefficient (S_D) = 0.54 (UBC-97, Vol-2, Pg. No. 35)

Table-6. Vulcanized Natural Rubber Compounds

Hardness IRHD ± 2	Young's Modulus E (MPa)	Shear Modulus G (MPa)	Material Constant k	Elongation at Break Min, %
37	1.35	0.40	0.87	650
40	1.50	0.45	0.85	600
45	1.80	0.54	0.80	600
50	2.20	0.64	0.73	500
55	3.25	0.81	0.64	500
60	4.45	1.06	0.57	400

Choosing 60 for analysis in critical circumstances

$$\begin{aligned}
 E &= 4.45 \\
 &= 4450 \text{ kN/m}^2 \\
 G &= 1.06 \\
 &= 1060 \text{ kN/m}^2 \\
 K &= 0.57 \\
 \epsilon_b &= 4 \\
 &= 400\% \\
 f_{py} &= 8500 \text{ kN/m}^2
 \end{aligned}$$

$$\sigma_a = 7840 \text{ kN/m}^2$$

Typically 7 to 8.5 Mpa, Consult the manufacturer

$$F_s = 164640 \text{ kN/m}^2$$

$$f_y = 274400 \text{ kN/m}^2$$

(A) LRB - Analysis

- i. The effective horizontal stiffness K_{effH}

$$K_{\text{effH}} = \frac{W}{g} \left(\frac{2\pi}{T_D} \right)^2$$

$$K_{\text{effH}} = 1601.35 \text{ kN/m}$$

Direction U_2 & U_3

- ii. Design displacement (D_D)

$$D_D = \left(\frac{g}{4\pi^2} \right) \times \frac{S_D T_D}{B_D}$$

$$= 0.33546 \text{ m.}$$

- iii. Yield Strength Q_d

$$Q_d = \frac{W_D}{4 \times D_D} = \frac{\pi}{4} \times K_{\text{effH}} \times \xi_{\text{effH}} \times D_D$$

$$= 42.191 \text{ kN}$$

- iv. Yield stiffness

$$K_U = 10 K_d$$

Where, K_d = Post yield stiffness,

K_U = Pre yield stiffness

Note- Based on the findings of the trials, the initial elastic stiffness was calculated to be between 9 and 16 K_d .

$$K_d = K_{\text{effH}} - \frac{Q_d}{D_D}$$

$$= 1475.58 \text{ kN/m.}$$

$$\begin{aligned} K_U &= 10 K_d \\ &= 14755.8 \text{ kN/m.} \end{aligned}$$

- v. Post yield stiffness ratio.

$$\begin{aligned} \frac{K_d}{K_U} &= \frac{1475.58}{14755.8} \\ &= 0.1 \end{aligned}$$

Direction U_2 & U_3

(B) LRB - Development

- i. Area of Lead Core (A_p)

$$\begin{aligned} A_p &= \frac{Q_d}{f_{py}} \\ &= 0.00496 \text{ m}^2 \end{aligned}$$

- ii. Dia of lead core (d_p)

$$\begin{aligned} A_p &= \frac{\pi d^2}{4} \\ d_p &= \sqrt{\frac{4A_p}{\pi}} \\ &= 0.0795 \text{ m.} \end{aligned}$$

- iii. Thickness of rubber layer (t_r)

$$\begin{aligned} t_r &= \frac{D_D}{\gamma_{\max}} \\ &= 0.67092 \text{ m.} \end{aligned}$$

- iv. The Shape factor (S)

$$\begin{aligned} \frac{E(1+2kS^2)}{G} &\geq 400, \\ S &= 9.09409 \end{aligned}$$

For $S < 10$, Take $S = 10$

- v. Compressive modulus of rubber & steel (E_c)

$$\begin{aligned} E_c &= E(1+2kS^2) \\ &= 511750 \text{ kN/m}^2 \end{aligned}$$

- vi. Effective area of bearing (A_o)

$$\begin{aligned} A_o &= W / \sigma_a \\ &= 0.31722 \text{ m}^2. \end{aligned}$$

- vii. Shear strain's effective area (A_1)

$$\begin{aligned} \frac{6SW}{E_c \times A_1} &\leq \frac{\epsilon_b}{3} \\ &= 0.21869 \text{ m}^2 \end{aligned}$$

- viii. Elastic Stiffness K_r

$$\begin{aligned} K_d &= K_r \times \frac{1+12 \times A_p}{A_o} \\ &= 1242.31 \text{ kN/m}. \end{aligned}$$

- ix. Effective area of individual rubber layer (A_{sf})

$$\begin{aligned} A_{sf} &= \frac{\pi d^2}{4} \\ &= 0.78632 \text{ m}^2. \end{aligned}$$

- x. Diameter of rubber (d)

$$\begin{aligned} d &= \sqrt{\frac{4A_{sf}}{\pi}} \\ &= 1.00059 \text{ m}. \end{aligned}$$

- xi. Effective vertical stiffness (k_v)

$$K_v = \frac{E_c \times A_{sf}}{t_r}$$

$$K_v = 599768 \text{ kN/m.} \quad \text{Direction } U_1$$

- xii. Reduction factor - Damping (β)

$$\beta = 2 \times \cos^{-1} \left(\frac{D_D}{d} \right)$$

$$= 2.457$$

- xiii. Reduced area (A_2)

$$A_2 = \frac{d^2 \times (\beta - \sin \beta)}{4}$$

$$= 0.4567 \text{ m}^2$$

- xiv. LRB - Details

$$A = 0.4567 \text{ m}^2 \quad (\text{Max Area of } A_0, A_1, \text{ \& } A_2)$$

$$d = 0.76255 \text{ m}$$

$$\text{No. of rubber layer (N)} = t_r/t \quad (\text{where } t = 0.02501)$$

$$= 26.8212$$

$$\text{Say (N)} = 27.00$$

- xv. Steel Plate thickness (t_s)

$$t_s = \frac{2 \times W \times 2t}{A \times F_s}$$

$$t_s = 0.00331 \geq 0.002 \text{ m.}$$

- xvi. Total height of bearing (h_b)

$$h_b = N \times (t_s + 2 \times 0.0025) + t_r$$

$$h_b = 0.89528 \text{ m.}$$

(C) Input Values in ETABS:

Link/Support Directional Properties

Identification

Property Name	U
Direction	U1
Type	Rubber Isolator
NonLinear	No

Linear Properties

Effective Stiffness	599768	kN/m
Effective Damping	0.05	kN-s/m

OK Cancel

**Figure-37. LRB Input Values in ETABS for Uniaxial Load 2487 KN
Direction U₁**

Link/Support Directional Properties

Identification

Property Name	U
Direction	U2
Type	Rubber Isolator
NonLinear	Yes

Linear Properties

Effective Stiffness	1601.35	kN/m
Effective Damping	0.05	kN-s/m

Shear Deformation Location

Distance from End-J	0	m
---------------------	---	---

Nonlinear Properties

Stiffness	14755.8	kN/m
Yield Strength	42.19	kN
Post Yield Stiffness Ratio	0.1	

OK Cancel

**Figure-38. LRB Input Values in ETABS for Uniaxial Load 2487 KN
Direction U₂ & U₃**

5.2.3 LRB for Axial Load - 3920 KN

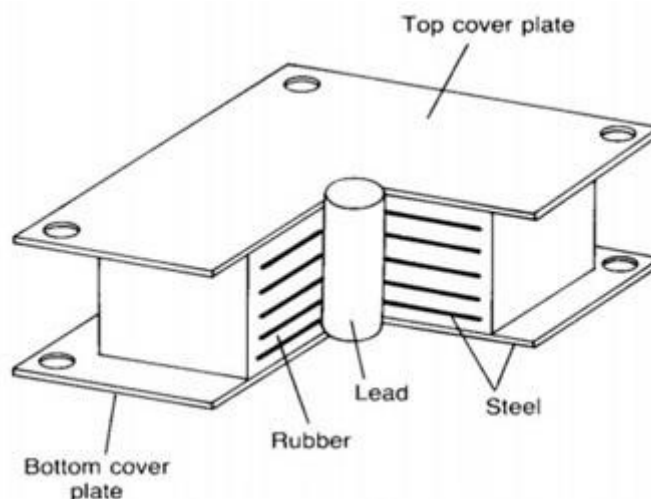


Figure-39. LRB Schematic

Axial Load (W)	= 3920 kN.
Time Period (T_D)	= 2.5 sec.
Design Shear Strain (γ_{\max})	= 50%
	= 0.5 kN/m ² .
Effective Damping (ξ_{eff})	= 5%
	= 0.05 For U1,U2,U3.

Table-7. Damping Coefficient, B_D or B_M

EFFECTIVE DAMPING, β_D OR β_M (PERCENTAGE OF CRITICAL)	B_D OR B_M FACTOR
$\leq 2\%$	0.8
5%	1.0
10%	1.2
20%	1.5
30%	1.7
40%	1.9
$\geq 50\%$	2.0

Table-8. Seismic Coefficient C_v

SOIL PROFILE TYPE	SEISMIC ZONE FACTOR, Z				
	$Z=0.075$	$Z=0.15$	$Z=0.2$	$Z=0.3$	$Z=0.4$
S_A	0.06	0.12	0.16	0.24	$0.32N_y$
S_B	0.08	0.15	0.20	0.30	$0.40N_y$
S_C	0.13	0.25	0.32	0.45	$0.56N_y$
S_D	0.18	0.32	0.40	0.54	$0.64N_y$
S_E	0.26	0.50	0.64	0.84	$0.96N_y$
S_F	See Footnote 1				

Damping Coefficient (B_D) = 1.0 (UBC-97, Vol-2, Pg. No. 414)

Seismic Coefficient (S_D) = 0.54 (UBC-97, Vol-2, Pg. No. 35)

Table-9. Vulcanized Natural Rubber Compounds

Hardness IRHD ± 2	Young's Modulus E (MPa)	Shear Modulus G (MPa)	Material Constant k	Elongation at Break Min, %
37	1.35	0.40	0.87	650
40	1.50	0.45	0.85	600
45	1.80	0.54	0.80	600
50	2.20	0.64	0.73	500
55	3.25	0.81	0.64	500
60	4.45	1.06	0.57	400

Choosing 60 for analysis in critical circumstances

$$\begin{aligned}
 E &= 4.45 \\
 &= 4450 \text{ kN/m}^2 \\
 G &= 1.06 \\
 &= 1060 \text{ kN/m}^2 \\
 K &= 0.57 \\
 \epsilon_b &= 4 \\
 &= 400\% \\
 f_{py} &= 8500 \text{ kN/m}^2
 \end{aligned}$$

$$\sigma_a = 7840 \text{ kN/m}^2$$

Typically 7 to 8.5 Mpa, Consult the manufacturer

$$F_s = 164640 \text{ kN/m}^2$$

$$f_y = 274400 \text{ kN/m}^2$$

(A) LRB - Analysis

- i. The effective horizontal stiffness K_{effH}

$$K_{\text{effH}} = \frac{W}{g} \left(\frac{2\pi}{T_D} \right)^2$$

$$K_{\text{effH}} = 2524.04 \text{ kN/m}$$

Direction U_2 & U_3

- ii. Design displacement (D_D)

$$D_D = \left(\frac{g}{4\pi^2} \right) \times \frac{S_D T_D}{B_D}$$

$$= 0.33546 \text{ m.}$$

- iii. Yield Strength Q_d

$$Q_d = \frac{W_D}{4 \times D_D} = \frac{\pi}{4} \times K_{\text{effH}} \times \xi_{\text{effH}} \times D_D$$

$$= 66.5012 \text{ kN}$$

- iv. Yield Stiffness

$$K_U = 10 K_d$$

Where, K_d = Post yield stiffness

K_U = Pre yield stiffness

Note- Based on the findings of the trials, the initial elastic stiffness was calculated to be between 9 and 16 K_d .

$$K_d = K_{\text{effH}} - \frac{Q_d}{D_D}$$

$$= 2325.81 \text{ kN/m.}$$

$$K_U = 10 K_d$$

$$= 23258.1 \text{ kN/m.}$$

- v. Post yield stiffness ratio.

$$\frac{K_d}{K_U} = \frac{2325.81}{23258.1}$$

$$= 0.1$$

Direction U2 & U3

(B) LRB - Development

- i. Area of Lead Core (A_p)

$$A_p = \frac{Q_d}{f_{py}}$$

$$= 0.00782 \text{ m}^2.$$

- ii. Dia of lead core (d_p)

$$A_p = \frac{\pi d^2}{4}$$

$$d_p = \sqrt{\frac{4A_p}{\pi}}$$

$$= 0.09981 \text{ m.}$$

- iii. Thickness of rubber layer (t_r)

$$t_r = \frac{D_D}{\gamma_{\max}}$$

$$= 0.67092 \text{ m.}$$

- iv. The Shape factor (S)

$$\frac{E(1+2kS^2)}{G} \geq 400,$$

$$S = 9.09409$$

For $S < 10$, Take $S = 10$

- v. Compressive modulus of rubber & steel (E_c)

$$\begin{aligned} E_c &= E (1+2kS^2) \\ &= 511750 \text{ kN/m}^2. \end{aligned}$$

- vi. Effective area of bearing (A_o)

$$\begin{aligned} A_o &= W / \sigma_a \\ &= 0.5 \text{ m}^2. \end{aligned}$$

- vii. Shear strain's effective area (A_1)

$$\begin{aligned} \frac{6SW}{E_c \times A_1} &\leq \frac{\epsilon_b}{3} \\ &= 0.3447 \text{ m}^2. \end{aligned}$$

- viii. Elastic Stiffness K_r

$$\begin{aligned} K_d &= K_r \times \frac{1+12 \times A_p}{A_o} \\ &= 1958.13 \text{ kN/m}. \end{aligned}$$

- ix. Effective area of individual rubber layer (A_{sf})

$$\begin{aligned} A_{sf} &= \frac{\pi d^2}{4} \\ &= 1.23939 \text{ m}^2. \end{aligned}$$

- x. Diameter of rubber (d)

$$\begin{aligned} d &= \sqrt{\frac{4A_{sf}}{\pi}} \\ &= 1.2562 \text{ m}. \end{aligned}$$

- xi. Effective vertical stiffness (k_v)

$$K_v = \frac{E_c \times A_{sf}}{t_r}$$

$$K_v = 945352 \text{ kN/m}.$$

Direction U_1

xii. Reduction factor - Damping (β)

$$\begin{aligned}\beta &= 2 \times \cos^{-1} \left(\frac{D_D}{d} \right) \\ &= 2.6\end{aligned}$$

xiii. Reduced area (A_2)

$$\begin{aligned}A_2 &= \frac{d^2 \times (\beta - \sin \beta)}{4} \\ &= 0.82236 \text{ m}^2.\end{aligned}$$

xiv. LRB - Details

$$\begin{aligned}A &= 0.82236 \text{ m}^2 && (\text{Max Area of } A_0, A_1, \text{ \& } A_2) \\ d &= 1.02326 \text{ m} \\ \text{No. of rubber layer (N)} &= t_r/t && (\text{where } t = 0.03141) \\ &= 21.3636 \\ \text{Say (N)} &= 22.00\end{aligned}$$

xv. Steel Plate thickness (t_s)

$$\begin{aligned}t_s &= \frac{2 \times W \times 2t}{A \times F_s} \\ t_s &= 0.00364 \geq 0.002 \text{ m}.\end{aligned}$$

xvi. Total height of bearing (h_b)

$$\begin{aligned}h_b &= N \times (t_s + 2 \times 0.0025) + t_r \\ h_b &= 0.86094 \text{ m}.\end{aligned}$$

(C) Input Values in ETABS:

Link/Support Directional Properties

Identification

Property Name	A
Direction	U1
Type	Rubber Isolator
NonLinear	No

Linear Properties

Effective Stiffness	345352	kN/m
Effective Damping	0.05	kN-s/m

OK Cancel

**Figure-40. LRB Input Values in ETABS for Axial Load 3920 KN
Direction U₁**

Link/Support Directional Properties

Identification

Property Name	A
Direction	U2
Type	Rubber Isolator
NonLinear	Yes

Linear Properties

Effective Stiffness	2524.04	kN/m
Effective Damping	0.05	kN-s/m

Shear Deformation Location

Distance from End-J	0	m
---------------------	---	---

Nonlinear Properties

Stiffness	23258.1	kN/m
Yield Strength	66.5	kN
Post Yield Stiffness Ratio	0.1	

OK Cancel

**Figure-41. LRB Input Values in ETABS for Axial Load 3920 KN
Direction U₂ & U₃**

5.3 Design of TFPB for G+12 Storey RC Structure.

For the analysis & design of TFPB, the cumulative load at the base is obtained from the fixed based design modal in ETABS-2016. This load is categorized into three groups viz. Axial load, Biaxial load and Uniaxial load.

5.3.1 TFPB for Biaxial Load - 1638 KN

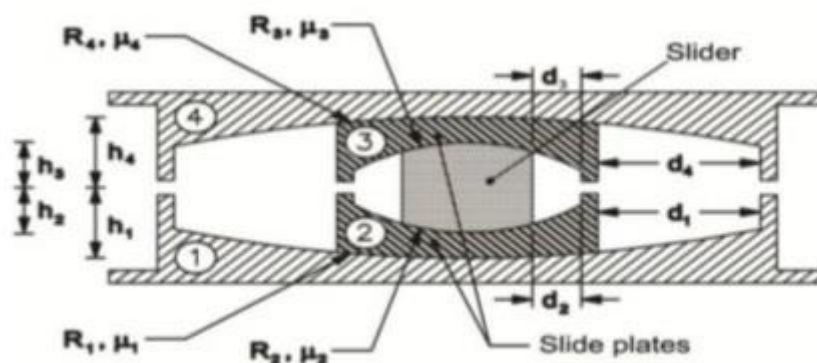


Figure-42. TFPB Schematic

(A) Geometrical, Frictional and D_D Computation

a. Geometrical features

$$\begin{aligned}
 R_4 &= R_1 &= 1778 \times 2 \\
 &&= 3556 \text{ mm.} \\
 &&= 3.556 \text{ m.} \\
 R_2 &= R_3 &= 647 \text{ mm} \\
 &&= 0.647 \text{ m} \\
 h_1 &= h_4 &= 161 \text{ mm} \\
 &&= 0.161 \text{ m} \\
 h_2 &= h_3 &= 121 \text{ mm}
 \end{aligned}$$

$$= 0.121 \text{ m}$$

$$d_1 = 566.02 \text{ mm}$$

$$d_2 = 81.05 \text{ mm}$$

$$\begin{aligned} R_{1\text{eff}4} &= R_{4\text{eff}4} = R_1 - h_1 \\ &= 3556 - 161 \\ &= 3395 \text{ mm.} \end{aligned}$$

$$\begin{aligned} R_{2\text{eff}4} &= R_{3\text{eff}4} = R_2 - h_2 \\ &= 647 - 121 \\ &= 526 \text{ mm.} \end{aligned}$$

$$\begin{aligned} d_4^* &= d_1^* = \frac{d_1 \times R_{1\text{eff}}}{R_1} \\ &= 540.39 \text{ mm} \\ &\approx 540.40 \text{ mm.} \end{aligned}$$

$$\begin{aligned} d_2^* &= d_3^* = \frac{d_2 \times R_{2\text{eff}}}{R_2} \\ &= 65.89 \text{ mm} \\ &\approx 65.90 \text{ mm.} \end{aligned}$$

b. Frictional characteristics Computation

At 1 & 4

$$P = W / A$$

$$\text{Here W Load} = 163.8 \text{ tonne or } 1638 \text{ KN.}$$

$$A = \pi r^2$$

$$\begin{aligned} r &= h_4 + h_1 \\ &= 161 + 161 \end{aligned}$$

$$r = 322 \text{ mm}$$

$$P = 0.000503 \text{ ton/mm}^2,$$

$$P = 0.000503 \times 1450$$

$$\begin{aligned}
 P &= 0.73 \text{ ksi}, & 1 \text{ ksi} &= \text{Kilo square inch} \\
 & & &= 1450 \text{ ton/mm}^2 \\
 3\text{- Friction Cycle} & & \mu &= 0.122 - 0.01 P, \\
 & & \mu &= 0.1147 \\
 \text{Adjust for high velocity} & & &= \mu - 0.0333 \\
 & & &= 0.1147 - 0.0333 \\
 & & &= 0.081 \text{ (Lower bound)} \\
 1 - \text{Friction Cycle} & & \mu &= 1.2 \times 0.081 \\
 & & &= 0.0977 \\
 \mu_4 &= \mu_1 = 0.081 \text{ (Lower bound)} \\
 \mu_4 &= \mu_1 = 0.098 \text{ (Upper bound)}
 \end{aligned}$$

At 2 and 3

$$\begin{aligned}
 P &= W / A \\
 \text{Here W Load} &= 163.8 \text{ tonne or } 1638 \text{ kN}, \\
 A &= \pi r^2 \\
 R &= h_2 + h_3 \\
 &= 121 + 121, \\
 &= 242 \text{ mm} \\
 P &= 0.000890 \text{ ton/mm}^2, \\
 P &= 0.000890 \times 1450 \\
 P &= 1.29 \text{ ksi}. & 1 \text{ ksi} &= \text{Kilo square inch} \\
 & & &= 1450 \text{ ton/mm}^2 \\
 3\text{- Friction Cycle} & & \mu &= 0.122 - 0.01 P \\
 & & &= 0.1091 \\
 \text{Adjust for high velocity} & & &= \mu - 0.036 \\
 & & &= 0.1091 - 0.036 \\
 & & &= 0.073 \text{ (Lower bound)} \\
 1 - \text{Friction Cycle} & & \mu &= 1.2 \times 0.073 \\
 & & &= 0.0877
 \end{aligned}$$

$$\begin{aligned} \mu_2 &= \mu_3 = 0.073 \text{ (Lower bound)} \\ \mu_2 &= \mu_3 = 0.088 \text{ (Upper bound)} \\ \mu &= \text{force at zero deformation} \\ \mu &= \mu_1 - (\mu_1 - \mu_2) \times \frac{R_{2eff}}{R_{1eff}} \text{ (Lower bound)} \\ \mu &= 0.080 \\ \mu &= \mu_1 - (\mu_1 - \mu_2) \times \frac{R_{2eff}}{R_{1eff}} \text{ (Upper bound)} \\ \mu &= 0.096 \end{aligned}$$

c. D_b Computation (Upper bound)

$$\begin{aligned} S_d &= 0.5074 \\ \mu &= 0.096 \\ \mu_1 &= 0.098 \\ D_y &= (\mu_1 - \mu_2) * R_{2eff} \\ D_y &= 0.005250 \\ F_d &= 0.2772 \\ W &= 163.8 \text{ Ton.} \\ \text{T.B.} &= 12 \text{ Nos. (where T.B. = Total Bearing)} \\ \Sigma F_d &= W \times \text{T.B.} \times F_d \\ &= 163.8 \times 12 \times 0.2772 \\ \Sigma F_d &= 544.95 \\ \Sigma w &= W \times \text{T.B.} \\ \Sigma w &= 1965.6 \text{ Ton.} \end{aligned}$$

i. **Design displacement** $D_D = 0.07202 \text{ m.}$

ii. **Effective stiffness, Q_d**

$$\begin{aligned} &= \mu * \Sigma w \\ &= 0.096 * 1965.6 \\ Q_d &= 188.98 \text{ Ton} \\ k_D &= \Sigma F_D / D_D \\ &= 544.95 / 0.07202 \end{aligned}$$

$$\begin{aligned}
 k_D &= 7566.63 \text{ Ton/m.} \\
 K_{\text{eff}} &= k_D + Q_D / D_D \\
 &= 7566.63 + 188.98 / 0.07202 \\
 K_{\text{eff}} &= 10190.63 \text{ Ton/m.}
 \end{aligned}$$

iii. **Effective period, T_{eff}**

$$\begin{aligned}
 T_{\text{eff}} &= [\sqrt{(\Sigma w) / (K_{\text{eff}} \times g))}] 2\pi \\
 T_{\text{eff}} &= 0.88103 \text{ sec.}
 \end{aligned}$$

iv. **Effective damping, β_{eff}**

$$\begin{aligned}
 \beta_D &= \frac{E}{2\pi K_{\text{eff}} \times D_D^2} = \frac{4\mu \Sigma w (D_D - D_y)}{2\pi K_{\text{eff}} \times D_D^2} \\
 \beta_{\text{eff}} &= \beta_D = 0.1520
 \end{aligned}$$

v. **Damping reduction coefficient, β**

$$\begin{aligned}
 \beta &= \left(\frac{\beta_{\text{eff}}}{0.05} \right)^{0.3} \\
 \beta &= 1.3959
 \end{aligned}$$

vi. **D_D^1**

$$\begin{aligned}
 D_D^1 &= \frac{T_{\text{eff}}^2 \times S_D!}{4\pi^2 \times \beta} \times g \\
 D_D^1 &= 0.0701 \text{ m}
 \end{aligned}$$

(B) ETABS links directional property computation (upper bound)

a. Principal Features

i. Determine bearing

The isolator had been envisioned as a cylinder with a height of 0.32 metres and a diameter of 0.305 metres

$$\begin{aligned}
 H &= 0.5 \text{ m} \\
 \emptyset &= 0.484 \text{ m}
 \end{aligned}$$

$$\begin{aligned}
 \text{Now, Area} \quad A &= \frac{\pi \times \phi^2}{4} \\
 &= \frac{\pi \times 0.484^2}{4} \\
 A &= 0.1840 \text{ m}^2 \\
 K_{\text{eff}} &= \frac{W}{R_{1\text{eff}}} + \frac{\mu W}{D_D} \\
 K_{\text{eff}} &= 266.91 \text{ Ton/m} \\
 I_1 &= \frac{K_{\text{eff}} \times h^3}{12E} = \frac{266.91 \times 0.5^3}{12E} \\
 &= 2.78035\text{E-}07 \text{ m}^4. \\
 E &= 1 \times 10^7 \text{ N/mm}^2.
 \end{aligned}$$

ii. Determine bearing mass

$$\begin{aligned}
 D_{\text{m-max}} &= 0.0702 \text{ m.} \\
 D_{\text{TM}} &= 1.15 \times D_{\text{m-max}} \\
 &= 1.15 \times 0.0702 \\
 D_{\text{TM}} &= 0.0807 \text{ m.} \\
 D &= 2 D_{\text{TM}} \\
 &= 2 \times 0.0807 \\
 D &= 0.16146 \text{ m.} \\
 w &= 0.241 D^2 - 0.00564 D \\
 w &= 0.0053721 \text{ Tonne} \\
 M &= w / g \\
 &= 0.005372 / 9.81 \\
 M &= 0.000548 \text{ Tonne sec}^2/\text{m.}
 \end{aligned}$$

b. Direction (U_1)

$$\begin{aligned}
 H &= 0.5 \text{ m} \\
 \varnothing &= 0.484 \text{ m} \\
 K_{\text{eff}} &= AE / L \\
 K_{\text{eff}} &= \mathbf{3679684.643 \text{ Ton/m.}} \\
 &\text{from } D_D \\
 K_{\text{eff}} &= 3679684.643 \text{ Ton/m.} \\
 \beta_{\text{eff}} &= 0.1520
 \end{aligned}$$

c. Direction ($U_2 - U_3$)**i. Determination of liner properties.**

$$\begin{aligned}
 K_{\text{eff}} &= 266.914 \text{ ton/m} \\
 &= \mathbf{2669.14 \text{ KN/m}} \\
 \beta_{\text{eff}} &= 0.1520 \\
 \text{Height for outer surface, } &= h_1 = h_4 = \mathbf{0.161 \text{ m.}} \\
 \text{Height for inner surface, } &= h_2 = h_3 = \mathbf{0.121 \text{ m.}}
 \end{aligned}$$

ii. Determination of Non - liner properties.

$$\begin{aligned}
 R_{2 \text{ eff}} &= 0.526 \text{ m.} \\
 D_y &= (\mu_1 - \mu_2) R_{2 \text{ eff}} \\
 &= (0.09769 - 0.08771) \times 0.526 \\
 D_y &= 0.00525 \text{ m.} \\
 \text{Stiffness (Outer Top)} &= \frac{\mu_1 W}{D_y} \\
 &= \frac{0.09769 \times 163.8}{0.00525} \\
 &= 3047.855 \text{ ton/m.} \\
 &= \mathbf{30478.55 \text{ KN/m.}} \\
 \text{Stiffness (Inner Top)} &= \frac{\mu_2 W}{D_y}
 \end{aligned}$$

$$\begin{aligned}
 &= \frac{0.08771 \times 163.8}{0.00526} \\
 &= 2736.448 \text{ ton/m.} \\
 &= \mathbf{27364.48 \text{ KN/m.}} \\
 \\
 \text{Friction Coefficient, Slow} &= \mu_1 = \mathbf{0.098 \text{ (Outer Top)}} \\
 &= \mu_2 = \mathbf{0.088 \text{ (Inner Top)}} \\
 \\
 \text{Friction Coefficient, Fast} &= 2 \times \mu_1 = \mathbf{0.195 \text{ (Outer Top)}} \\
 &= 2 \times \mu_2 = \mathbf{0.175 \text{ (Inner Top)}} \\
 \\
 \text{Rate Parameter} &= \frac{\text{Friction Coeff. Slow}}{\text{Friction Coeff. Fast}} \\
 &= 0.098 / 0.195 \\
 &= 0.5 \\
 &= \mathbf{0.0005 \text{ sec/mm}} \\
 \\
 \text{Radius of sliding surface} \\
 \\
 \text{Outer Top} &= R_{1\text{eff}} = \mathbf{3.395 \text{ m.}} \\
 \\
 \text{Inner Top} &= R_{2\text{eff}} = \mathbf{0.526 \text{ m.}} \\
 \\
 \text{Stop distance} \\
 \\
 \text{Outer Top } u_1^* &= 2 D_y + 2 d_1^* \\
 &= 1.09130 \text{ m.} \\
 &= \mathbf{1091.30 \text{ mm}} \\
 \\
 \text{Inner Top } u_2^* &= 2 D_y \\
 &= 0.0105 \text{ m.} \\
 &= \mathbf{10.5 \text{ mm.}}
 \end{aligned}$$

(C) Input Values in ETABS:

Link/Support Directional Properties

Identification

Property Name	B
Direction	U1
Type	Triple Pendulum Isolator
NonLinear	Yes

Linear Properties

Effective Stiffness	36796846.43	kN/m
Effective Damping	1.396	kN-s/m

Nonlinear Properties

Stiffness	36796846.43	kN/m
Damping Coefficient	1.396	kN-s/m

OK Cancel

**Figure-43. TFPB Input Values in ETABS for Biaxial Load 1638 KN
Direction U₁**

Link/Support Directional Properties

Identification

Property Name: Type:

Direction: NonLinear:

Linear Properties

Effective Stiffness - U2: kN/m Effective Stiffness - U3: kN/m

Effective Damping - U2: kN-s/m Effective Damping - U3: kN-s/m

Shear Deformation Location

Distance from End-J - U2: m Distance from End-J - U3: m

Height and Symmetry of Sliding Surfaces

Height for Outer Surfaces: m ☒ Outer Bottom Surface is Symmetric to Outer Top Surface

Height for Inner Surfaces: m ☒ Inner Bottom Surface is Symmetric to Inner Top Surface

Nonlinear Properties for Directions U2 and U3

	Outer Top	Outer Bottom	Inner Top	Inner Bottom	
Stiffness	<input type="text" value="30478.548"/>	<input type="text" value="30478.548"/>	<input type="text" value="27364.48"/>	<input type="text" value="27364.48"/>	kN/m
Friction Coefficient, Slow	<input type="text" value="0.09769"/>	<input type="text" value="0.09769"/>	<input type="text" value="0.0877"/>	<input type="text" value="0.0877"/>	
Friction Coefficient, Fast	<input type="text" value="0.19538"/>	<input type="text" value="0.19538"/>	<input type="text" value="0.17541"/>	<input type="text" value="0.17541"/>	
Rate Parameter	<input type="text" value="0.0005"/>	<input type="text" value="0.0005"/>	<input type="text" value="0.0005"/>	<input type="text" value="0.0005"/>	sec/mm
Radius of Sliding Surface	<input type="text" value="3.395"/>	<input type="text" value="3.395"/>	<input type="text" value="0.526"/>	<input type="text" value="0.526"/>	m
Stop Distance	<input type="text" value="1091.3"/>	<input type="text" value="1091.3"/>	<input type="text" value="10.5"/>	<input type="text" value="10.5"/>	mm

**Figure-44. TFPB Input Values in ETABS for Biaxial Load 1638 KN
Direction U₂ & U₃**

5.3.2 TFPB for Uniaxial Load - 2487 KN

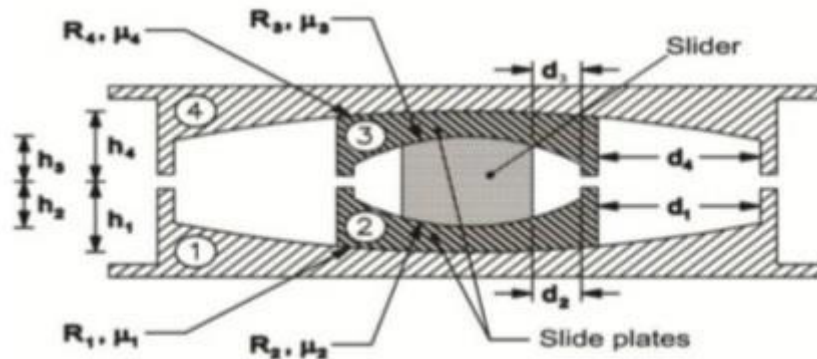


Fig. 45. TFPB Schematic

(A) Geometrical, Frictional and D_D Computation

a. Geometrical features

$$\begin{aligned}
 R_4 &= R_1 &= 1778 \times 2 \\
 &&= 3556 \text{ mm} \\
 &&= 3.556 \text{ mtrs.} \\
 R_2 &= R_3 &= 647 \text{ mm} \\
 &&= 0.647 \text{ mtrs} \\
 h_1 &= h_4 &= 161 \text{ mm} \\
 &&= 0.161 \text{ mtrs} \\
 h_2 &= h_3 &= 121 \text{ mm} \\
 &&= 0.121 \text{ mtrs} \\
 d_1 &= 566.02 \text{ mm} \\
 d_2 &= 81.05 \text{ mm} \\
 R_{1\text{eff}} &= R_{4\text{eff}} &= R_1 - h_1 \\
 &&= 3556 - 161 \\
 &&= 3395 \text{ mm.}
 \end{aligned}$$

$$\begin{aligned}
 R_{2\text{eff}} &= R_{3\text{eff}} &= R_2 - h_2 \\
 & &= 647 - 121 \\
 & &= 526 \text{ mm.} \\
 d_4^* &= d_1^* &= \frac{d_1 \times R_{1\text{eff}}}{R_1} \\
 & &= 540.39 \text{ mm} \\
 & &\approx 540.40 \text{ mm.} \\
 d_2^* &= d_3^* &= \frac{d_2 \times R_{2\text{eff}}}{R_2} \\
 & &= 65.89 \text{ mm} \\
 & &\approx 65.90 \text{ mm.}
 \end{aligned}$$

b. Frictional Characteristics Computation

At 1 and 4

$$P = W / A$$

$$\text{Here W Load} = 248.7 \text{ tonne or } 2487 \text{ KN}$$

$$A = \pi r^2$$

$$\begin{aligned}
 R &= h_4 + h_1 \\
 &= 161 + 161
 \end{aligned}$$

$$r = 322 \text{ mm}$$

$$P = 0.000764 \text{ ton/mm}^2,$$

$$P = 0.000764 \times 1450$$

$$\begin{aligned}
 P &= 01.11 \text{ ksi,} & 1 \text{ ksi} &= \text{Kilo square inch} \\
 & & &= 1450 \text{ ton/mm}^2
 \end{aligned}$$

$$\begin{aligned}
 3\text{- Friction Cycle} \quad \mu &= 0.122 - 0.01 P \\
 \mu &= 0.1109
 \end{aligned}$$

$$\begin{aligned}
 \text{Adjust for high velocity} &= \mu - 0.0333 \\
 &= 0.1109 - 0.0333 \\
 &= 0.078 \text{ (Lower bound)}
 \end{aligned}$$

$$\begin{aligned}
 1\text{- Friction Cycle} \quad \mu &= 1.2 \times 0.078 \\
 &= 0.0932
 \end{aligned}$$

$$\mu_1 = \mu_4 = 0.078 \text{ (Lower bound)}$$

$$\mu_1 = \mu_4 = 0.093 \text{ (Upper bound)}$$

At 2 and 3

$$P = W / A$$

$$\text{Here } W \text{ Load} = 248.7 \text{ ton or } 2487 \text{ kN}$$

$$A = \pi r^2$$

$$r = h_2 + h_3$$

$$= 121 + 121,$$

$$r = 242 \text{ mm}$$

$$P = 0.001352 \text{ ton/mm}^2$$

$$P = 0.001352 \times 1450$$

$$P = 1.96 \text{ ksi.} \quad 1 \text{ ksi} = \text{Kilo square inch}$$

$$= 1450 \text{ ton/mm}^2$$

$$\begin{aligned} 3\text{- Friction Cycle } \mu &= 0.122 - 0.01 P \\ &= 0.1024 \end{aligned}$$

$$\begin{aligned} \text{Adjust for high velocity} &= \mu - 0.036 \\ &= 0.1024 - 0.036 \\ &= 0.066 \text{ (Lower bound)} \end{aligned}$$

$$\begin{aligned} 1\text{- Friction Cycle } \mu &= 1.2 \times 0.066 \\ &= 0.0797 \end{aligned}$$

$$\mu_2 = \mu_3 = 0.066 \text{ (Lower bound)}$$

$$\mu_2 = \mu_3 = 0.080 \text{ (Upper bound)}$$

$$\mu = \text{force at zero deformation}$$

$$\mu = \mu_1 - (\mu_1 - \mu_2) \times \frac{R_{2\text{eff}}}{R_{1\text{eff}}} \text{ (Lower bound)}$$

$$\mu = 0.076$$

$$\mu = \mu_1 - (\mu_1 - \mu_2) \times \frac{R_{2\text{eff}}}{R_{1\text{eff}}} \text{ (Upper bound)}$$

$$\mu = 0.091$$

c. D_D Computation (Upper bound)

$$\begin{aligned}
 S_d &= 0.5074 \\
 \mu &= 0.091 \\
 \mu_1 &= 0.093 \\
 D_y &= (\mu_1 - \mu_2) * R_{2eff} \\
 D_y &= 0.007088 \\
 F_d &= 0.2772 \\
 W &= 248.7 \text{ Ton} \\
 \text{T.B.} &= 12 \text{ Nos. (Where T.B. = Total Bearing)} \\
 \Sigma F_d &= W \times \text{T.B.} \times F_d \\
 &= 248.7 \times 12 \times 0.2772 \\
 \Sigma F_d &= 827.40 \\
 \Sigma W &= W \times \text{T.B.} \\
 \Sigma W &= 2984.4 \text{ Tonne}
 \end{aligned}$$

$$\text{i. Design displacement } D_D = 0.07202 \text{ mtrs.}$$

$$\begin{aligned}
 \text{ii. Effective stiffness, } Q_D &= \mu * \Sigma W \\
 &= 0.091 * 2984.4 \\
 Q_D &= 271.78 \text{ Ton} \\
 k_D &= \Sigma F_D / D_D \\
 &= 827.40 / 0.07202 \\
 k_D &= 11488.53 \text{ Ton/m.} \\
 K_{eff} &= k_D + Q_D / D_D \\
 &= 11488.53 + 271.78 / 0.07202 \\
 K_{eff} &= 15262.22 \text{ Ton/m.}
 \end{aligned}$$

$$\begin{aligned}
 \text{iii. Effective period, } T_{eff} &= [\sqrt{(\Sigma W) / (K_{eff} \times g))}] 2\pi \\
 T_{eff} &= 0.88708 \text{ sec.}
 \end{aligned}$$

iv. **Effective damping, β_{eff}**

$$\beta_D = \frac{E}{2\pi K_{\text{eff}} \times D_D^2} = \frac{4\mu \sum w(D_D - D_y)}{2\pi K_{\text{eff}} \times D_D^2}$$

$$\beta_{\text{eff}} = \beta_D = 0.1419$$

v. **Damping reduction coefficient, β**

$$\beta = \left(\frac{\beta_{\text{eff}}}{0.05} \right)^{0.3}$$

$$\beta = 1.3675$$

vi. **D_D^1**

$$D_D^1 = \frac{S_{D1} \times T_{\text{eff}}^2}{4\pi^2 \times \beta} \times g$$

$$D_D^1 = 0.0726 \text{ mtrs}$$

(B) ETABS link directional property computation (upper bound)**a. Principal features****i. Determine bearing**

The isolator had been envisioned as a cylinder with a height of 0.32 metres and a diameter of 0.305 metres

$$H = 0.5 \text{ m}$$

$$\varnothing = 0.484 \text{ m}$$

$$\begin{aligned} \text{Now, C/S Area} \quad A &= \frac{\pi \times \varnothing^2}{4} \\ &= \frac{\pi \times 0.484^2}{4} \\ A &= 0.1840 \text{ m}^2 \end{aligned}$$

$$K_{\text{eff}} = \frac{W}{R_{1\text{eff}}} + \frac{\mu w}{D_D}$$

$$K_{\text{eff}} = 387.73 \text{ Ton/m}$$

$$I_1 = \frac{K_{\text{eff}} \times h^3}{12E} = \frac{387.73 \times 0.5^3}{12E}$$

$$= 4.03884\text{E-}07 \text{ m}^4.$$

$$E = 1 \times 10^7 \text{ N/mm}^2$$

ii. Determine bearing mass

$$D_{m\text{-max}} = 0.0702 \text{ m.}$$

$$D_{TM} = 1.15 \times D_{m\text{-max}}$$

$$= 1.15 \times 0.0702$$

$$D_{TM} = 0.0807 \text{ m.}$$

$$D = 2 D_{TM}$$

$$= 2 \times 0.0807$$

$$D = 0.16146 \text{ m.}$$

$$w = 0.241 D^2 - 0.00564 D$$

$$w = 0.0053721 \text{ tonne}$$

$$M = w / g$$

$$= 0.005372 / 9.81$$

$$M = 0.000548 \text{ tonne sec}^2/\text{m.}$$

b. Direction (U_1)

$$H = 0.5 \text{ m}$$

$$\varnothing = 0.484 \text{ m}$$

$$K_{\text{eff}} = AE / L$$

$$K_{\text{eff}} = 3679684.643 \text{ ton/m.}$$

from D_D

$$K_{\text{eff}} = 3679684.643 \text{ ton/m.}$$

$$\beta_{\text{eff}} = 0.1419$$

c. Direction ($U_2 - U_3$)**i. Determination of liner properties.**

$$K_{\text{eff}} = 387.729 \text{ ton/m}$$

$$= 3877.29 \text{ KN/m}$$

$$\beta_{\text{eff}} = 0.1419$$

$$\text{Height for outer surface, } = h_1 = h_4 = 0.161 \text{ m.}$$

$$\text{Height for inner surface, } = h_2 = h_3 = 0.121 \text{ m.}$$

ii. Determination of Non - liner properties.

$$R_{2 \text{ eff}} = 0.526 \text{ m.}$$

$$D_y = (\mu_1 - \mu_2) R_{2 \text{ eff}}$$

$$= (0.093155 - 0.079680) \times 0.526$$

$$D_y = 0.00709 \text{ m.}$$

$$\begin{aligned} \text{Stiffness (Outer Top)} &= \frac{\mu_1 w}{D_y} \\ &= \frac{0.093155 \times 248.7}{0.00709} \\ &= 3268.561 \text{ ton/m.} \\ &= 32685.61 \text{ KN/m.} \end{aligned}$$

$$\begin{aligned} \text{Stiffness (Inner Top)} &= \frac{\mu_2 w}{D_y} \\ &= \frac{0.079680 \times 248.7}{0.00709} \\ &= 2795.747 \text{ ton/m.} \\ &= 27957.47 \text{ KN/m.} \end{aligned}$$

$$\text{Friction Coefficient, Slow} = \mu_1 = 0.093 \text{ (Outer Top)}$$

$$= \mu_2 = 0.080 \text{ (Inner Top)}$$

$$\text{Friction Coefficient, Fast} = 2 \times \mu_1 = 0.186 \text{ (Outer Top)}$$

$$= 2 \times \mu_2 = 0.159 \text{ (Inner Top)}$$

$$\text{Rate Parameter} = \frac{\text{Friction Coeff. Slow}}{\text{Friction Coeff. Fast}}$$

$$= 0.093 / 0.186$$

$$= 0.5$$

$$= 0.0005 \text{ sec/mm}$$

Radius of sliding surface

$$\text{Outer Top} = R_{1 \text{ eff}} = 3.395 \text{ m.}$$

$$\text{Inner Top} = R_{2 \text{ eff}} = 0.526 \text{ m.}$$

Stop distance

$$\text{outer Top } u_1^* = 2 D_y + 2 d_1^*$$

$$= 1.09498 \text{ m.}$$

$$= 1094.98 \text{ mm}$$

$$\text{Inner Top } u_2^* = 2 D_y$$

$$= 0.0142 \text{ m.}$$

$$= 14.18 \text{ mm.}$$

(C) Input Values in ETABS:

Link/Support Directional Properties

Identification

Property Name	U
Direction	U1
Type	Triple Pendulum Isolator
NonLinear	Yes

Linear Properties

Effective Stiffness	36796846.43	kN/m
Effective Damping	1.367	kN-s/m

Nonlinear Properties

Stiffness	36796846.43	kN/m
Damping Coefficient	1.367	kN-s/m

OK Cancel

**Figure-46. TFPB Input Values in ETABS for Uniaxial Load 2487 KN
Direction U₁**

Link/Support Directional Properties

Identification

Property Name: Type:

Direction: NonLinear:

Linear Properties

Effective Stiffness - U2: kN/m Effective Stiffness - U3: kN/m

Effective Damping - U2: kN-s/m Effective Damping - U3: kN-s/m

Shear Deformation Location

Distance from End-J - U2: m Distance from End-J - U3: m

Height and Symmetry of Sliding Surfaces

Height for Outer Surfaces: m ☒ Outer Bottom Surface is Symmetric to Outer Top Surface

Height for Inner Surfaces: m ☒ Inner Bottom Surface is Symmetric to Inner Top Surface

Nonlinear Properties for Directions U2 and U3

	Outer Top	Outer Bottom	Inner Top	Inner Bottom	
Stiffness	<input type="text" value="32685.609"/>	<input type="text" value="32685.609"/>	<input type="text" value="27957.47"/>	<input type="text" value="27957.47"/>	kN/m
Friction Coefficient, Slow	<input type="text" value="0.09315"/>	<input type="text" value="0.09315"/>	<input type="text" value="0.079679"/>	<input type="text" value="0.079679"/>	
Friction Coefficient, Fast	<input type="text" value="0.1863"/>	<input type="text" value="0.1863"/>	<input type="text" value="0.159359"/>	<input type="text" value="0.159359"/>	
Rate Parameter	<input type="text" value="0.0005"/>	<input type="text" value="0.0005"/>	<input type="text" value="0.0005"/>	<input type="text" value="0.0005"/>	sec/mm
Radius of Sliding Surface	<input type="text" value="3.395"/>	<input type="text" value="3.395"/>	<input type="text" value="0.526"/>	<input type="text" value="0.526"/>	m
Stop Distance	<input type="text" value="1094.976"/>	<input type="text" value="1094.976"/>	<input type="text" value="14.176"/>	<input type="text" value="14.176"/>	mm

**Figure-47. TFPB Input Values in ETABS for Uniaxial Load 2487 KN
Direction U₂ & U₃**

5.3.3 TFPB for Axial Load - 3920 KN

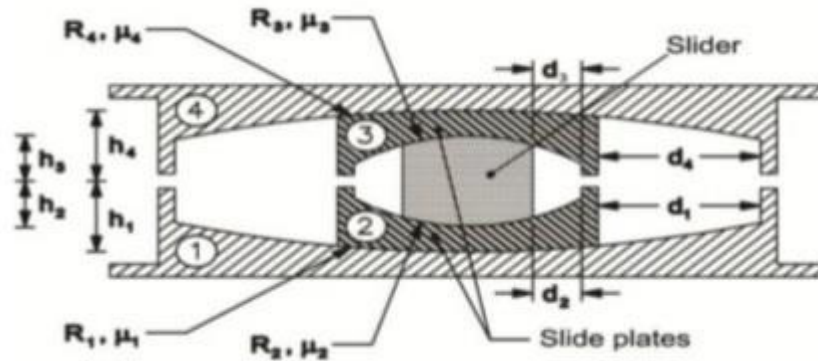


Figure-48. TFPB Schematic

(A) Geometrical, Frictional and D_D Computation

a. Geometrical features

$$\begin{aligned}
 R_4 &= R_1 &= 1778 \times 2 \\
 &&= 3556 \text{ mm} \\
 &&= 3.556 \text{ m} \\
 R_2 &= R_3 &= 647 \text{ mm} \\
 &&= 0.647 \text{ m} \\
 h_1 &= h_4 &= 161 \text{ mm} \\
 &&= 0.161 \text{ m} \\
 h_2 &= h_3 &= 121 \text{ mm} \\
 &&= 0.121 \text{ m} \\
 d_1 &= 566.02 \text{ mm} \\
 d_2 &= 81.05 \text{ mm} \\
 R_{1\text{eff}} &= R_{4\text{eff}} &= R_1 - h_1 \\
 &&= 3556 - 161 \\
 &&= 3395 \text{ mm}
 \end{aligned}$$

$$\begin{aligned}
 R_{2\text{eff}} &= R_{3\text{eff}} &= R_2 - h_2 \\
 & &= 647 - 121 \\
 & &= 526 \text{ mm.} \\
 d_4^* &= d_1^* &= \frac{d_1 \times R_{1\text{eff}}}{R_1} \\
 & &= 540.39 \text{ mm} \\
 & &\approx 540.40 \text{ mm.} \\
 d_2^* &= d_3^* &= \frac{d_2 \times R_{2\text{eff}}}{R_2} \\
 & &= 65.89 \text{ mm} \\
 & &\approx 65.90 \text{ mm.}
 \end{aligned}$$

b. Frictional Characteristics Computation

At 1 and 4

$$P = W / A$$

$$\text{Here W Load} = 392.0 \text{ tonne or } 3920 \text{ KN,}$$

$$A = \pi r^2$$

$$\begin{aligned}
 r &= h_4 + h_1 \\
 &= 161 + 161
 \end{aligned}$$

$$r = 322 \text{ mm}$$

$$P = 0.001203 \text{ ton/mm}^2$$

$$P = 0.001203 \times 1450$$

$$\begin{aligned}
 P &= 1.74 \text{ ksi,} & 1 \text{ ksi} &= \text{Kilo square inch} \\
 & & &= 1450 \text{ ton/mm}^2
 \end{aligned}$$

$$\begin{aligned}
 3\text{- Friction Cycle} \quad \mu &= 0.122 - 0.01 P \\
 \mu &= 0.1046
 \end{aligned}$$

$$\begin{aligned}
 \text{Adjust for high velocity} &= \mu - 0.0333 \\
 &= 0.1046 - 0.0333 \\
 &= 0.071 \text{ (Lower bound)}
 \end{aligned}$$

$$\begin{aligned}
 1\text{- Friction Cycle} \quad \mu &= 1.2 \times 0.071 \\
 &= 0.0855
 \end{aligned}$$

$$\mu_1 = \mu_4 = 0.071 \text{ (Lower bound)}$$

$$\mu_1 = \mu_4 = 0.086 \text{ (Upper bound)}$$

At 2 and 3

$$P = W / A$$

$$\text{Here } W \text{ Load} = 392.0 \text{ tonne or } 3920 \text{ KN}$$

$$A = \pi r^2$$

$$\begin{aligned} r &= h_2 + h_3 \\ &= 121 + 121 \\ &= 242 \text{ mm} \end{aligned}$$

$$P = 0.002131 \text{ ton/mm}^2,$$

$$P = 0.002131 \times 1450$$

$$\begin{aligned} P &= 3.09 \text{ ksi.} \quad 1 \text{ ksi} = \text{Kilo square inch} \\ &= 1450 \text{ ton/mm}^2 \end{aligned}$$

$$\begin{aligned} \text{3- Friction Cycle } \mu &= 0.122 - 0.01 P \\ &= 0.0911 \end{aligned}$$

$$\begin{aligned} \text{Adjust for high velocity} &= \mu - 0.036 \\ &= 0.0911 - 0.036 \\ &= 0.055 \text{ (Lower bound)} \end{aligned}$$

$$\begin{aligned} \text{1 - Friction Cycle } \mu &= 1.2 \times 0.055 \\ &= 0.0661 \end{aligned}$$

$$\mu_2 = \mu_3 = 0.055 \text{ (Lower bound)}$$

$$\mu_2 = \mu_3 = 0.066 \text{ (Upper bound)}$$

$$\mu = \text{force at zero deformation}$$

$$\mu = \mu_1 - (\mu_1 - \mu_2) \times \frac{R_{2\text{eff}}}{R_{1\text{eff}}} \text{ (Lower bound)}$$

$$\mu = 0.069$$

$$\mu = \mu_1 - (\mu_1 - \mu_2) \times \frac{R_{2\text{eff}}}{R_{1\text{eff}}} \text{ (Upper bound)}$$

$$\mu = 0.082$$

c. D_D Computation (Upper bound)

$$\begin{aligned}
 S_d &= 0.5074 \\
 \mu &= 0.082 \\
 \mu_1 &= 0.086 \\
 D_y &= (\mu_1 - \mu_2) * R_{2eff} \\
 D_y &= 0.010190 \\
 F_d &= 0.2772 \\
 W &= 392 \text{ Ton} \\
 \text{T.B.} &= 12 \text{ Nos. (Where T.B. = Total Bearing)} \\
 \Sigma F_d &= W \times \text{T.B.} \times F_d \\
 &= 392 \times 12 \times 0.2772 \\
 \Sigma F_d &= 1304.15 \\
 \Sigma W &= W \times \text{T.B.} \\
 \Sigma W &= 4704 \text{ Ton}
 \end{aligned}$$

i. Design displacement, D_D = 0.07202 m.

ii. Effective stiffness, Q_d

$$\begin{aligned}
 &= \mu * \Sigma W \\
 &= 0.082 * 2832 \\
 Q_d &= 388.07 \text{ Ton} \\
 k_D &= \Sigma F_D / D_D \\
 &= 1304.15 / 0.07202 \\
 k_D &= 18108.18 \text{ Ton/m.} \\
 K_{eff} &= k_D + Q_D / D_D \\
 &= 18108.18 + 388.07 / 0.07202 \\
 K_{eff} &= 23496.59 \text{ Ton/m.}
 \end{aligned}$$

iii. Effective period, T_{eff}

$$\begin{aligned}
 T_{eff} &= [\sqrt{(\Sigma W) / (K_{eff} \times g)}] 2\pi \\
 T_{eff} &= 0.89759 \text{ sec.}
 \end{aligned}$$

iv. **Effective damping, β_{eff}**

$$\beta_D = \frac{E}{2\pi K_{\text{eff}} \times D_D^2} = \frac{4\mu \Sigma w (D_D - D_y)}{2\pi K_{\text{eff}} \times D_D^2}$$

$$\beta_{\text{eff}} = \beta_D = 0.1253$$

v. **Damping reduction Coefficient, β**

$$\beta = \left(\frac{\beta_{\text{eff}}}{0.05} \right)^{0.3}$$

$$\beta = 1.3174$$

vi. **D_D^1**

$$D_D^1 = \frac{S_{D1} \times T_{\text{eff}}^2}{4\pi^2 \times \beta} \times g$$

$$D_D^1 = 0.0771 \text{ m.}$$

(B) ETABS links directional property computation (upper bound)**a. Principal features****i. Determine bearing**

The isolator had been envisioned cylinder with a height of 0.32 metres and a diameter of 0.305 metres

$$H = 0.5 \text{ m.}$$

$$\varnothing = 0.484 \text{ m}$$

$$\begin{aligned} \text{Now, Area} \quad A &= \frac{\pi \times \varnothing^2}{4} \\ &= \frac{\pi \times 0.484^2}{4} \\ A &= 0.1840 \text{ m}^2 \end{aligned}$$

$$K_{\text{eff}} = \frac{W}{R_{1\text{eff}}} + \frac{\mu w}{D_D}$$

$$K_{\text{eff}} = 564.50 \text{ Ton/m}$$

$$I_1 = \frac{K_{\text{eff}} \times h^3}{12E} = \frac{564.50 \times 0.5^3}{12E}$$

$$= 5.88019\text{E-}07 \text{ m}^4.$$

$$E = 1 \times 10^7 \text{ N/mm}^2$$

ii. **Determine bearing mass**

$$D_{m\text{-max}} = 0.0702 \text{ mtrs.}$$

$$D_{TM} = 1.15 \times D_{m\text{-max}}$$

$$= 1.15 \times 0.0702$$

$$D_{TM} = 0.0807 \text{ mtrs.}$$

$$D = 2 D_{TM}$$

$$= 2 \times 0.0807$$

$$D = 0.16146 \text{ mtrs.}$$

$$w = 0.241 D^2 - 0.00564 D$$

$$w = 0.0053721 \text{ tonne.}$$

$$M = w / g$$

$$= 0.005372 / 9.81$$

$$M = 0.000548 \text{ tonne sec}^2/\text{m.}$$

b. Direction (U_1)

$$H = 0.5 \text{ m}$$

$$\emptyset = 0.484 \text{ m}$$

$$K_{\text{eff}} = AE / L$$

$$K_{\text{eff}} = 3679684.643 \text{ ton/m.}$$

$$\mathbf{K_{\text{eff}} = 36796846.43 \text{ KN/m.}}$$

from D_D

$$K_{\text{eff}} = 3679684.64 \text{ ton/m.}$$

$$\beta_{\text{eff}} = 0.1253$$

c. Direction (U₂ - U₃)

i. Determination of liner properties.

$$K_{\text{eff}} = 564.498 \text{ ton/m}$$

$$= 5644.98 \text{ KN/m}$$

$$\beta_{\text{eff}} = 0.1253$$

$$\text{Height for outer surface, } = h_1 = h_4 = \mathbf{0.161 \text{ m}}$$

$$\text{Height for inner surface, } = h_2 = h_3 = \mathbf{0.121 \text{ m}}$$

ii. Determination of Non - liner properties.

$$R_{2\text{eff}} = 0.526 \text{ mtrs.}$$

$$D_y = (\mu_1 - \mu_2) R_{2\text{eff}}$$

$$= (0.08550 - 0.06613) \times 0.526$$

$$D_y = \mathbf{0.01091 \text{ mtrs.}}$$

$$\begin{aligned} \text{Stiffness (Outer Top)} &= \frac{\mu_1 W}{D_y} \\ &= \frac{0.08550 \times 392}{0.01091} \\ &= 3289.068 \text{ ton/m.} \\ &= \mathbf{32890.68 \text{ KN/m.}} \end{aligned}$$

$$\begin{aligned} \text{Stiffness (Inner Top)} &= \frac{\mu_2 W}{D_y} \\ &= \frac{0.06613 \times 392}{0.01091} \\ &= 2543.821 \text{ ton/m.} \\ &= \mathbf{25438.21 \text{ KN/m.}} \end{aligned}$$

$$\text{Friction Coefficient, Slow} = \mu_1 = \mathbf{0.086 \text{ (Outer Top)}}$$

$$= \mu_2 = \mathbf{0.066 \text{ (Inner Top)}}$$

$$\text{Friction Coefficient, Fast} = 2 \times \mu_1 = 0.171 \text{ (Outer Top)}$$

$$= 2 \times \mu_2 = 0.132 \text{ (Inner Top)}$$

$$\text{Rate Parameter} = \frac{\text{Friction Coeff. Slow}}{\text{Friction Coeff. Fast}}$$

$$= 0.086 / 0.171$$

$$= 0.5$$

$$= 0.0005 \text{ sec/mm}$$

Radius of sliding surface

$$\text{Outer Top} = R_{1 \text{ eff}} = 3.395 \text{ mtrs.}$$

$$\text{Inner Top} = R_{2 \text{ eff}} = 0.526 \text{ mtrs.}$$

Stop distance

$$\text{Outer Top } u_1^* = 2 D_y + 2 d_1^*$$

$$= 1.10118 \text{ mtrs.}$$

$$= 1101.18 \text{ mm}$$

$$\text{Inner Top } u_2^* = 2 D_y$$

$$= 0.0204 \text{ mtrs.}$$

$$= 20.380 \text{ mm.}$$

(C) Input Values in ETABS:

Link/Support Directional Properties

Identification

Property Name	A
Direction	U1
Type	Triple Pendulum Isolator
NonLinear	Yes

Linear Properties

Effective Stiffness	36796846.43	kN/m
Effective Damping	1.317	kN-s/m

Nonlinear Properties

Stiffness	36796846.43	kN/m
Damping Coefficient	1.317	kN-s/m

OK Cancel

**Figure-49. TFPB Input Values in ETABS for Axial Load 3920 KN
Direction U₁**

Link/Support Directional Properties

Identification

Property Name: A Type: Triple Pendulum Isolator

Direction: U2; U3 NonLinear: Yes

Linear Properties

Effective Stiffness - U2: 5644.98 kN/m Effective Stiffness - U3: 5644.98 kN/m

Effective Damping - U2: 1.317 kN-s/m Effective Damping - U3: 1.317 kN-s/m

Shear Deformation Location

Distance from End-J - U2: 0 m Distance from End-J - U3: 0 m

Height and Symmetry of Sliding Surfaces

Height for Outer Surfaces: 0.161 m ☒ Outer Bottom Surface is Symmetric to Outer Top Surface

Height for Inner Surfaces: 0.121 m ☒ Inner Bottom Surface is Symmetric to Inner Top Surface

Nonlinear Properties for Directions U2 and U3

	Outer Top	Outer Bottom	Inner Top	Inner Bottom	
Stiffness	32890.679	32890.679	25438.208	25438.208	kN/m
Friction Coefficient, Slow	0.0855	0.0855	0.0661	0.0661	
Friction Coefficient, Fast	0.171	0.171	0.13225	0.13225	
Rate Parameter	0.0005	0.0005	0.0005	0.0005	sec/mm
Radius of Sliding Surface	3.395	3.395	0.526	0.526	m
Stop Distance	1101.18	1101.18	20.38	20.38	mm

OK Cancel

**Figure-50. TFPB Input Values in ETABS for Axial Load 3920 KN
Direction U₂ & U₃**

5.4 Design of LRB for G+22 Storey RC Structure.

For the analysis & design of LRB, the cumulative load at the base is obtained from the fixed based design modal in ETABS-2016. This load is categorized into three groups viz. Axial load, Biaxial load and Uniaxial load.

5.4.1 LRB for Biaxial Load - 3342 KN

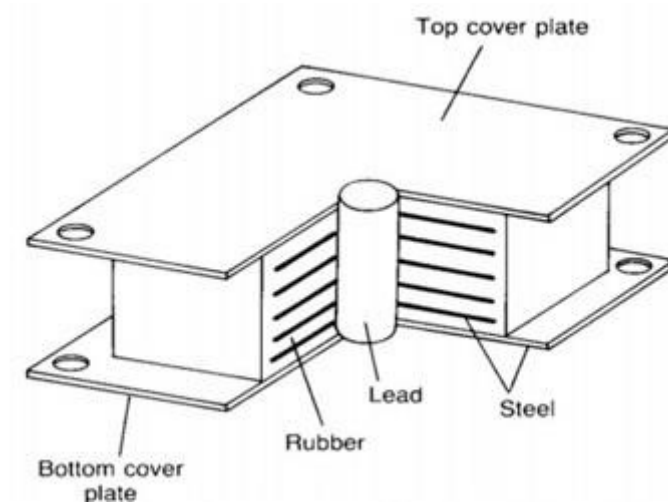


Figure-51. LRB Schematic

Biaxial Load (W)	= 3342 kN.
Time Period (TD)	= 2.5 sec.
Design Shear Strain (γ_{max})	= 50%
	= 0.5 kN/m ² .
Effective Damping (ξ_{eff})	= 5%
	= 0.05 For U1,U2,U3.

Table-10. Damping Coefficient, B_D or B_M

EFFECTIVE DAMPING, β_D OR β_M (PERCENTAGE OF CRITICAL)	B_D OR B_M FACTOR
$\leq 2\%$	0.8
5%	1.0
10%	1.2
20%	1.5
30%	1.7
40%	1.9
$\geq 50\%$	2.0

Table-11. Seismic Coefficient C_v

SOIL PROFILE TYPE	SEISMIC ZONE FACTOR, Z				
	$Z=0.075$	$Z=0.15$	$Z=0.2$	$Z=0.3$	$Z=0.4$
S_A	0.06	0.12	0.16	0.24	$0.32N_v$
S_B	0.08	0.15	0.20	0.30	$0.40N_v$
S_C	0.13	0.25	0.32	0.45	$0.56N_v$
S_D	0.18	0.32	0.40	0.54	$0.64N_v$
S_E	0.26	0.50	0.64	0.84	$0.96N_v$
S_F	See Footnote 1				

Damping Coefficient (B_D) = 1.0 (UBC-97, Vol-2, Pg. No. 414)

Seismic Coefficient (S_D) = 0.54 (UBC-97, Vol-2, Pg. No. 35)

Table-12. Vulcanized Natural Rubber Compounds

Hardness IRHD ± 2	Young's Modulus E (MPa)	Shear Modulus G (MPa)	Material Constant k	Elongation at Break Min, %
37	1.35	0.40	0.87	650
40	1.50	0.45	0.85	600
45	1.80	0.54	0.80	600
50	2.20	0.64	0.73	500
55	3.25	0.81	0.64	500
60	4.45	1.06	0.57	400

Choosing 60 for analysis in critical circumstances

$$\begin{aligned} E &= 4.45 \\ &= 4450 \text{ kN/m}^2 \end{aligned}$$

$$\begin{aligned} G &= 1.06 \\ &= 1060 \text{ kN/m}^2 \end{aligned}$$

$$K = 0.57$$

$$\begin{aligned} \varepsilon_b &= 4 \\ &= 400\% \end{aligned}$$

$$f_{py} = 8500 \text{ kN/m}^2$$

$$\sigma_a = 7840 \text{ kN/m}^2$$

Typically 7 to 8.5 Mpa, Consult the manufacturer

$$F_s = 164640 \text{ kN/m}^2$$

$$f_y = 274400 \text{ kN/m}^2$$

(A) LRB - Analysis

- i. The effective horizontal stiffness K_{effH}

$$K_{\text{effH}} = \frac{W}{g} \left(\frac{2\pi}{T_D} \right)^2$$

$$K_{\text{effH}} = 2151.88 \text{ kN/m} \quad \text{Direction } U_2 \text{ \& } U_3$$

- ii. Design displacement (D_D)

$$D_D = \left(\frac{g}{4\pi^2} \right) \times \frac{S_D T_D}{B_D}$$

$$= 0.33546 \text{ m.}$$

- iii. Yield Strength Q_d

$$Q_d = \frac{W_D}{4 \times D_D} = \frac{\pi}{4} \times K_{\text{effH}} \times \xi_{\text{effH}} \times D_D$$

$$= 56.6957 \text{ kN}$$

iv. Yield Stiffness

$$K_U = 10 K_d$$

Where, K_d = Post yield stiffness

K_U = Pre yield stiffness

Note- Based on the findings of the trials, the initial elastic stiffness was calculated to be between 9 and 16 K_d .

$$K_d = K_{effH} - \frac{Q_d}{D_D}$$

$$= 1982.87 \text{ kN/m.}$$

$$K_U = 10 K_d$$

$$= \mathbf{19828.7 \text{ kN/m.}}$$

v. Post yield stiffness ratio.

$$\frac{K_d}{K_U} = \frac{1982.87}{19828.7}$$

$$= \mathbf{0.1}$$

Direction U_2 & U_3

(B) LRB - Developmenti. Area of Lead Core (A_p)

$$A_p = \frac{Q_d}{f_{py}}$$

$$= 0.00667 \text{ m}^2.$$

ii. Dia of lead core (d_p)

$$A_p = \frac{\pi d^2}{4}$$

$$d_p = \sqrt{\frac{4A_p}{\pi}}$$

$$= 0.09216 \text{ m.}$$

iii. Thickness of rubber layer (t_r)

$$t_r = \frac{D_D}{\gamma_{\max}}$$

$$= 0.67092 \text{ m.}$$

- iv. The Shape factor (S)

$$\frac{E(1+2kS^2)}{G} \geq 400,$$

$$S = 9.09409$$

For $S < 10$, Take $S = 10$

- v. Compressive modulus of rubber & steel (E_c)

$$\begin{aligned} E_c &= E(1+2kS^2) \\ &= 511750 \text{ kN/m}^2. \end{aligned}$$

- vi. Effective area of bearing (A_o)

$$\begin{aligned} A_o &= W / \sigma_a \\ &= 0.42628 \text{ m}^2. \end{aligned}$$

- vii. Shear strain's effective area (A_1)

$$\begin{aligned} \frac{6SW}{E_c \times A_1} &\leq \frac{\epsilon_b}{3} \\ &= 0.29387 \text{ m}^2. \end{aligned}$$

- viii. Elastic Stiffness K_r

$$\begin{aligned} K_d &= K_r \times \frac{1+12 \times A_p}{A_o} \\ &= 1669.41 \text{ kN/m.} \end{aligned}$$

- ix. Effective area of individual rubber layer (A_{sf})

$$\begin{aligned} A_{sf} &= \frac{\pi d^2}{4} \\ &= 1.05665 \text{ m}^2. \end{aligned}$$

- x. Diameter of rubber (d)

$$d = \sqrt{\frac{4A_{sf}}{\pi}}$$

$$= 1.1599 \text{ m.}$$

- xi. Effective vertical stiffness (kv)

$$K_v = \frac{E_c \times A_{sf}}{t_r}$$

$$K_v = 805961 \text{ kN/m.} \quad \text{Direction } U_1$$

- xii. Reduction factor - Damping (β)

$$\beta = 2 \times \cos^{-1} \left(\frac{D_D}{d} \right)$$

$$= 2.555$$

- xiii. Reduced area (A_2)

$$A_2 = \frac{d^2 \times (\beta - \sin \beta)}{4}$$

$$= 0.67318 \text{ m}^2$$

- xiv. LRB - Details

$$A = 0.67318 \text{ m}^2 \quad (\text{Max Area of } A_0, A_1, \text{ \& } A_2)$$

$$d = 0.92581 \text{ m}$$

$$\text{No. of rubber layer (N)} = t_r/t \quad (\text{where } t = 0.029)$$

$$= 23.1373$$

$$\text{Say (N)} = 24.00$$

- xv. Steel Plate thickness (t_s)

$$t_s = \frac{2 \times W \times 2t}{A \times F_s}$$

$$t_s = 0.0035 \geq 0.002 \text{ m.}$$

- xvi. Total height of bearing (h_b)
- $$h_b = N \times (t_s + 2 \times 0.0025) + t_r$$
- $$h_b = 0.87486 \text{ m.}$$

(C) Input Values in ETABS:

The screenshot shows the 'Link/Support Directional Properties' dialog box. The 'Identification' section includes fields for Property Name (B), Direction (U1), Type (Rubber Isolator), and NonLinear (No). The 'Linear Properties' section includes fields for Effective Stiffness (305961 kN/m) and Effective Damping (0.05 kN-s/m). The dialog has OK and Cancel buttons at the bottom.

**Figure-52. LRB Input Values in ETABS for Biaxial Load 3342 KN
Direction U₁**

Link/Support Directional Properties

Identification

Property Name	B
Direction	U2
Type	Rubber Isolator
NonLinear	Yes

Linear Properties

Effective Stiffness	2151.88	kN/m
Effective Damping	0.05	kN-s/m

Shear Deformation Location

Distance from End-J	0	m
---------------------	---	---

Nonlinear Properties

Stiffness	19828.7	kN/m
Yield Strength	56.7	kN
Post Yield Stiffness Ratio	0.1	

OK Cancel

**Figure-53. LRB Input Values in ETABS for Biaxial Load 3342 KN
Direction U_2 & U_3**

5.4.2 LRB for Uniaxial Load - 4627 KN

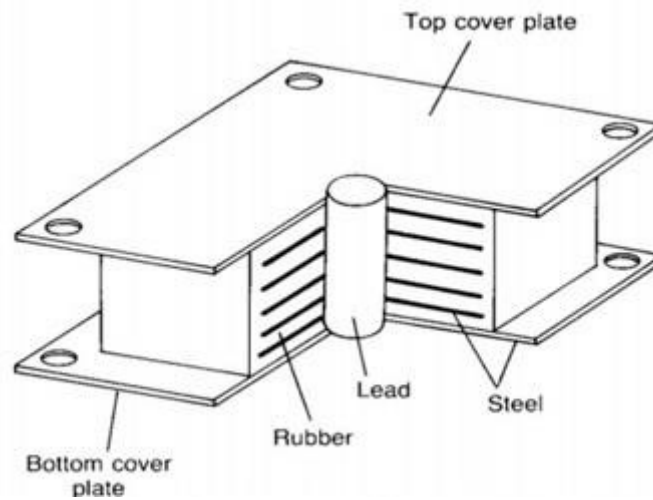


Figure-54. LRB Schematic

Uniaxial Load (W)	= 4627 kN.
Time Period (TD)	= 2.5 sec.
Design Shear Strain (γ_{\max})	= 50%
	= 0.5 kN/m ² .
Effective Damping (ξ_{eff})	= 5%
	= 0.05 For U1,U2,U3.

Table-13. Damping Coefficient, B_D or B_M

EFFECTIVE DAMPING, β_D OR β_M (PERCENTAGE OF CRITICAL)	B_D OR B_M FACTOR
$\leq 2\%$	0.8
5%	1.0
10%	1.2
20%	1.5
30%	1.7
40%	1.9
$\geq 50\%$	2.0

Table-14. Seismic Coefficient C_v

SOIL PROFILE TYPE	SEISMIC ZONE FACTOR, Z				
	$Z=0.075$	$Z=0.15$	$Z=0.2$	$Z=0.3$	$Z=0.4$
S_A	0.06	0.12	0.16	0.24	$0.32N_v$
S_B	0.08	0.15	0.20	0.30	$0.40N_v$
S_C	0.13	0.25	0.32	0.45	$0.56N_v$
S_D	0.18	0.32	0.40	0.54	$0.64N_v$
S_E	0.26	0.50	0.64	0.84	$0.96N_v$
S_F	See Footnote 1				

Damping Coefficient (B_D) = 1.0 (UBC-97, Vol-2, Pg. No. 414)

Seismic Coefficient (S_D) = 0.54 (UBC-97, Vol-2, Pg. No. 35)

Table-15. Vulcanized Natural Rubber Compounds

Hardness IRHD ± 2	Young's Modulus E (MPa)	Shear Modulus G (MPa)	Material Constant k	Elongation at Break Min, %
37	1.35	0.40	0.87	650
40	1.50	0.45	0.85	600
45	1.80	0.54	0.80	600
50	2.20	0.64	0.73	500
55	3.25	0.81	0.64	500
60	4.45	1.06	0.57	400

Choosing 60 for analysis in critical circumstances

$$\begin{aligned}
 E &= 4.45 \\
 &= 4450 \text{ kN/m}^2 \\
 G &= 1.06 \\
 &= 1060 \text{ kN/m}^2 \\
 K &= 0.57 \\
 \epsilon_b &= 4 \\
 &= 400\%
 \end{aligned}$$

$$f_{py} = 8500 \text{ kN/m}^2$$

$$\sigma_a = 7840 \text{ kN/m}^2$$

Typically 7 to 8.5 Mpa, Consult the manufacturer

$$F_s = 164640 \text{ kN/m}^2$$

$$f_y = 274400 \text{ kN/m}^2$$

(A) LRB - Analysis

- i. The effective horizontal stiffness K_{effH}

$$K_{effH} = \frac{W}{g} \left(\frac{2\pi}{T_D} \right)^2$$

$$K_{effH} = 2979.27 \text{ kN/m} \quad \text{Direction } U_2 \text{ \& } U_3$$

- ii. Design displacement (D_D)

$$D_D = \left(\frac{g}{4\pi^2} \right) \times \frac{S_D T_D}{B_D}$$

$$= 0.33546 \text{ m.}$$

- iii. Yield Strength Q_d

$$Q_d = \frac{W_D}{4 \times D_D} = \frac{\pi}{4} \times K_{effH} \times \xi_{effH} \times D_D$$

$$= 78.4952 \text{ kN}$$

- iv. Yield Stiffness

$$K_U = 10 K_d$$

Where, K_d = Post yield stiffness

K_U = Pre yield stiffness

Note- Based on the findings of the trials, the initial elastic stiffness was calculated to be between 9 and 16 K_d .

$$K_d = K_{effH} - \frac{Q_d}{D_D}$$

$$= 2745.28 \text{ kN/m.}$$

$$\begin{aligned} K_U &= 10 K_d \\ &= 27452.8 \text{ kN/m.} \end{aligned}$$

- v. Post yield stiffness ratio.

$$\begin{aligned} \frac{K_d}{K_U} &= \frac{2745.28}{27452.8} \\ &= 0.1 \end{aligned}$$

Direction U₂ & U₃

(B) LRB - Development

- i. Area of Lead Core (A_p)

$$\begin{aligned} A_p &= \frac{Q_d}{f_{py}} \\ &= 0.00923 \text{ m}^2. \end{aligned}$$

- ii. Dia of lead core (d_p)

$$\begin{aligned} A_p &= \frac{\pi d^2}{4} \\ d_p &= \sqrt{\frac{4A_p}{\pi}} \\ &= 0.10843 \text{ m.} \end{aligned}$$

- iii. Thickness of rubber layer (t_r)

$$\begin{aligned} t_r &= \frac{D_D}{\gamma_{\max}} \\ &= 0.67092 \text{ m.} \end{aligned}$$

- iv. The Shape factor (S)

$$\frac{E(1+2kS^2)}{G} \geq 400,$$

$$S = 9.09409$$

For S < 10, Take S = 10

- v. Compressive modulus of rubber & steel (E_c)

$$\begin{aligned} E_c &= E(1+2kS^2) \\ &= 511750 \text{ kN/m}^2. \end{aligned}$$

- vi. Effective area of bearing (A_o)

$$\begin{aligned} A_o &= W / \sigma_a \\ &= 0.59018 \text{ m}^2. \end{aligned}$$

- vii. Shear strain's effective area (A_1)

$$\begin{aligned} \frac{6SW}{E_c \times A_1} &\leq \frac{\epsilon_b}{3} \\ &= 0.40687 \text{ m}^2. \end{aligned}$$

- viii. Elastic Stiffness K_r

$$\begin{aligned} K_d &= K_r \times \frac{1+12 \times A_p}{A_o} \\ &= 2311.29 \text{ kN/m}. \end{aligned}$$

- ix. Effective area of individual rubber layer (A_{sf})

$$\begin{aligned} A_{sf} &= \frac{\pi d^2}{4} \\ &= 1.46293 \text{ m}^2. \end{aligned}$$

- x. Diameter of rubber (d)

$$\begin{aligned} d &= \sqrt{\frac{4A_{sf}}{\pi}} \\ &= 1.36479 \text{ m}. \end{aligned}$$

- xi. Effective vertical stiffness (k_v)

$$K_v = \frac{E_c \times A_{sf}}{t_r}$$

$$K_v = 1115853 \text{ kN/m}.$$

Direction U_1

- xii. Reduction factor - Damping (β)

$$\begin{aligned}\beta &= 2 \times \cos^{-1} \left(\frac{D_D}{d} \right) \\ &= 2.645\end{aligned}$$

- xiii. Reduced area (A_2)

$$\begin{aligned}A_2 &= \frac{d^2 \times (\beta - \sin \beta)}{4} \\ &= 1.00982 \text{ m}^2\end{aligned}$$

- xiv. LRB - Details

$$A = 1.00982 \text{ m}^2 \quad (\text{Max Area of } A_0, A_1, \text{ \& } A_2)$$

$$d = 1.13391 \text{ m}$$

$$\begin{aligned}\text{No. of rubber layer (N)} &= t_r/t \quad (\text{where } t = 0.03412) \\ &= 19.6638\end{aligned}$$

$$\text{Say (N)} = 20$$

- xv. Steel Plate thickness (t_s)

$$t_s = \frac{2 \times W \times 2t}{A \times F_s}$$

$$t_s = 0.0038 \geq 0.002 \text{ m.}$$

- vi. Total height of bearing (h_b)

$$h_b = N \times (t_s + 2 \times 0.0025) + t_r$$

$$h_b = 0.84689 \text{ m.}$$

(C) Input Values in ETABS:

Link/Support Directional Properties

Identification

Property Name	U
Direction	U1
Type	Rubber Isolator
NonLinear	No

Linear Properties

Effective Stiffness	1115853	kN/m
Effective Damping	0.05	kN-s/m

OK Cancel

**Figure-55. LRB Input Values in ETABS for Uniaxial Load 4627 KN
Direction U₁**

Link/Support Directional Properties

Identification

Property Name	U
Direction	U2
Type	Rubber Isolator
NonLinear	Yes

Linear Properties

Effective Stiffness	2979.27	kN/m
Effective Damping	0.05	kN-s/m

Shear Deformation Location

Distance from End-J	0	m
---------------------	---	---

Nonlinear Properties

Stiffness	27452.8	kN/m
Yield Strength	78.5	kN
Post Yield Stiffness Ratio	0.1	

OK Cancel

**Figure-56. LRB Input Values in ETABS for Uniaxial Load 4627 KN
Direction U₂ & U₃**

5.4.3 LRB for Axial Load - 6860 KN

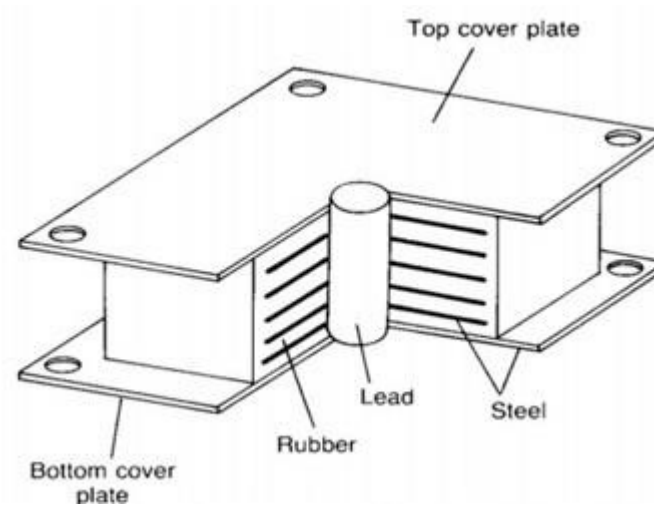


Figure-57. LRB Schematic

Axial Load (W)	= 6860 kN.
Time Period (TD)	= 2.5 sec.
Design Shear Strain (γ_{\max})	= 50%
	= 0.5 kN/m ² .
Effective Damping (ξ_{eff})	= 5%
	= 0.05 For U1,U2,U3.

Table-16. Damping Coefficient, B_D or B_M

EFFECTIVE DAMPING, β_D OR β_M (PERCENTAGE OF CRITICAL)	B_D OR B_M FACTOR
$\leq 2\%$	0.8
5%	1.0
10%	1.2
20%	1.5
30%	1.7
40%	1.9
$\geq 50\%$	2.0

Table-17. Seismic Coefficient C_v

SOIL PROFILE TYPE	SEISMIC ZONE FACTOR, Z				
	$Z=0.075$	$Z=0.15$	$Z=0.2$	$Z=0.3$	$Z=0.4$
S_A	0.06	0.12	0.16	0.24	$0.32N_v$
S_B	0.08	0.15	0.20	0.30	$0.40N_v$
S_C	0.13	0.25	0.32	0.45	$0.56N_v$
S_D	0.18	0.32	0.40	0.54	$0.64N_v$
S_E	0.26	0.50	0.64	0.84	$0.96N_v$
S_F	See Footnote 1				

Damping Coefficient (B_D) = 1.0 (UBC-97, Vol-2, Pg. No. 414)

Seismic Coefficient (S_D) = 0.54 (UBC-97, Vol-2, Pg. No. 35)

Table-18. Vulcanized Natural Rubber Compounds

Hardness IRHD ± 2	Young's Modulus E (MPa)	Shear Modulus G (MPa)	Material Constant k	Elongation at Break Min, %
37	1.35	0.40	0.87	650
40	1.50	0.45	0.85	600
45	1.80	0.54	0.80	600
50	2.20	0.64	0.73	500
55	3.25	0.81	0.64	500
60	4.45	1.06	0.57	400

Choosing 60 for analysis in critical circumstances

$$\begin{aligned}
 E &= 4.45 \\
 &= 4450 \text{ kN/m}^2 \\
 G &= 1.06 \\
 &= 1060 \text{ kN/m}^2 \\
 K &= 0.57 \\
 \epsilon_b &= 4 \\
 &= 400\%
 \end{aligned}$$

$$f_{py} = 8500 \text{ kN/m}^2$$

$$\sigma_a = 7840 \text{ kN/m}^2$$

Typically 7 to 8.5 Mpa, Consult the manufacturer

$$F_s = 164640 \text{ kN/m}^2$$

$$f_y = 274400 \text{ kN/m}^2$$

(A) LRB - Analysis

- i. The effective horizontal stiffness K_{effH}

$$K_{\text{effH}} = \frac{W}{g} \left(\frac{2\pi}{T_D} \right)^2$$

$$K_{\text{effH}} = 4417.08 \text{ kN/m} \quad \text{Direction } U_2 \text{ \& } U_3$$

- ii. Design displacement (D_D)

$$D_D = \left(\frac{g}{4\pi^2} \right) \times \frac{S_D T_D}{B_D}$$

$$= 0.33546 \text{ m.}$$

- iii. Yield Strength Q_d

$$Q_d = \frac{W_D}{4 \times D_D} = \frac{\pi}{4} \times K_{\text{effH}} \times \xi_{\text{effH}} \times D_D$$

$$= 116.377 \text{ kN}$$

- iv. Yield Stiffness

$$K_U = 10 K_d$$

Where, K_d = Post yield stiffness,

K_U = Pre yield stiffness

Note- Based on the findings of the trials, the initial elastic stiffness was calculated to be between 9 and 16 K_d .

$$K_d = K_{\text{effH}} - \frac{Q_d}{D_D}$$

$$= 4070.16 \text{ kN/m.}$$

$$\begin{aligned} K_U &= 10 K_d \\ &= 40701.6 \text{ kN/m.} \end{aligned}$$

- v. Post yield stiffness ratio.

$$\begin{aligned} \frac{K_d}{K_U} &= \frac{4070.16}{40701.6} \\ &= 0.1 \end{aligned}$$

Direction U₂ & U₃

(B) LRB - Development

- i. Area of Lead Core (A_p)

$$\begin{aligned} A_p &= \frac{Q_d}{f_{py}} \\ &= 0.01369 \text{ m}^2. \end{aligned}$$

- ii. Dia of lead core (d_p)

$$\begin{aligned} A_p &= \frac{\pi d^2}{4} \\ d_p &= \sqrt{\frac{4A_p}{\pi}} \\ &= 0.13203 \text{ m.} \end{aligned}$$

- iii. Thickness of rubber layer (t_r)

$$\begin{aligned} t_r &= \frac{D_D}{\gamma_{\max}} \\ &= 0.67092 \text{ m.} \end{aligned}$$

- iv. The Shape factor (S)

$$\frac{E(1+2kS^2)}{G} \geq 400,$$

$$S = 9.09409$$

For S < 10, Take S = 10

- v. Compressive modulus of rubber & steel (E_c)

$$\begin{aligned} E_c &= E(1+2kS^2) \\ &= 511750 \text{ kN/m}^2. \end{aligned}$$

- vi. Effective area of bearing (A_o)

$$\begin{aligned} A_o &= W / \sigma_a \\ &= 0.875 \text{ m}^2. \end{aligned}$$

- vii. Shear strain's effective area (A_1)

$$\begin{aligned} \frac{6SW}{E_c \times A_1} &\leq \frac{\epsilon_b}{3} \\ &= 0.60322 \text{ m}^2. \end{aligned}$$

- viii. Elastic Stiffness K_r

$$\begin{aligned} K_d &= K_r \times \frac{1+12 \times A_p}{A_o} \\ &= 3426.73 \text{ kN/m}. \end{aligned}$$

- ix. Effective area of individual rubber layer (A_{sf})

$$\begin{aligned} A_{sf} &= \frac{\pi d^2}{4} \\ &= 2.16894 \text{ m}^2. \end{aligned}$$

- x. Diameter of rubber (d)

$$\begin{aligned} d &= \sqrt{\frac{4A_{sf}}{\pi}} \\ &= 1.6618 \text{ m}. \end{aligned}$$

- xi. Effective vertical stiffness (k_v)

$$K_v = \frac{E_c \times A_{sf}}{t_r}$$

$$K_v = 1654366 \text{ kN/m}.$$

Direction U_1

xii. Reduction factor - Damping (β)

$$\begin{aligned}\beta &= 2 \times \cos^{-1} \left(\frac{D_D}{d} \right) \\ &= 2.735\end{aligned}$$

xiii. Reduced area (A_2)

$$\begin{aligned}A_2 &= \frac{d^2 \times (\beta - \sin \beta)}{4} \\ &= 1.61519 \text{ m}^2\end{aligned}$$

xiv. LRB - Details

$$A = 1.61519 \text{ m}^2 \quad (\text{Max Area of } A_0, A_1, \text{ \& } A_2)$$

$$d = 1.43406 \text{ m}$$

$$\begin{aligned}\text{No. of rubber layer (N)} &= t_r/t \quad (\text{where } t = 0.04154) \\ &= 16.1493\end{aligned}$$

$$\text{Say (N)} = 17$$

xv. Steel Plate thickness (t_s)

$$t_s = \frac{2 \times W \times 2t}{A \times F_s}$$

$$t_s = 0.00429 \geq 0.002 \text{ m.}$$

xvi. Total height of bearing (h_b)

$$h_b = N \times (t_s + 2 \times 0.0025) + t_r$$

$$h_b = 0.8288 \text{ m.}$$

(C) Input Values in ETABS:

Link/Support Directional Properties

Identification

Property Name	A
Direction	U1
Type	Rubber Isolator
NonLinear	No

Linear Properties

Effective Stiffness	1654366	kN/m
Effective Damping	0.05	kN-s/m

OK Cancel

**Figure-58. LRB Input Values in ETABS for Axial Load 6860 KN
Direction U₁**

Link/Support Directional Properties

Identification

Property Name	A
Direction	U2
Type	Rubber Isolator
NonLinear	Yes

Linear Properties

Effective Stiffness	4417.08	kN/m
Effective Damping	0.05	kN-s/m

Shear Deformation Location

Distance from End-J	0	m
---------------------	---	---

Nonlinear Properties

Stiffness	40701.6	kN/m
Yield Strength	116.38	kN
Post Yield Stiffness Ratio	0.1	

OK Cancel

**Figure-59. LRB Input Values in ETABS for Axial Load 6860 KN
Direction U₂ & U₃**

5.5 Design of TFPB for G+22 Storey RC Structure.

For the analysis & design of TFPB, the cumulative load at the base is obtained from the fixed based design modal in ETABS-2016. This load is categorized into three groups viz. Axial load, Biaxial load and Uniaxial load.

5.5.1 TFPB for Biaxial Load - 3342 KN

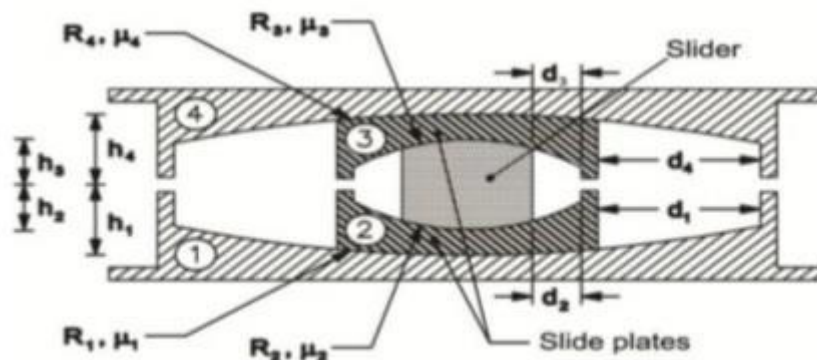


Figure-60. TFPB Schematic

(A) Geometrical, Frictional and D_D Computation

a. Geometrical features

$$\begin{aligned}
 R_4 &= R_1 &= 1778 \times 2 \\
 &&= 3556 \text{ mm} \\
 &&= 3.556 \text{ mtrs.} \\
 R_2 &= R_3 &= 647 \text{ mm} \\
 &&= 0.647 \text{ mtrs} \\
 h_1 &= h_4 &= 161 \text{ mm} \\
 &&= 0.161 \text{ mtrs} \\
 h_2 &= h_3 &= 121 \text{ mm} \\
 &&= 0.121 \text{ mtrs} \\
 d_1 &= 566.02 \text{ mm}
 \end{aligned}$$

$$d_2 = 81.05 \text{ mm}$$

$$\begin{aligned} R_{1\text{eff}} &= R_{4\text{eff}} &= R_1 - h_1 \\ & &= 3556 - 161 \\ & &= 3395 \text{ mm} \end{aligned}$$

$$\begin{aligned} R_{2\text{eff}} &= R_{3\text{eff}} &= R_2 - h_2 \\ & &= 647 - 121 \\ & &= 526 \text{ mm} \end{aligned}$$

$$\begin{aligned} d_4^* &= d_1^* &= \frac{d_1 \times R_{1\text{eff}}}{R_1} \\ & &= 540.39 \text{ mm} \\ & &\approx 540.40 \text{ mm} \end{aligned}$$

$$\begin{aligned} d_2^* &= d_3^* &= \frac{d_2 \times R_{2\text{eff}}}{R_2} \\ & &= 65.89 \text{ mm} \\ & &\approx 65.90 \text{ mm.} \end{aligned}$$

b. Frictional Characteristics Computation

At 1 and 4

$$P = W / A$$

$$\text{Here W Load} = 334.2 \text{ tonne or } 3342 \text{ KN,}$$

$$A = \pi r^2$$

$$\begin{aligned} r &= h_4 + h_1 \\ &= 161 + 161 \end{aligned}$$

$$r = 322 \text{ mm}$$

$$P = 0.001026 \text{ ton/mm}^2,$$

$$P = 0.001026 \times 1450$$

$$\begin{aligned} P &= 1.49 \text{ ksi,} & 1 \text{ ksi} &= \text{Kilo square inch} \\ & & &= 1450 \text{ ton/mm}^2 \end{aligned}$$

$$\begin{aligned} \text{3- Friction Cycle} & \mu &= 0.122 - 0.01 P, \end{aligned}$$

$$\mu = 0.1071$$

$$\begin{aligned}
 \text{Adjust for high velocity} &= \mu - 0.0333 \\
 &= 0.1071 - 0.0333 \\
 &= 0.074 \text{ (Lower bound)} \\
 1 - \text{Friction Cycle} \quad \mu &= 1.2 \times 0.074 \\
 &= 0.0886 \\
 \mu_1 &= \mu_4 = 0.074 \text{ (Lower bound)} \\
 \mu_1 &= \mu_4 = 0.089 \text{ (Upper bound)}
 \end{aligned}$$

At 2 and 3

$$P = W / A$$

$$\text{Here W Load} = 334.2 \text{ tonne or } 3342 \text{ KN,}$$

$$A = \pi r^2$$

$$\begin{aligned}
 r &= h_2 + h_3 \\
 &= 121 + 121 \\
 &= 242 \text{ mm}
 \end{aligned}$$

$$P = 0.001816 \text{ ton/mm}^2,$$

$$P = 0.001816 \times 1450$$

$$\begin{aligned}
 P &= 2.63 \text{ ksi.} \quad 1 \text{ ksi} = \text{Kilo square inch} \\
 &= 1450 \text{ ton/mm}^2
 \end{aligned}$$

$$\begin{aligned}
 3 - \text{Friction Cycle} \quad \mu &= 0.122 - 0.01 P \\
 &= 0.0957
 \end{aligned}$$

$$\begin{aligned}
 \text{Adjust for high velocity} &= \mu - 0.036 \\
 &= 0.0957 - 0.036 \\
 &= 0.060 \text{ (Lower bound)}
 \end{aligned}$$

$$\begin{aligned}
 1 - \text{Friction Cycle} \quad \mu &= 1.2 \times 0.060 \\
 &= 0.0716
 \end{aligned}$$

$$\text{Lower bound} \quad \mu_2 = \mu_3 = 0.060$$

$$\text{Upper bound} \quad \mu_2 = \mu_3 = 0.072$$

$$\mu = \text{force at zero deformation}$$

$$\mu = \mu_1 - (\mu_1 - \mu_2) \times \frac{R_{2\text{eff}}}{R_{1\text{eff}}} \text{ (Lower bound)}$$

$$\mu = 0.072$$

$$\mu = \mu_1 - (\mu_1 - \mu_2) \times \frac{R_{2eff}}{R_{1eff}} \quad (\text{Upper bound})$$

$$\mu = 0.086$$

c. D_b Computation (Upper bound)

$$S_d = 0.5074$$

$$\mu = 0.086$$

$$\mu_1 = 0.089$$

$$D_y = (\mu_1 - \mu_2) * R_{2eff}$$

$$D_y = 0.008939$$

$$F_d = 0.2772$$

$$W = 334.2 \text{ Ton}$$

$$\text{T.B.} = 12 \text{ Nos. (Where T.B. = Total Bearing)}$$

$$\Sigma F_d = W \times \text{T.B.} \times F_d$$

$$= 334.2 \times 12 \times 0.2772$$

$$\Sigma F_d = 1111.86$$

$$\Sigma W = W \times \text{T.B.}$$

$$\Sigma W = 4010.4 \text{ Ton}$$

i. Design displacement, D_D = 0.07202 m.

ii. Effective stiffness, Q_d = $\mu * \Sigma W$

$$= 0.086 * 4010.4$$

$$Q_d = 344.71 \text{ Ton}$$

$$k_D = \Sigma F_D / D_D$$

$$= 1111.86 / 0.07202$$

$$k_D = 15438.15 \text{ Ton/m.}$$

$$K_{eff} = k_D + Q_D / D_D$$

$$= 15438.15 + 344.71 / 0.07202$$

$$K_{eff} = 20224.50 \text{ Ton/m.}$$

iii. **Effective period, T_{eff}**

$$T_{\text{eff}} = [\sqrt{(\sum w)/(K_{\text{eff}} \times g))}] 2\pi$$

$$T_{\text{eff}} = 0.89331 \text{ sec.}$$

iv. **Effective damping, β_{eff}**

$$\beta_D = \frac{E}{2\pi K_{\text{eff}} \times D_D^2} = \frac{4\mu \sum w (D_D - D_y)}{2\pi K_{\text{eff}} \times D_D^2}$$

$$\beta_{\text{eff}} = \beta_D = 0.1320$$

v. **Damping reduction Coefficient, β**

$$\beta = \left(\frac{\beta_{\text{eff}}}{0.05}\right)^{0.3}$$

$$\beta = 1.3380$$

vi. **D_D^1**

$$D_D^1 = \frac{S_D \times T_{\text{eff}}^2}{4\pi^2 \times \beta} \times g$$

$$D_D^1 = 0.0752 \text{ mtrs}$$

(B) ETABS links directional property computation (upper bound)**a. Principal features****i. Determine bearing**

The isolator had been envisioned cylinder with a height of 0.32 metres and a diameter of 0.305 metres

$$H = 0.5 \text{ m}$$

$$\varnothing = 0.484 \text{ m}$$

$$\begin{aligned} \text{Now, Area} \quad A &= \frac{\pi \times \varnothing^2}{4} \\ &= \frac{\pi \times 0.484^2}{4} \\ A &= 0.1840 \text{ m}^2 \end{aligned}$$

$$\begin{aligned}
 K_{\text{eff}} &= \frac{W}{R_{1\text{eff}}} + \frac{\mu w}{D_D} \\
 K_{\text{eff}} &= 497.30 \text{ Ton/m} \\
 I_1 &= \frac{K_{\text{eff}} \times h^3}{12E} = \frac{497.30 \times 0.5^3}{12E} \\
 &= 5.18022\text{E-}07 \text{ m}^4. \\
 E &= 1 \times 10^7 \text{ N/mm}^2
 \end{aligned}$$

ii. **Determine bearing mass**

$$\begin{aligned}
 D_{\text{m-max}} &= 0.0702 \text{ m.} \\
 D_{\text{TM}} &= 1.15 \times D_{\text{m-max}} \\
 &= 1.15 \times 0.0702 \\
 D_{\text{TM}} &= 0.0807 \text{ m.} \\
 D &= 2 D_{\text{TM}} \\
 &= 2 \times 0.0807 \\
 D &= 0.16146 \text{ m.} \\
 w &= 0.241 D^2 - 0.00564 D \\
 w &= 0.0053721 \text{ tonne.} \\
 M &= w / g \\
 &= 0.005372 / 9.81 \\
 M &= 0.000548 \text{ tonne sec}^2/\text{m.}
 \end{aligned}$$

b. Direction (U₁)

$$\begin{aligned}
 H &= 0.5 \text{ m} \\
 \varnothing &= 0.484 \text{ m} \\
 K_{\text{eff}} &= AE / L \\
 K_{\text{eff}} &= 3679684.643 \text{ ton/m.} \\
 \mathbf{K_{\text{ef}}} &= \mathbf{36796846.43 \text{ KN/m.}}
 \end{aligned}$$

from D_D

$$K_{\text{eff}} = 3679684.64 \text{ ton/m.}$$

$$\beta_{\text{eff}} = 0.1320$$

c. Direction ($U_2 - U_3$)

i. Determination of liner properties.

$$K_{\text{eff}} = 497.301 \text{ ton/m}$$

$$= 4973.01 \text{ KN/m}$$

$$\beta_{\text{eff}} = 0.1320$$

$$\text{Height for outer surface, } = h_1 = h_4 = 0.161 \text{ m.}$$

$$\text{Height for inner surface, } = h_2 = h_3 = 0.121 \text{ m.}$$

ii. Determination of Non - liner properties.

$$R_{2 \text{ eff}} = 0.526 \text{ mtrs.}$$

$$D_y = (\mu_1 - \mu_2) R_{2 \text{ eff}}$$

$$= (0.08859 - 0.07159) \times 0.526$$

$$D_y = 0.00894 \text{ mtrs.}$$

$$\begin{aligned} \text{Stiffness (Outer Top)} &= \frac{\mu_1 W}{D_y} \\ &= \frac{0.08859 \times 334.2}{0.00894} \\ &= 3312.041 \text{ ton/m.} \\ &= 33120.41 \text{ KN/m.} \end{aligned}$$

$$\begin{aligned} \text{Stiffness (Inner Top)} &= \frac{\mu_2 W}{D_y} \\ &= \frac{0.07159 \times 334.2}{0.00894} \\ &= 2676.680 \text{ ton/m.} \end{aligned}$$

$$= 26766.80 \text{ KN/m.}$$

$$\begin{aligned} \text{Friction Coefficient, Slow} &= \mu_1 = 0.089 \text{ (Outer Top)} \\ &= \mu_2 = 0.072 \text{ (Inner Top)} \end{aligned}$$

$$\begin{aligned} \text{Friction Coefficient, Fast} &= 2 \times \mu_1 = 0.177 \text{ (Outer Top)} \\ &= 2 \times \mu_2 = 0.143 \text{ (Inner Top)} \end{aligned}$$

$$\begin{aligned} \text{Rate Parameter} &= \frac{\text{Friction Coeff. Slow}}{\text{Friction Coeff. Fast}} \\ &= 0.089 / 0.177 \\ &= 0.5 \\ &= 0.0005 \text{ sec/mm} \end{aligned}$$

Radius of sliding surface

$$\begin{aligned} \text{Outer Top} &= R_{1 \text{ eff}} = 3.395 \text{ m} \\ \text{Inner Top} &= R_{2 \text{ eff}} = 0.526 \text{ m} \end{aligned}$$

Stop distance

$$\begin{aligned} \text{Outer Top } u_1^* &= 2 D_y + 2 d_1^* \\ &= 1.09868 \text{ m} \\ &= 1098.68 \text{ mm} \\ \text{Inner Top } u_2^* &= 2 D_y \\ &= 0.0179 \text{ m} \\ &= 17.878 \text{ mm} \end{aligned}$$

(C) Input Values in ETABS:

Link/Support Directional Properties

Identification

Property Name	B
Direction	U1
Type	Triple Pendulum Isolator
NonLinear	Yes

Linear Properties

Effective Stiffness	36796846.43	kN/m
Effective Damping	1.338	kN-s/m

Nonlinear Properties

Stiffness	36796846.43	kN/m
Damping Coefficient	1.338	kN-s/m

OK Cancel

**Figure-61. TFPB Input Values in ETABS for Biaxial Load 3342 KN
Direction U₁**

Link/Support Directional Properties

Identification

Property Name: B Type: Triple Pendulum Isolator

Direction: U2; U3 NonLinear: Yes

Linear Properties

Effective Stiffness - U2: 4973.014 kN/m Effective Stiffness - U3: 4973.014 kN/m

Effective Damping - U2: 1.338 kN-s/m Effective Damping - U3: 1.338 kN-s/m

Shear Deformation Location

Distance from End-J - U2: 0 m Distance from End-J - U3: 0 m

Height and Symmetry of Sliding Surfaces

Height for Outer Surfaces: 0.161 m ☒ Outer Bottom Surface is Symmetric to Outer Top Surface

Height for Inner Surfaces: 0.121 m ☒ Inner Bottom Surface is Symmetric to Inner Top Surface

Nonlinear Properties for Directions U2 and U3

	Outer Top	Outer Bottom	Inner Top	Inner Bottom	
Stiffness	33120.415	33120.415	26766.8	26766.8	kN/m
Friction Coefficient, Slow	0.088587	0.088587	0.071593	0.071593	
Friction Coefficient, Fast	0.177175	0.177175	0.143187	0.143187	
Rate Parameter	0.0005	0.0005	0.0005	0.0005	sec/mm
Radius of Sliding Surface	3.395	3.395	0.526	0.526	m
Stop Distance	1098.677	1098.677	17.877	17.877	mm

OK Cancel

**Figure-62. TFPB Input Values in ETABS for Biaxial Load 3342 KN
Direction U₂ & U₃**

5.5.2 TFPB for Uniaxial Load - 4627 KN

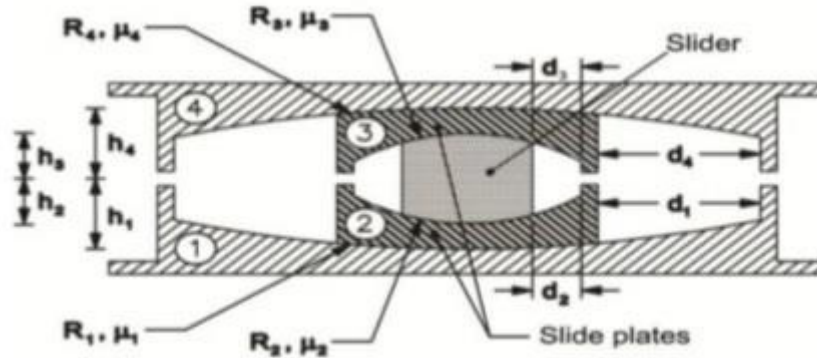


Figure-63. TFPB Schematic

(A) Geometrical, Frictional and D_D Computation

a. Geometrical features

$$\begin{aligned}
 R_4 &= R_1 = 1778 \times 2 \\
 &= 3556 \text{ mm} \\
 &= 3.556 \text{ m} \\
 R_2 &= R_3 = 647 \text{ mm} \\
 &= 0.647 \text{ m} \\
 h_1 &= h_4 = 161 \text{ mm} \\
 &= 0.161 \text{ m} \\
 h_2 &= h_3 = 121 \text{ mm} \\
 &= 0.121 \text{ m} \\
 d_1 &= 566.02 \text{ mm} \\
 d_2 &= 81.05 \text{ mm} \\
 R_{1\text{eff}} &= R_{4\text{eff}} = R_1 - h_1
 \end{aligned}$$

$$\begin{aligned}
 &= 3556 - 161 \\
 &= 3395 \text{ mm} \\
 R_{2\text{eff}} &= R_{3\text{eff}} &= R_2 - h_2 \\
 &= 647 - 121 \\
 &= 526 \text{ mm} \\
 d_4^* &= d_1^* &= \frac{d_1 \times R_{1\text{eff}}}{R_1} \\
 &= 540.39 \text{ mm} \\
 &\approx 540.40 \text{ mm.} \\
 d_2^* &= d_3^* &= \frac{d_2 \times R_{2\text{eff}}}{R_2} \\
 &= 65.89 \text{ mm} \\
 &\approx 65.90 \text{ mm.}
 \end{aligned}$$

b. Frictional Characteristics Computation

At surfaces 1 and 4

$$P = W / A$$

$$\text{Here W Load} = 462.7 \text{ tonne or } 4627 \text{ KN,}$$

$$A = \pi r^2$$

$$r = h_4 + h_1$$

$$= 161 + 161$$

$$r = 322 \text{ mm}$$

$$P = 0.001420 \text{ ton/mm}^2,$$

$$P = 0.001420 \times 1450$$

$$P = 02.06 \text{ ksi, } 1 \text{ ksi} = \text{Kilo square inch}$$

$$= 1450 \text{ ton/mm}^2$$

$$3\text{- Friction Cycle } \mu = 0.122 - 0.01 P$$

$$\mu = 0.1014$$

$$\text{Adjust for high velocity} = \mu - 0.0333$$

$$= 0.1014 - 0.0333$$

$$\begin{aligned}
 &= 0.068 \text{ (Lower bound)} \\
 \text{1 - Friction Cycle} \quad \mu &= 1.2 \times 0.068 \\
 &= 0.0817
 \end{aligned}$$

$$\begin{aligned}
 \mu_1 &= \mu_4 = 0.068 \text{ (Lower bound)} \\
 \mu_1 &= \mu_4 = 0.082 \text{ (Upper bound)}
 \end{aligned}$$

At 2 and 3

$$P = W / A$$

$$\text{Here W Load} = 462.7 \text{ tonne or } 4627 \text{ KN,}$$

$$A = \pi r^2$$

$$\begin{aligned}
 r &= h_2 + h_3 \\
 &= 121 + 121 \\
 &= 242 \text{ mm}
 \end{aligned}$$

$$P = 0.002515 \text{ ton/mm}^2$$

$$P = 0.002515 \times 1450$$

$$\begin{aligned}
 P &= 3.65 \text{ ksi.} \quad 1 \text{ ksi} = \text{Kilo square inch} \\
 &= 1450 \text{ ton/mm}^2
 \end{aligned}$$

$$\begin{aligned}
 \text{3- Friction Cycle} \quad \mu &= 0.122 - 0.01 P \\
 &= 0.0855
 \end{aligned}$$

$$\begin{aligned}
 \text{Adjust for high velocity} &= \mu - 0.036 \\
 &= 0.0855 - 0.036 \\
 &= 0.050 \text{ (Lower bound)}
 \end{aligned}$$

$$\begin{aligned}
 \text{1 - Friction Cycle} \quad \mu &= 1.2 \times 0.050 \\
 &= 0.0594
 \end{aligned}$$

$$\mu_2 = \mu_3 = 0.050 \text{ (Lower bound)}$$

$$\mu_2 = \mu_3 = 0.059 \text{ (Upper bound)}$$

$$\mu = \text{force at zero deformation}$$

$$\mu = \mu_1 - (\mu_1 - \mu_2) \times \frac{R_{2\text{eff}}}{R_{1\text{eff}}} \text{ (Lower bound)}$$

$$\mu = 0.065$$

$$\mu = \mu_1 - (\mu_1 - \mu_2) \times \frac{R_{2\text{eff}}}{R_{1\text{eff}}} \text{ (Upper bound)}$$

$$\mu = 0.078$$

c. D_D Computation (Upper bound)

$$S_d = 0.5074$$

$$\mu = 0.078$$

$$\mu_1 = 0.082$$

$$D_y = (\mu_1 - \mu_2) * R_{2eff}$$

$$D_y = 0.011721$$

$$F_d = 0.2772$$

$$W = 462.7 \text{ Ton}$$

$$T.B. = 12 \text{ Nos. (Where T.B. = Total Bearing)}$$

$$\begin{aligned} \Sigma F_d &= W \times T.B. \times F_d \\ &= 462.7 \times 12 \times 0.2772 \end{aligned}$$

$$\Sigma F_d = 1539.36$$

$$\Sigma W = W \times T.B.$$

$$\Sigma W = 5552.4 \text{ Ton}$$

i. Design displacement, D_D = 0.07202 mtrs.

ii. Effective stiffness, Q_d

$$\begin{aligned} &= \mu * \Sigma W \\ &= 0.078 * 5552.4 \\ Q_d &= 434.59 \text{ Ton} \\ k_D &= \Sigma F_D / D_D \\ &= 1539.36 / 0.07202 \\ k_D &= 21374.12 \text{ Ton/m.} \\ K_{eff} &= k_D + Q_D / D_D \\ &= 21374.12 + 434.59 / 0.07202 \\ K_{eff} &= 27408.45 \text{ Ton/m.} \end{aligned}$$

iii. Effective period, T_{eff}

$$\begin{aligned} T_{eff} &= [\sqrt{((\Sigma W) / (K_{eff} \times g))}] 2\pi \\ T_{eff} &= 0.90291 \text{ sec.} \end{aligned}$$

iv. **Effective damping, β_{eff}**

$$\beta_D = \frac{E}{2\pi K_{\text{eff}} \times D_D^2} = \frac{4\mu \Sigma w(D_D - D_y)}{2\pi K_{\text{eff}} \times D_D^2}$$

$$\beta_{\text{eff}} = \beta_D = 0.1174$$

v. **Damping reduction Coefficient, β**

$$\beta = \left(\frac{\beta_{\text{eff}}}{0.05} \right)^{0.3}$$

$$\beta = 1.2917$$

vi. **D_D^1**

$$D_D^1 = \frac{S_{D1} \times T_{\text{eff}}^2}{4\pi^2 \times \beta} \times g$$

$$D_D^1 = 0.0796 \text{ mtrs}$$

(B) ETABS links directional property Computation (upper bound)**a. Principal features****i. Determine bearing**

The isolator had been envisioned cylinder with a height of 0.32 metres and a diameter of 0.305 metres

$$H = 0.5 \text{ m.}$$

$$\varnothing = 0.484 \text{ m,}$$

$$\begin{aligned} \text{Now, Area} \quad A &= \frac{\pi \times \varnothing^2}{4} \\ &= \frac{\pi \times 0.484^2}{4} \\ A &= 0.1840 \text{ m}^2 \end{aligned}$$

$$K_{\text{eff}} = \frac{W}{R_{1\text{eff}}} + \frac{\mu w}{D_D}$$

$$K_{\text{eff}} = 639.15 \text{ Ton/m}$$

$$\begin{aligned} I_1 &= \frac{K_{\text{eff}} \times h^3}{12E} = \frac{639.15 \times 0.5^3}{12E} \\ &= 6.65781\text{E-}07 \text{ m}^4 \end{aligned}$$

$$E = 1 \times 10^7 \text{ N/mm}^2$$

ii. **Determine bearing mass**

$$D_{m-\max} = 0.0702 \text{ m.}$$

$$\begin{aligned} D_{TM} &= 1.15 \times D_{m-\max} \\ &= 1.15 \times 0.0702 \end{aligned}$$

$$D_{TM} = 0.0807 \text{ m.}$$

$$\begin{aligned} D &= 2 D_{TM} \\ &= 2 \times 0.0807 \end{aligned}$$

$$D = 0.16146 \text{ m.}$$

$$w = 0.241 D^2 - 0.00564 D$$

$$w = 0.0053721 \text{ tonne.}$$

$$\begin{aligned} M &= w / g \\ &= 0.005372 / 9.81 \end{aligned}$$

$$M = 0.000548 \text{ tonne sec}^2/\text{m.}$$

b. Direction (U_1)

$$H = 0.5 \text{ m}$$

$$\varnothing = 0.484 \text{ m}$$

$$K_{\text{eff}} = AE / L$$

$$K_{\text{eff}} = 3679684.643 \text{ ton/m.}$$

$$K_{\text{eff}} = \mathbf{36796846.43 \text{ KN/m.}}$$

from D_D

$$K_{\text{eff}} = 3679684.64 \text{ ton/m.}$$

$$\beta_{\text{eff}} = 0.1174$$

c. Direction ($U_2 - U_3$)**i. Determination of liner properties.**

$$K_{\text{eff}} = 639.150 \text{ ton/m}$$

$$= 6391.50 \text{ KN/m}$$

$$\beta_{\text{eff}} = 0.1174$$

$$\text{Height for outer surface, } = h_1 = h_4 = \mathbf{0.161 \text{ mtrs.}}$$

$$\text{Height for inner surface, } = h_2 = h_3 = \mathbf{0.121 \text{ mtrs.}}$$

ii. Determination of Non - liner properties.

$$R_{2\text{eff}} = 0.526 \text{ mtrs.}$$

$$D_y = (\mu_1 - \mu_2) R_{2\text{eff}}$$

$$= (0.08172 - 0.05944) \times 0.526$$

$$D_y = 0.01172 \text{ mtrs.}$$

$$\begin{aligned} \text{Stiffness (Outer Top)} &= \frac{\mu_1 W}{D_y} \\ &= \frac{0.08172 \times 462.7}{0.01172} \\ &= 3226.231 \text{ ton/m.} \\ &= \mathbf{32262.31 \text{ KN/m.}} \end{aligned}$$

$$\begin{aligned} \text{Stiffness (Inner Top)} &= \frac{\mu_2 W}{D_y} \\ &= \frac{0.05944 \times 462.7}{0.01172} \\ &= 2346.573 \text{ ton/m.} \\ &= \mathbf{23465.73 \text{ KN/m.}} \end{aligned}$$

$$\text{Friction Coefficient, Slow} = \mu_1 = \mathbf{0.082 \text{ (Outer Top)}}$$

$$= \mu_2 = \mathbf{0.059 \text{ (Inner Top)}}$$

$$\begin{aligned}\text{Friction Coefficient, Fast} &= 2 \times \mu_1 = \mathbf{0.163 \text{ (Outer Top)}} \\ &= 2 \times \mu_2 = \mathbf{0.119 \text{ (Inner Top)}}\end{aligned}$$

$$\begin{aligned}\text{Rate Parameter} &= \frac{\text{Friction Coeff. Slow}}{\text{Friction Coeff. Fast}} \\ &= 0.082 / 0.163 \\ &= 0.5 \\ &= \mathbf{0.0005 \text{ sec/mm}}\end{aligned}$$

Radius of sliding surface

$$\begin{aligned}\text{Outer Top} &= R_{1 \text{ eff}} = \mathbf{3.395 \text{ mtrs.}} \\ \text{Inner Top} &= R_{2 \text{ eff}} = \mathbf{0.526 \text{ mtrs.}}\end{aligned}$$

Stop distance

$$\begin{aligned}\text{Outer Top } u_1^* &= 2 D_y + 2 d_1^* \\ &= 1.10424 \text{ mtrs.} \\ &= \mathbf{1104.24 \text{ mm}}\end{aligned}$$

$$\begin{aligned}\text{Inner Top } u_2^* &= 2 D_y \\ &= 0.0234 \text{ mtrs.} \\ &= \mathbf{23.441 \text{ mm.}}\end{aligned}$$

(C) Input Values in ETABS:

Link/Support Directional Properties

Identification

Property Name	U
Direction	U1
Type	Triple Pendulum Isolator
NonLinear	Yes

Linear Properties

Effective Stiffness	36796846.43	kN/m
Effective Damping	1.292	kN-s/m

Nonlinear Properties

Stiffness	36796846.43	kN/m
Damping Coefficient	1.292	kN-s/m

OK Cancel

**Figure-64. TFPB Input Values in ETABS for Uniaxial Load 4627 KN
Direction U₁**

Link/Support Directional Properties

Identification

Property Name: U Type: Triple Pendulum Isolator

Direction: U2; U3 NonLinear: Yes

Linear Properties

Effective Stiffness - U2: 6391.499 kN/m Effective Stiffness -U3: 6391.499 kN/m

Effective Damping - U2: 1.292 kN-s/m Effective Damping -U3: 1.292 kN-s/m

Shear Deformation Location

Distance from End-J - U2: 0 m Distance from End-J - U3: 0 m

Height and Symmetry of Sliding Surfaces

Height for Outer Surfaces: 0.161 m ☒ Outer Bottom Surface is Symmetric to Outer Top Surface

Height for Inner Surfaces: 0.121 m ☒ Inner Bottom Surface is Symmetric to Inner Top Surface

Nonlinear Properties for Directions U2 and U3

	Outer Top	Outer Bottom	Inner Top	Inner Bottom	
Stiffness	32262.308	32262.308	23465.73	23465.73	kN/m
Friction Coefficient, Slow	0.081723	0.081723	0.05944	0.05944	
Friction Coefficient, Fast	0.163446	0.163446	0.11888	0.11888	
Rate Parameter	0.0005	0.0005	0.0005	0.0005	sec/mm
Radius of Sliding Surface	3.395	3.395	0.526	0.526	m
Stop Distance	1104.24	1104.24	23.44	23.44	mm

OK Cancel

**Figure-65. TFPB Input Values in ETABS for Uniaxial Load 4627 KN
Direction U₂ & U₃**

5.5.3 TFPB for Axial Load - 6860 KN

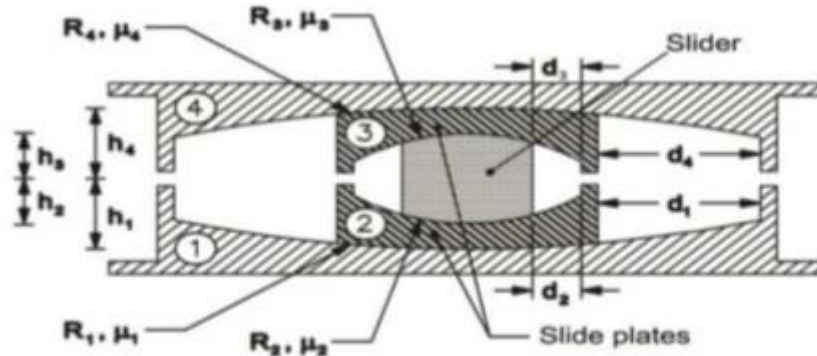


Figure-66. TFPB Schematic

(A) Geometrical, Frictional and D_D Computation

a. Geometrical features

$$\begin{aligned}
 R_4 &= R_1 &= 1778 \times 2 \\
 &&= 3556 \text{ mm} \\
 &&= 3.556 \text{ m} \\
 R_2 &= R_3 &= 647 \text{ mm} \\
 &&= 0.647 \text{ m} \\
 h_1 &= h_4 &= 161 \text{ mm} \\
 &&= 0.161 \text{ m} \\
 h_2 &= h_3 &= 121 \text{ mm} \\
 &&= 0.121 \text{ m} \\
 d_1 &= 566.02 \text{ mm} \\
 d_2 &= 81.05 \text{ mm} \\
 R_{1\text{eff}} &= R_{4\text{eff}} &= R_1 - h_1 \\
 &&= 3556 - 161 \\
 &&= 3395 \text{ mm}
 \end{aligned}$$

$$\begin{aligned}
 R_{2\text{eff}} &= R_{3\text{eff}} &= R_2 - h_2 \\
 & &= 647 - 121 \\
 & &= 526 \text{ mm} \\
 d_4^* &= d_1^* &= \frac{d_1 \times R_{1\text{eff}}}{R_1} \\
 & &= 540.39 \text{ mm} \\
 & &\approx 540.40 \text{ mm} \\
 d_2^* &= d_3^* &= \frac{d_2 \times R_{2\text{eff}}}{R_2} \\
 & &= 65.89 \text{ mm} \\
 & &\approx 65.90 \text{ mm}
 \end{aligned}$$

b. Frictional Characteristics Computation

At 1 and 4

$$P = W / A$$

$$\text{Here } W \text{ Load} = 686.0 \text{ tonne or } 6860 \text{ KN}$$

$$A = \pi r^2$$

$$\begin{aligned}
 r &= h_4 + h_1 \\
 &= 161 + 161
 \end{aligned}$$

$$r = 322 \text{ mm}$$

$$P = 0.002106 \text{ ton/mm}^2,$$

$$P = 0.002106 \times 1450$$

$$\begin{aligned}
 P &= 3.05 \text{ ksi}, & 1 \text{ ksi} &= \text{Kilo square inch} \\
 & & &= 1450 \text{ ton/mm}^2
 \end{aligned}$$

$$\begin{aligned}
 \text{3- Friction Cycle } \mu &= 0.122 - 0.01 P, \\
 \mu &= 0.0915
 \end{aligned}$$

$$\begin{aligned}
 \text{Adjust for high velocity} &= \mu - 0.0333 \\
 &= 0.0915 - 0.0333 \\
 &= 0.058 \text{ (Lower bound)}
 \end{aligned}$$

$$\begin{aligned}
 \text{1 - Friction Cycle } \mu &= 1.2 \times 0.058 \\
 &= 0.0698
 \end{aligned}$$

$$\mu_1 = \mu_4 = 0.058 \text{ (Lower bound)}$$

$$\mu_1 = \mu_4 = 0.070 \text{ (Upper bound)}$$

At 2 and 3

$$P = W / A$$

$$\text{Here } W \text{ Load} = 686.0 \text{ tonne or } 6860 \text{ KN}$$

$$A = \pi r^2$$

$$\begin{aligned} r &= h_2 + h_3 \\ &= 121 + 121 \\ &= 242 \text{ mm} \end{aligned}$$

$$P = 0.003729 \text{ ton/mm}^2,$$

$$P = 0.003729 \times 1450$$

$$\begin{aligned} P &= 5.41 \text{ ksi.} \quad 1 \text{ ksi} = \text{Kilo square inch} \\ &= 1450 \text{ ton/mm}^2 \end{aligned}$$

$$\begin{aligned} \text{3- Friction Cycle } \mu &= 0.122 - 0.01 P \\ &= 0.0679 \end{aligned}$$

$$\begin{aligned} \text{Adjust for high velocity} &= \mu - 0.036 \\ &= 0.0679 - 0.036 \\ &= 0.032 \text{ (Lower bound)} \end{aligned}$$

$$\begin{aligned} \text{1 – Friction Cycle } \mu &= 1.2 \times 0.032 \\ &= 0.0383 \end{aligned}$$

$$\mu_2 = \mu_3 = 0.032 \text{ (Lower bound)}$$

$$\mu_2 = \mu_3 = 0.038 \text{ (Upper bound)}$$

$$\mu = \text{force at zero deformation}$$

$$\mu = \mu_1 - (\mu_1 - \mu_2) \times \frac{R_{2\text{eff}}}{R_{1\text{eff}}} \text{ (Lower bound)}$$

$$\mu = 0.054$$

$$\mu = \mu_1 - (\mu_1 - \mu_2) \times \frac{R_{2\text{eff}}}{R_{1\text{eff}}} \text{ (Upper bound)}$$

$$\mu = 0.065$$

c. D_D Computation (Upper bound)

$$\begin{aligned}
 S_d &= 0.5074 \\
 \mu &= 0.065 \\
 \mu_1 &= 0.070 \\
 D_y &= (\mu_1 - \mu_2) * R_{2eff} \\
 D_y &= 0.016555 \\
 F_d &= 0.2772 \\
 W &= 686 \text{ Ton} \\
 \text{T.B.} &= 12 \text{ Nos. (Where T.B. = Total Bearing)} \\
 \Sigma F_d &= W \times \text{T.B.} \times F_d \\
 &= 686 \times 12 \times 0.2772 \\
 \Sigma F_d &= 2282.26 \\
 \Sigma W &= W \times \text{T.B.} \\
 \Sigma W &= 8232 \text{ Tonne}
 \end{aligned}$$

i. **Design displacement, D_D** = 0.07202 m.

ii. **Effective stiffness, Q_d**

$$\begin{aligned}
 &= \mu * \Sigma W \\
 &= 0.065 * 8232 \\
 Q_d &= 534.41 \text{ Ton} \\
 k_D &= \Sigma F_D / D_D \\
 &= 2282.26 / 0.07202 \\
 k_D &= 31689.31 \text{ Ton/m.} \\
 K_{eff} &= k_D + Q_D / D_D \\
 &= 31689.31 + 534.41 / 0.07202 \\
 K_{eff} &= 39109.67 \text{ Ton/m.}
 \end{aligned}$$

iii. **Effective period, T_{eff}**

$$\begin{aligned}
 T_{eff} &= \left[\sqrt{(\Sigma W) / (K_{eff} \times g)} \right] 2\pi \\
 T_{eff} &= 0.92036 \text{ sec.}
 \end{aligned}$$

iv. **Effective damping, β_{eff}**

$$\beta_D = \frac{E}{2\pi K_{\text{eff}} \times D_D^2} = \frac{4\mu \Sigma w(D_D - D_y)}{2\pi K_{\text{eff}} \times D_D^2}$$

$$\beta_{\text{eff}} = \beta_D = 0.0930$$

v. **Damping reduction Coefficient, β**

$$\beta = \left(\frac{\beta_{\text{eff}}}{0.05} \right)^{0.3}$$

$$\beta = 1.2047$$

vi. **D_D^1**

$$D_D^1 = \frac{S_{D1} \times T_{\text{eff}}^2}{4\pi^2 \times \beta} \times g$$

$$D_D^1 = 0.0887 \text{ mtrs}$$

(B) ETABS links directional property computation (upper bound)**a. Principal features****i. Determine bearing**

The isolator had been envisioned as a cylinder with a height of 0.32 metres and a diameter of 0.305 metres

$$H = 0.5 \text{ m}$$

$$\varnothing = 0.484 \text{ m}$$

$$\begin{aligned} \text{Now, Area} \quad A &= \frac{\pi \times \varnothing^2}{4} \\ &= \frac{\pi \times 0.484^2}{4} \\ A &= 0.1840 \text{ m}^2 \end{aligned}$$

$$K_{\text{eff}} = \frac{W}{R_{1\text{eff}}} + \frac{\mu w}{D_D}$$

$$K_{\text{eff}} = 820.42 \text{ Ton/m}$$

$$\begin{aligned} I_1 &= \frac{K_{\text{eff}} \times h^3}{12E} = \frac{820.42 \times 0.5^3}{12E} \\ &= 8.54609\text{E-}07 \text{ m}^4. \end{aligned}$$

$$E = 1 \times 10^7 \text{ N/mm}^2$$

ii. Determine bearing mass

$$D_{m-\max} = 0.0702 \text{ m.}$$

$$\begin{aligned} D_{TM} &= 1.15 \times D_{m-\max} \\ &= 1.15 \times 0.0702 \end{aligned}$$

$$D_{TM} = 0.0807 \text{ m.}$$

$$\begin{aligned} D &= 2 D_{TM} \\ &= 2 \times 0.0807 \end{aligned}$$

$$D = 0.16146 \text{ m.}$$

$$w = 0.241 D^2 - 0.00564 D$$

$$w = 0.0053721 \text{ tonne.}$$

$$\begin{aligned} M &= w / g \\ &= 0.005372 / 9.81 \end{aligned}$$

$$M = 0.000548 \text{ tonne sec}^2/\text{m.}$$

b. Direction (U_1)

$$H = 0.5 \text{ m}$$

$$\varnothing = 0.484 \text{ m}$$

$$K_{\text{eff}} = AE / L$$

$$K_{\text{eff}} = 3679684.643 \text{ ton/m.}$$

$$K_{\text{eff}} = \mathbf{36796846.43 \text{ KN/m.}}$$

from D_D

$$K_{\text{eff}} = 3679684.64 \text{ ton/m.}$$

$$\beta_{\text{eff}} = 0.0930$$

c. Direction ($U_2 - U_3$)**i. Determination of liner properties.**

$$K_{\text{eff}} = 820.425 \text{ ton/m}$$

$$= 8204.25 \text{ KN/m}$$

$$\beta_{\text{eff}} = 0.0930$$

$$\text{Height for outer surface, } = h_1 = h_4 = 0.161 \text{ mtrs.}$$

$$\text{Height for inner surface, } = h_2 = h_3 = 0.121 \text{ mtrs.}$$

ii. Determination of Non - liner properties.

$$R_{2 \text{ eff}} = 0.526 \text{ mtrs.}$$

$$D_y = (\mu_1 - \mu_2) R_{2 \text{ eff}}$$

$$= (0.06980 - 0.03832) \times 0.526$$

$$D_y = 0.01655 \text{ mtrs.}$$

$$\begin{aligned} \text{Stiffness (Outer Top)} &= \frac{\mu_1 W}{D_y} \\ &= \frac{0.06980 \times 686}{0.01655} \\ &= 2892.227 \text{ ton/m.} \\ &= 28922.27 \text{ KN/m.} \end{aligned}$$

$$\begin{aligned} \text{Stiffness (Inner Top)} &= \frac{\mu_2 W}{D_y} \\ &= \frac{0.03832 \times 686}{0.01655} \\ &= 1588.044 \text{ ton/m.} \\ &= 15880.44 \text{ KN/m.} \end{aligned}$$

$$\begin{aligned} \text{Friction Coefficient, Slow} &= \mu_1 = 0.070 \text{ (Outer Top)} \\ &= \mu_2 = 0.038 \text{ (Inner Top)} \end{aligned}$$

$$\begin{aligned}\text{Friction Coefficient, Fast} &= 2 \times \mu_1 = \mathbf{0.140 \text{ (Outer Top)}} \\ &= 2 \times \mu_2 = \mathbf{0.077 \text{ (Inner Top)}}\end{aligned}$$

$$\begin{aligned}\text{Rate Parameter} &= \frac{\text{Friction Coeff. Slow}}{\text{Friction Coeff. Fast}} \\ &= 0.070 / 0.140 \\ &= 0.5 \\ &= \mathbf{0.0005 \text{ sec/mm}}\end{aligned}$$

Radius of sliding surface

$$\begin{aligned}\text{Outer Top} &= R_{1 \text{ eff}} = \mathbf{3.395 \text{ mtrs.}} \\ \text{Inner Top} &= R_{2 \text{ eff}} = \mathbf{0.526 \text{ mtrs.}}\end{aligned}$$

Stop distance

$$\begin{aligned}\text{Outer Top } u_1^* &= 2 D_y + 2 d_1^* \\ &= 1.11391 \text{ mtrs.} \\ &= \mathbf{1113.91 \text{ mm}}\end{aligned}$$

$$\begin{aligned}\text{Inner Top } u_2^* &= 2 D_y \\ &= 0.0331 \text{ mtrs.} \\ &= \mathbf{33.109 \text{ mm.}}\end{aligned}$$

(C) Input Values in ETABS:

Link/Support Directional Properties

Identification

Property Name	A
Direction	U1
Type	Triple Pendulum Isolator
NonLinear	Yes

Linear Properties

Effective Stiffness	36796846.43	kN/m
Effective Damping	1.205	kN-s/m

Nonlinear Properties

Stiffness	36796846.43	kN/m
Damping Coefficient	1.205	kN-s/m

OK Cancel

**Figure-67. TFPB Input Values in ETABS for Axial Load 6860 KN
Direction U₁**

Link/Support Directional Properties

Identification

Property Name: Type:

Direction: NonLinear:

Linear Properties

Effective Stiffness - U2: kN/m Effective Stiffness - U3: kN/m

Effective Damping - U2: kN-s/m Effective Damping - U3: kN-s/m

Shear Deformation Location

Distance from End-J - U2: m Distance from End-J - U3: m

Height and Symmetry of Sliding Surfaces

Height for Outer Surfaces: m ☒ Outer Bottom Surface is Symmetric to Outer Top Surface

Height for Inner Surfaces: m ☒ Inner Bottom Surface is Symmetric to Inner Top Surface

Nonlinear Properties for Directions U2 and U3

	Outer Top	Outer Bottom	Inner Top	Inner Bottom	
Stiffness	<input type="text" value="28922.265"/>	<input type="text" value="28922.265"/>	<input type="text" value="15880.44"/>	<input type="text" value="15880.44"/>	kN/m
Friction Coefficient, Slow	<input type="text" value="0.069795"/>	<input type="text" value="0.069795"/>	<input type="text" value="0.03832"/>	<input type="text" value="0.03832"/>	
Friction Coefficient, Fast	<input type="text" value="0.13959"/>	<input type="text" value="0.13959"/>	<input type="text" value="0.076645"/>	<input type="text" value="0.076645"/>	
Rate Parameter	<input type="text" value="0.0005"/>	<input type="text" value="0.0005"/>	<input type="text" value="0.0005"/>	<input type="text" value="0.0005"/>	sec/mm
Radius of Sliding Surface	<input type="text" value="3.395"/>	<input type="text" value="3.395"/>	<input type="text" value="0.526"/>	<input type="text" value="0.526"/>	m
Stop Distance	<input type="text" value="1113.909"/>	<input type="text" value="1113.909"/>	<input type="text" value="33.109"/>	<input type="text" value="33.109"/>	mm

**Figure-68. TFPB Input Values in ETABS for Axial Load 6860 KN
Direction U₂ & U₃**

5.6 Summary

The Base Isolation System's attributes are discussed in this chapter.: 1) Lead Rubber Bearing (LRB) in Direction U_1 viz. Effective stiffness & Effective damping for linear properties and in Direction U_2 & U_3 viz. Effective stiffness & Effective damping for linear properties and Stiffness, Yield strength & post yield strength ratio for non-linear properties. 2) Triple Friction Pendulum Bearing (TFPB) in Direction U_1 viz. Effective stiffness & Effective damping for linear properties and in Direction U_2 & U_3 viz. Effective stiffness & Effective damping for linear properties and Height of outer & inner surface, Stiffness, friction coefficient for slow & fast, Rate parameter, Radius of sliding surface and stop distance for non-linear properties are design according to axial load, biaxial load and Tri-axial load (Cumulative load from fixed base modal). Using this link/support properties the design of case(a)-Model-2 & 3 and case(b)-Model 5-6 are analyzed and the results will be compare with fixed base support in next chapter.

CHAPTER – VI

ANALYSIS OF RESULTS



6.1 Preamble

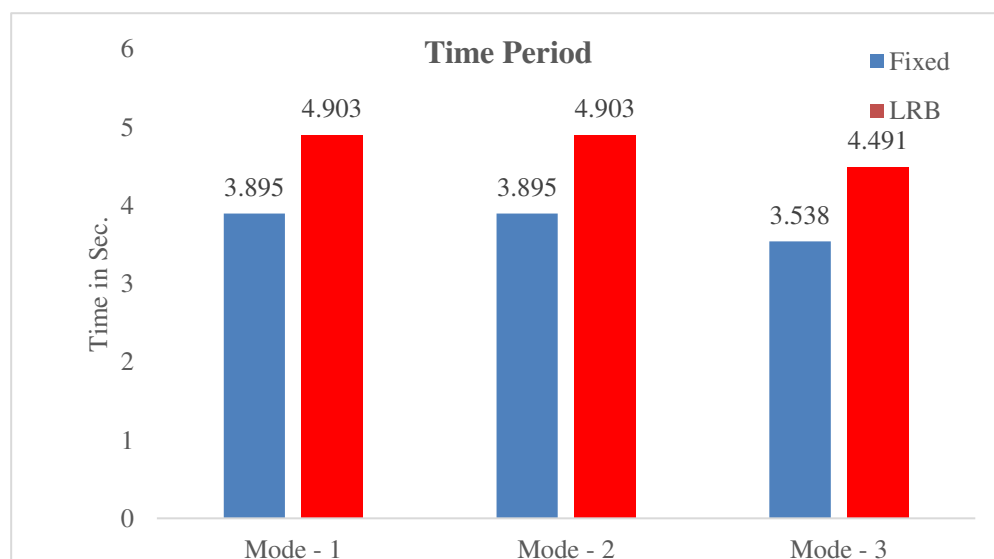
In this chapter the result obtained from all the model: Time period, Base Shear, Storey-Drift, Storey-Displacement, Steel reduction and overall cost economy is analyzed and a Results summary is made for comparison along with graph.

6.2 Result Comparison for Case (a) G+12 Storey Reinforced Concrete (RC) Structure. (Case-I with Case-II).

6.2.1 Time Period.

Table-19. Comparison of Time Period of Fixed Base Structure (Case-I) and LRB Base Structure (Case-II).

Time Period (Sec)			
	Fixed Base	LRB Base	Remark
Mode - 1	3.895	4.903	
Mode - 2	3.895	4.903	
Mode - 3	3.538	4.491	



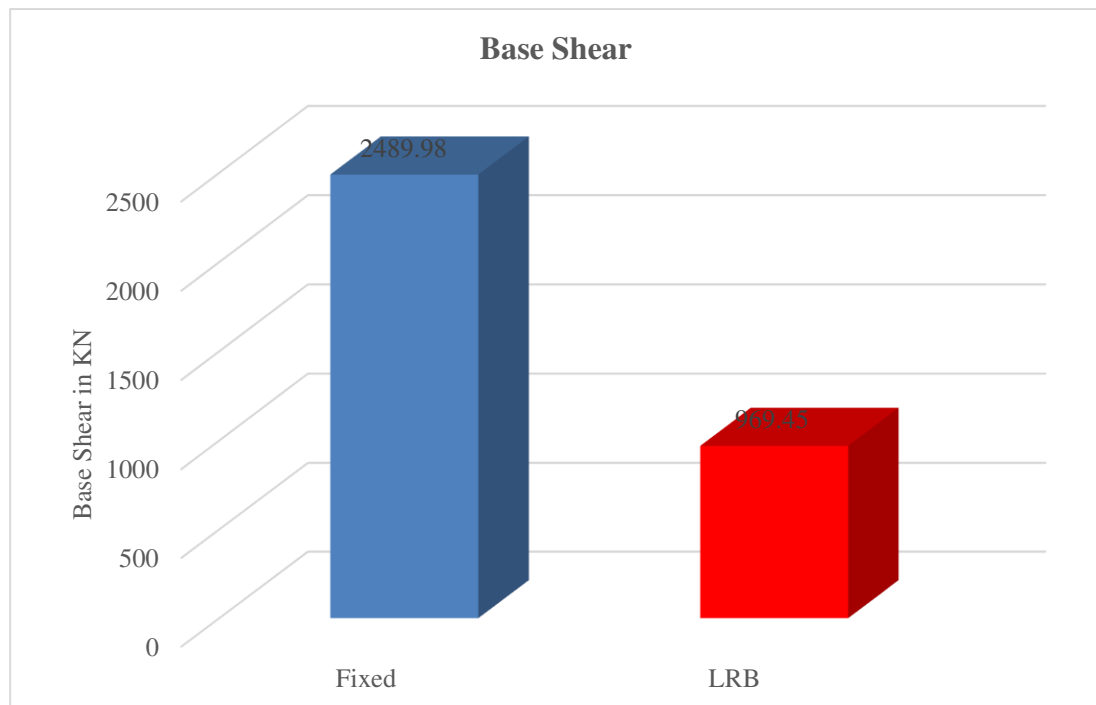
Graph-1. Parametric Change of Time Period of Fixed Base Structure (Case-I) and LRB Base Structure (Case-II).

The Time Period of G+12 Storey reinforced concrete structure for case (a) Case-I: Fixed base structure and Case-II: LRB base structure is shown in table-19 and parametric change in form of graph is shown in graph-1. The time period in Case-II is raised by 26.23% as compared to Case-I.

6.2.2 Base Shear.

Table-20. Comparison of Base Shear of Fixed Base Structure (Case-I) and LRB Base Structure (Case-II).

Base Shear (KN)			
	Fixed Base	LRB Base	Remark
Base Shear	2489.98	969.45	



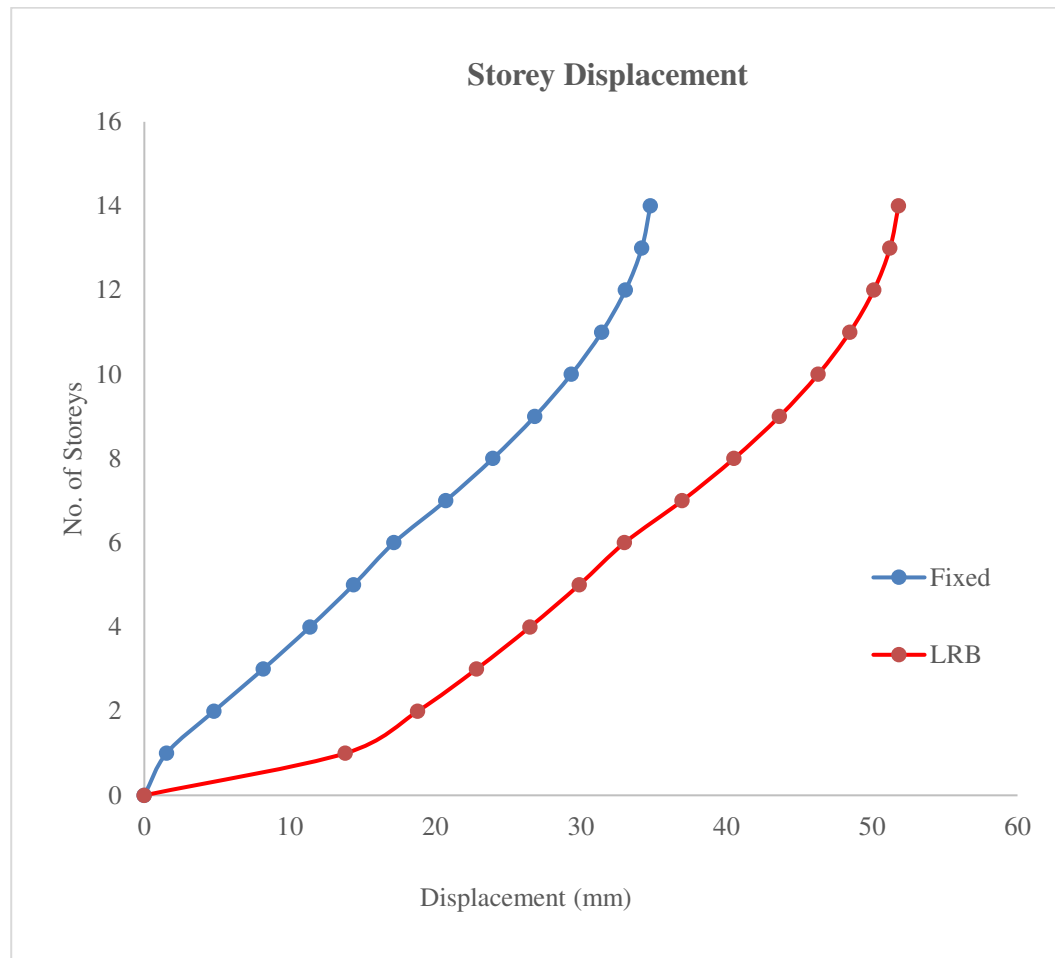
Graph-2. Parametric Change of Base Shear of Fixed Base Structure (Case-I) and LRB Base Structure (Case-II).

The Base Shear of G+12 Storey reinforced concrete structure for case (a) Case-I: Fixed Base Structure and Case-II: LRB Base Structure is shown in table-20 and parametric change in form of graph is shown in graph-2. The Base shear in Case-II is reduced by 61.07% as compared to Case-I.

6.2.3 Storey-Displacement.

Table-21. Comparison of Storey-Displacement of Fixed Base Structure (Case-I) and LRB Base Structure (Case-II).

Storey-Displacement			
Storey	Fixed Base	LRB Base	Remark
Storey -13	34.769	51.824	
Storey -12	34.184	51.24	
Storey -11	33.061	50.127	
Storey -10	31.428	48.471	
Storey -9	29.336	46.299	
Storey -8	26.831	43.639	
Storey -7	23.947	40.518	
Storey -6	20.711	36.961	
Storey -5	17.152	33.002	
Storey -4	14.377	29.884	
Storey -3	11.382	26.501	
Storey -2	8.171	22.829	
Storey -1	4.784	18.786	
Ground	1.527	13.819	

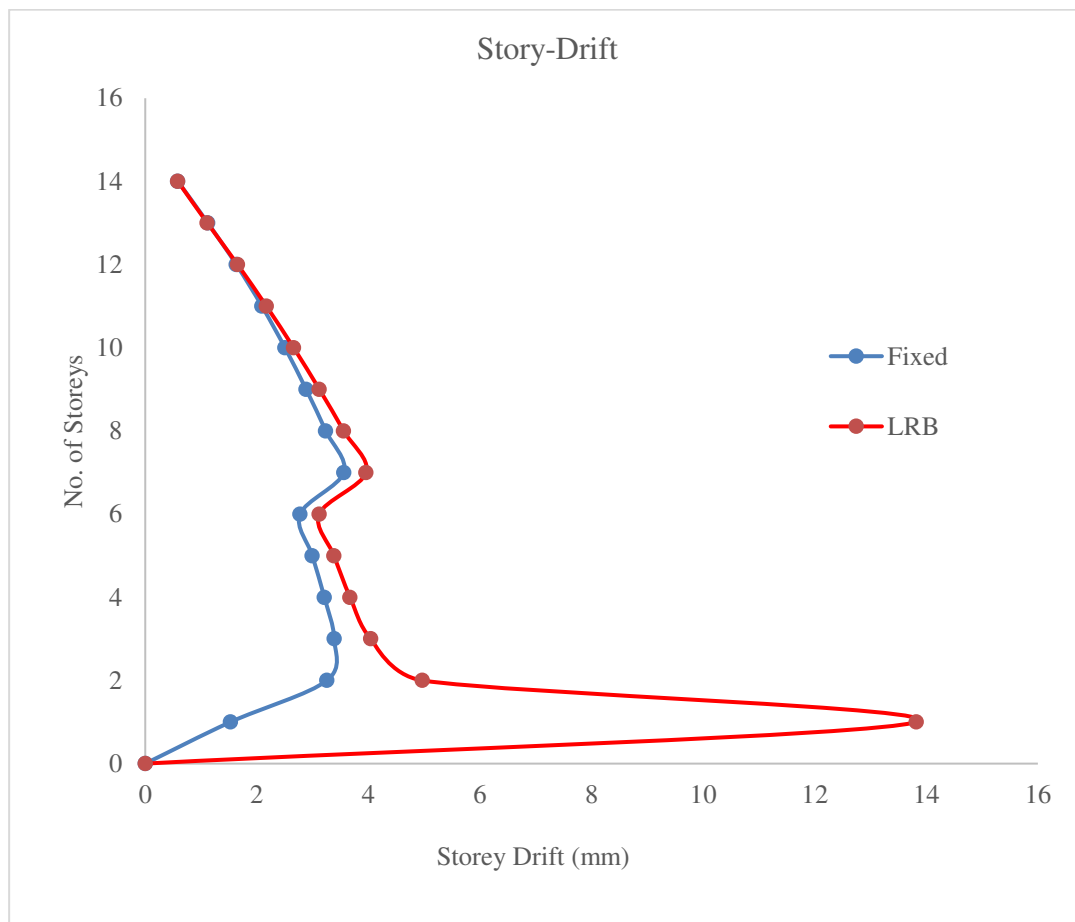


Graph-3. Parametric Change of Storey-Displacement of Fixed Base Structure (Case-I) and LRB Base Structure (Case-II).

The Storey-Displacement of G+12 Storey reinforced concrete structure for case (a) Case-I: Fixed Base Structure and Case-II: LRB Base Structure is shown in table-21 and parametric change in form of graph is shown in graph-3. The Storey-Displacement in Case-II is raised by 58.74% as compared to Case-I.

6.2.4 Storey-Drift.**Table-22. Comparison of Storey-Drift of Fixed Base Structure (Case-I) and LRB Base Structure (Case-II).**

Storey-Drift			
Storey	Fixed Base	LRB Base	Remark
Storey -13	0.585	0.584	
Storey -12	1.123	1.113	
Storey -11	1.633	1.656	
Storey -10	2.092	2.172	
Storey -9	2.505	2.66	
Storey -8	2.884	3.121	
Storey -7	3.236	3.557	
Storey -6	3.559	3.959	
Storey -5	2.775	3.118	
Storey -4	2.995	3.383	
Storey -3	3.211	3.672	
Storey -2	3.387	4.043	
Storey -1	3.257	4.967	
Ground	1.527	13.819	



Graph-4. Parametric Change of Storey-Drift of Fixed Base Structure (Case-I) and LRB Base Structure (Case-II).

The Storey-Drift of G+12 Storey reinforced concrete structure for case (a) Case-I: Fixed Base Structure and Case-II: LRB Base Structure is shown in table-22. The storey-drift follows a non-linear pattern which can be observed in graph as shown in graph-4. The Storey-Drift is reduced by 64.06% which makes the structure ideally stiff & provides less damage to the structure. The storey-drift obtained are well within the limit as per IS 1893:2016.

6.2.5 Steel Reduction.

Table-23. Comparison of Steel Reduction of Fixed Base Structure (Case-I) and LRB Base Structure (Case-II).

Steel Reduction (%)			
Sr. No.	Description	Fixed Base (mm ²)	LRB Base (mm ²)
1	Column-Biaxial	77586	61581
2	Column-Uniaxial	764810	552144
3	Column-Axial	1606393	1433588
Reinforcement in Column=		2448789	2047313
Reinforcement Reduction in Column =		16.39%	
1	Beam	2898050	2629336
Reinforcement Reduction in Beam =		9.27%	
Total Reinforcement Reduction =		25.67%	

The Steel Reduction of G+12 Storey reinforced concrete structure for case (a) Case-I: Fixed Base Structure and Case-II: LRB Base Structure is shown in table-23. The Steel in Case-II is reduced by 25.67% as compared to Case-I.

6.2.6 Overall Cost Economy.

Table-24. Comparison of Overall Cost Economy of Fixed Base Structure (Case-I) and LRB Base Structure (Case-II).

Overall Cost Economy				
Sr. No.	Description	Quantity	Units	Remark
1	Approx Reinforcement Quantity	5	Kg/Sft	
2	Total Reinforcement Reduction (Approx 26%)	1.3	Kg/Sft	
3	Total Cost Reduction due to LRB (Round off)	95	Rs.	Steel 70 Rs./Kg
4	Cost of Lead Rubber Bearing	200	Rs./Sft	
5	Net Cost for Lead Rubber Bearing	105	Rs.	
6	Approx. cost of Construction	1500	Rs./Sft	
7	Effective Incremental in Construction Cost	7.00	%	

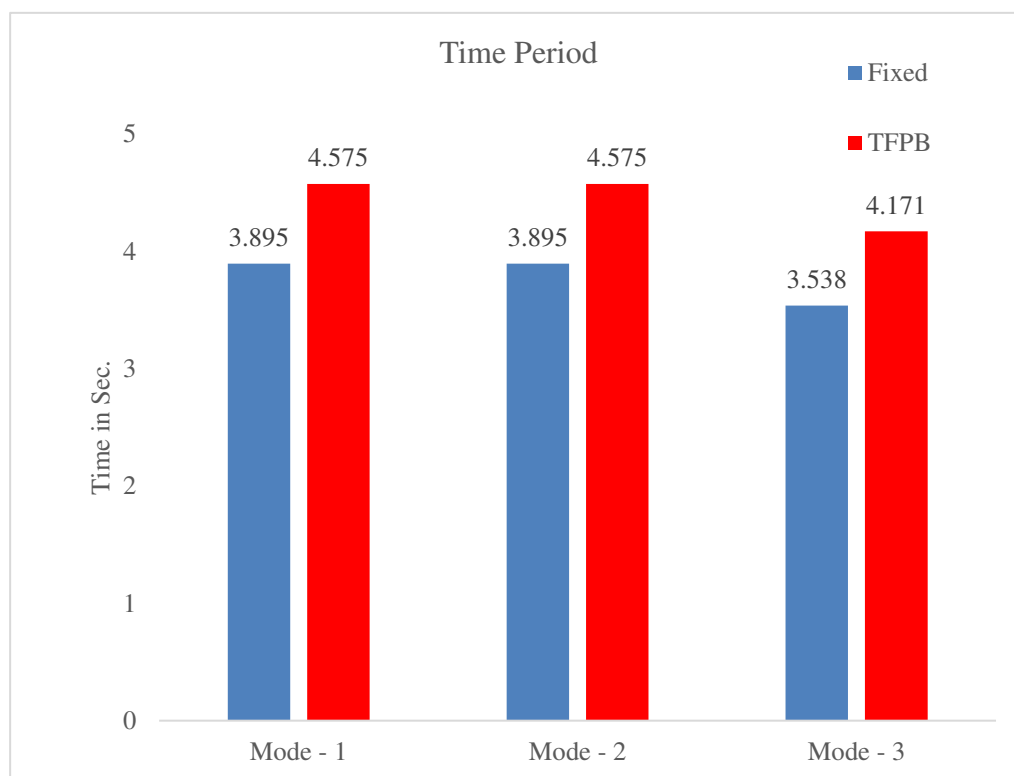
The Overall Cost Economy of G+12 Storey reinforced concrete structure for case (a) Case-I: Fixed Base Structure and Case-II: LRB Base Structure is shown in table-24. The Overall cost economy of Case-II is raised by 7.00% as compared to Case-I.

6.3 Result Comparison for Case (a) G+12 Storey Reinforced Concrete (RC) Structure. (Case-I with Case-III).

6.3.1 Time Period.

Table-25. Comparison of Time Period of Fixed Base Structure (Case-I) and TFPB Base Structure (Case-III).

Time Period (Sec)			
	Fixed Base	TFPB Base	Remark
Mode - 1	3.895	4.575	
Mode - 2	3.895	4.575	
Mode - 3	3.538	4.171	



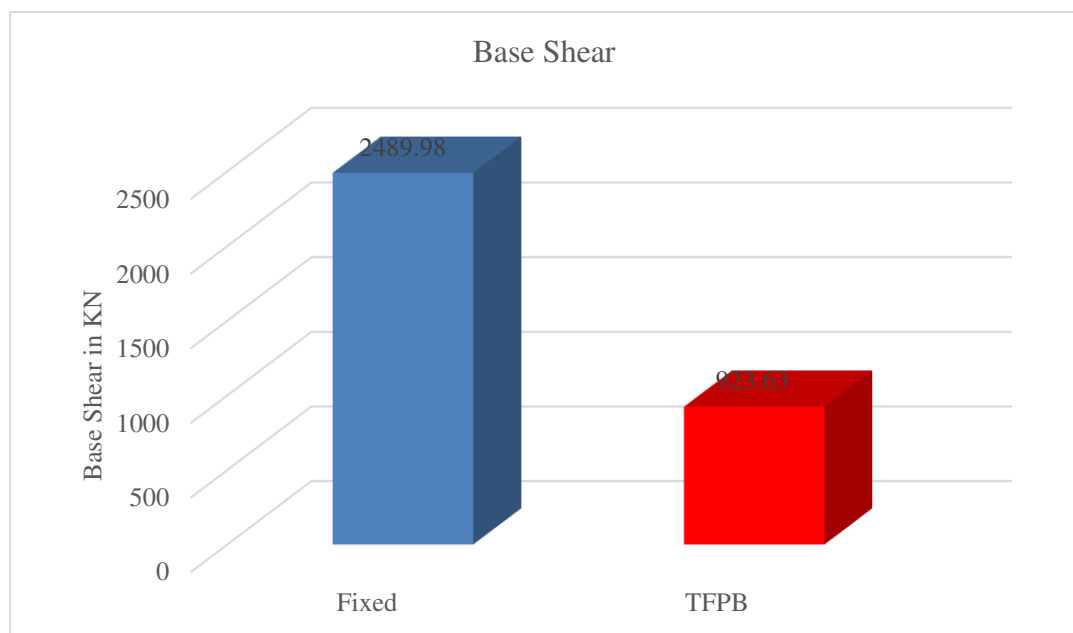
Graph-5. Parametric Change of Time Period of Fixed Base Structure (Case-I) and TFPB Base Structure (Case-III).

The Time Period of G+12 Storey reinforced concrete structure for case (a) Case-I: Fixed Base Structure and Case-III: TFPB Base Structure is shown in table-25 and parametric change in form of graph is shown in graph-5. The time period in Case-III is raised by 17.60% as compared to Case-I.

6.3.2 Base Shear.

Table-26. Comparison of Base Shear of Fixed Base Structure (Case-I) and TFPB Base Structure (Case-III).

Base Shear (KN)			
	Fixed Base	TFPB Base	Remark
Base Shear	2489.98	923.63	



Graph-6. Parametric Change of Base Shear of Fixed Base Structure (Case-I) and TFPB Base Structure (Case-III).

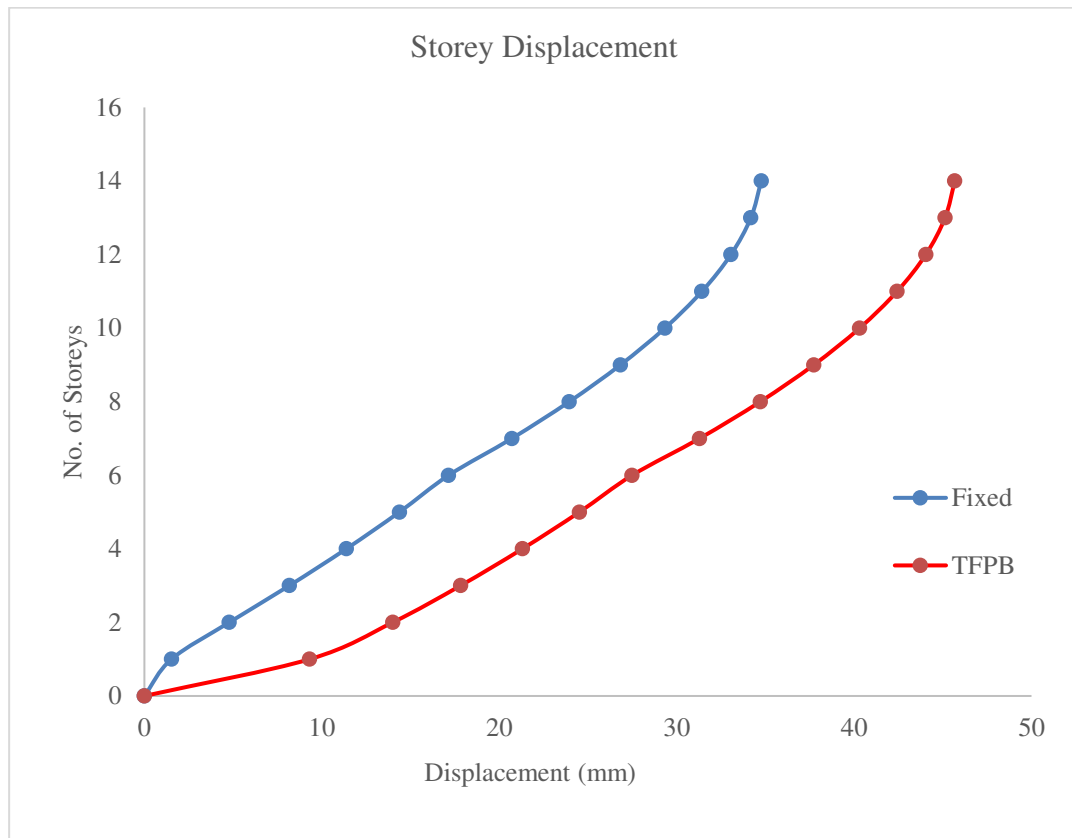
The Base Shear of G+12 Storey reinforced concrete structure for case (a) Case-I: Fixed Base Structure and Case-III: TFPB Base Structure is shown in table-26 and

parametric change in form of graph is shown in graph-6. The Base shear in Case-III is reduced by 62.91% as compared to Case-I.

6.3.3 Storey-Displacement.

Table-27. Comparison of Storey-Displacement of Fixed Base Structure (Case-I) and TFPB Base Structure (Case-III).

Storey-Displacement			
Storey	Fixed Base	TFPB Base	Remark
Storey -13	34.769	45.68	
Storey -12	34.184	45.127	
Storey -11	33.061	44.044	
Storey -10	31.428	42.428	
Storey -9	29.336	40.312	
Storey -8	26.831	37.729	
Storey -7	23.947	34.713	
Storey -6	20.711	31.29	
Storey -5	17.152	27.494	
Storey -4	14.377	24.523	
Storey -3	11.382	21.306	
Storey -2	8.171	17.822	
Storey -1	4.784	13.997	
Ground	1.527	9.314	

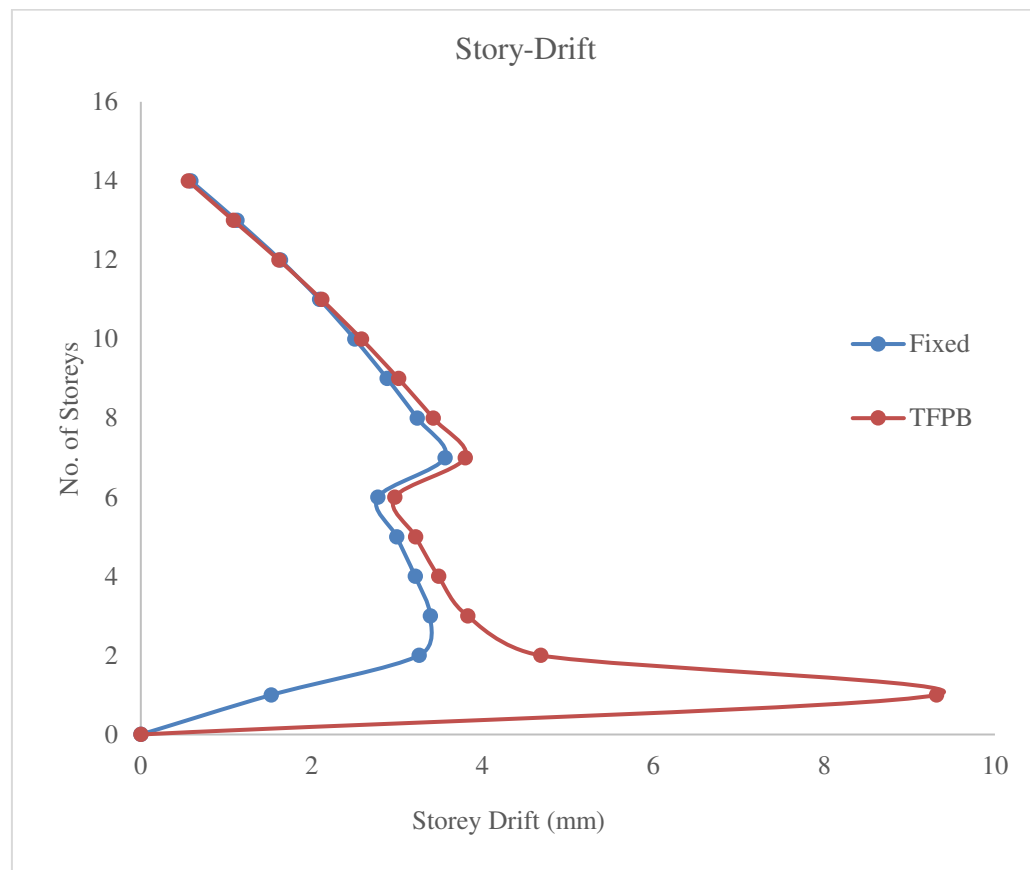


Graph-7. Parametric Change of Storey-Displacement of Fixed Base Structure (Case-I) and TFPB Base Structure (Case-III).

The Storey-Displacement of G+12 Storey reinforced concrete structure for case (a) Case-I: Fixed Base Structure and Case-III: TFPB Base Structure is shown in table-27 and parametric change in form of graph is shown in graph-7. The Storey-Displacement in Case-III is raised by 49.41% as compared to Case-I.

6.3.4 Storey-Drift.**Table-28. Comparison of Storey-Drift of Fixed Base Structure (Case-I) and TFPB Base Structure (Case-III).**

Storey-Drift			
Storey	Fixed Base	TFPB Base	Remark
Storey -13	0.585	0.553	
Storey -12	1.123	1.083	
Storey -11	1.633	1.616	
Storey -10	2.092	2.116	
Storey -9	2.505	2.583	
Storey -8	2.884	3.016	
Storey -7	3.236	3.423	
Storey -6	3.559	3.796	
Storey -5	2.775	2.971	
Storey -4	2.995	3.217	
Storey -3	3.211	3.484	
Storey -2	3.387	3.825	
Storey -1	3.257	4.683	
Ground	1.527	9.314	



Graph-8. Parametric Change of Storey-Drift of Fixed Base Structure (Case-I) and TFPB Base Structure (Case-III).

The Storey-Drift of G+12 Storey reinforced concrete structure for case (a) Case-I: Fixed Base Structure and Case-III: TFPB Base Structure is shown in table-28. The storey-drift follows a non-linear pattern which can be observed in graph as shown in graph-8. The Storey-Drift is reduced by 49.72% which makes the structure ideally stiff & provides less damage to the structure. The storey-drift obtained are well within the limit as per IS 1893:2016.

6.3.5 Steel Reduction.

Table-29. Comparison of Steel Reduction of Fixed Base Structure (Case-I) and TFPB Base Structure (Case-III).

Steel Reduction (%)			
Sr. No.	Description	Fixed Base (mm ²)	TFPB Base (mm ²)
1	Column-Biaxial	77586	61998
2	Column-Uniaxial	764810	557424
3	Column-Axial	1606393	1431680
Reinforcement in Column=		2448789	2448789
Reinforcement Reduction in Column =		16.24%	
1	Beam	2898050	2595148
Reinforcement Reduction in Beam =		10.45%	
Total Reinforcement Reduction =		26.69%	

The Steel Reduction of G+12 Storey reinforced concrete structure for case (a) Case-I: Fixed Base Structure and Case-III: TFPB Base Structure is shown in table-29. The Steel in Case-III is reduced by 26.69% as compared to Case-I.

6.3.6 Overall Cost Economy.

Table-30. Comparison of Overall Cost Economy of Fixed Base Structure (Case-I) and TFPB Base Structure (Case-III).

Overall Cost Economy				
Sr. No.	Description	Quantity	Units	Remark
1	Approx Reinforcement Quantity	5	Kg/Sft	
2	Total Reinforcement Reduction (Approx 27%)	1.35	Kg/Sft	
3	Total Cost Reduction due to TFPB (Round off)	100	Rs.	Steel 70 Rs./Kg
4	Cost of Triple Friction Pendulum Bearing	160	Rs./Sft	
5	Net Cost for Friction Pendulum Bearing	60	Rs.	
6	Approx. cost of Construction	1500	Rs./Sft	
7	Effective Incremental in Construction Cost	4.00	%	

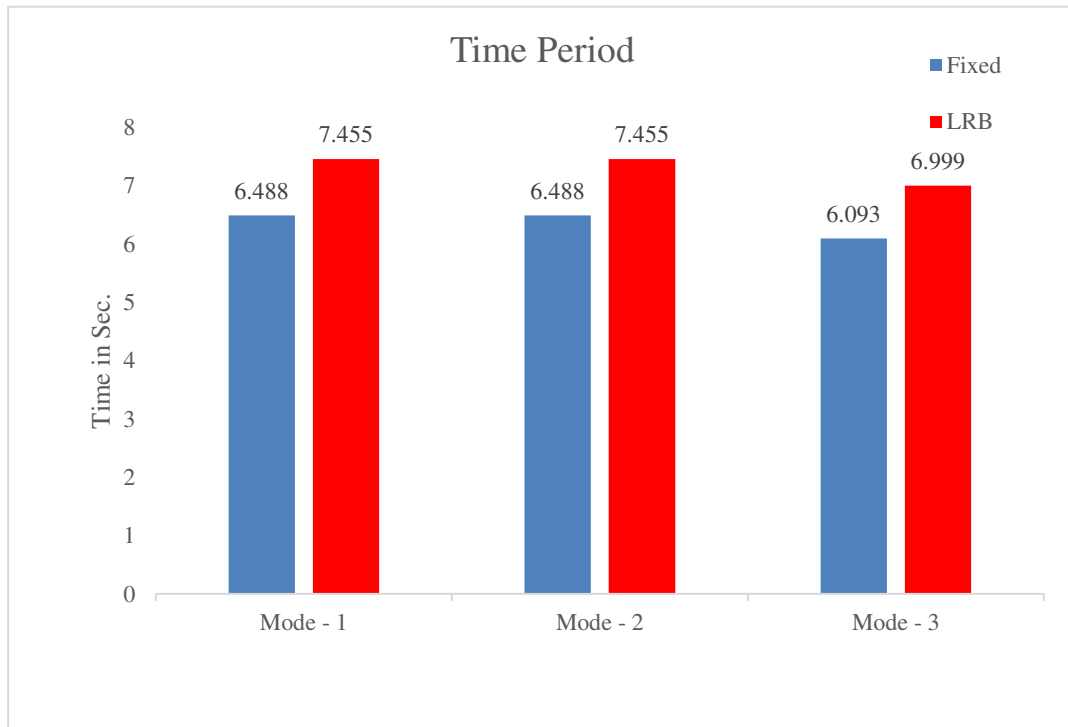
The Overall Cost Economy of G+12 Storey reinforced concrete structure for case (a) Case-I: Fixed Base Structure and Case-III: TFPB Base Structure is shown in table-30. The Overall cost economy of Case-III is raised by 4.00% as compared to Case-I.

6.4 Result Comparison for Case (b) G+22 Storey Reinforced Concrete (RC) Structure. (Case-IV with Case-V).

6.4.1 Time Period.

Table-31. Comparison of Time Period of Fixed Base Structure (Case-IV) and LRB Base Structure (Case-V).

Time Period (Sec)			
	Fixed Base	LRB Base	Remark
Mode - 1	6.488	7.455	
Mode - 2	6.488	7.455	
Mode - 3	6.093	6.999	



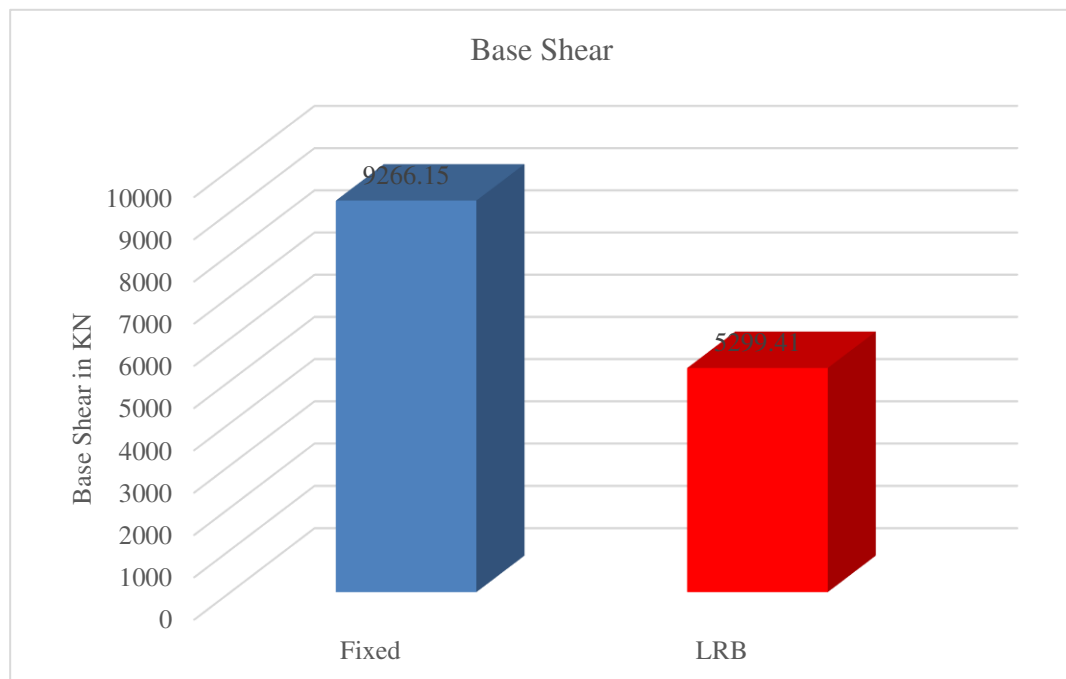
Graph-9. Parametric Change of Time Period of Fixed Base Structure (Case-IV) and LRB Base Structure (Case-V).

The Time Period of G+22 Storey reinforced concrete structure for case (b) Case-IV: Fixed Base Structure and Case-V: LRB Base Structure is shown in table-31 and parametric change in form of graph is shown in graph-9. The time period in Case-V is raised by 14.89% as compared to Case-IV.

6.4.2 Base Shear.

Table-32. Comparison of Base Shear of Fixed Base Structure (Case-IV) and LRB Base Structure (Case-V).

Base Shear (KN)			
	Fixed Base	LRB Base	Remark
Base Shear	9266.15	5299.41	



Graph-10. Parametric Change of Base Shear of Fixed Base Structure (Case-IV) and LRB Base Structure (Case-V).

The Base Shear of G+22 Storey reinforced concrete structure for case (b) Case-IV: Fixed Base Structure and Case-V: LRB Base Structure is shown in table-32 and parametric change in form of graph is shown in graph-10. The Base shear in

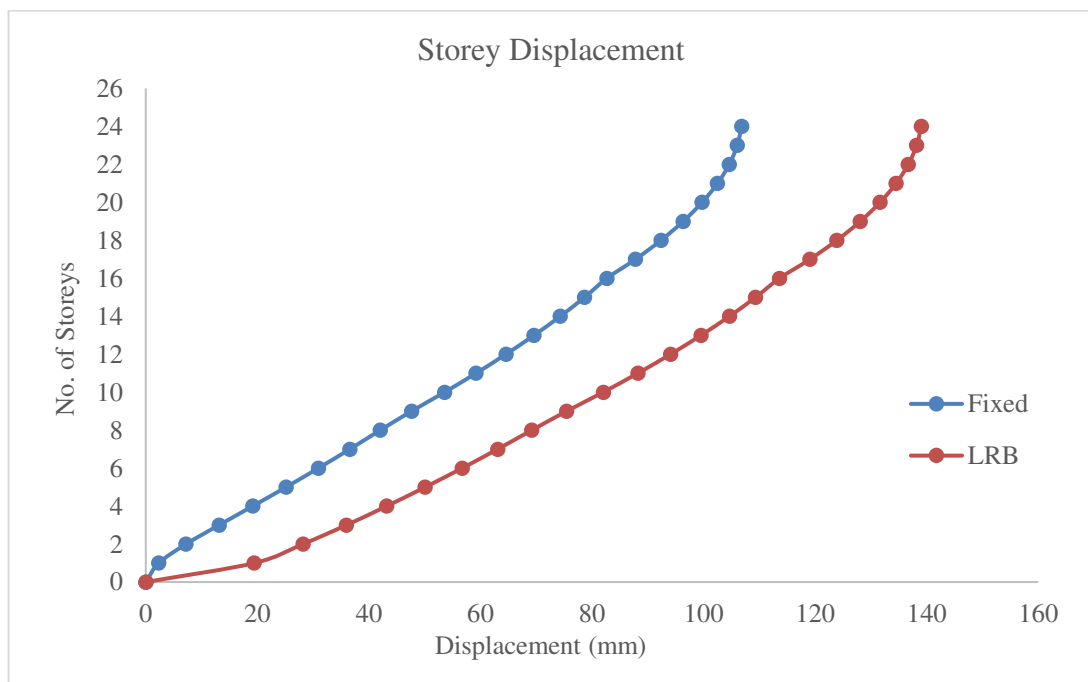
Case-V is reduced by 42.81% as compared to Case-IV.

6.4.3 Storey-Displacement.

Table-33. Comparison of Storey-Displacement of Fixed Base Structure (Case-IV) and LRB Base Structure (Case-V).

Storey-Displacement			
Storey	Fixed Base	LRB Base	Remark
Storey -23	106.815	139.022	
Storey -22	106.042	138.201	
Storey -21	104.613	136.714	
Storey -20	102.506	134.524	
Storey -19	99.746	131.648	
Storey -18	96.356	128.1	
Storey -17	92.365	123.901	
Storey -16	87.797	119.07	
Storey -15	82.685	113.632	
Storey -14	78.674	109.333	
Storey -13	74.318	104.644	
Storey -12	69.613	99.555	
Storey -11	64.576	94.078	
Storey -10	59.224	88.227	
Storey -9	53.575	82.016	

Storey -8	47.653	75.462	
Storey -7	42.036	69.205	
Storey -6	36.594	63.097	
Storey -5	30.962	56.73	
Storey -4	25.152	50.102	
Storey -3	19.191	43.203	
Storey -2	13.142	35.98	
Storey -1	7.217	28.187	
Ground	2.343	19.449	



Graph-11. Parametric Change of Storey-Displacement of Fixed Base Structure (Case-IV) and LRB Base Structure (Case-V).

The Storey-Displacement of G+22 Storey reinforced concrete structure for case (b) Case-IV: Fixed Base Structure and Case-V: LRB Base Structure is shown in

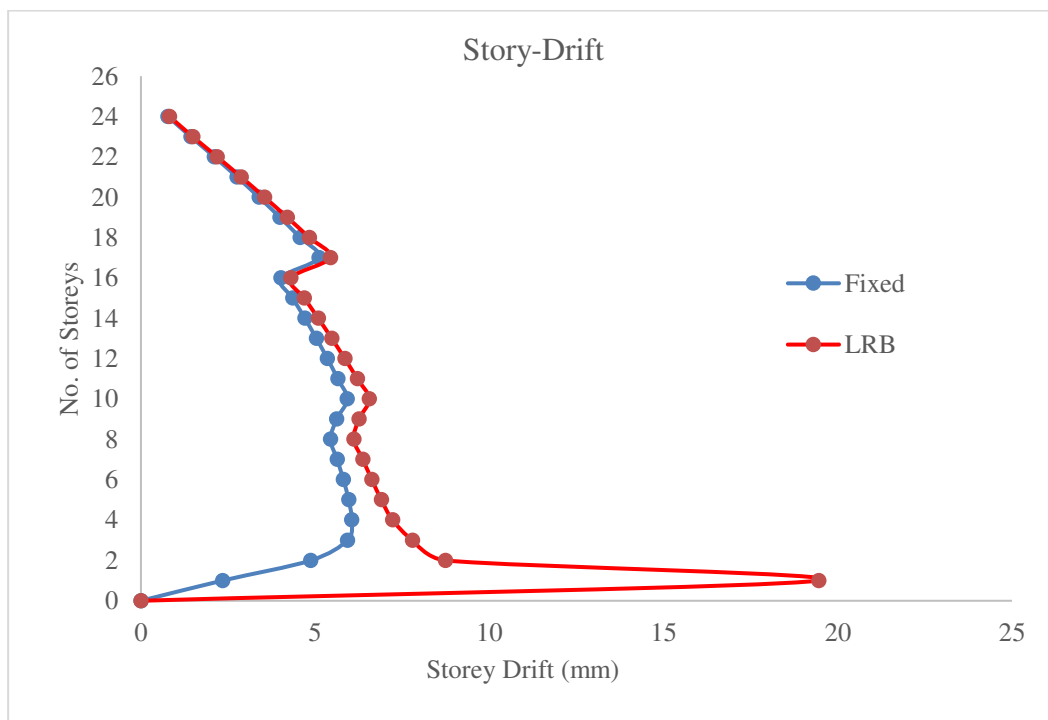
table-33 and parametric change in form of graph is shown in graph-11. The Storey-Displacement in Case-V is raised by 39.76% as compared to Case-IV.

6.4.4 Storey-Drift.

Table-34. Comparison of Storey-Drift of Fixed Base Structure (Case-IV) and LRB Base Structure (Case-V).

Storey-Drift			
Storey	Fixed Base	LRB Base	Remark
Storey -23	0.773	0.821	
Storey -22	1.429	1.487	
Storey -21	2.107	2.19	
Storey -20	2.76	2.876	
Storey -19	3.39	3.548	
Storey -18	3.991	4.199	
Storey -17	4.568	4.831	
Storey -16	5.112	5.438	
Storey -15	4.011	4.299	
Storey -14	4.356	4.689	
Storey -13	4.705	5.089	
Storey -12	5.037	5.477	
Storey -11	5.352	5.851	
Storey -10	5.649	6.211	

Storey -9	5.922	6.554	
Storey -8	5.617	6.257	
Storey -7	5.442	6.108	
Storey -6	5.632	6.367	
Storey -5	5.81	6.628	
Storey -4	5.961	6.899	
Storey -3	6.049	7.223	
Storey -2	5.925	7.793	
Storey -1	4.874	8.738	
Ground	2.343	19.449	



Graph-12. Parametric Change of Storey-Drift of Fixed Base Structure (Case-IV) and LRB Base Structure (Case-V).

The Storey-Drift of G+22 Storey reinforced concrete structure for case (b) Case-IV: Fixed Base Structure and Case-V: LRB Base Structure is shown in table-34. The storey-drift follows a non-linear pattern which can be observed in graph as shown in graph-12. The Storey-Drift is reduced by 55.07% which makes the structure ideally stiff & provides less damage to the structure. The storey-drift obtained are well within the limit as per IS 1893:2016.

6.4.5 Steel Reduction.

Table-35. Comparison of Steel Reduction of Fixed Base Structure (Case-IV) and LRB Base Structure (Case-V).

Steel Reduction (%)			
Sr. No.	Description	Fixed Base (mm ²)	LRB Base (mm ²)
1	Column-Biaxial	265416	225700
2	Column-Uniaxial	4513480	3995044
3	Column-Axial	16957790	15971568
Reinforcement in Column=		21736686	20192312
Reinforcement Reduction in Column =		7.10%	
1	Beam	17355952	14908932
Reinforcement Reduction in Beam =		14.10%	
Total Reinforcement Reduction =		21.20%	

The Steel Reduction of G+22 Storey reinforced concrete structure for case (b) Case-IV: Fixed Base Structure and Case-V: LRB Base Structure is shown in table-35. The Steel in Case-V is reduced by 21.20% as compared to Case-IV.

6.4.6 Overall Cost Economy.

Table-36. Comparison of Overall Cost Economy of Fixed Base Structure (Case-IV) and LRB Base Structure (Case-V).

Overall Cost Economy				
Sr. No.	Description	Quantity	Units	Remark
1	Approx Reinforcement Quantity	5	Kg/Sft	
2	Total Reinforcement Reduction (Approx 22%)	1.1	Kg/Sft	
3	Total Cost Reduction due to LRB (Round off)	80	Rs.	Steel 70 Rs./Kg
4	Cost of Lead Rubber Bearing	200	Rs./Sft	
5	Net Cost for Lead Rubber Bearing	120	Rs.	
6	Approx. cost of Construction	1500.00	Rs./Sft	
7	Effective Incremental in Construction Cost	8.00	%	

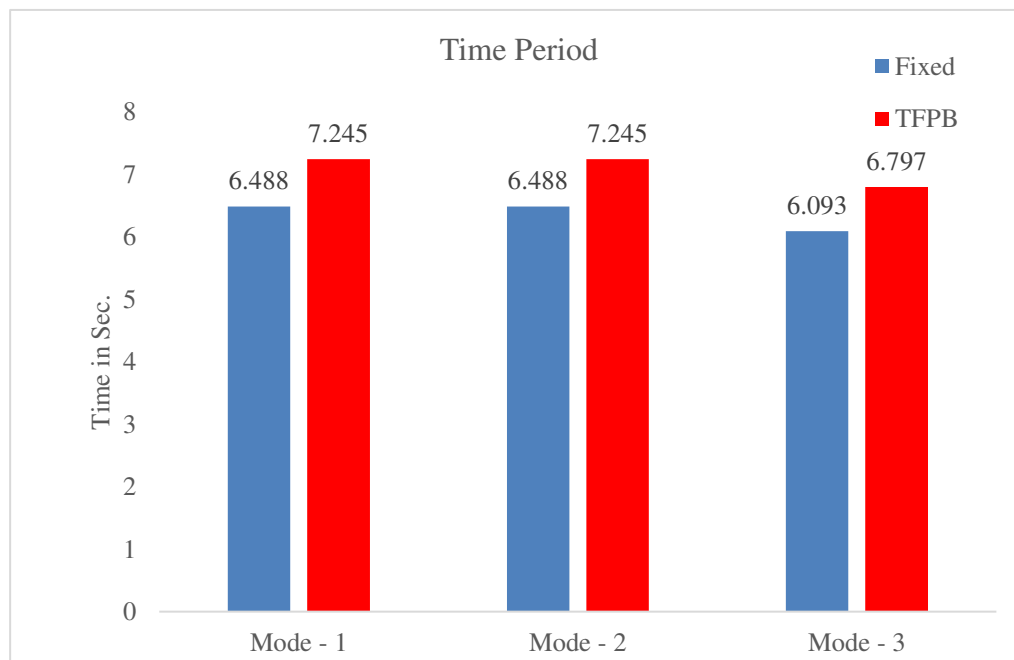
The Overall Cost Economy of G+22 Storey reinforced concrete structure for case (b) Case-IV: Fixed Base Structure and Case-V: LRB Base Structure is shown in table-36. The Overall cost economy of Case-V is raised by 8.00% as compared to Case-IV.

6.5 Result Comparison for Case (a) G+22 Storey Reinforced Concrete (RC) Structure. (Case-IV with Case-VI).

6.5.1 Time Period.

Table-37. Comparison of Time Period of Fixed Base Structure (Case-IV) and TFPB Base Structure (Case-VI).

Time Period (Sec)			
	Fixed Base	TFPB Base	Remark
Mode - 1	6.488	7.245	
Mode - 2	6.488	7.245	
Mode - 3	6.093	6.797	



Graph-13. Parametric Change of Time Period of Fixed Base Structure (Case-IV) and TFPB Base Structure (Case-VI).

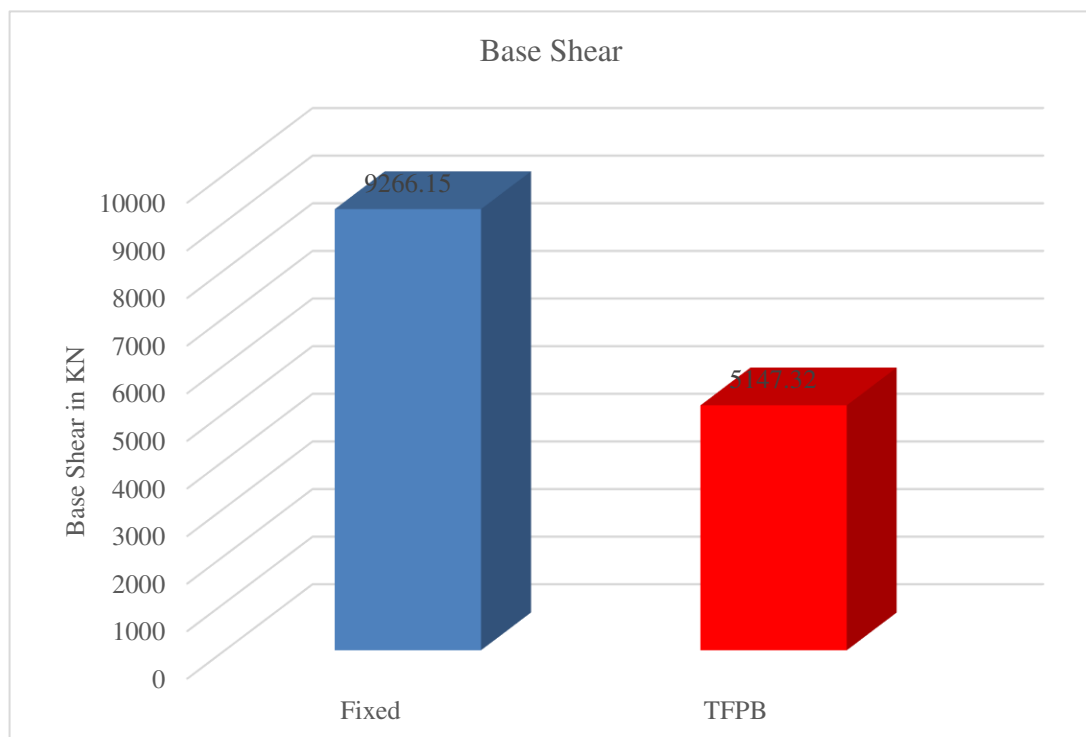
The Time Period of G+22 Storey reinforced concrete structure for case (b) Case-IV: Fixed Base Structure and Case-VI: TFPB Base Structure is shown in table-37

and parametric change in form of graph is shown in graph-13. The time period in Case-VI is raised by 11.63% as compared to Case-IV.

6.5.2 Base Shear.

Table-38. Comparison of Base Shear of Fixed Base Structure (Case-IV) and TFPB Base Structure (Case-VI).

Base Shear (KN)			
	Fixed Base	TFPB Base	Remark
Base Shear	9266.15	5147.32	



Graph-14. Parametric Change of Base Shear of Fixed Base Structure (Case-IV) and TFPB Base Structure (Case-VI).

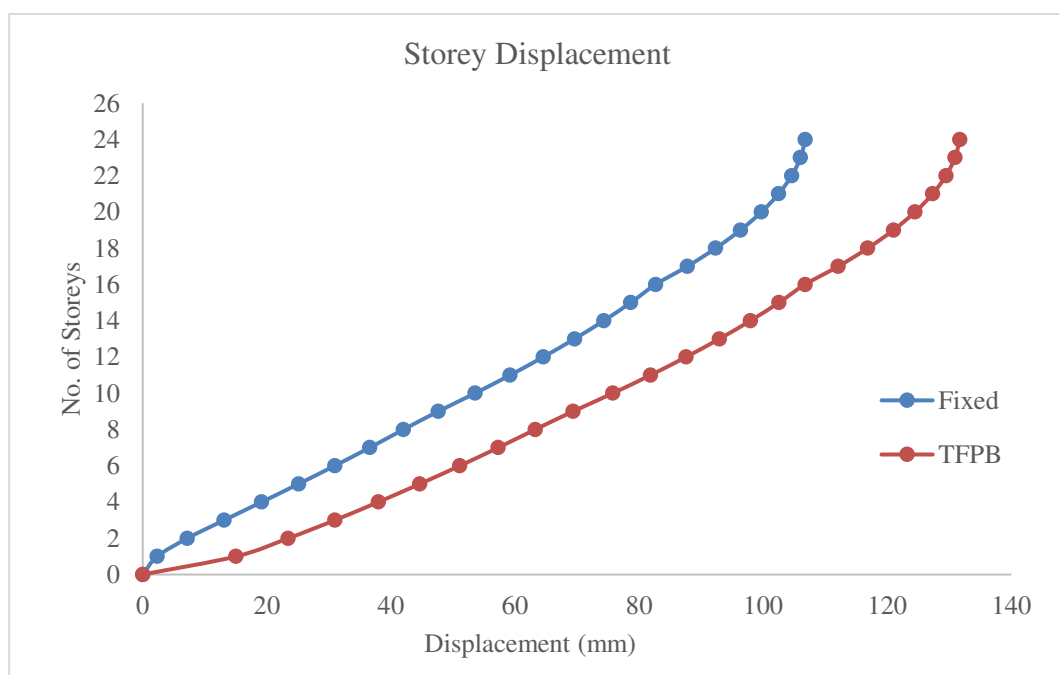
The Base Shear of G+22 Storey reinforced concrete structure for case (b) Case-IV: Fixed Base Structure and Case-VI: TFPB Base Structure is shown in table-38 and parametric change in form of graph is shown in graph-14. The Base shear in Case-VI is reduced by 44.45% as compared to Case-IV.

6.5.3 Storey-Displacement.

Table-39. Comparison of Storey-Displacement of Fixed Base Structure (Case-IV) and TFPB Base Structure (Case-VI).

Storey-Displacement			
Storey	Fixed Base	TFPB Base	Remark
Storey -23	106.815	131.724	
Storey -22	106.042	130.937	
Storey -21	104.613	129.484	
Storey -20	102.506	127.335	
Storey -19	99.746	124.505	
Storey -18	96.356	121.012	
Storey -17	92.365	116.877	
Storey -16	87.797	112.12	
Storey -15	82.685	106.77	
Storey -14	78.674	102.55	
Storey -13	74.318	97.95	
Storey -12	69.613	92.96	
Storey -11	64.576	87.593	
Storey -10	59.224	81.863	
Storey -9	53.575	75.786	
Storey -8	47.653	69.381	

Storey -7	42.036	63.273	
Storey -6	36.594	57.322	
Storey -5	30.962	51.125	
Storey -4	25.152	44.683	
Storey -3	19.191	37.991	
Storey -2	13.142	30.997	
Storey -1	7.217	23.473	
Ground	2.343	15.06	



Graph-15. Parametric Change of Storey-Displacement of Fixed Base Structure (Case-IV) and TFPB Base Structure (Case-VI).

The Storey-Displacement of G+22 Storey reinforced concrete structure for case (b) Case-IV: Fixed Base Structure and Case-VI: TFPB Base Structure is shown in table-39 and parametric change in form of graph is shown in graph-15. The

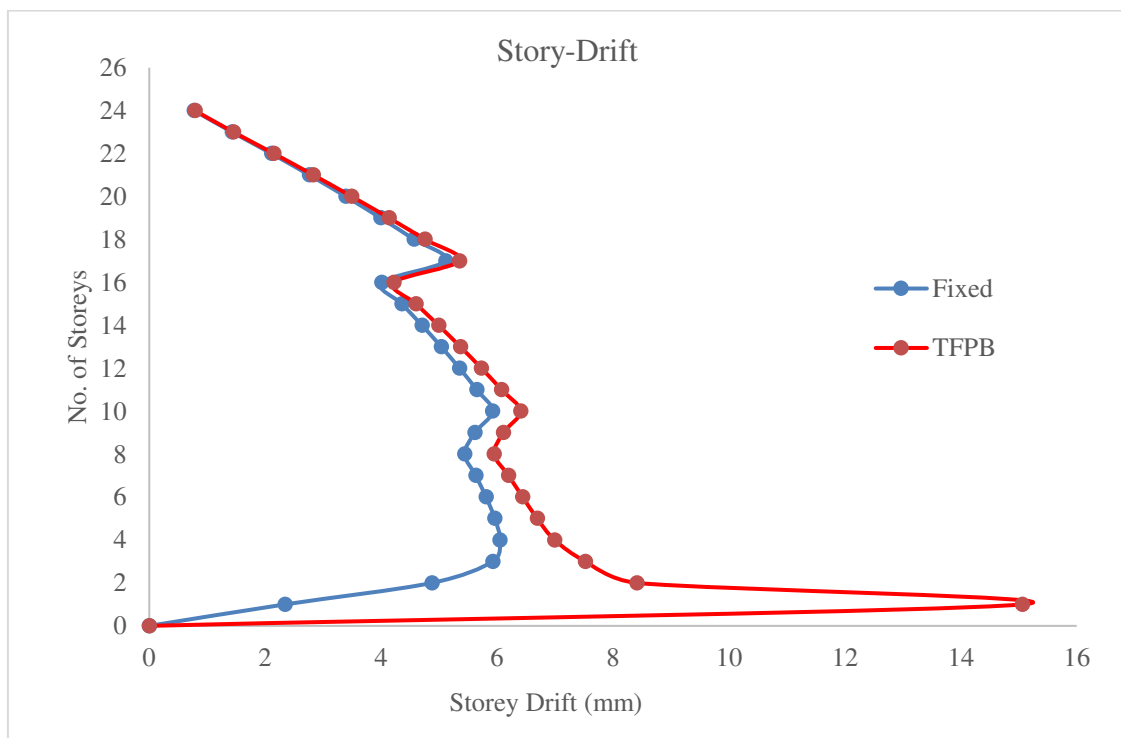
Storey-Displacement in Case-VI is raised by 30.94% as compared to Case-IV.

6.5.4 Storey-Drift.

Table-40. Comparison of Storey-Drift of Fixed Base Structure (Case-IV) and TFPB Base Structure (Case-VI).

Storey-Drift			
Storey	Fixed Base	TFPB Base	Remark
Storey -23	0.773	0.787	
Storey -22	1.429	1.453	
Storey -21	2.107	2.149	
Storey -20	2.76	2.83	
Storey -19	3.39	3.493	
Storey -18	3.991	4.135	
Storey -17	4.568	4.757	
Storey -16	5.112	5.35	
Storey -15	4.011	4.22	
Storey -14	4.356	4.6	
Storey -13	4.705	4.99	
Storey -12	5.037	5.367	
Storey -11	5.352	5.73	
Storey -10	5.649	6.077	

Storey -9	5.922	6.405	
Storey -8	5.617	6.108	
Storey -7	5.442	5.951	
Storey -6	5.632	6.197	
Storey -5	5.81	6.442	
Storey -4	5.961	6.692	
Storey -3	6.049	6.994	
Storey -2	5.925	7.524	
Storey -1	4.874	8.413	
Ground	2.343	15.06	



Graph-16. Parametric Change of Storey-Drift of Fixed Base Structure (Case-IV) and TFPB Base Structure (Case-VI).

The Storey-Drift of G+22 Storey reinforced concrete structure for case (b) Case-IV: Fixed Base Structure and Case-VI: TFPB Base Structure is shown in table-40. The storey-drift follows a non-linear pattern which can be observed in graph as shown in graph-16. The Storey-Drift is reduced by 44.14% which makes the structure ideally stiff & provides less damage to the structure. The storey-drift obtained are well within the limit as per IS 1893:2016.

6.5.5 Steel Reduction.

Table-41. Comparison of Steel Reduction of Fixed Base Structure (Case-IV) and TFPB Base Structure (Case-VI).

Steel Reduction (%)			
Sr. No.	Description	Fixed Base (mm ²)	TFPB Base (mm ²)
1	Column-Biaxial	265416	229720
2	Column-Uniaxial	4513480	4021152
3	Column-Axial	16957790	15960503
Reinforcement in Column=		21736686	20211375
Reinforcement Reduction in Column =		7.02%	
1	Beam	17355952	14759524
Reinforcement Reduction in Beam =		14.96%	
Total Reinforcement Reduction =		21.98%	

The Steel Reduction of G+22 Storey reinforced concrete structure for case (b) Case-IV: Fixed Base Structure and Case-VI: TFPB Base Structure is shown in table-41. The Steel in Case-VI is reduced by 21.98% as compared to Case-IV.

6.5.6 Overall Cost Economy.

Table-42. Comparison of Overall Cost Economy of Fixed Base Structure (Case-IV) and TFPB Base Structure (Case-VI).

Overall Cost Economy				
Sr. No.	Description	Quantity	Units	Remark
1	Approx Reinforcement Quantity	5	Kg/Sft	
2	Total Reinforcement Reduction (Approx 22%)	1.1	Kg/Sft	
3	Total Cost Reduction due to TFPB (Round off)	80	Rs.	Steel 70 Rs./Kg
4	Cost of Triple Friction Pendulum Bearing	160	Rs./Sft	
5	Net Cost for Friction Pendulum Bearing	80	Rs.	
6	Approx. cost of Construction	1500.00	Rs./Sft	
7	Effective Incremental in Construction Cost	5.33	%	

The Overall Cost Economy of G+22 Storey reinforced concrete structure for case (b) Case-IV: Fixed Base Structure and Case-VI: TFPB Base Structure is shown in table-42. The Overall cost economy of Case-VI is raised by 5.33% as compared to Case-IV.

6.6 Summary

In this chapter, comparison of Time period, Base shear, Storey-displacement, Storey-drift, Percentage reduction of steel and overall cost economy is done and their parametric change is shown in the form of graph. The summary of analysis of result is shown below.

Table-43. Summary of Result Analysis

S.N.	Description	LRB Base	TFPB Base
For G+12 Storey Reinforced Concrete Structure			
1	Time Period	26.23%	17.60%
2	Base Shear	61.07%	62.91%
3	Storey-Displacement	58.74%	49.41%
4	Storey-Drift	64.06%	49.72%
5	Percentage Steel Reduction	25.67%	26.69%
6	Overall Cost Economy	7.00%	4.00%
For G+22 Storey Reinforced Concrete Structure			
1	Time Period	14.89%	11.63%
2	Base Shear	42.81%	44.45%
3	Storey-Displacement	39.76%	30.94%
4	Storey-Drift	55.07%	44.14%
5	Percentage Steel Reduction	21.20%	21.98%
6	Overall Cost Economy	8.00%	5.33%

CHAPTER – VII

CONCLUSIONS



The primary goal of this effort was to analyze and construct a medium-rise reinforced concrete framework that used base isolation bearings. When opposed to a fixed base construction, base isolator bearing optimization produces better outcomes. Time duration, base shear, storey displacement, storey drift, percentage of steel reduction, and overall cost economy are several of the characteristics that examined for their effect.

In the present study, a G+12 storey & G+22 storey RC building was analyzed using response spectrum method for Case (a) G+12 Storey RC Structure viz. Case-I: Fixed base structure, Case-II: LRB base structure & Case-III: TFPB base structure and Case (b) G+22 Storey RC Structure Viz. Case-IV: Fixed base structure, Case-V: LRB base structure & Case-VI: TFPB base structure. According to chapter 6's (Analysis of Results) findings, base isolation systems are more important during earthquakes than fixed based framework.

The Time period in Case-II & Case-V is increased by 26.23% and 14.89% respectively and in Case-III & Case-VI is increased by 17.60% and 11.63% respectively which result into increase in reaction time of structure during earthquake against fixed base framework Case-I & Case-IV.

The Base shear in Case-II & Case-V is reduced by 61.07% and 42.81% respectively and in Case-III & Case-VI is reduced by 62.91% and 44.45% respectively which reduces the seismic effect on framework during earthquake against fixed base framework Case-I & Case-IV.

The Storey-displacement in Case-II & Case-V is increased by 58.74% and 39.76% respectively and in Case-III & Case-VI is increased by 49.41% and 30.94% respectively makes framework more flexible during earthquake against fixed base framework Case-I & Case-IV.

The Storey-drift in Case-II & Case-V is reduced by 64.06% and 55.07% respectively and in Case-III & Case-VI is increased by 49.72% and 44.14% respectively which makes the structure ideally stiff & Compared to fixed Case-I & Case-IV, the structure sustains less damage. The storey-drift obtained are well within the limit as per IS 1893:2016.

The percentage of steel in Case-II & Case-V is reduced by 25.67% and 21.20% respectively and in Case-III & Case-VI is reduced by 26.69% and 21.98% respectively which result into cost saving against fixed base framework Case-I & Case-IV.

The Overall cost economy in Case-II & Case-V the construction cost is fairly increased by 7.00% and 8.00% respectively and in Case-III & Case-VI the construction cost is fairly increased by 4.00% and 5.33% respectively as against to fixed base framework Case-I & Case-IV.

From the above studied, we can conclude that the effectiveness of the LRB based isolated structure is better TFPB based isolated structure. Base isolation system plays a vital role at the time of earthquake and perform well compare to fixed base structure. Cost difference is also very limitedly increased by approx. 7.0 to 8.0% for LRB and 4.0 to 6.0% for TFPB. With base isolation system provision, a structure is offered a discount of approx. 30% by Insurance Company. With base isolation system provision, maintenance cost of the structure is reduced which increases the life of structure compared to fixed base structure.

7.1 Future Work

Here we have consider square building with residential usage loading criteria from Indian Standards and height limitation of 45 meter and 70 meter according to the DCR. One can take rectangle / square building and can go beyond 70 meter height and also can analyze for commercial buildings.

CHAPTER – VIII

BIBLIOGRAPHY



REFERENCES

1. Domenicoa, D. D., Gandellib, E., & Virginio. (2020). Effective base isolation combining low-friction curved surface sliders and hysteretic gap dampers. *Soil Dynamics and Earthquake Engineering*, 1-20.
2. Deringol, A. H., & Gunyesi, E. M. (2020). Single and combined used of friction-damped and base-isolated system in ordinary buildings. *Journal of Constructional Steel Research*, 1-18.
3. Lina, Y.-S., Chana, R. W., & Tagawa, H. (2020). Earthquake early warning-enabled smart base isolation system. *Automation in Construction*, 1-12.
4. Angelis, F. D., & Cancellara, D. (2019). Dynamic analysis and vulnerability reduction of asymmetric structures: Fixed base vs base isolated system. *Composite Structures*, 203-220.
5. Khana, B. L., Azeem, M. A., & Usman, M. A. (2019). Effect of near and far Field Earthquakes on performance of various base isolation systems. *International Conference on Fracture and Structural Integrity*, 108-118.
6. Calvia, P. M., & Calvib, G. M. (2018). Historical development of friction-based seismic isolation systems. *Soil Dynamics and Earthquake Engineering*, 14-30
7. Santhosh, H. P., Harsha, M. S., Manohar, K., & Pradeep, B. B. (2017). Seismic Isolation of RC framed Structures with and Without Infills. *International Journal of Civil Engineering and Technology (IJCIET)*, 316-327.
8. Cancellara, D., & Angelis, F. D. (2016). Assessment and dynamic nonlinear analysis of different base isolation system for a multi-storey RC building irregular in plan. *Computers and Structures*, 1-15.
9. Somasekhariah, H. M., Dharmesh, N., & Ghouse, M. (2016). A Comparative study on RC frame structure considering Lead Rubber Bearing and Triple Friction Pendulum Bearing. *International Journal of Innovative Research in Science, Engineering and Technology*, 14907-14918.
10. Nitya , M., & Arathi , S. (2016). Study on the earthquake response of a RC building with base isolation. *International journal of science and research*, 1002-1005.

11. Thomas, T., & Mathai, A. (. (2016). Study of base isolation using friction pendulum bearing system. *Journal of Mechanical and Civil Engineering*, 19-23.
12. Vijaykumar, M., Manivel, S., & Arokiaprakash, A. (2016). A study on seismic performance of RCC frame with various bracing systems using base isolation technique. *International journal of applied engineering research*, 7030-7033.
13. Prasada Rao, D. V., & Sulochana, G. (2016). Modelling of an infill wall for the Analysis of a Building frame subjected to Lateral force. *International Journal of Civil Engineering and Technology*, 180-187.
14. Desai, M., & John, R. (2015). Seismic performance of base isolated multi-storey building. *International journal of scientific & engineering research*, 84-89.
15. Naveen, K., Prabhakara, H., & Eramma, H. (2015). Base isolation of mass irregular RC multi-storey building. *International research journal of engineering and technology*, 902-906.
16. Noorzai, M., Bajad, M., & Dodal, N. (2015). Study response of fixed base and isolation base. *International journal of innovative research in science, engineering and technology*, 3674-3681.
17. Ghodke, R. B., & Admane, S. V. (2015). Effect of base-isolation for building structures. *International journal of science, engineering and technology research*, 971-974.
18. Dia, N. E., & Mustafa, W. A. (2015). Seismic base isolation in reinforced concrete structures. *International journal of research studies in science, engineering and technology*, 1-13.
19. Khan, M., & Bakre, S. (2015). Design and study of seismic base isolators. *Journal of basic and applied engineering research*, 734- 739.
20. Barmo, A., Mualla, I. H., & Hasan, H. T. (2015). The behaviour of multi-story buildings seismically isolated hybrid isolation (friction, rubber and with the addition of rotational friction dampers). *Open journal of earthquake research*, 1-13.
21. Keerthana, S., Sathish Kumar, K., & Balamonica, K. (2015). Seismic response reduction of structures using base isolation. *International journal of innovative science, engineering and technology*, 33-40.

22. Warriar, G. A., Balamonica, K., & Sathish Kumar, K. (2015). Study on laminated rubber bearing base isolators for seismic protection of structures. *International journal of research in engineering and technology*, 466-476.
23. El-Bayoumi, K., Naguib, M., & Fikry, S. A. (2015). Dynamic analysis of high rise seismically isolated building. *American journal of civil engineering*, 43-50.
24. Khooshki, M. E., & Shahri, A. A. (2015). Seismic response controlling of structures with a new semi base isolation devices. *Walia journal*, 30-38.
25. Reddy, A. R., & Ramesh, V. (2015). Seismic analysis of Base Isolated Building in RC framed structures. *International journal of civil and structural engineering research*, 170-176.
26. Taywade, P. W., & Savale, M. N. (2015). Sustainability of structure using base isolation techniques for seismic protection. *International journal of innovative research in science, engineering and technology*, 1215-1228.
27. El-Bayoumi, K. (2015). Modelling of Triple Friction Pendulum Bearing in SAP2000. *International journal of advances in engineering and technology*, 1964-1971.
28. Arya, G., Alice, T. V., & Mathai, A. (2015). Seismic analysis of high damping rubber bearings for base isolation. *International journal of research in engineering and technology*, 321-327.
29. Ramani, T. (2015). Smart Base Isolators for Seismic Control of Structures. *Vellore Institute of Technology*, Chennai.
30. Warriar, G. A., & Sathish Kumar, K. (2015). Response Control of Structures using Base Isolation.
31. Moretti, S., Trozzo, A. C., Terzic, V., Cimellaro, G. P., & Mahin, S. (2014). Utilizing base-isolation systems to increase earthquake resiliency of healthcare and school buildings. *4th International conference on building resilience*, 969-976.
32. Nautiyal, P., Singh, S., & Batham, G. (2013). A COMPARATIVE STUDY OF THE EFFECT OF INFILL WALLS ON SEISMIC PERFORMANCE OF REINFORCED CONCRETE BUILDINGS. *International Journal of Civil Engineering and Technology (IJCET)*, 208-218.
33. Rezaei, S., Amiri, G. G., & Namiranian, P. (2014). Effects of Triple Pendulum

- Bearing on Seismic response of Isolated Buildings under near field excitations. *Earthquake engineering and Structural dynamics*.
34. Kubo, T., Yamamoto, T., & Sato, K. (2014). A seismic design of nuclear reactor building structures applying seismic isolation system in a high seismicity region – A feasibility case study in Japan. *Nuclear engineering and technology*, 581-594.
 35. Nhan, D. D. (2013). Predicting the displacement of Triple Pendulum Bearings in a full scale shaking experiment using a three dimensional element. *Earthquake engineering & Structural dynamics*.
 36. EFILOGLU, M. (2013). Understanding the concepts of base isolation.
 37. Nautiyal, P., Singh, S., & Batham, G. (2013). A Comparative study of the effect of infill walls on seismic Performance of Reinforced Concrete Buildings. *International Journal of Civil Engineering and Technology*, 208-218.
 38. Petti, L., Polichetti, F., & Lodato, A. (2013). Modelling and analysis of Base Isolated Structures with Friction Pendulum System considering near fault events. *Open journal of civil engineering*, 86-93.
 39. Jamnekar, V. P., & Durge, P. V. (2013). Seismic evaluation of brick.
 40. Computers and Structures (2012). SAP2000 Integrated Finite Element Analysis and Design of Structures, Analysis Reference. Berkeley, California, USA: Computers and Structures. 29
 41. Wancheng, Y., Binbin, W., Pakchui, C., Xinjian, C., & Zhaojun, R. (2012). Seismic performance of cable-sliding friction bearing system for isolated bridges. *Earthquake Engineering and Engineering Vibration*, 173-183
 42. Malekzadeh, M., & Taghikhany, T. (2012). Multi-Stage performance of seismically isolated bridge using Triple Pendulum Bearing. *Advances in structural engineering*.
 43. T. Okazaki, E, Sato K. Kajiwar, K. Ryan and S. Mahin, (2012). Defense Base Isolation Tests: Performance of Triple-Pendulum Bearings. 15 WCEE, LISBOA2012.
 44. UC Berkeley (2010). Peer ground motion database. Technical report, *Pacific Earth- quake Engineering Research Center*: 26
 45. Kravchuk, N., Colquhoun, R., & Porbaha, A. (2008). Development of a friction pendulum bearing base isolation system for earthquake engineering

- education. *American society for engineering education*.
46. Hussain, S., Lee, D., & Retamal, E. Viscous damping for base isolated structures.
 47. Deb, S.K. (2004). Seismic base isolation – An overview. *Geotechnics and earthquake hazards*, 1426-1430.
 48. Kunde , M. C., & Jangid, R. S. (2003). Seismic behavior of isolated bridges: A state of the-art review. *Electronic Journal of Structural Engineering*, 3, 140 170. 9, 18, 19, 20, 21.
 49. Connor, J. (2002). Introduction to Structural Motion Control. *Massachusetts Institute of Technology*. 12, 31, 34, 39
 50. Trombetti, C., Ceccoli, C., & Silvestri, L. (2001). A simplified approach to the analysis of torsional problems in seismic base isolated structures. In A. Singh (Ed.), *Creative Systems in Structural and Construction Engineering*.
 51. Naeim, F., & Kelly, J. (1999). Design of Isolated Structures from Theory to Practice. *John Wiley Sons.*, 19, 20
 52. Charng, P. H. (1998). Base Isolation for Multistorey Building Structures. Ph. D. thesis, *University of Canterbury*.
 53. Tsai, C. (1997). Finite element formulations for friction pendulum seismic isolation bearings. *International Journal for Numerical methods in Engineering*, 29-49
 54. Krawinkler, H. and M. Rahnama (1992). Effects of soft soils on design spectra. In A. Balkema (Ed.), Proceedings of the Tenth. *World Conference on Earthquake Engineering*, 5841-5844
 55. Mokha, A., Constantinou, M., Reinhorn, A., & Zayas, V. (1991). Experimental study of friction-pendulum isolation system. *Journal of Structural Engineering.*, 1201-1217
 56. Andriono, T. (1990). Seismic Resistant Design of Base Isolated Multistorrey Structures. Ph.D. thesis, *University of Canterbury*.
 57. Jenkins, H. Velocity Displacement for NS El Centro Acceleration. *Mercer University*.
 58. Mostaghel, N., & Khodaverdia, M. (1987). Dynamics of resilient-friction base isolator. *Earthquake Engineering and Structural Dynamics.*, 379-390
 59. Zayas, V., Low, S., & Mahin, S. (1987). The fps earthquake resisting system,

- experimental report. Technical Report UCB/EERC-87/01,, *Earthquake Engineering Research Center, University of California, Berkeley.*
60. Ehrlich, E., Flexner, S. B., Carruth, G., & Hawkins, J. (1980). *Oxford American Dictionary*. Avon Books.
61. Skinner, R., & McVerry, G. (1975). Base isolation for increased earthquake resistance of buildings. *Bulletin of New Zealand Society for Earthquake Engineering*, 93-101

I.S. CODE

62. IS 456:2000 Plain and Reinforced Concrete - Code of Practice.
63. IS: 875 (part 1-5) Standards for structural safety building loading - code of practice.
64. IS 1893:2016 Criteria for Earthquake Resistant Design of Structures - Part 1: General Provisions and Buildings
65. IS 13920:2016 Ductile Design and Detailing of Reinforced Concrete Structures Subjected to Seismic Forces - Code of Practice.
66. SP: 16 Design aids for reinforced concrete.
67. IBC 2000 International Building Code.
68. UBC 1997 Uniform Building Code - Structural Design Requirements.

BOOK

69. Dr. Jain k., Explanatory example on Indian seismic code IS 1893 (Part-1).
70. Dr. Shah H.J. & Dr. Jain Sudhir k., Design example of a six storey building.
71. Earthquake tips (1 to 24), Learning earthquake design and construction.

WEBSITE

72. <https://www.youtube.com/watch?v=J2eHCxB-K7s>
73. <https://www.youtube.com/watch?v=Tqr0k4Dw2FM>
74. <https://www.youtube.com/watch?v=thIRPajbxTU>
75. <https://www.youtube.com/watch?v=LTa9q6noUAQ>
76. <https://www.youtube.com/watch?v=Foo06lqMepU>

- 77. https://www.youtube.com/watch?v=PlpJx_UffBM
- 78. <https://www.youtube.com/watch?v=e3Erp-6FNsg>
- 79. <https://www.youtube.com/watch?v=Nc4JcWn6nYs>
- 80. <https://www.youtube.com/watch?v=sJQCWfXSgSs>
- 81. <https://www.youtube.com/watch?v=DuDf8jFBEOk>

PUBLICATIONS



A Study on Different Types of Base Isolation System over Fixed Based



M. Tamim Tanwer, Tanveer Ahmed Kazi and Mayank Desai

Abstract Based isolation is a technique which is used to prevent or reduce damage to a structure at a time of earthquake. It is a design principle by which flexible supports (isolators) are installed under every supporting point of a structure. It is generally located across a foundation (substructure) and superstructure. Seismic hazards are key concern for a earthquake prone areas of the world. Performance-based earthquake design has brought recent technological advances which has established new approach to construct earthquake resistant structure. Base isolation systems are progressively used technique for advanced earthquake resistance structure. The effect of different types of base isolator over earthquake resistant structures is studied in this paper. The work focuses on comparative study of different types of base isolators such as lead rubber bearings (LRB), friction pendulum bearings (FPB), elastomeric rubber bearing (ERB), high damping rubber bearings (HDRB), and low damping rubber bearing (LDRB) and compared for time period, base shear, fundamental period, frequency, storey drift, time history analysis, and displacement of the fixed base.

Keywords Base isolation system • Lead rubber bearings (LRB)
Friction pendulum bearings (FPB) • Elastomeric rubber bearing (ERB)
High damping rubber bearings (HDRB) • Low damping rubber bearing (LDRB)
Earthquake

M. Tamim Tanwer (✉)
Pacific University, 76/77 Amber Colony Harinagar-1, Udhna, Surat
Gujarat 394210, India
e-mail: tamimtanwer@gmail.com

T. A. Kazi
Pacific University, Pacific Hills, Pratapnagar Extension, Airport Road, Debari,
Udaipur 313003, India
e-mail: tanveerkz79@gmail.com

M. Desai
SVNIT Surat, Keval Chowk, SVNIT Campus, Athwa, Surat, Gujarat 395007, India
e-mail: dmayank@gmail.com

1 Introduction

An earthquake is one of nature's most dangerous disasters which results in significant loss of life and terrible harm to the property, especially man-made structures. An earthquake is a shaking of the earth surface which results from the sudden release of accumulated energy in the tectonic plates of the earth lithosphere and due to which seismic waves occurs. Earthquake is a natural calamity which has destroyed millions of lives throughout in the past historic time. Due to earthquake, a force is precipitate from the earth lithosphere and which lasted for short duration of time.

Base isolation system is a technique introduced in a structure which separates the structure from damaging induced by seismic waves and it will prevent the superstructures from engrossing the earthquake force. Base isolator mechanism helps to increase the natural time period of the structure and decreases the earthquake acceleration response. The base isolation system rests on the structural bearing which lies between the superstructure and substructure and helps to dissolve the horizontal displacement, rotation or translation. The bearing which helps to prevents translation is known as a fixed bearing or fix-point bearing and if this bearing is fixed in all directions, then it is known as a guided bearing or unidirectional movable bearing. Earthquakes study provides guidance to architects and engineers with a number of important design criteria foreign to the normal design process. From the well-established methods reviewed by many researchers, base isolation system proves to be the most effective solution for a broad range of earthquake design problems and the effect of these systems over seismic responses of the structures are studied in this paper.

2 Objective of Study

The key objective of the base isolation system is to save the structure from earthquake's effect or to minimize the earthquake's effect. Many comparative researches have disclosed that the reaction of the isolated structure is remarkably less than the fixed (regular) base structure. The main objective of the study is to compare different types of base isolators such as lead rubber bearings (LRB), Friction pendulum bearings (FPB), elastomeric rubber bearing (ERB), high damping rubber bearings (HDRB), and low damping rubber bearing (LDRB) with time period, base shear, fundamental period, frequency, storey drift, time history analysis, and displacement of the fixed base.

3 Literature Study

Nitya and Arathi [1] have published a research paper for “Study of earthquake response of a RC building with base isolation” on International Journal of Science and Research (IJSR). In this research, a RCMR frame structure of G+6 storey’s with fixed base and with base isolation system is considered. Analysis is performed by using SAP 2000. They come to a conclusion that the base isolation system substantially increases the time period of the structure. It reduces correspondingly the base shear up to 75% as compared to fixed one. With the increase in fundamental period, RCMR frame with base isolation system completely removed the structure from the resonance range of the seismic waves. Analysis shows that the fundamental period of the structure is approximately twice for the isolated structure. Increment in fundamental period reduces the maximum acceleration and hence it reduces the earthquake force from the structure. From the tables and graphs, it gets clear that the storey displacements are much higher for isolated buildings, also the displacement of all the storeys are almost same. The isolator with rubber has more displacement as of friction isolator (Fig. 1).

Thomas and Mathai [2] have published a research paper for “Study of base isolation using friction pendulum bearing system” on Journal of Mechanical and Civil Engineering. They had created FEM model of base isolator in ANSYS 14.5 software. They had analyzed and compared the behavior of the friction pendulum bearing with rubber base isolator. Static analysis of base isolator as nonlinear is performed for different storey under different load value. They came to a conclusion that as we increase the number of storey load value, then stress intensity value also gets increased. The stress intensity value was found under permissible limits up to 30-storeys and we can design the base isolators for 22 storeys to 30 storey buildings. From this analysis, it gets clear that the slider movement produced a dynamic friction force which provides the required damping for engrossing the earthquake energy (Fig. 2).

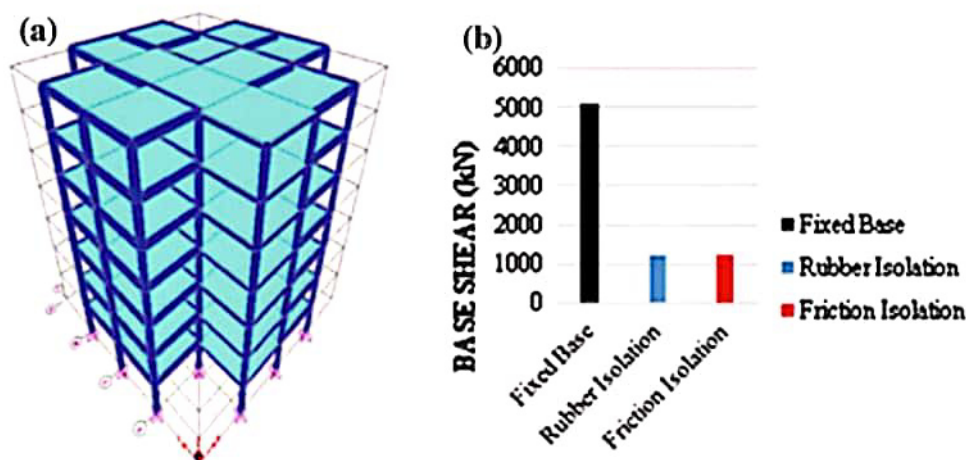


Fig. 1 a Perspective view of model, b comparison of base shear

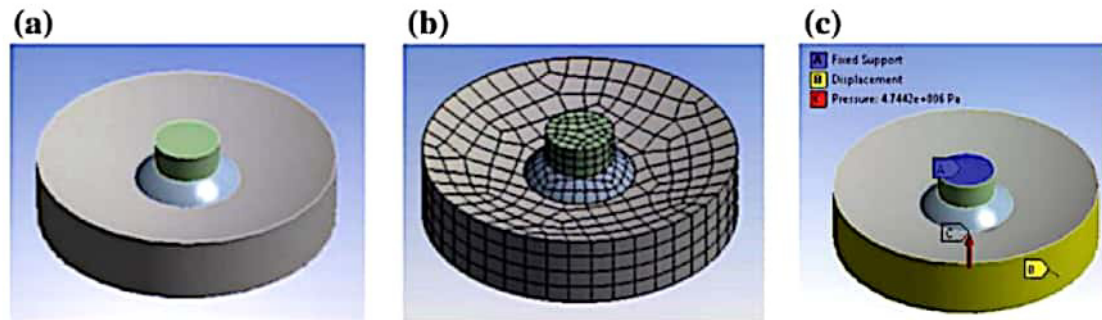


Fig. 2 a Model of the base isolator, b mesh configuration of the base isolator, c boundary condition of base isolator

Vijaykumar et al. [3] have published a research paper for “A Study on Seismic Performance of RCC Frame with Various Bracing Systems using Base Isolation Technique” on International Journal of Applied Engineering Research. In these research paper, a G+25 storey building square in plan is analyzed using design software SAP 2000. They come to a conclusion that the performance of the structure with base isolation systems proves more effective than a fixed base. The structure is analyzed for displacement and drift parameters and they noted that displacement in base isolation structure is high compared to fixed base. The main factor responsible for collapse of structure is its storey drift. The research shows that storey drift in base isolation structure is very much reduced compared to regular base structure. Though the cost of installation adds to drawback of base isolation, the performance proves its necessity in hospitals, public places, and essential buildings. Hence from the study, it can be observed that the bracing system performs better by the use of base isolation in seismic prone area (Fig. 3).

Desai and John [4] have published a research paper for “Seismic Performance of Base Isolated Multi-Storey Building” on International Journal of Scientific and Engineering Research. In this research paper, Dynamic Response Spectrum Analysis is worked out for 8-storey office building. The structure is analyzed with fixed

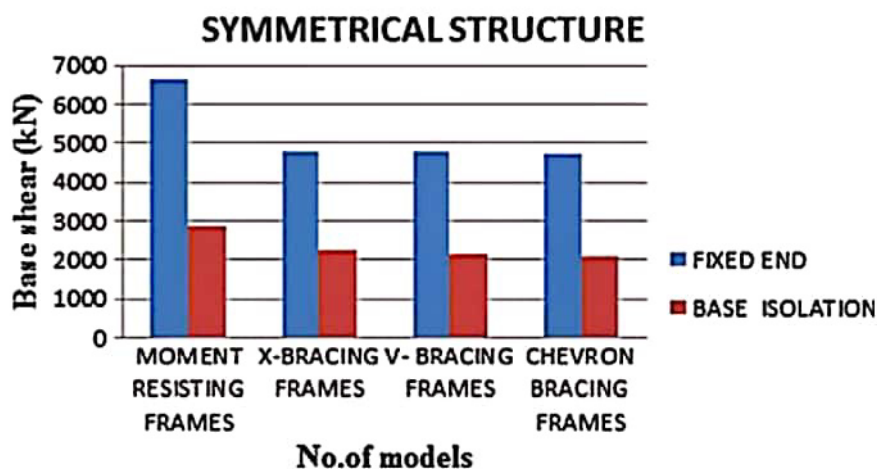
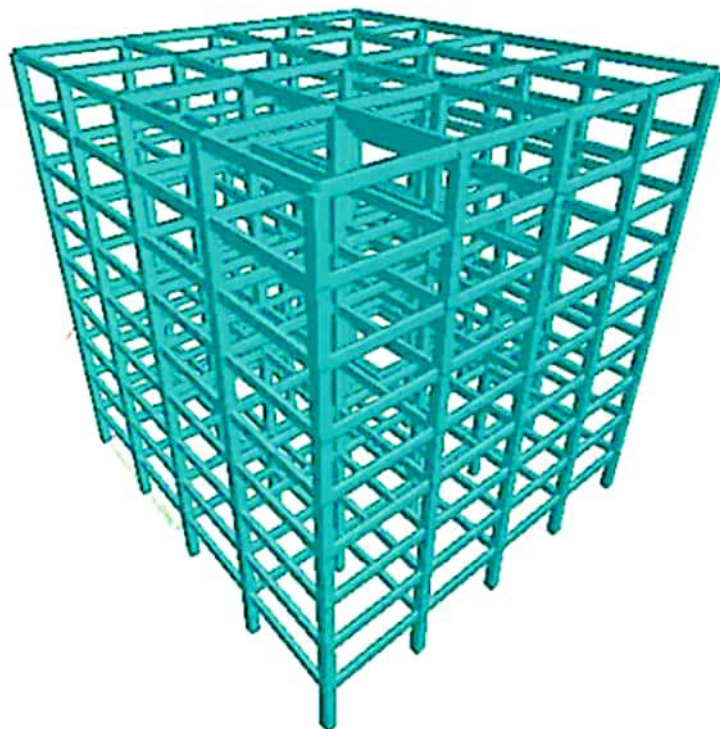


Fig. 3 Comparison of base shear

base structure and with different types of base isolator. Comparative study of different parameters like frequency, spectral acceleration, base shear, displacement, and storey drift is worked out without provision of base isolator and with provision of different base isolators. From the summary of results, it can be seen that In base-isolated structure, frequency has reduced as compared to the fixed base structure. Fundamental mode is more effective in seismic analysis. Frequency is minimum in LRB structure in fundamental mode compared to HDRB and LDRB. Acceleration has reduced when isolators are provided. LRB structure gives the least acceleration compared to HDRB and LDRB isolators. Base shear reduces considerably in base-isolated structure. The base shear in LRB structure is reduced to 47%, in HDRB structure it reduced to 33% and in LDRB structure it reduced to 34%, respectively, as compared to the fixed base structure. Displacement is very high in LRB, HDRB, and LDRB compared to fixed base structure. The Average displacement is maximum in LRB as compared to HDRB and LDRB. Storey drift has reduced considerably by provision of isolator. The reduction in storey drift at 9 m height are 13%, 13%, and 15%, respectively for HDRB, LDRB and LRB structures as compared to the fixed base structure. It can be concluded that the performance of the structure with base isolation systems proves more effective than a fixed base. Performance of LRB proves more effective as compared to the HDRB and LDRB (Fig. 4).

Naveen et al. [5] have published a research paper for “Base Isolation of Mass Irregular RC Multi-Storey Building” on International Research Journal of Engineering and Technology (IRJET). In this research paper, a G+9 storey building square is analyzed using design software SAP 2000. They come to a conclusion that the reduction in lateral displacement at top storey of regular structure was found to

Fig. 4 Perspective view of 8-storey office building model



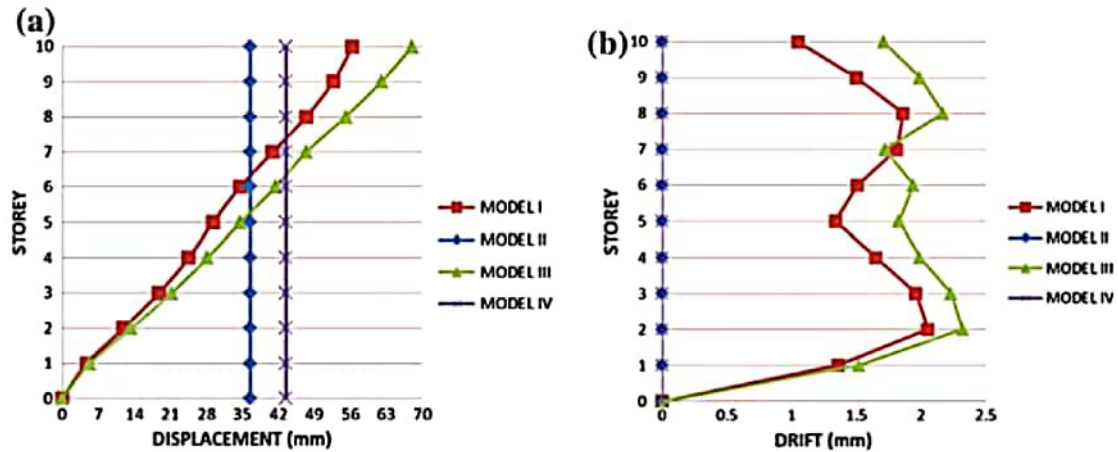


Fig. 5 a Graph showing displacement (mm) of all IV module, b graph showing drift (mm) of all IV module

be 35% whereas in mass irregular structure the lateral displacement at top storey was 36% from the history time analysis of El centro earthquake. From the analysis of lateral displacements in both directions, it came to know that torsion occurs due to mass irregularity in a structure. No inter-storey drifts was found in base-isolated structure, whereas in mass irregular structure large amount of inter-storey drifts found, which means that the structure takes rigid body movements in base-isolated structure as compared to a fixed base structure (Fig. 5).

Noorzai et al. [6] have published a research paper for “Study Response of Fixed Base and Isolation Base” on International Journal of Innovative Research in Science Engineering and Technology. In their research (G+25), RCC frame structure with fixed base and with isolated LRB base was analyzed and design using design software ETABS. They come to a conclusion that the structure with isolated base discloses less lateral deflection. The lateral displacement at base in base-isolated structure never equals zero and less amount of moment is generated than the fixed base structure. The base isolation systems separate the structure from the earthquake-induced load and also maintain larger fundamental lateral period as compared to a fixed base structure. Base isolation system also known as seismic base isolation is one of the most recent technique to protect the structure against seismic forces. It also helps in pertaining the passive vibration control to structure. Structure with isolated base separates the substructure and superstructure during the earthquake, and as a result, the substructure will move along the ground and the superstructure will be dormant. LRB proves to be the most effective base isolators as compared to fixed base and any other types of isolators (Fig. 6).

Ghodke and Admane [7] have published a research paper for “Effect Of Base-Isolation for Building Structures” on International Journal of Science, Engineering and Technology Research (IJSETR). In this research paper, a G+5 storey building is analyzed using design software SAP 2000. They come to a conclusion that with increasing the height of the structure, displacement is decreasing in

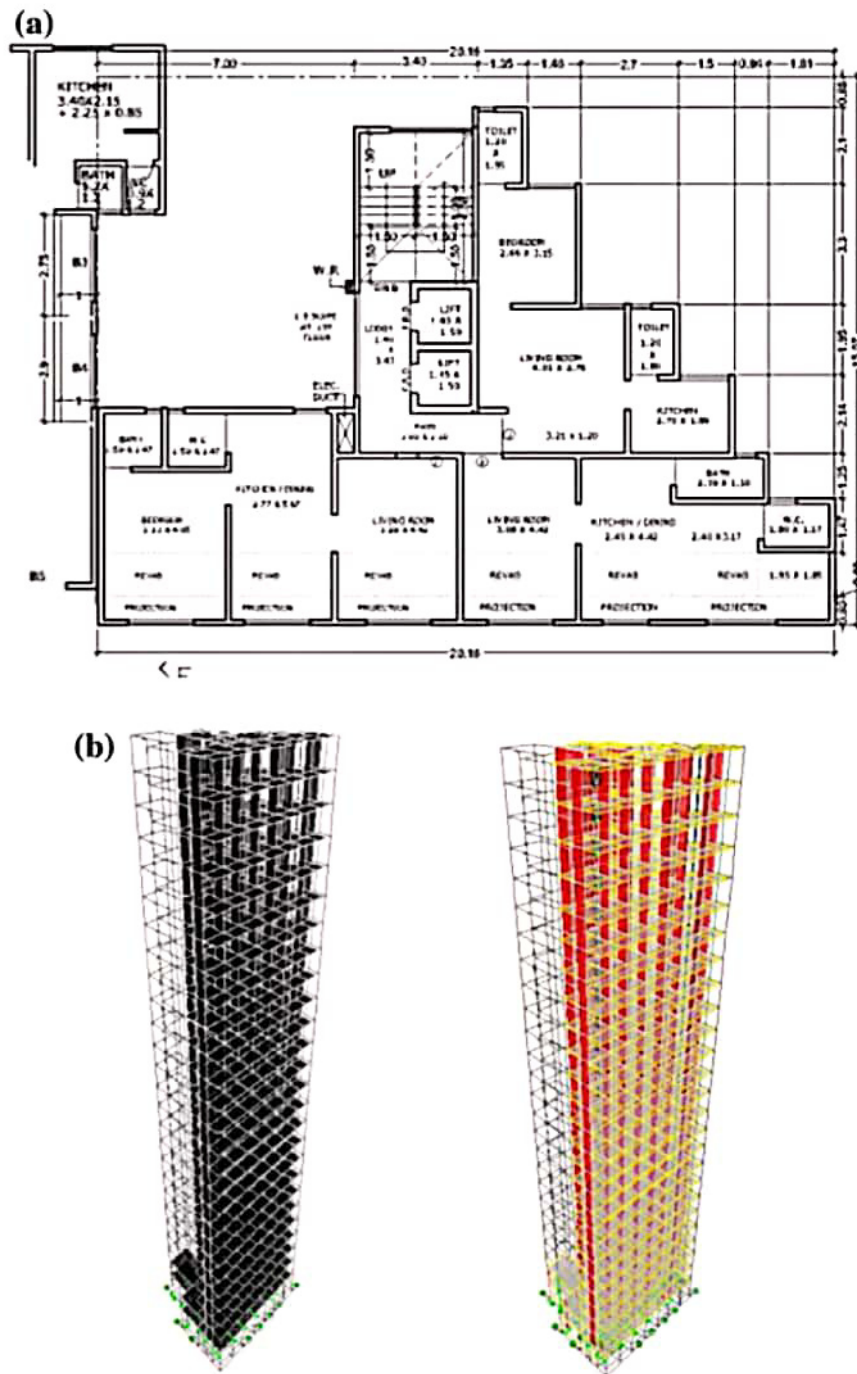


Fig. 6 a G+25 storey plan, b analytical models

base-isolated structure. The displacement is less in isolated—base structure than to a fixed base (Fig. 7).

Nassani and Wassef [8] have published a research paper for “Seismic Base Isolation in Reinforced Concrete Structures” on International Journal of Research Studies in Science, Engineering and Technology. G+4 storeys are analyzed with isolated base and without isolated base. The analysis was performed in design software SAP2000. They come to a conclusion that the structure with isolated base

reduces the base shear and storey drifts, on the other hand, it also increased the displacement as compared to fixed base systems where base shear and storey drift are too high and the displacement of structure get decreased (Fig. 8).

4 Conclusion

The base isolation system substantially increases the time period of the structure. It reduces correspondingly the base shear up to 75% as compared to fixed one. Fundamental period of the structure is approximately twice for the isolated structure. Fundamental modes prove more effective in seismic analysis. Performance of the structure with base isolation systems proves more effective than a fixed base. In base-isolated structure frequency has reduced as compared to the fixed base structure. Storey drift has considerably reduced by provision of a base isolator. The reduction in storey drift at 9 m height are 13%, 13%, and 15%, respectively, for HDRB, LDRB, and LRB structures as compared to the non-isolated structure. Performance of lead rubber bearing is better as compared to the HDR bearing and LDR bearing. In a time history analysis for EI Centro, earthquake reduction in top storey lateral displacement is 35% in 10 storied fixed base structures, whereas the reduction of lateral displacement is 36% in 10 storied mass irregular structures. No inter-storey drifts were found in base-isolated structure, whereas in mass irregular structure large amount of inter-storey drifts found, which means that the structure takes rigid body movements in base-isolated structure as compared to a fixed base structure. The base isolation systems separate the structure from the earthquake-induced load and also maintain larger fundamental lateral period as compared to a fixed base structure. It is concluded that with increasing the height of the structure, displacement is decreasing in base-isolated structure.

References

1. Nitya, M., Arathi, S.: Study on the earthquake response of a RC building with base isolation. *Int. J. Sci. Res.* **5**, 1002–1005 (2016)
2. Thomas, T., Mathai, A.: Study of base isolation using friction pendulum bearing system. *J. Mech. Civil Eng.* 19–23 (2016)
3. Vijaykumar, M., Manivel, S., Arokiaprakash, A.: A study on seismic performance of RCC frame with various bracing systems using base isolation technique. *Int. J. Appl. Eng. Res.* **11**, 7030–7033 (2016)
4. Desai, M., John, R.: Seismic performance of base isolated multi-storey building. *Int. J. Sci. Eng. Res.* **6**, 84–89 (2015)
5. Naveen, K., Prabhakara, H.R., Eramma, H.: Base isolation of mass irregular RC multi-storey building. *Int. Res. J. Eng. Technol.* **2**, 902–906 (2015)
6. Noorzai, M., Bajad, M.N., Dodal, N.: Study response of fixed base and isolation base. *Int. J. Innov. Res. Sci. Eng. Technol.* **4**, 3674–3681 (2015)

7. Ghodke, R.B., Admane, S.V.: Effect of base-isolation for building structures. *Int. J. Sci. Eng. Technol. Res.* **4**, 971–974 (2015)
8. Nassani, D.E., Wassef, M.A.: Seismic base isolation in reinforced concrete structures. *Int. J. Res. Stud. Sci. Eng. Technol.* **2**, pp. 1–13 (2015)
9. Kravchuk, N., Colquhoun, R., Porbaha, A.: Development of a friction pendulum bearing base isolation system for earthquake engineering education. In: *Proceedings of the 2008 American Society for Engineering Education Pacific Southwest Annual Conference*, Pittsburg, Pennsylvania, June (2008)
10. Keerthana, S., Sathish Kumar, K., Balamonica, K.: Seismic response reduction of structures using base isolation
11. Taywade, P.W., Savale, M.N.: Sustainability of structure using base isolation techniques for seismic protection. *Int. J. Innov. Res. Sci. Eng. Technol.* **4**(3) (2015)
12. Kooshki, M.E., Shahri, A.A.: Seismic response controlling of structures with a new semi base isolation device (2015)
13. Deb, S.K.: Seismic base isolation—an overview. *Current Sci.* 1426–1430 (2004)
14. Kelly, J.M.: *Earthquake-Resistant Design with Rubber* (1993)
15. Moretti, S., et al.: Utilizing base-isolation systems to increase earthquake resiliency of healthcare and school buildings. *Proced. Econ. Finance* **18**, 969–976 (2014)
16. Nitya, M., Arathi, S.: Design and study of seismic base isolators. *J. Basic Appl. Eng. Res.* **2** (9), 734–739 (2015)
17. Hussain, S., Lee, D., Retamal, E.: Viscous damping for base isolated structures. Taylor Devices (1998). <http://www.taylordevices.com/Tech-Paper-archives/literature-pdf/36-Viscous-Damping.pdf>
18. Kubo, T., et al.: A seismic design of nuclear reactor building structures applying seismic isolation system in a high seismicity region—a feasibility case study in Japan. *Nucl. Eng. Technol.* **46**(5), 581–594 (2014)
19. Arya, G., Alice, T.V., Alice, M.: Seismic analysis of high damping rubber bearings for base isolation



COMPARATIVE STUDY ON LEAD RUBBER BEARING (LRB) BASE ISOLATION SYSTEM ON G+12 & G+22 STORY RCC STRUCTURE OVER FIXED BASED FOR INDIAN SUBCONTINENT

M. Tamim Tanwer

Research Scholar, Pacific Academy of Higher Education & Research University-Udaipur, Rajasthan, India.

Prof. Dr. Tanveer Ahmed Kazi

Professor, Pacific Academy of Higher Education & Research University-Udaipur, Rajasthan, India.

Prof. Dr. Mayank Desai

Assistant Professor, Sardar Vallabhbhai National Institute of Technology-Surat, Gujarat, India.

ABSTRACT

Earthquake is a very dangerous natural disaster which occurs by movement of the tectonic plates in the core of earth. Due to earthquake many structures collapse which result into human life losses. Base Isolation System is the technique to absorb the earthquake forces and reduces the earthquake effects in the structure at the time of earthquake. In this paper, we are considering the design of G+12 & G+22 story RCC building with fixed base and with base isolation system. Lead rubber bearing (LRB) is used for the design of based isolated structure. Analyzing and designed of these two type of buildings are carried out by response spectrum method in ETABS 2016 software. After analyzing the Structure, time period, base shear, story displacement, story-drift, percentage reduction in steel and overall cost economy will be obtained for both type of structure. From this study, it is found that time period and story displacement increased while base shear, story drift, percentage of steel and overall cost is reduced with provision of Lead Rubber Bearing (LRB) as base isolators.

Keywords: Earthquake, Base Isolation System, Lead Rubber Bearings, Time Period, Base Shear, Story Drift, Story Displacement, Reinforcement, Cost Economy, Response

Cite this Article: M.Tamim Tanwer, Prof.Dr.Tanveer Ahmed Kazi and Prof.Dr.Mayank Desai, Comparative Study on Lead Rubber Bearing (LRB) Base Isolation System on G+12 & G+22 Story RCC Structure Over Fixed Based for Indian Subcontinent. International Journal of Civil Engineering and Technology 10 (11), 2019, pp. 423-433.

<https://iaeme.com/Home/issue/IJCIET?Volume=11&Issue=11>

1. INTRODUCTION

1.1. General

Earthquake is occurring due to movement of the tectonic plates in core of the earth. It is a horizontal movement of earth surface. By earthquake the top surface of earth is shake and foundation is also shake with them. Results the superstructure experience seismic forces and structural members are may collapse. Due to collapse of the structure humans can buried under debris. Peoples are lost their life and also their properties. We cannot construct earthquake proof structure but we can construct earthquake resistant structure.

1.2. Base Isolation System

Base isolation system is also famous in the name of seismic isolation system. It is a method which is protect the structure against seismic force. Base isolation is the effective technique of earthquake engineering appurtenance to the no action in structural vibration control technologies. The System is innovated by Dr. Bill Robinson at New Zealand in 1974. It is very popular system to protect the structures from seismic forces. This technique is useful for new structures as well as can also use in old structure. The base isolation is installing between the foundation and superstructure. It is not allowed to transfer the seismic forces from ground to the superstructure. Base isolation is work as a suspension type system and absorb seismic forces without transferring to superstructure.

Lead Rubber Bearings is very popular and expanded all over worldwide. It is also used in India. The first lead rubber bearing installed in India at G.K. general Hospital, Bhuj, Gujarat in 2001. In this hospital total 280 bearings are used. The LRB is made with rubber and lead core.

Lead Rubber Bearings are made up of alternate layers of hot vulcanized rubber and steel laminates with a cylindrical lead core in the center of the bearing. The energy can be dissipated by providing the lead core, by its yielding, it is allowed to achieve an equivalent with viscous damping coefficient about 30 %. The lead rubber bearings may show that the best economic solution for seismic base isolation problems because it brings the functions of vertical support, hardness at service load levels and horizontal flexibility at seismic load.

2. LITERATURE REVIEW

Khin Thanda Htun, Kyaw Kaung Cho (2019), has published a paper title “**Experimental in Structural Dynamics (Base Isolation System: Modelling)**” in International Journal of Trend in Scientific Research and Development (**IJTSRD**). The authors has determined dynamic behaviour of a steel structure model for without base isolated structure and with base isolated structure. They concluded that, the experimental result shows that the system used for base isolation reduced the time period of the structure and the relative displacement of the top with respect to the support. The base isolated system introduces in the structure make the structure more flexible thus reduced the effect of the earthquake loads on the structure. The base isolated method largely depends on the behaviours of the springs attached which provided the stability to the structure.

The experimental results are also affected by the distribution of the sensors. The mass of the sensor also contributes to the response of the structure. The sensor arrangement had mass concentration in every floor. The sensor arrangement should be arranged that there is no mass concentration and thus result minimum contribution to the structural response. [1]

Dhiraj Narayan Sahoo, Dr. Pravat Kumar Parhi (2018), has published a paper title “Base Isolation of Residential Building using Lead Rubber Bearing Technique” in International Journal of Engineering, Research and Technology (IJERT). They has designed G+10 and G+15 buildings with fixed base and with base isolation techniques. They design the buildings for Bhubaneswar, Odisha which is located in earthquake zone II.

The designing of buildings was completed in ETABS software. In base isolation system they used lead rubber bearings in their buildings. They concluded that, the time period of structure increases approximate 2 times after providing the base isolator to fixed base structure. Due to this increase in the time period, structure experiences less amount of seismic force. The lateral earthquake load, storey shear, column force and moment are reduced to significant amount due to base isolator to the structure. The maximum storey displacement in base isolated structure increases. The maximum storey stiffness of structure decreases in base isolated structure. From the above results, the damage to the base isolated structure will be less as compared to fixed base structure. [2]

Manoj Prajapati, Dr. Savita Maru (2018), has published a paper title “**Base Isolation for Earthquake Resistance: A Review**” in International research Journal of Engineering and Technology (IRJET). They has concluded from review that researchers introduce the new technology of base isolation system which protects building to damage under seismic action and the results like drift, displacement and base shear are better with building performance in case of base isolation then fixed base. Further, some more concluded points are: cost can be reasonable using software simulating applications, high rise building can be design for safety using design software’s, column beam design to optimize the size and strength, quality with cost optimize it can be design for future construction, effective planning and control can be performed for high rise building using simulation and design software’s. [3]

Saurabh P. Kharat, Dinesh N. Biradar, Ajay S. Sagekar, Prathamesh V. Chavan, Prof. Reshma Saikh (2018), has published a paper title “Case study on Lead Rubber Isolation Bearing” They concluded that, the study shows the effectiveness of the LRB base isolation system in terms of reduced structural responses under seismic loading. As the base isolators are extensively used worldwide in high seismic areas in near future, we will accept the same in India also. At least in seismic zone IV and V the use of base isolators has to be encouraged as they are technically very effective and economically feasible. The use of base isolators reduces inter-story drift and structural damages during earthquake. The building will be ready to occupy with the minor repair. The results of this work demonstrated that base isolators are excellent seismic control devices for high raise symmetric buildings. Base isolation method has proved to be a reliable method of earthquake resistant design. [4]

3. SAMPLE MODEL DETAILS

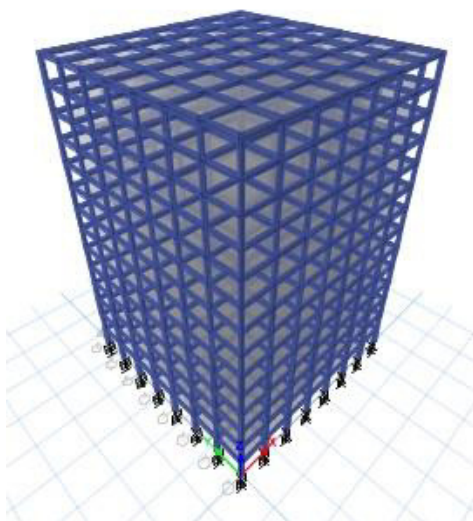


Figure 1: (G+12 Storey)

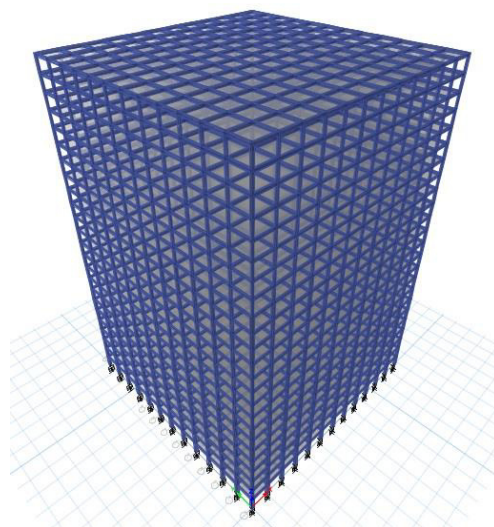


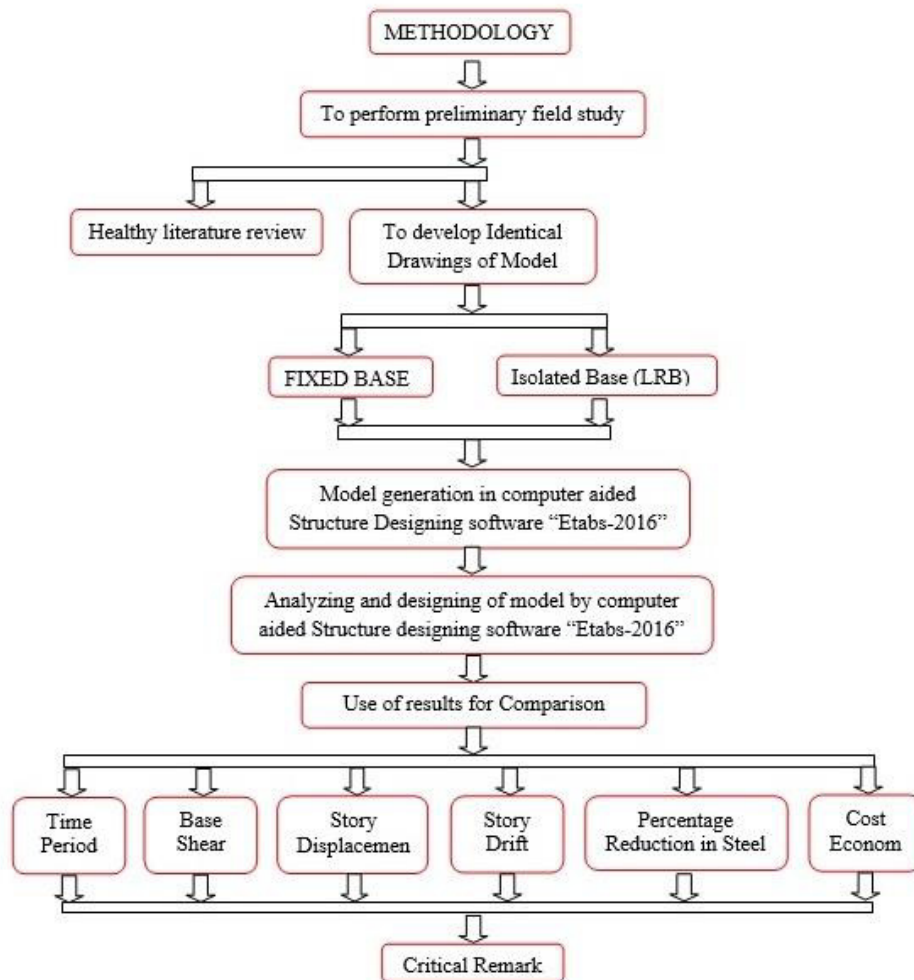
Figure 2: (G+22 Storey)

Sample Modal – 1 & 2	G+12 (7 Bay x 7 Bay)	Sample Modal – 3 & 4	G+22 (12 Bay x 12 Bay)
Beam	= 230 x 450 mm	Beam	= 230 x 450 mm
Column	= 300 x 300 (Storey 8 to Terrace) 375 x 375 (Plinth to Storey 7) 450 x 450 (Base)	Column	= 300 x 300 (Storey 16 to Terrace) 375 x 375 (Storey 8 to Storey 16) 450 x 450 (Plinth to Storey 7) 525 x 525 (Base)
Floor to Floor Height	= 3.0 m.	Wall Thickness	= 115 mm.
Floor Load		Floor Finish	= 1 KN/m ²
Live Load	= 3 KN/m ²	Seismic Zone	= Zone 3
Earthquake Load		Percentage Damping	= 5%
EQ load	= Response Spectrum Method		
Soil Type	= Hard Soil (Type-I)		
Modal Method	= SRSS		
Material			
Grade of Concrete	= M20 [20 N/mm ²]	Grade of Steel	= Fe500 [500 N/mm ²]
Unit weight of Concrete	= 25 KN/m ²	Unit weight of brick masonry	= 20 KN/m ²
Design basis	= Limit State Method (IS: 456-2000)		

The sample model of 7 bay x 7 bay for G+12 story building & 12 bay x 12 bay for G+22 Story building (1 bay = 4 m.) is taken with Seismic Zone III on hard soil type – I with the above following details is considered for Analysis & Design.

1. Model 1: - G+12 storey building with fixed base.
2. Model 2: - G+12 storey building with LRB base isolation.
1. Model 1: - G+22 storey building with fixed base.
2. Model 2: - G+22 storey building with LRB base isolation.

4. METHODOLOGY



5. ANALYSIS & DESIGN OF LEAD RUBBER BEARING (LRB)

For the Analysis & Design of Lead Rubber Bearing, the cumulative load at the base is obtained from the fixed based design model in Etabs. This load are categorized into three group's viz. Biaxial, Uniaxial and Axial loaded. Sample Calculation for one group is shown below.

Biaxial Load (W) = 1638 kN.

Time Period (T_D) = 2.5 sec.

Design Shear Strain (γ_{max}) = 50% = 0.5 kN/m².

Effective Damping (ξ_{eff}) = 5 % = 0.05 For U_1 , U_2 , U_3 .

TABLE A-16-C—DAMPING COEFFICIENTS, B_D AND B_M

EFFECTIVE DAMPING, B_D or B_M (percentage of critical) ^{1,2}	B_D or B_M FACTOR
≤ 2	0.8
5	1.0
10	1.2
20	1.5
30	1.7
40	1.9
≥ 50	2.0

TABLE 16-R—SEISMIC COEFFICIENT C_v

SOIL PROFILE TYPE	SEISMIC ZONE FACTOR, Z				
	Z = 0.075	Z = 0.15	Z = 0.2	Z = 0.3	Z = 0.4
S_d	0.06	0.12	0.16	0.24	$0.32N_f$
S_B	0.08	0.15	0.20	0.30	$0.40N_f$
S_C	0.13	0.25	0.32	0.45	$0.56N_f$
S_D	0.18	0.32	0.40	0.54	$0.64N_f$
S_E	0.26	0.50	0.64	0.84	$0.96N_f$
S_F	See Footnote 1				

Comparative Study on Lead Rubber Bearing (LRB) Base Isolation System on G+12 & G+22 Story RCC Structure Over Fixed Based for Indian Subcontinent

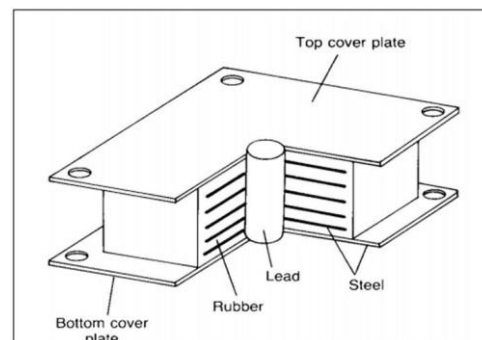
Damping Coefficient (B_D) = 1 (UBC-97, Vol-2, Pg. No. 414)

Seismic Coefficient (S_D) = 0.54 (UBC-97, Vol-2, Pg. No. 35)

Selecting 60 as Rubber Hardness for analysis in critical conditions

Hardness IRHD ± 2	Young's Modulus E (MPa)	Shear Modulus G (MPa)	Material Constant k	Elongation at Break Min, %
37	1.35	0.40	0.87	650
40	1.50	0.45	0.85	600
45	1.80	0.54	0.80	600
50	2.20	0.64	0.73	500
55	3.25	0.81	0.64	500
60	4.45	1.06	0.57	400

Table 5.4: Vulcanized Natural Rubber Compounds



Young's Modulus (E)	= 4.45Mpa 4450 kN/m ²	Modification factor (k)	= 0.57
Shear modulus (G)	= 1.06 Mpa 1060 kN/m ²	Elongation of rubber at break (ϵ_b)	= 4 (400%)
Allowable normal stress	= 7840 kN/m ² .	Yield strength of core(f_{py})	= 8500 kN/m ² .
Consulted manufacture, usually 7 to 8.5 Mpa Page No.132, Table 5.7			
Yield strength of steel plate (f_y)	= 274400 kN/m ² .	Shear Yield strength of steel (F_s)	= 164640 kN/m ² .

Part-1 Analysis of LRB

a) Effective Horizontal stiffness K_{effH}

$$K_{effH} = \frac{W}{g} \left(\frac{2\pi}{T_D} \right)^2 \quad K_{effH} = 1054.69 \text{ kN/m}$$

U_2 & U_3 Linear effective stiffness

b) Lateral displacement or Design displacement (DD)

$$D_D = \left(\frac{g}{4\pi^2} \right) \times \frac{S_D T_D}{B_D} = 0.335 \text{ m.}$$

c) Strength or short term yield force Q_d

$$Q_d = \frac{W_D}{4 \times D_D} = \frac{\pi}{2} \times K_{effH} \times \xi_{effH} \times D_D = 27.788 \text{ kN}$$

d) Post-yield horizontal stiffness K_d

K_U = Pre yield stiffness, K_d = Post yield stiffness, Where $K_U = 10 K_d$

Note- Initial elastic stiffness was estimated from experimental results in the range of 9 to 16 K_d

$$K_d = K_{effH} - \frac{Q_d}{D_D} = 971.854 \text{ kN/m.}$$

$$K_U = 10 K_d$$

e) Post yield stiffness ratio.

$$\frac{K_d}{K_U} = \frac{971.854}{9718.54} = 0.1 \quad U_2 \text{ \& } U_3 \text{ Post yield stiffness ratio.}$$

Part-2 Design of LRB

a) Lead Core Area A_p

$$A_p = \frac{Q_d}{f_{py}} = 0.00327 \text{ m}^2$$

b) Dia. of lead core d_p

$$A_p = \frac{\pi d_p^2}{4} \Rightarrow d_p = \sqrt{\frac{4A_p}{\pi}} = 0.06452 \text{ m.}$$

c) Total height of rubber layer t_r

$$t_r = \frac{D_D}{\gamma_{max}} = 0.67092 \text{ m.}$$

d) Shape factor S

$$\frac{E(1+2kS^2)}{G} \geq 400, S = 9.09409,$$

For $S < 10$, Take $S = 10$

e) Compressive modulus of rubber & steel (E_c)

$$E_c = E(1+2kS^2) = 511750 \text{ kN/m}^2.$$

f) Effective area of bearing A_o

$$A_o = W / \text{Allowable normal stress.} = 0.20893 \text{ m}^2.$$

g) Effective area from the shear strain A_1

$$\frac{6SW}{E_c \times A_1} \leq \frac{\epsilon_b}{3} = 0.14404 \text{ m}^2.$$

h) Elastic Stiffness K_r of the bearing

$$K_d = K_r \times \frac{1+12 \times A_p}{A_o} = 818.219 \text{ kN/m}.$$

i) Effective area of individual rubber layer (A_{sf})

$$A_{sf} = \frac{\pi d^2}{4} = 0.51789 \text{ m}^2.$$

j) Diameter of Rubber (d)

$$d = \sqrt{\frac{4A_{sf}}{\pi}} = 0.81203 \text{ m}.$$

k) Effective vertical stiffness (k_v)

$$K_v = \frac{E_c \times A_{sf}}{t_r}, K_v = 395022 \text{ kN/m}, U_1 \text{ Vertical Linear effective stiffness.}$$

l) Damping reduction factor (β)

$$\beta = 2 \times \cos^{-1} \left(\frac{D_p}{d} \right) = 2.29$$

m) Reduced area (A_2)

$$A_2 = \frac{d^2 \times (\beta - \sin \beta)}{4} = 0.25348 \text{ m}^2.$$

n) Details of Lead Rubber Bearing

$$A = 0.25348 \text{ m}^2 \text{ (max Area of } A_o, A_1, \text{ \& } A_2), d = 0.56811 \text{ m}.$$

$$\text{No. of layer (N)} = t_r/t, \text{ Where } t = 0.0203$$

$$N = 33.0491 \text{ say } N = 34.00$$

Total height of bearing (h)

$$h = t_r + N \times (t_s + 2 \times 0.0025), h = 0.94929 \text{ m}.$$

Steel Plate thickness (t_s)

$$t_s = \frac{2 \times W \times 2t}{A \times F_s}, t_s = 0.00319 \geq 0.002 \text{ m}.$$

Input Values for Etabs :

		G+12 Storey			G+22 Storey			
Direction U1	Cumulative Load	Biaxial	Uniaxial	Axial	Biaxial	Uniaxial	Axial	Units
		1638 KN	2487 KN	3920 KN	3342 KN	4627 KN	6860 KN	
	Linear Properties							
	Effective Stiffness	395022	599768	945352	805961	1115853	1654366	
Direction U2 & U3	Effective Damping	0.05	0.05	0.05	0.05	0.05	0.05	KN-s/m
	Linear Properties							
	Effective Horizontal Stiffness	1054.69	1601.35	2524.043	2151.88	2979.27	4417.08	
	Effective Damping	0.05	0.05	0.05	0.05	0.05	0.05	KN-s/m
	Non Linear Properties							
	Pre-yield Stiffness	9718.54	14755.8	23258.05	19828.7	27452.8	40701.6	
	Strength	27.788	42.191	66.501	56.696	78.495	116.377	KN
	Post Yield Stiffness ratio	0.1	0.1	0.1	0.1	0.1	0.1	

6. RESULTS

6.1. Time Period

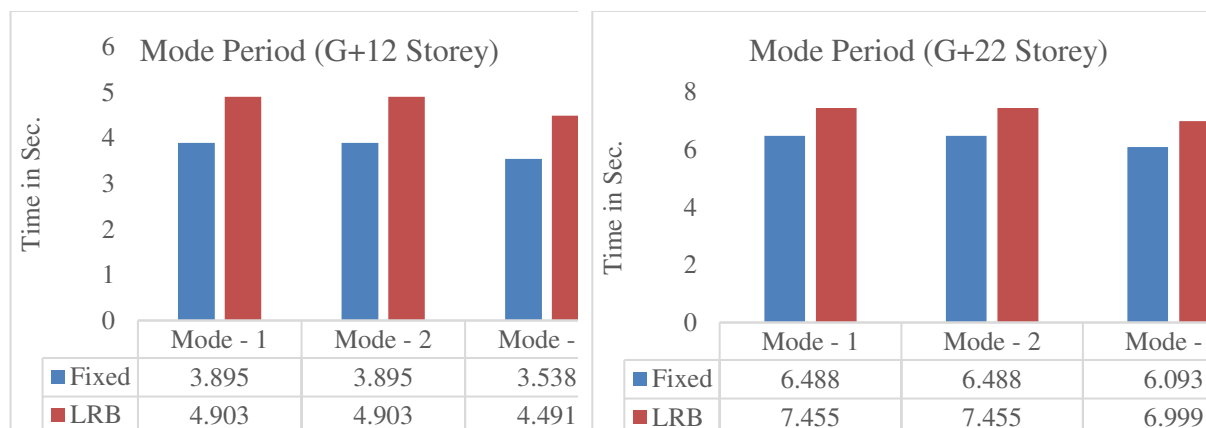


Figure 3: Time Period of G+12 & G+22 Storey models

Figure 3 shows the time period for fixed base and LRB base of G+12 & G+22 Storey models. Time period of base isolated structure over fixed base structure of G+12 & G+22 Storey is increased by 26.23% and 14.89 % respectively.

6.2. Base Shear

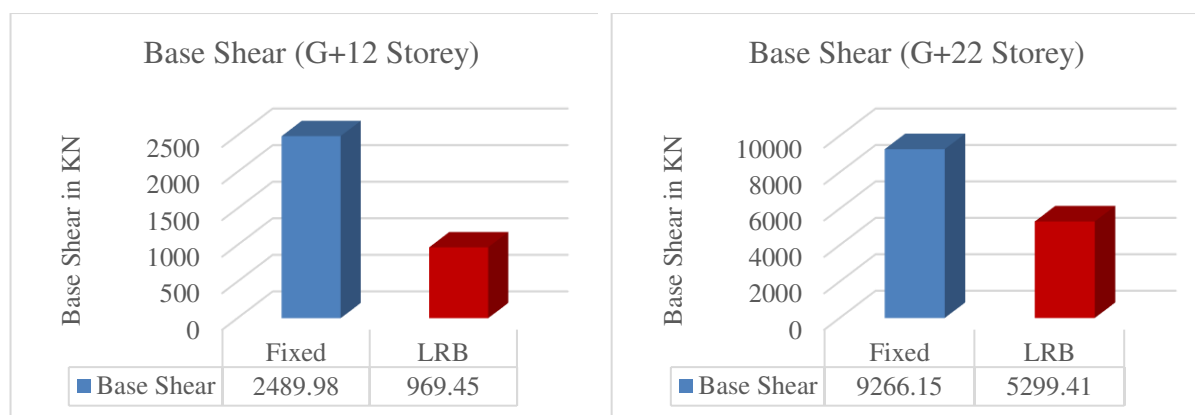


Figure 4: Base Shear of G+12 & G+22 Storey models

Figure 4 shows the base shear for fixed base and LRB base of G+12 & G+22 Storey models. Base shear of base isolated structure over fixed base structure of G+12 & G+22 Storey is decreased by 61.07% and 42.81 % respectively.

6.3. Storey-Drift

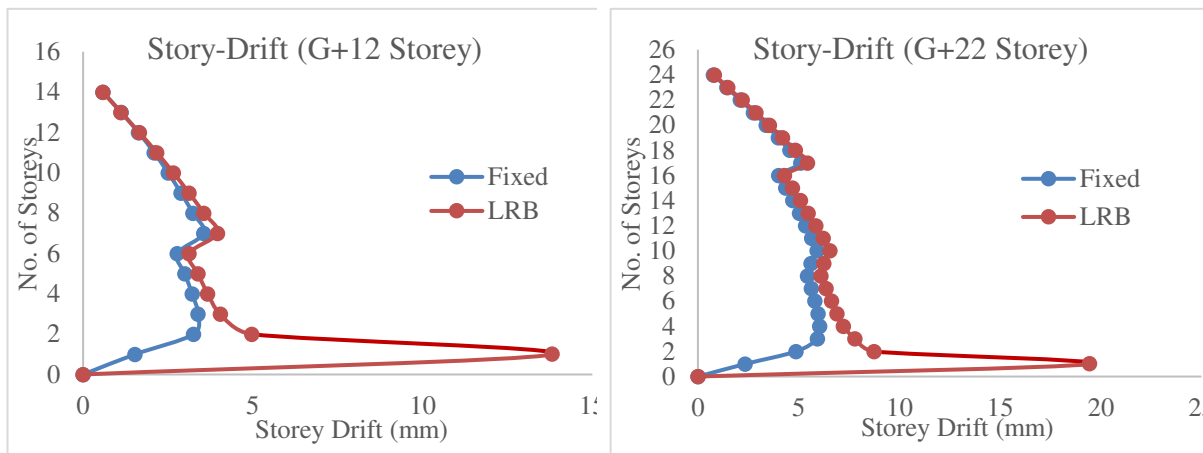


Figure 5: Storey-Drift of G+12 & G+22 Storey models

Figure 5 shows the storey-Drift for fixed base and LRB base of G+12 & G+22 Storey models. Storey-Drift of base isolated structure over fixed base structure of G+12 & G+22 Storey is reduced well within the limit as per IS1893 and in higher stories which makes structure safe against earthquake.

6.4. Storey Displacement

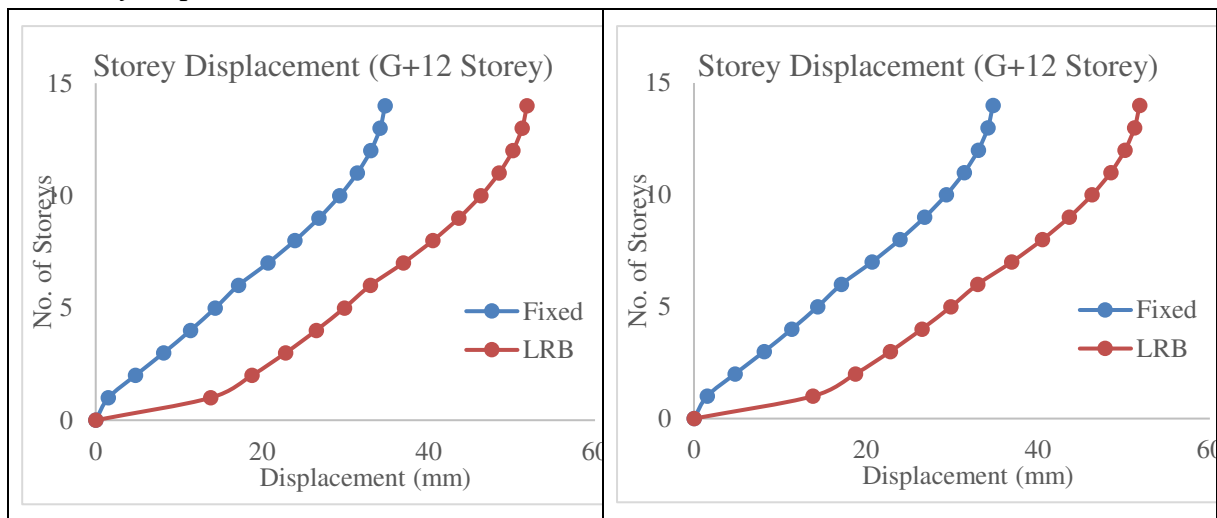


Figure 6: Storey Displacement of G+12 & G+22 Storey models.

Figure 6 shows the storey displacement for fixed base and LRB base of G+12 & G+22 Storey models. Storey displacement of base isolated structure over fixed base structure of G+12 & G+22 Storey is increased by 58.74% and 39.76 % respectively.

6.5. Percentage Reduction in Steel

G+12 Storey				G+22 Storey		
Sr.No.	Description	Fixed	LRB	Fixed	LRB	Remark
1	Column-Biaxial	77586	61581	265416	225700	
2	Column-Uniaxial	764810	552144	4513480	3995044	
3	Column-Axial	1606393	1433588	16957790	15971568	
Total Reinforcement in mm ² =		2448789	2047313	21736686	20192312	
Reinforcement Reduction in Column =		16.39%		7.10%		
1	Beam	2898050	2629336	17355952	14908932	
Reinforcement Reduction in Beam =		9.27%		14.10%		
Total Reinforcement Reduction =		25.67%		21.20%		

Above table shows the percentage reduction in steel for fixed base and LRB base of G+12 & G+22 Storey models. Percentage reduction in steel of base isolated structure over fixed base structure of G+12 & G+22 Storey is decreased by 25.67% and 21.20 % respectively.

6.6. Cost Economy

Sr.No.	Description	Quantity	Units	Remark
1	Approx. Reinforcement Quantity	5	Kg/Sft	
2	Total Reinforcement Reduction (approx. 26%)	1.3	Kg/Sft	
3	Total Cost Reduction due to LRB (Round off)	65	Rs.	Steel 50 Rs./Kg
4	Cost of Lead Rubber Bearing	150	Rs./Sft	
5	Net Cost for Lead Rubber Bearing	85	Rs.	
6	Approx. cost of Construction	1200	Rs./Sft	
7	Effective Incremental in Construction Cost	7.14	%	G+12 Storey
		8.57	%	G+22 Storey

Above table shows the cost economy for fixed base and LRB base of G+12 & G+22 Storey models. Effective incremental in construction cost of base isolated structure over fixed base structure of G+12 & G+22 Storey is increased by 7.14% and 8.57 % respectively.

7. CONCLUSION

In the present study, a G+12 storey & G+22 storey RC building was analysed using response spectrum method for both fixed and Lead Rubber Bearing (LRB) isolation. From the above result it can be concluded that Lead Rubber Bearing plays a vital role during earthquake as its increase the time period by 26.23% and 14.89% respectively which result into increase in reaction time of structure during earthquake, storey displacement by 15.87% and 22.07 % respectively which make structure more flexible, reduces base shear by 61.07% and 42.81 % respectively which reduces the seismic effect on structure and storey drift is reduced well within the limit as per IS1893 which makes structure safe against earthquake. Using of LRB as base isolators over fixed base decrease the steel quantity by 25.67% and 21.20% respectively and which results in reduction of cost economy by fairly incremental of construction cost by 7.14% and 8.57%.

From the above studied, we can conclude that the performance of the LRB based isolated structure is better than fixed base structure. Cost difference is also very limitedly increased by approx. 7 to 8 %. Also discount of 30% is offered by Insurance Company to a base isolated structure and the maintenance of the (LRB) base isolated structure is very low as compared to fixed base structure.

REFERENCES

- [1] Khin Thanda Htun, Kyaw Kaung Cho (2019), "Experimental in Structural Dynamics (Base Isolation System: Modelling)" IJTSRD volume 3, Issue 3 e-ISSN 2456-6470 (2019).
- [2] Dhiraj Narayan Sahoo, Dr. Pravat Kumar Parhi, "Base Isolation of Residential Building using Lead Rubber Bearing Technique" IJERT volume7, Issue 5, ISSN: 2278-0181 (2018).
- [3] Manoj Prajapati, Dr. Savita Maru, "Base Isolation for Earthquake Resistance: A Review" IJRASET volume 6, Issue 7, ISSN: 2321-9653 (2018).
- [4] Saurabh P. Kharat, Dinesh N. Biradar, Ajay S. Sagekar, Prathamesh V. Chavan, Prof. Reshma Saikh, "Case study on Lead Rubber Isolation Bearing" IRJET volume 5, Issue 3, e-ISSN: 2395-0056 (2018).
- [5] Prof. R. B. Ghodke, Dr. S. V. Admane, "Effect of Base Isolation for Building Structures" IJSETR volume 4, Issue 4, ISSN: 2278-7798 (2015).
- [6] Nirav G. Patel, "Study on a Base Isolation System" IJISSET ISSN 2348-7968 (2014).
- [7] O. V. Mkrtychev, G.A. Dzhinchvelashvili, A. A. Bunov, "Study of Lead Rubber Bearings Operation with Varying Height Buildings at Earthquake" XXIII R-S-P seminar, TFoCE (2014).
- [8] Prashika Tamang, Bijay Kumar Gupta, Bidisha Rai, Karsang Chukey Bhutia, Chungku Shepa, "Study on Earthquake Resistant Building (Base Isolation)" IJETT volume 33, Number 9, ISSN: 2231-5381 (2016).
- [9] Poornima B S, Dr. B S Jayashankar Babu, "Comparative Study on Seismic Response of Regular and Irregular RC Framed Buildings with HDRB, LRB and FPS Base Isolation Systems" IJRASET volume 7 ISSN: 2321-9653 (2019).
- [10] Mital Desai, Prof. Roshni John, "Seismic performance of Base Isolated Multi-storey Building" IJSER volume 6 ISSN 2229-5518 (2015).
- [11] Mithun, Dileep Kumar U, "Comparative Study on Seismic Response of Irregular Structure with Lead Rubber Bearing and Friction Pendulum Bearing Base Isolation System" IJIRSET volume 6 ISSN 2319-8753 (2017).
- [12] Sindhala Raju, Dr. Chenna Rajaram, "Seismic Base Isolation of Multi- Storey Building" IJECS VOLUME 6 ISSN 2348-117X (2017).
- [13] Sabale Nikhil Laxman, Ansari Ubaid, Karale Sandip A. "Base Isolation Study for Multistoried Buildings" IJARIE volume 3 ISSN 2395-4396 (2017).
- [14] Naveen K, Dr H. R. Prabhakara, Dr. H. Eramma, "Base Isolation of Mass Irregular RC Multi-storey Building" IRJET volume 2 ISSN 2395-0056 (2015).
- [15] Nithin A. V., Jayalekshmi R., "Seismic Analysis of Multi-storey RC Buildings supported on single and combined Base Isolation Systems" IJSER volume 8 ISSN 2229-5518 (2017).
- [16] IS 1893:2016 Criteria for Earthquake Resistant Design of Structures - Part 1: General Provisions and Buildings.
- [17] IS 456:2000 Plain and Reinforced Concrete - Code of Practice.
- [18] IBC 2000 International Building Code.
- [19] UBC 1997 Uniform Building Code - Structural Design Requirements.



COMPARATIVE STUDY ON TRIPLE FRICTION PENDULUM BEARING (TFPB) BASE ISOLATION SYSTEM ON G+12 & G+22 STORY RCC STRUCTURE OVER FIXED BASED FOR INDIAN SUBCONTINENT

M. Tamim Tanwer

Research Scholar, Pacific Academy of Higher Education & Research University-Udaipur,
Rajasthan, India.

Prof. (Dr.) Tanveer Ahmed Kazi

Professor, Pacific Academy of Higher Education & Research University-Udaipur,
Rajasthan, India.

Prof. (Dr.) Mayank Desai

Assistant Professor, Sardar Vallabhbhai National Institute of Technology-Surat, Gujarat,
India.

ABSTRACT

Earthquake is a very dangerous natural disaster which occurs by movement of the tectonic plates in the core of earth. Due to earthquake many structures collapse which result into human life losses. Base Isolation System is the technique to absorb the earthquake forces and reduces the earthquake effects in the structure at the time of earthquake. In this paper, we are considering the design of G+12 & G+22 story RCC building with fixed base and with base isolation system. Triple Friction Pendulum Bearing (TFPB) is used for the design of based isolated structure. Analyzing and designed of these two type of buildings are carried out by response spectrum method in ETABS 2016 software. After analyzing the Structure, time period, base shear, story displacement, story-drift, percentage reduction in steel and overall cost economy will be obtained for both type of structure. From this study, it is found that time period and story displacement increased while base shear, story drift, percentage of steel and overall cost is reduced with provision of Triple Friction Pendulum Bearing (TFPB) as base isolators.

Key words: Earthquake, Base Isolation System, Triple Friction Pendulum Bearings, Time Period, Base Shear, Story Drift, Story Displacement, Reinforcement, Cost Economy, Response Spectrum Method, Seismic forces, ETABS 2016.

Cite this Article: M. Tamim Tanwer, Tanveer Ahmed Kazi and Mayank Desai, Comparative study on Triple Friction Pendulum Bearing (TFPB) Base Isolation System on G+12 & G+22 story RCC Structure over Fixed Based for Indian Subcontinent, *International Journal of Advanced Research in Engineering and Technology (IJARET)*, 2020, 11(11), pp. 2637-2651

<https://iaeme.com/Home/issue/IJARET?Volume=11&Issue=11>

1. INTRODUCTION

1.1. General

Earthquake is occurring due to movement of the tectonic plates in core of the earth. It is a horizontal movement of earth surface. By earthquake the top surface of earth is shake and foundation is also shake with them. Results the superstructure experience seismic forces and structural members are may collapse. Due to collapse of the structure humans can buried under debris. Peoples are lost their life and also their properties. We cannot construct earthquake proof structure but we can construct earthquake resistant structure.

1.2. Base Isolation System

Base isolation system is also famous in the name of seismic isolation system. It is a method which is protect the structure against seismic force. Base isolation is the effective technique of earthquake engineering appurtenance to the no action in structural vibration control technologies. The System is innovated by Dr. Bill Robinson at New Zealand in 1974. It is very popular system to protect the structures from seismic forces. This technique is useful for new structures as well as can also use in old structure. The base isolation is installing between the foundation and superstructure. It is not allowed to transfer the seismic forces from ground to the superstructure. Base isolation is work as a suspension type system and absorb seismic forces without transferring to superstructure.

The TFPB consists of a spherical stainless steel surface and a slider, covered by a Teflon-based composite material. During severe ground motion, the slider moves on the spherical surface lifting the structure and dissipating energy by friction between the spherical surface and the slider. This isolator uses its surface curvature to generate the restoring force from the pendulum action of the weight of the structure on the TFPB.

2. LITERATURE REVIEW

Nitya M and Arathi S (July-2016) has published a research paper for “**Study of earthquake response of a RC building with base isolation**” on International Journal of Science and Research (IJSR). In this research a reinforced concrete moment resisting frame of G+6 storey with and without base isolation are considered. Analysis is done by using SAP 2000 software. They conclude that The Base isolation substantially increases the time period of the building & hence correspondingly reduces the base shear .The base shear is reduced up to 75 % of that of fixed one. The increase in period for structure with isolated base makes sure that the structure being completely removed from the resonance range of the earthquake. Analysis shows that the fundamental period of the structure is approximately doubled for the isolated structure. Increment in fundamental period reduces the maximum acceleration and hence the earthquake induced forces in the structure. From the tables and graphs it is clear that the storey displacements are much higher for isolated buildings, also the displacement of all the storey's are almost same. The isolator with rubber has more displacement compared to friction isolator. [1]

Tessy Thomas and Dr. Alice Mathai (ICETEM-2016) has published a research paper for “**Study of base isolation using friction pendulum bearing system**” on Journal of Mechanical

and Civil Engineering. In this research Finite element model of base isolator is created in ANSYS 14.5 software. The behaviour of the friction pendulum as base isolator also analysed. The nonlinear static analysis of base isolator is done for different storey load values. It is concluded that as the number of storey load value increases, stress intensity value also increases. The stress intensity value obtained up to 30-storeyes is within the permissible limits and base isolator can be designed for 22 to 30 storeyed building. From this analysis it is clear that the movement of slider generates a dynamic friction force that provides the required damping for absorbing the energy of the earthquake. [2]

M.Vijayakumar, Mr. S.Manivel and Mr. A.Arokiaprakash (2016) has published a research paper for “**A Study on Seismic Performance of RCC Frame with Various Bracing Systems using Base Isolation Technique**” on International Journal of Applied Engineering Research. In these research paper a G+25 storey building square in plan is analysed using SAP 2000 software. They conclude that the performance of building with base isolation technique is much better than fixed base one. The parameters such as displacement and drift have been analysed. Hence it is seen that displacement is higher in base isolation when compared to fixed base. The main factor governing the building is its storey drift. The study shows that drift is very much reduced in base isolation. Though the cost of installation adds to drawback of base isolation, but the performance proves its necessity in hospitals, public places and essential buildings. Hence from the study, it can be observed that various bracing system performs better by the use of base isolation in seismic prone area. [3]

3. SAMPLE MODEL DETAILS

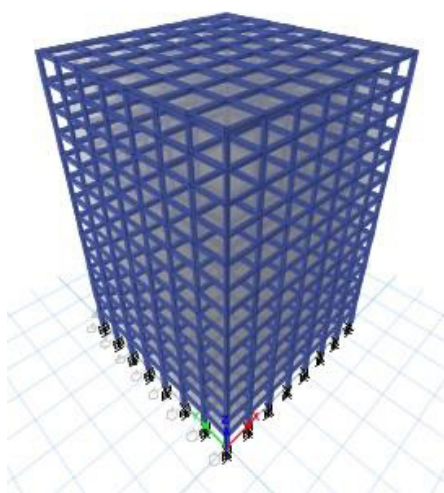


Figure 1: (G+12 Storey)

Sample Modal – 1 & 2
 Beam = 230 x 450 mm
 Column = 300 x 300 (Storey 8 to Terrace)
 375 x 375 (Plinth to Storey 7)
 450 x 450 (Base)

Floor to Floor Height = 3.0 m.

Floor Load

Live Load = 3 KN/m²

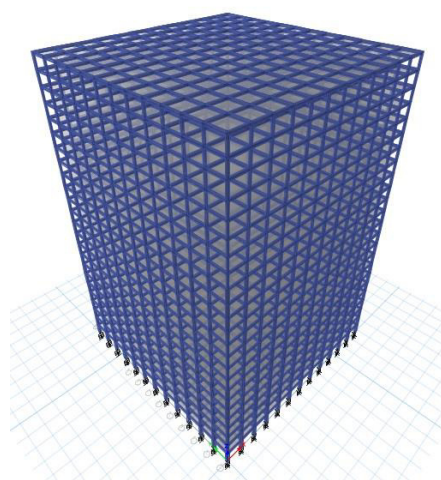


Figure 2: (G+22 Storey)

Sample Modal – 3 & 4
 Beam = 230 x 450 mm
 Column = 300 x 300 (Storey 16 to Terrace)
 375 x 375 (Storey 8 to Storey 16)
 450 x 450 (Plinth to Storey 7)
 525 x 525 (Base)

Wall Thickness = 115 mm.

Floor Finish = 1 KN/m²

Comparative study on triple friction pendulum bearing (TFPB) base isolation system on G+12 & G+22 story RCC structure over fixed based for Indian subcontinent

Earthquake Load

EQ load = Response Spectrum Method Seismic Zone = Zone 3

Soil Type = Hard Soil (Type-I) Percentage Damping = 5%

Modal Method = SRSS

Material

Grade of Concrete = M20 [20 N/mm^2] Grade of Steel = Fe500 [500 N/mm^2]

Unit weight of = 25 KN/m^2 Unit weight of = 20 KN/m^2

Concrete brick masonry

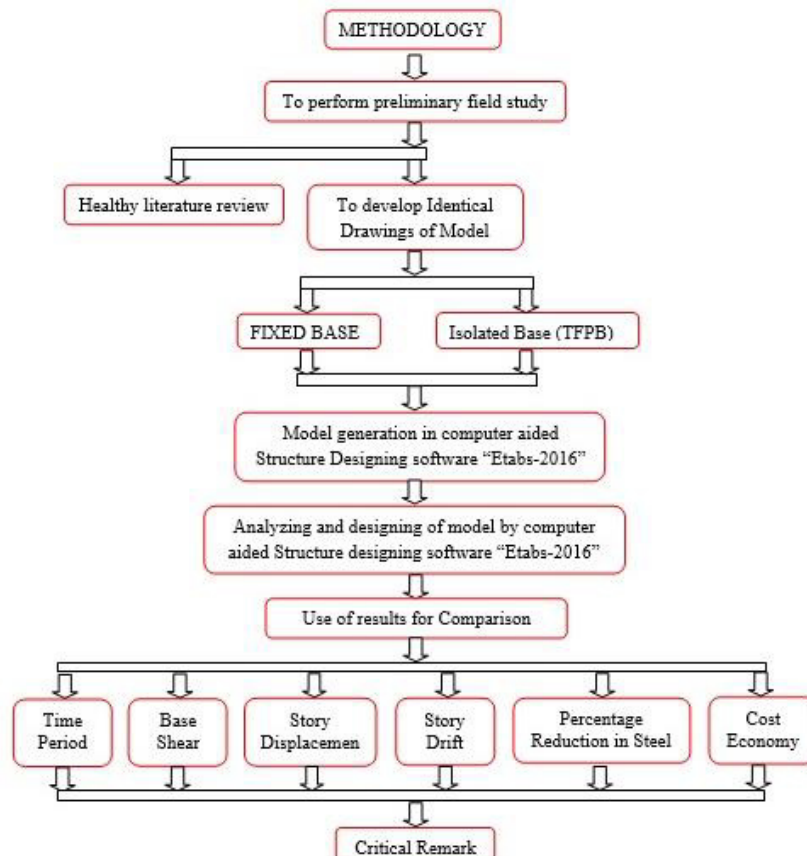
Design basis = Limit State Method (IS: 456-2000)

The sample model of 7 bay x 7 bay for G+12 story building & 12 bay x 12 bay for G+22 Story building (1 bay = 4 m.) is taken with Seismic Zone III on hard soil type – I with the above following details is considered for Analysis & Design.

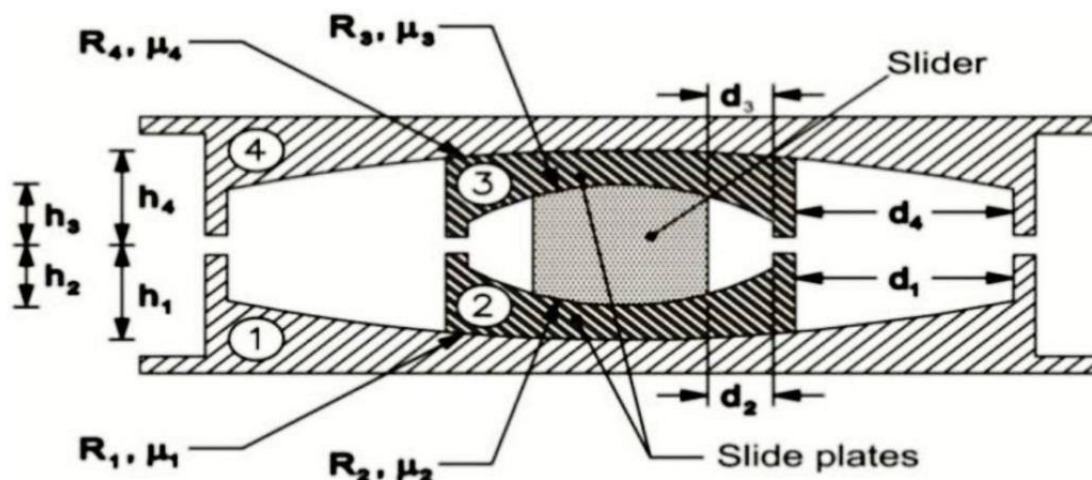
1. Model 1: - G+12 storey building with fixed base. 1. Model 1: - G+22 storey building with fixed base.

2. Model 2: - G+12 storey building with TFPB base isolation. 2. Model 2: - G+22 storey building with TFPB base isolation.

4. METHODOLOGY



5. ANALYSIS & DESIGN OF TRIPLE FRICTION PENDULUM BEARING (TFPB)



For the Analysis & Design of Triple Friction Pendulum Bearing, the cumulative load at the base is obtained from the fixed based design model in Etabs. This load are categorized into three group's viz. Biaxial, Uniaxial and Axial loaded. Sample Calculation for one group is shown below.

Biaxial Load (W) = 1638 kN.

(A) Calculation of geometric, frictional and D_D

1) Geometric Properties

$$R_1 = R_4 = 1778 \times 2 = 3556 \text{ mm} = 3.556 \text{ m.}$$

$$R_2 = R_3 = 647 \text{ mm} = 0.647 \text{ m.}$$

$$h_1 = h_4 = 161 \text{ mm} = 0.161 \text{ m.}$$

$$h_2 = h_3 = 121 \text{ mm} = 0.121 \text{ m.}$$

$$d_1 = 566.02 \text{ mm} \quad d_2 = 81.05 \text{ mm}$$

$$R_{1\text{eff}4} = R_{4\text{eff}4} = R_1 - h_1 = 3556 - 161 = 3395 \text{ mm.}$$

$$R_{2\text{eff}4} = R_{3\text{eff}4} = R_2 - h_2 = 647 - 121 = 526 \text{ mm.}$$

$$d_1^* = d_4^* = \frac{d_1 \times R_{1\text{eff}}}{R_1} = 540.39 \text{ mm} \approx 540.40 \text{ mm.} \quad d_2^* = d_3^* = \frac{d_2 \times R_{2\text{eff}}}{R_2} = 65.89 \text{ mm} \approx 65.90 \text{ mm.}$$

2) Calculating Frictional Properties of the bearing

Bearing pressure at surfaces 1 and 4

$$P = \text{Load} / \text{Area} \quad \text{Load } W = 163.8 \text{ ton (1638 kN)}$$

$$\text{Area } A = \pi \times r^2$$

$$r = h_1 + h_4 = 161 + 161 = 322 \text{ mm.}$$

$$P = 0.000503 \text{ ton/mm}^2,$$

$$P = 0.000503 \times 1450 = 0.73 \text{ ksi.}$$

$$1 \text{ ksi} = \text{Kilo square inch} = 1450 \text{ ton/mm}^2.$$

$$3\text{- Cycle friction, } \mu = 0.122 - 0.01 P,$$

$$\mu = 0.1147$$

$$\text{Adjust for high velocity} = \mu - 0.033 = 0.1147 - 0.033 \\ = 0.081 \text{ (Lower bound friction)}$$

$$\text{I - cycle friction } \mu = 1.2 \times 0.081 = 0.0977 \\ \text{Say} = 0.098$$

$$\text{Lower bound } \mu_1 = \mu_4 = 0.081 \quad \text{Upper bound } \mu_1 = \mu_4 = 0.098$$

Bearing pressure at surfaces 2 and 3

$$P = \text{Load} / \text{Area} \quad \text{Load } W = 163.8 \text{ ton (1638 kN)} \quad \text{Area } A = \pi \times r^2$$

$$r = h_2 + h_3 = 121 + 121 = 242 \text{ mm.} \quad P = 0.00089 \text{ ton/mm}^2 = 1.29 \text{ ksi.}$$

$$1 \text{ ksi} = 1450 \text{ ton/mm}^2.$$

$$\text{3- Cycle friction, } \mu = 0.122 - 0.01 P, \\ \mu = 0.1091$$

$$\text{Adjust for high velocity} = \mu - 0.036 = 0.1091 - 0.036 \\ = 0.073 \text{ (Lower bound friction)}$$

$$\text{I - cycle friction } \mu = 1.2 \times 0.073 = 0.0877 \\ \text{Say} = 0.088$$

$$\text{Lower bound } \mu_2 = \mu_3 = 0.073 \quad \text{Upper bound } \mu_2 = \mu_3 = 0.088$$

μ = force at zero displacement divided by the normal load

$$\text{For Lower bound, } \mu = \mu_1 - (\mu_1 - \mu_2) \times \frac{R_{2\text{eff}}}{R_{1\text{eff}}} \\ \mu = 0.080$$

$$\text{For Upper bound, } \mu = \mu_1 - (\mu_1 - \mu_2) \times \frac{R_{2\text{eff}}}{R_{1\text{eff}}} \\ \mu = 0.096$$

3) D_D Calculation (Upper bound Analysis)

$$S_d = 0.5074, \quad \mu = 0.096 \quad \mu_1 = 0.098 \quad Dy = (\mu_1 - \mu_2) * R_{2\text{eff}} = 0.005250,$$

$$F_d = 0.277243, \quad W = 163.8 \text{ Ton.}$$

$$\text{No. of Bearing} = 12$$

$$\Sigma F_d = F_d \times W \times \text{Total Bearing} \quad \Sigma F_d = 0.277243 \times 163.8 \times 12 = 544.95$$

$$\Sigma W = \text{Load} \times \text{No. of bearing} \quad \Sigma W = 1965.6 \text{ tons}$$

$$\text{i. Let the displacement be } D_D = 0.07202 \text{ m.}$$

$$\text{ii. Effective stiffness, } Q_d = \mu * \Sigma W \quad = 0.096 \times 1965.6 \\ Q_d = 188.98 \text{ ton}$$

$$k_D = \Sigma F_D / D_D = 544.95 / 0.07202$$

$$k_D = 7566.63 \text{ ton/m.}$$

$$K_{\text{eff}} = k_D + (Q_d / D_D) = 7566.63 + (188.98 / 0.07202).$$

$$K_{\text{eff}} = 10190.63 \text{ ton/m.}$$

iii. Effective period, $T_{\text{eff}} = 2\pi\sqrt{(\Sigma w)/(K_{\text{eff}} \times g)}$

$$T_{\text{eff}} = 0.88103 \text{ sec.}$$

iv. Effective damping, $\beta_D = \frac{E}{2\pi K_{\text{eff}} \times D_D^2} = \frac{4\mu \Sigma w (D_D - D_y)}{2\pi K_{\text{eff}} \times D_D^2}$

$$\beta_{\text{eff}} = \beta_D = 0.1520 \text{ (15.20\%)}$$

Refer Eq. 17.5-2 & 17.8-7, ASCE 7-10 for iii & iv.

v. Damping reduction factor, $\beta = \left(\frac{\beta_{\text{eff}}}{0.05}\right)^{0.3}$

$$\beta = 1.3959$$

vi. $D_D^1 = \frac{S_D \times T_{\text{eff}}^2}{4\pi^2 \times \beta} \times g$

$$D_D^1 = 0.0701 \text{ m.}$$

(B) Calculating SAP2000 or Etabs links / support property data (upper bound)

1) Main Properties

i. Rotational Inertia

Considering the isolator with diameter $\varnothing = 0.305 \text{ m.}$ (cylinder), $h = 0.32 \text{ m}$ (Total height)

$$\varnothing = 0.484 \text{ m, } h = 0.5 \text{ m. } A = \frac{\pi \times \varnothing^2}{4} = \frac{\pi \times 0.484^2}{4}$$

$$A = 0.1840 \text{ m}^2$$

$$K_{\text{eff}} = \frac{W}{R_{1\text{eff}}} + \frac{\mu W}{D_D}$$

$$K_{\text{eff}} = 266.91 \text{ ton/m}$$

$$I_1 = \frac{K_{\text{eff}} \times h^3}{12E} = \frac{638.012 \times 0.5^3}{12 \times 10000000}$$

$$= 2.78035\text{E-}07 \text{ m}^4.$$

Note:- Young's modulus 'E' was assumed $1 \times 10^7 \text{ N/mm}^2$ equal to half of actual steel modulus as the bearing is not a solid piece of metal. $E = 1.00\text{E+}07 \text{ N/mm}^2.$

ii. Determine of Bearing mass

$$D_{\text{m-max}} = 0.0702 \text{ m. } D_{\text{TM}} = 1.15 \times 0.0702$$

refer (Eq. 17.5.3.5 – ASCE 7-10)

$$D_{\text{TM}} = 0.0807 \text{ m.}$$

$$D = 2 D_{\text{TM}} = 2 \times 0.0807$$

$$D = 0.16146 \text{ m.}$$

$$W = 0.241 D^2 - 0.00564 D$$

$$W = 0.0053721 \text{ ton.}$$

$$M = w / g = 0.005372 / 9.81$$

$$M = 0.000548 \text{ ton sec}^2/\text{m.}$$

2) Directional properties (U_1)

$$\varnothing = 0.484 \text{ m, } h \text{ or } L = 0.5 \text{ m}$$

$$\text{Effective stiffness} = AE / L$$

$$K_{\text{eff}} = 3679684.643 \text{ ton/m.}$$

$$K_{\text{eff}} = 36796846.43 \text{ KN/m.}$$

Effective damping from the D_D calculation

$$K_{\text{eff}} = 3679684.64 \text{ ton/m.}$$

$$\beta_{\text{eff}} = 0.1520 \text{ (15.20\%)}$$

3) Directional properties ($U_2 - U_3$)

i. Determination of liner properties.

Effective stiffness $K_{\text{eff}} = 266.914 \text{ ton/m.} = 2669.14 \text{ KN/m.}$ Effective damping $\beta_{\text{eff}} = 0.1520$

$$\text{Height for outer surface} = h_1 = h_4 = 161 \text{ mm (0.161 m.)}$$

$$\text{Height for Inner surface} = h_2 = h_3 = 121 \text{ mm (0.121 m.)}$$

ii. Determination of Non - liner properties.

$$\text{Stiffness} = \frac{\mu_1 w}{D_y}$$

$$D_y = (\mu_1 - \mu_2) R_{2\text{eff}} = (0.098 - 0.088) \times 0.526$$

$$D_y = 0.00525 \text{ m.}$$

$$\text{Stiffness of outer surface} = \frac{\mu_1 w}{D_y} = \frac{0.098 \times 163.8}{0.00525} = 3047.855 \text{ ton/m.} = 30478.55 \text{ KN/m.}$$

$$\text{Stiffness of Inner surface} = \frac{\mu_2 w}{D_y} = \frac{0.088 \times 163.8}{0.00525} = 2736.448 \text{ ton/m.} = 27364.48 \text{ KN/m.}$$

$$\text{Friction slow} = \mu_1 \text{ for outer surface} = 0.098$$

$$= \mu_2 \text{ for Inner surface} = 0.088$$

$$\text{Friction fast} = 2 \times \mu_1 \text{ for outer surface} = 0.195$$

$$= 2 \times \mu_2 \text{ for Inner surface} = 0.175$$

$$\text{Rate Parameter} = \text{Friction slow} / \text{Friction fast} = 0.098 / 0.195 = 0.5 = 0.0005$$

❖ Radius of sliding surface

$$\text{For outer} = R_{1\text{eff}} = 3.395 \text{ m.}$$

$$\text{For inner} = R_{2\text{eff}} = 0.526 \text{ m.}$$

❖ Stop distance

$$\text{For outer surface } u_1^* = 2 D_y + 2 d_1^* = 1.09130 \text{ m.} = 1091.30 \text{ mm.}$$

$$\text{For Inner surface } u_2^* = 2 D_y = 0.0105 \text{ m.} = 10.50 \text{ mm.}$$

Input Values for Etabs:

The image shows two screenshots of the 'Link/Support Directional Properties' dialog box in ETABS. The left screenshot shows the 'Identification' and 'Linear Properties' tabs. The right screenshot shows the 'Linear Properties' and 'Nonlinear Properties' tabs.

Left Screenshot (Identification and Linear Properties):

- Identification:** Property Name: B, Direction: U1, Type: Triple Pendulum Isolator, NonLinear: Yes.
- Linear Properties:** Effective Stiffness: 36796846.43 kN/m, Effective Damping: 1.396 kN-s/m.
- Nonlinear Properties:** Stiffness: 36796846.43 kN/m, Damping Coefficient: 1.396 kN-s/m.

Right Screenshot (Linear Properties and Nonlinear Properties):

- Identification:** Property Name: B, Direction: U2: U3, Type: Triple Pendulum Isolator, NonLinear: Yes.
- Linear Properties:** Effective Stiffness - U2: 2669.136 kN/m, Effective Stiffness - U3: 2669.136 kN/m, Effective Damping - U2: 1.396 kN-s/m, Effective Damping - U3: 1.396 kN-s/m.
- Shear Deformation Location:** Distance from End-J - U2: 0 m, Distance from End-J - U3: 0 m.
- Height and Symmetry of Sliding Surfaces:** Height for Outer Surfaces: 0.161 m, Height for Inner Surfaces: 0.121 m. Checkboxes: ☒ Outer Bottom Surface is Symmetric to Outer Top Surface, ☒ Inner Bottom Surface is Symmetric to Inner Top Surface.
- Nonlinear Properties for Directions U2 and U3:**

	Outer Top	Outer Bottom	Inner Top	Inner Bottom	
Stiffness	30478.548	30478.548	27364.48	27364.48	kN/m
Friction Coefficient, Slow	0.09769	0.09769	0.0877	0.0877	
Friction Coefficient, Fast	0.19538	0.19538	0.17541	0.17541	
Rate Parameter	0.0005	0.0005	0.0005	0.0005	sec/mm
Radius of Sliding Surface	3.395	3.395	0.526	0.526	m
Stop Distance	1091.3	1091.3	10.5	10.5	mm

G+12 Storey Model								
Direction U1	Load	1638 KN		2487 KN		3920 KN		
	Linear Properties							
	Effective Stiffness	36796846.43		36796846.43		36796846.43		KN/m
	Effective Damping	1.396		1.367		1.317		KN-s/m
	Non-Linear Properties							
	Effective Stiffness	36796846.43		36796846.43		36796846.43		KN/m
	Effective Damping	1.396		1.367		1.317		KN-s/m
Direction U2 & U3	Linear Properties							
	Effective Stiffness	2669.14		3877.29		5644.98		KN/m
	Effective Damping	1.396		1.367		1.317		KN-s/m
	Ht. for outer Surface	0.161		0.161		0.161		m
	Ht. for inner Surface	0.121		0.121		0.121		m
	Non-Linear Properties							
		Outer Top	Inner Top	Outer Top	Inner Top	Outer Top	Inner Top	

Comparative study on triple friction pendulum bearing (TFPB) base isolation system on G+12 & G+22 story RCC structure over fixed based for Indian subcontinent

	Stiffness	30478.5 5	27364.48	32685.61	27957.47	32890.68	25438.21	KN/m
	Friction Coeff. Slow	0.0977	0.0877	0.0931	0.0797	0.0855	0.0661	
	Friction Coeff. Fast	0.1954	0.1754	0.1863	0.1593	0.1710	0.1322	
	Rate Parameter	0.0005	0.0005	0.0005	0.0005	0.0005	0.0005	Sec/mm
	sliding surface (R)	3.395	0.526	3.395	0.526	3.395	0.526	m
	Stop Distance	1091.30	10.50	1094.98	14.18	1101.18	20.38	mm
G+22 Storey Model								
Direction U1	Load	3342 KN		4627 KN		6860 KN		
	Linear Properties							
	Effective Stiffness	36796846.43		36796846.43		36796846.43		KN/m
	Effective Damping	1.338		1.292		1.205		KN-s/m
	Non-Linear Properties							
	Effective Stiffness	36796846.43		36796846.43		36796846.43		KN/m
	Effective Damping	1.338		1.292		1.205		KN-s/m
Direction U2 & U3	Linear Properties							
	Effective Stiffness	4973.01		6391.50		8204.24		KN/m
	Effective Damping	1.338		1.292		1.205		KN-s/m
	Height for Outer Surface	0.161		0.161		0.161		m
	Height for Inner Surface	0.121		0.121		0.121		m
	Non-Linear Properties							
		Outer Top	Inner Top	Outer Top	Inner Top	Outer Top	Inner Top	
	Stiffness	33120.4 1	26766.80	32262.31	23465.73	28922.27	15880.44	KN/m
	Friction Coefficient Slow	0.0886	0.0716	0.0817	0.0594	0.0698	0.0383	
	Friction Coefficient Fast	0.1771	0.1432	0.1634	0.1189	0.1396	0.0766	

	Rate Parameter	0.0005	0.0005	0.0005	0.0005	0.0005	0.0005	Sec/mm
	Radius of sliding surface	3.395	0.526	3.395	0.526	3.395	0.526	m
	Stop Distance	1098.68	17.88	1104.24	23.44	1113.91	33.11	mm

6. Results

6.1. Time Period

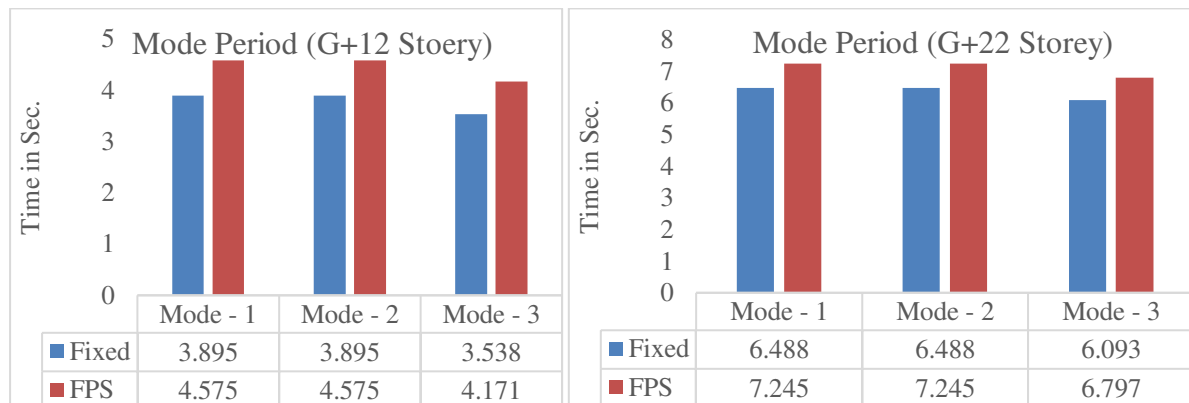


Figure 3: Time Period of G+12 & G+22 Storey models

Figure 3 shows the time period for fixed base and TFPB base of G+12 & G+22 Storey models. Time period of base isolated structure over fixed base structure of G+12 & G+22 Storey is increased by 17.60% and 11.63 % respectively.

6.2. Base Shear

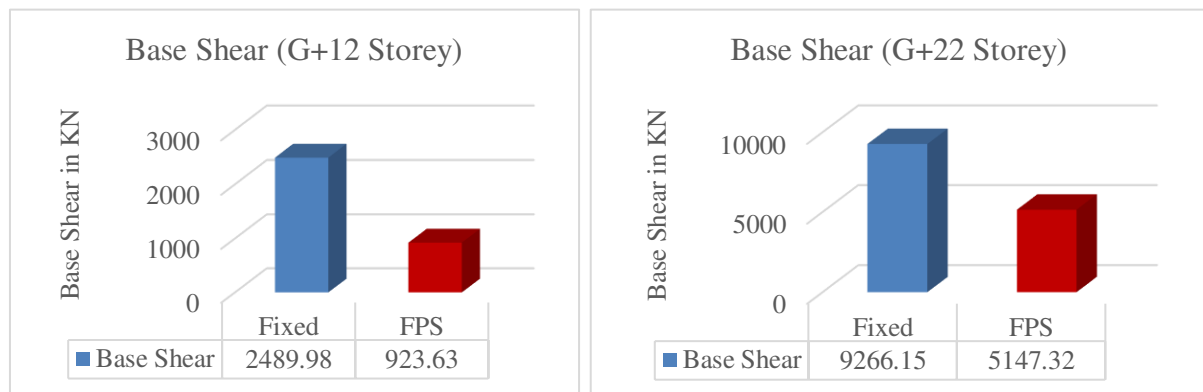


Figure 4: Base Shear of G+12 & G+22 Storey models

Figure 4 shows the base shear for fixed base and TFPB base of G+12 & G+22 Storey models. Base shear of base isolated structure over fixed base structure of G+12 & G+22 Storey is decreased by 62.91% and 44.45 % respectively.

6.3. Storey-Drift

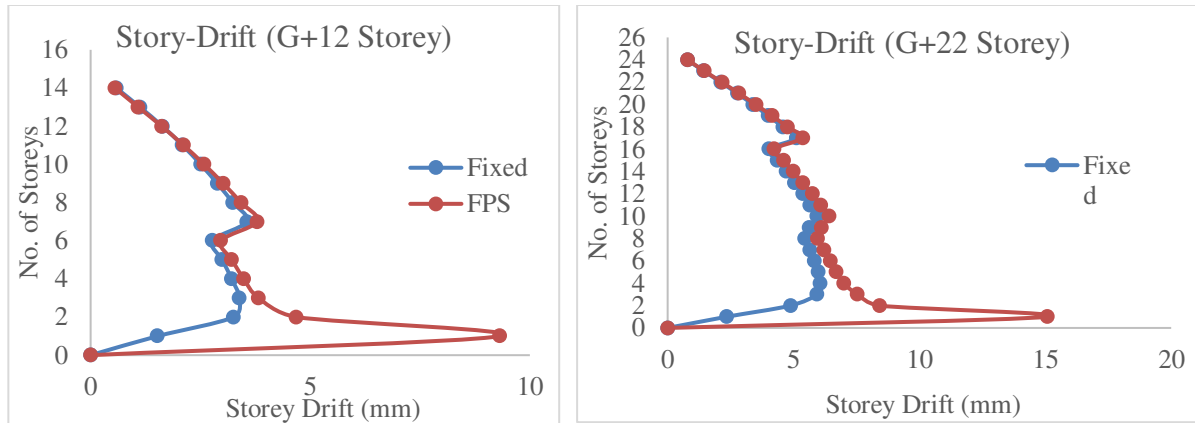


Figure 5: Storey-Drift of G+12 & G+22 Storey models

Figure 5 shows the storey-Drift for fixed base and TFPB base of G+12 & G+22 Storey models. Storey-Drift of base isolated structure over fixed base structure of G+12 & G+22 Storey is reduced well within the limit as per IS1893 and in higher stories which makes structure safe against earthquake.

6.4. Storey Displacement

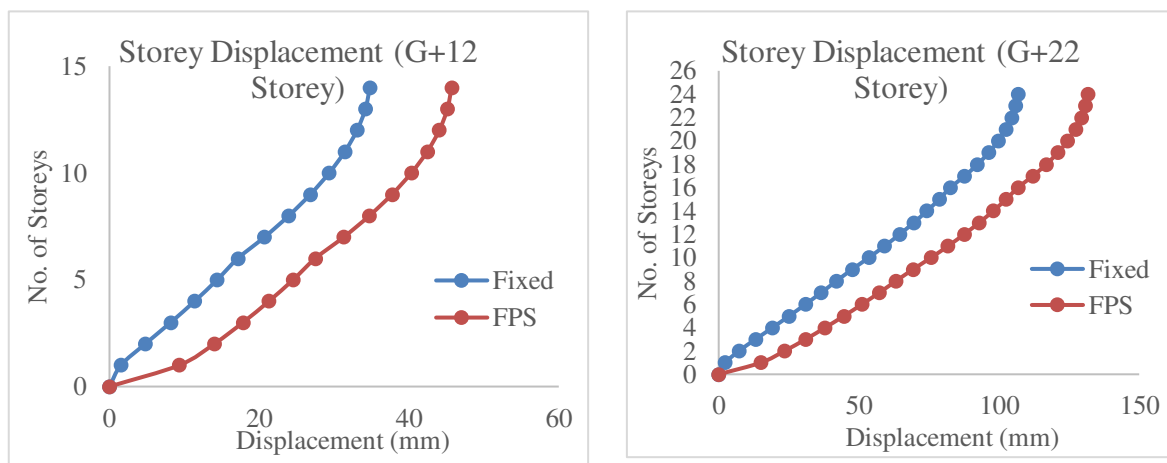


Figure 6: Story Displacement of G+12 & G+22 Storey models.

Figure 6 shows the storey displacement for fixed base and TFPB base of G+12 & G+22 Storey models. Storey displacement of base isolated structure over fixed base structure of G+12 & G+22 Storey is increased by 49.41% and 30.94 % respectively.

6.5. Percentage Reduction in Steel

G+12 Storey				G+22 Storey		
Sr.No.	Description	Fixed	TFPB	Fixed	TFPB	Remark
1	Column-Biaxial	77586	61998	265416	229720	
2	Column-Uniaxial	764810	557424	4513480	4021152	
3	Column-Axial	1606393	1431680	16957790	15960503	
Total Reinforcement in mm ² =		2448789	2051102	21736686	20211375	
Reinforcement Reduction in Column =		16.24%		7.02%		
1	Beam	2898050	2595148	17355952	14759524	
Reinforcement Reduction in Beam =		10.45%		14.96%		
Total Reinforcement Reduction =		26.69%		21.98%		

Above table shows the percentage reduction in steel for fixed base and TFPB base of G+12 & G+22 Storey models. Percentage reduction in steel of base isolated structure over fixed base structure of G+12 & G+22 Storey is decreased by 26.69% and 21.98 % respectively.

6.6. Cost Economy

Sr.No.	Description	Quantity	Units	Remark
1	Approx Reinforcement Quantity	5	Kg/Sft	
2	Total Reinforcement Reduction (Approx 27%)	1.35	Kg/Sft	
3	Total Cost Reduction due to TFPB (Round off)	68	Rs.	Steel 50 Rs./Kg
4	Cost for Triple Friction Pendulum Bearing	110	Rs./Sft	

Comparative study on triple friction pendulum bearing (TFPB) base isolation system on G+12 & G+22 story RCC structure over fixed based for Indian subcontinent

5	Net Cost for Triple Friction Pendulum Bearing	42	Rs.	
6	Approx cost of Construction	1200	Rs./Sft	
7	Effective Incremental in Construction Cost	3.57	%	G+12 Storey
		4.64	%	G+22 Storey

Above table shows the cost economy for fixed base and TFPB base of G+12 & G+22 Storey models. Effective incremental in construction cost of base isolated structure over fixed base structure of G+12 & G+22 Storey is increased by 3.57% and 4.64 % respectively.

7. CONCLUSION

In the present study, a G+12 storey & G+22 storey RC building was analysed using response spectrum method for both fixed and Triple Friction Pendulum Bearing (TFPB) isolation. From the above result it can be concluded that Triple Friction Pendulum Bearing plays a vital role during earthquake as its increase the time period by 17.60% and 11.63% respectively which result into increase in reaction time of structure during earthquake, storey displacement by 49.41% and 30.94% respectively which make structure more flexible, reduces base shear by 62.91% and 44.45% respectively which reduces the seismic effect on structure and storey drift is reduced well within the limit as per IS1893 which makes structure safe against earthquake. Using of TFPB as base isolators over fixed base decrease the steel quantity by 26.69% and 21.98% respectively and which results in reduction of cost economy by fairly incremental of construction cost by 3.57% and 4.64%.

From the above studied, we can conclude that the performance of the TFPB based isolated structure is better than fixed base structure. Cost difference is also very limitedly increased by approx. 3 to 4 %. Also discount of 30% is offered by Insurance Company to a base isolated structure and the maintenance of the (TFPB) base isolated structure is very low as compared to fixed base structure.

REFERENCES

- [1] Nitya, M., &Arathi, S. (July-2016). Study on the earthquake response of a RC building with base isolation. International journal of science and research, 5, 1002-1005.
- [2] Thomas, T., &Mathai, A. (2016).Study of base isolation using friction pendulum bearing system.Journal of Mechanical and Civil Engineering, 19-23.
- [3] Vijaykumar, M., Manivel, S., &Arokiaprakash, A. (2016).A study on seismic performance of RCC frame with various bracing systems using base isolation technique. International journal of applied engineering research, 11, 7030-7033.

- [4] Naveen, K., Prabhakara, H.R., &Eramma, H. (Oct-2015). Base isolation of mass irregular RC multi-storey building.International research journal of engineering and technology, 2, 902-906.
- [5] Desai, M., & John, R. (Dec-2015). Seismic performance of base isolated multi-storey building. International journal of scientific & engineering research, 6, 84-89.
- [6] Noorzai, M., Bajad, M.N., &Dodal, N. (May-2015). Study response of fixed base and isolation base. International journal of innovative research in science, engineering and technology, 4, 3674-3681.
- [7] Ghodke, R.B., &Admane, S.V. (April-2015). Effect of base-isolation for building structures.International journal of science, engineering and technology research, 4, 971-974.
- [8] Nassani, D.E., &Wassef, M.A. (Feb-2015). Seismic base isolation in reinforced concrete structures.International journal of research studies in science, engineering and technology, 2, 1-13.
- [9] Moretti, S., Trozzo, A., Terzic, V., Cimellaro, G.P., &Mahin, S. (Sept-2014). Utilizing base-isolation systems to increase earthquake resiliency of healthcare and school buildings. 4th International conference on building resilience, 14, 969-976.
- [10] Khan, M., &Bakre S.V. (April-June 2015). Design and study of seismic base isolators.Journal of basic and applied engineering research, 2, 734-739.
- [11] Barmo, A., Mualla, I.H., &Hasan, H.T. (Feb-2015). The behaviour of multi-story buildings seismically isolated hybrid isolation (friction, rubber and with the addition of rotational friction dampers). Open journal of earthquake research, 4, 1-13.
- [12] Keerthana, S., Sathishkumar, K., &Balamonica, K. (Feb-2015).Seismic response reduction of structures using base isolation.International journal of innovative science, engineering and technology, 2, 33-40. [13] Sabale Nikhil Laxman, Ansari Ubaid, Karale Sandip A. **“Base Isolation Study for Multistoried Buildings”** IJARIE volume 3 ISSN 2395-4396 (2017).
- [13] Nithin A. V., Jayalekshmi R., **“Seismic Analysis of Multi-storey RC Buildings supported on single and combined Base Isolation Systems”** IJSER volume 8 ISSN 2229-5518 (2017).
- [14] Santhosh H.P., Harsha M.S., Manohar K & Pradeepa B.B. (Feb-2017). “Seismic isolation of RC framed structure with and without infills.” International Journal of Civil Engineering and Technology (IJCET) Volume 8 ISSN 0976-6316.
- [15] Dr. H.M. Somasekharaiah, Er. Dharmesh N. & Mohammed Ghouse. (Aug-2016).”A comparative study on RC frame structure considering lead rubber bearing and triple friction pendulum bearing.” International journal of innovative research in science engineering and technology. Volume -4, Issue-8 ISSN 2319-8753.
- [16] IS 1893:2016 Criteria for Earthquake Resistant Design of Structures - Part 1: General Provisions and Buildings.
- [17] IS 456:2000 Plain and Reinforced Concrete - Code of Practice.
- [18] IBC 2000 International Building Code.
- [19] UBC 1997 Uniform Building Code - Structural Design Requirements.

CERTIFICATE





IAEME PUBLICATION

Publishers of High Quality Peer Reviewed Refereed Scientific,
Engineering & Technology, Medicine and Management International Journals

INTERNATIONAL JOURNAL OF CIVIL ENGINEERING AND TECHNOLOGY (IJCIET)



Certificate of Publication

This is to certify that the research paper entitled "**COMPARATIVE STUDY ON LEAD RUBBER BEARING (LRB) BASE ISOLATION SYSTEM ON G+12 & G+22 STORY RCC STRUCTURE OVER FIXED BASED FOR INDIAN SUBCONTINENT**" authored by "**M. Tamim Tanwer ; Prof. Dr. Tanveer Ahmed Kazi ; Prof. Dr. Mayank Desai** " had been reviewed by the Editorial Board and published in "INTERNATIONAL JOURNAL OF CIVIL ENGINEERING AND TECHNOLOGY (IJCIET), Volume 10, Issue 11, November 2019, pp. 423-433; ISSN Print: 0976-6308 and ISSN Online: 0976-6316;"

Article Id - IJCIET_10_11_043

Date of Publication - 30 November 2019

Article Link - https://iaeme.com/Home/article_id/IJCIET_10_11_043

Chief Editor

Plot: 03, Flat- S 1, PoomalaiSantosh Pearls Apartment, Plot No. 10, VaikoSalai 6th Street, Jai Shankar Nagar,
Palavakkam, Chennai - 600 041, Tamilnadu, India. E-mail: editor@iaeme.com



IAEME PUBLICATION

Publishers of High Quality Peer Reviewed Refereed Scientific,
Engineering & Technology, Medicine and Management International Journals

INTERNATIONAL JOURNAL OF ADVANCED RESEARCH IN ENGINEERING AND TECHNOLOGY (IJARET)



Certificate of Publication

This is to certify that the research paper entitled "**COMPARATIVE STUDY ON TRIPLE FRICTION PENDULUM BEARING (TFPB) BASE ISOLATION SYSTEM ON G+12 & G+22 STORY RCC STRUCTURE OVER FIXED BASED FOR INDIAN SUBCONTINENT**" authored by "**Mr.M. Tamim Tanwer ; Prof.Dr.Tanveer Ahmed Kazi ; Prof.Dr.Mayank Desai** " had been reviewed by the Editorial Board and published in "INTERNATIONAL JOURNAL OF ADVANCED RESEARCH IN ENGINEERING AND TECHNOLOGY (IJARET), Volume 11, Issue 11, November 2020, pp. 2637-2651; ISSN Print: 0976-6480 and ISSN Online: 0976-6499;"

Article Id - IJARET_11_11_262

Date of Publication - 30 November 2020

Article Link - https://iaeme.com/Home/article_id/IJARET_11_11_262

Chief Editor

Plot: 03, Flat- S 1, PoomalaiSantosh Pearls Apartment, Plot No. 10, VaikoSalai 6th Street, Jai Shankar Nagar,
Palavakkam, Chennai - 600 041, Tamilnadu, India. E-mail: editor@iaeme.com

22nd ISTE State Annual Faculty Convention 2017



Indian Society for Technical Education
A. D. Patel Institute of Technology (ADIT)



Certificate

This is to certify that a paper titled Introduction to base isolation system was presented in National Conference on "Engineering Innovations for Social and Environmental Development", during 22nd ISTE State Annual Faculty Convention, jointly organized by ISTE Gujarat Section and A.D. Patel Institute of Technology, New Vallabh Vidyanagar, Anand on 30th December, 2017 authored by M.Tamim.A.Tanzwer, Mr. Sabban Shaikh, Mr. Jignesh Panchal.

Dr. A.S. Nandane
Convenor-ISTE State Convention

Dr. R.K. Jain
Principal, ADIT

Prof. K. M. Bhavsar
Chairman-ISTE Gujarat Section

Third International Conference on
INFORMATION AND COMMUNICATION TECHNOLOGY
FOR INTELLIGENT SYSTEMS





Certificate

This is to certify that Prof. Dr. Mr. / Ms. B. M. Tamim Tawwal
participated in International Conference on ICT for Intelligent Systems (ICTIS 2018) held during 6 - 7 April, 2018
at Hotel Pride Plaza, Ahmedabad, INDIA.

He / She also presented a paper / delivered an invited talk / chaired a technical session titled A Study
on different types of Base Isolation System over
We wish his / her the best for future endeavours.



Dr. Priyanka Sharma
Professor, Raksha Shakti University


Bharat Patel
Chairman, CEDB, IE(I)


Mihir Chauhan
Organizing Secretary, ICTIS - 2018



 Springer


Gujarat
Innovation
Society



ICRAET-2022

Certificate

This certificate is awarded to

DR/PROF/Mr/Ms. M. Tamim Tanweer..... of

*PAHER University..... for being a paper presenter/participant/Chaired
on title...Analysis & design of Lead Rubber bearing (LRB) in*

*International Conference on Recent Advancements in Engineering & Technology-2022
organized by SS College of Engineering, Udaipur on 18th - 19th February.*

M. Firdos Sheikh
conference convener,
SS college of engineering



Dr. Prashant sharma
Principal,
SS college of engineering



Indian Institute of
Industrial Engineering



4TH INTERNATIONAL CONFERENCE ON CREATIVITY & INNOVATION IN TECHNOLOGY DEVELOPMENT

Certificate

This certificate is awarded to

Dr. Prof./Mr/Ms. M. Tamim. Tan. of
PAHER. University. for being a Paper Presenter/Participant/Chaired
on title .Analysis. & Design. of Triple. fiction. pendulum. in
4th International Conference on Creativity & Innovation in Technology

Date : 23/12/2022

Place : Udaipur

Development organized on 9-10th December 2022.

Convenor
Dr. Prashant Sharma
Principal, SSCE

Convenor
Dr. Deepak Tak
Principal, SSPC

Co-Convenor
Mr Piyush Sharma
HOD EE

Co-Convenor
Mr. Dheeraj Soni
HOD ME

Co-Convenor
Mr. M. Firdos Sheikh
HOD CSE

PLAGIARISM REPORT



ANALYTICAL STUDY OF BASE ISOLATION SYSTEM ON MEDIUM-RISE REINFORCED CONCRETE BUILDING FOR INDIAN SUBCONTINENT

ORIGINALITY REPORT

4%

SIMILARITY INDEX

3%

INTERNET SOURCES

1%

PUBLICATIONS

1%

STUDENT PAPERS

PRIMARY SOURCES

1

www.ijirset.com

Internet Source

1%

2

repository.its.ac.id

Internet Source

1%

3

M. S. Mounashree, H. Hema, S. M. Harisha. "Chapter 10 Comparative Study on Influence of Lead Rubber Bearing on RC Structures with Flat Slab and Conventional Slab System Under Seismic Loading", Springer Science and Business Media LLC, 2019

Publication

<1%

4

vdocuments.net

Internet Source

<1%

5

Cenk Alhan, Furkan Şahin. "Protecting vibration-sensitive contents: an investigation of floor accelerations in seismically isolated buildings", Bulletin of Earthquake Engineering, 2011

Publication

<1%

6

www.ijamtes.org

Internet Source

<1 %

7

Submitted to Nottingham Trent University

Student Paper

<1 %

8

Submitted to Higher Education Commission
Pakistan

Student Paper

<1 %

9

docplayer.net

Internet Source

<1 %

10

1library.net

Internet Source

<1 %

11

peer.berkeley.edu

Internet Source

<1 %

12

Submitted to Engineers Australia

Student Paper

<1 %

Exclude quotes Off

Exclude bibliography Off

Exclude matches < 14 words